University of Stavanger

FACULTY OF SCIENCE AND TECHNOLOGY

MASTER'S THESIS

Study programme/specialisation: Engineering Structures and Materials / Civil Engineering Structures	Spring semester, 2020 Open
Author: Ran Zhao and Joanna Syper	
Programme coordinator: Sudath Siriwardane Supervisor(s): Jasna B. Jakobsen (UiS) Jungao Wang (External, Statens vegvesen)	
Title of master's thesis: Dynamic response of a floating bridge under wind conditions from field measurements	
Credits: 30	
Keywords: Bjørnafjorden Floating bridge Cable-stayed Bridge Finite Element Method Abaqus Fortran	Number of pages: ……134…… + supplemental material/other: ……52…… Stavanger, ……28.06.2020…….. date/year

ABSTRACT

The long and slender floating structures across the wide and deep waters are exposed for considerable environmental loads. In this study, the dynamic response of a curved floating pontoon bridge supported by side mooring lines subjected to aerodynamic loads is investigated. The studied concept K12_05 is one of the concepts suggested by The Norwegian Public Roads Administration for fjord crossing at Bjørnafjorden.

The finite element model of the Bjørnafjorden floating bridge is developed in the Abaqus software. The studied floating bridge concept has a complex geometry with variable curvature along the vertical and horizontal plane. The bridge is firstly examined in modal analysis in terms of eigenfrequencies and eigenmodes. Bridge responses under static wind considering various wind directions and different spatial distributions are studied. Furthermore, bridge dynamic responses considering aerodynamic loads characterized by quasi-static buffeting theory are studied by using time domain analysis. The turbulent wind field is simulated considering wind spectral and coherence parameters given by the design guidelines and from field measurements. Fortran subroutines are developed to integrate with Abaqus to calculate the instantaneous wind loads. Six realizations of each characteristic wind condition are generated to represent the randomness of the wind field in time domain. The bridge dynamic responses are presented and discussed in the forms of mean displacement, standard deviation and maximum responses. The power spectral density of the bridge response is also calculated and compared with modal information of the structure. Finally, sensitivity analysis on wind spectral and coherence parameters was studied.

PREFACE

This master thesis is the completion of the master's degree in civil engineering structures at the Department of Mechanical and Structural Engineering and Materials Science at University of Stavanger. This work was performed during the spring semester of 2020.

We would like to give very special thanks for the guidance of Dr. Jungao Wang from The Norwegian Public Roads Administration. We are greatly appreciative of the knowledge that Dr. Jungao shared with us and for his time spent helping us with this study. It is because of his guidance and persistent help that this work came into existence.

Sincere thanks to Prof. Jasna B. Jakobsen for insightful comments and suggestions throughout this thesis work. We could not have achieved these results without a strong support group. We are grateful for all the support and every video meeting undertaken during this unusual time of pandemic.

Many thanks also to the help we received from the Faculty of Science and Technology who provided us with Abaqus license which enabled us to continue working from home during the lockdown.

Finally, for our parents and friends who supported us with love and understanding.

Ran Zhao

Joanna Syper

CONTENTS

LIST OF FIGURES

LIST OF TABLES

1. Introduction

1.1. The Coastal Highway Route E39

The Coastal Highway Route E39 which starts in the city of Kristiansand in the south part of Norway and runs to the city of Trondheim is approximately 1100 km long and requires using of seven different ferry connections which makes a travel time last for 21 hours. The Norwegian Public Roads Administration undertakes the ambitious improvements of E39 by replacing ferries with bridges and tunnels which eventually will reduce the driving time by half and save massive amount of waiting time. This long-term goal of transforming the E39 into ferry-free highway is estimated for about NOK 340 billion and is the largest infrastructure project in modern Norwegian history [3].

Figure 1: The Coastal Highway Route E39 [4]

In order to link Western Norway together different fjord crossing solutions are considered for each of fjord crossing projects. Some of them uses familiar technologies like tunnel or suspension bridge solutions, when the other more demanding fjord crossings projects requires development of new technologies [5]. Because the concept must cross the fjords of large width and depth and resists high environmental loads the existing methods and design rules are not sufficient to obtain the adequate solution.

One of the most demanding concepts of Ferry Free project is crossing of Bjørnafjorden, located 30 km south of Bergen, which has a water depth of around 550m and width of nearly 5 km. To replace today's ferry connection, the crossing path is planned from an island called Svarvahelleholmen in the south to Søre in the north and that will ensure the great connection between two large Norwegian cities – Stavanger and Bergen. The wide distance between two shores makes it impossible to use conventional bridge concept for the fjord-crossing. Therefore, a floating bridge with a span of the cable-stayed part is chosen as a concept for the longest crossing proposed on The Coastal Highway Route E39-project.

1.2. Bjørnafjorden bridge concept

Various bridge concepts have been considered in the selection of the preferred design concept for Bjørnafjorden crossing and there are four existing design proposals:

Concept K11_07: Floating bridge consists of a straight cable-stayed bridge plus a curved floating pontoon bridge. The bridge is only anchored at two ends.

Concept K12_05: Floating bridge with similar shape as concept K11 but supported additionally by side mooring lines.

Concept K13_06: Straight floating bridge with both side anchorage and end anchorage.

Concept K14_7: Side-anchored floating bridge consists of a straight cable-stayed bridge plus a S-shaped floating pontoon bridge.

In this thesis, concept K12_05 is studied. Concept K12_05 presents a C-shaped floating bridge with a total arch length of 5530 meters. The bridge consists of two parts: a cable-stayed bridge which is built to provide the ships with an access to enter the fjord and the remaining is floating pontoon bridge.

Looking from the plan view, the southern cable-stayed bridge is straight, and the floating bridge is bent with an arch radius of 5000 meters. The curved shape design is applied to provide a higher stiffness in the transverse direction. Detailed information of the plane curvature is provided in the table below. The bridge is sectioned into many segments according to the road system. Each segment can be identified by two profile numbers, and the difference between profile numbers indicates the arch length of the segment in meter. The southern end of the

bridge has a profile number of 38530 and the northern end of 44060, which means that the arch length of the bridge in total is 5530 meters.

Table 1: Plan curvature

Profile number (m)	**38530 - 39310**	**39310 - 44060**
Plan curvature	Radius = ∞	Radius = 5000 m

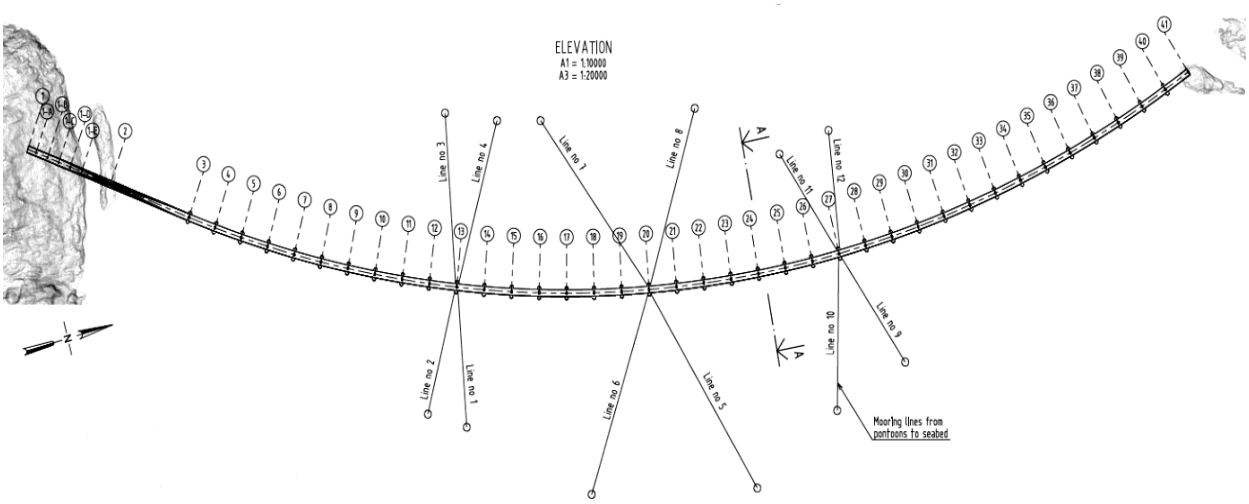

Figure 2: Plan view of Bjørnafjorden bridge - concept K12 [11]

The curvature and the elevation in the vertical plane vary along the entire bridge span. The bridge starts at an elevation of 66.662 meters above the mean sea level and ends at 11.615 meters. The varying curvatures of the southern part ensure a smooth transition from the high bridge to the low bridge.

Table 2: Vertical curvature and slope

Profile number (m)	**38530 - 39359.7**	**39359.7 - 40210.3**	**40210.3 - 40750.1**	**40750.1 - 43602.8**	**43602.8 - 44060**
Vertical Curvature	R = 35000m	S = -3.00%	R = 18000m	S = 0.00%	R = 16000

The southern cable-stayed bridge is held by a 220 meters height tower with 72 cables and the floating low bridge is supported by 38 steel pontoons with a spacing of 125 meters. Three pontons are mounted with side mooring lines as an additional support of the floating pontoon

bridge to increase the horizontal stiffness and to provide additional viscous damping. The 35 conventional pontoons without mooring lines are designed to have a draft of 5 meters while 7.5 meters draft is designed for the 3 moored pontoons.

1.3. Thesis description

The study of large floating structures exposed for considerable environmental loads is a very complex task. Therefore, a few simplifications have been made to complete this master thesis work within limited time period. The major simplification refers to hydrodynamic effects where the wave loads acting on pontoons were neglected. Furthermore, the cable-stayed bridge part was neglected in the bridge response analysis to speed up the simulation, and the low bridge part is still supposed to represent the global bridge behavior under wind loads.

The objective of this thesis work was 1) to construct the complete Finite Element Model of the structure in Abaqus and 2) to develop the wind load model as a subroutine in Fortran for Abaqus to simulate the wind-induced bridge responses and 3) to understand the bridge response under various wind conditions including the wind directionality, various mean wind spatial distribution and different wind field based on the design guidelines N400 and field measurements and 4) to find the dominant wind parameter that affect the bridge response through sensitivity study.

Over writing this thesis work following key steps were undertaken:

Chapter 1: Introduction on the Bjørnafjorden bridge project and basic information about the concepts for the fjord crossing proposed by The Norwegian Public Roads Administration are included. The chapter presents detailed information about the concept K12 which is a subject of this study and about its vertical and horizontal bridge profile.

Chapter 2: The beam theory and its application in Finite Element Methods that served as a basis for the modeling of beam elements in Abaqus software are described. The equation of motion of multi-degree-of-freedom systems and the eigenfrequencies of the structure as a significant part of structural engineering are presented. Mass and stiffness matrices for Rayleigh viscous damping and graphical representation of their combination are also included.

Chapter 3: Finite Element Model of the Bjørnafjorden bridge in Abaqus along with assumptions made is presented. Determination of the global coordinates due to variable curvature along the vertical and horizontal plane are described, as well as the input file building process for Abaqus

software with cited commands from [12]. The detailed information about dimensions, properties and functions of the elements that the whole structure consists of are presented. Verification of the loads with attached screenshots of the model from Abaqus illustrating the process of achieving the static equilibrium for cable-stayed and floating part of the bridge are included.

Chapter 4: Applicable theory related to aerodynamic effects as the wind loads is the subject of major interest in this chapter. The mean wind speed as well as wind turbulence single point statistics and coherence parameters are seduced. Some parts are presented in detail such as important buffeting wind theory. The chapter contains the graphical representation of instantaneous wind flow and displacements of the cross-section due to the turbulent wind. Chapter 4.3 provides information of how the dynamic wind field is generated in MATLAB. The FORTRAN subroutines describing the wind loads acting on the structure in global coordinates are discussed in Chapter 4.4.

Chapter 5: The results on the eigenfrequency of the model with and without mooring lines from the modal analysis of the low bridge are discussed.

Chapter 6: The presentation of the low bridge response under various static wind conditions are presented and discussed.

Chapter 7: The dynamic response of the low bridge is presented and discussed.

Chapter 8: The sensitivity study on of the A parameters in wind spectra and C parameters in wind coherence on the bridge response is presented and discussed.

2. Structural modeling theory

2.1. Beam theory

The Euler-Bernoulli is the classical theory to describe the deformations of the beam under axial forces and bending. It assumes that the cross section of the beam is perpendicular to the neutral axis, that the plane section remains the same before and after deformation and that the deformed beam angles are very small. On the other hand, the Timoshenko theory is an extended version of Euler-Bernoulli and it says that the deformed cross-section is not necessarily perpendicular to the neutral axis.

The major difference between two theories is that Timoshenko takes shear deformation into account in determining the flexural behavior while Euler-Bernoulli assumes shear deformations to be negligible. In the Timoshenko beam theory plane cross sections stay plane but no longer normal to the longitudinal axis. The shear deformation is the distinction between the normal to the longitudinal axis and the plane cross section rotation. Mathematically, the fundamental difference is that the Euler-Bernoulli theory requires increased order of parametric continuity in comparison to the Timoshenko beam theory. The first one is mostly applied for beams which are thin when the other one for thick members. The reason for that is that shear deflections are comparatively small for long thin beams and so the results show little difference in such cases. When beams are short and thick and the material shear modulus is low, the difference becomes noticeable as the shear deflections become more important.

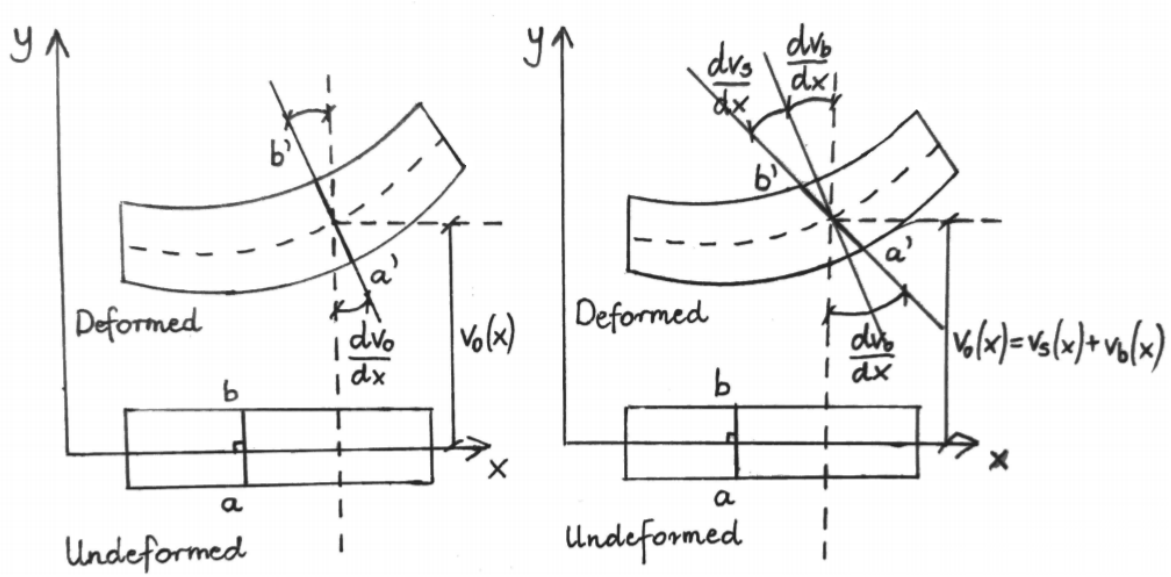

Figure 3: Representation of two beam theories (left column: Bernoulli; right column: Timoshenko)

The relations presented on the picture above shows that when the cross section deforms in the Euler-Bernoulli theory, the rotation occurs only due to bending $\frac{dv_o}{dx}$ as the plane section remains normal to the longitudinal axis. While in Timoshenko theory the cross-section deformation consists of bending part, $\frac{dv_b}{dx}$, and shear deformation part, $\frac{dv_s}{dx}$ [8].

2.2. Beam theory in Finite Element Method

To perform finite element analysis of the structure the beam members are idealized as a group of one or more finite elements. The number of elements is determined to represent the continuous structure with sufficient accuracy. The most common 3D beam elements have two end nodes and six degree of freedom per node: three translations and three rotations.

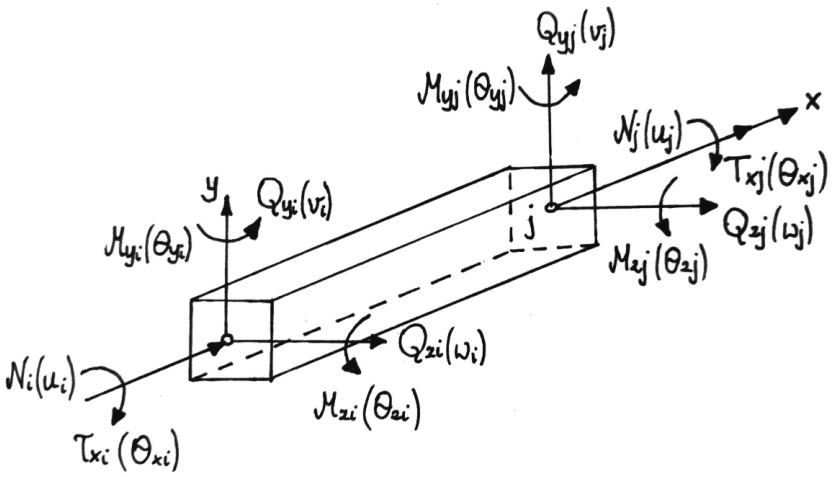

Figure 4: 3D beam element

The rotation of the cross section in Euler-Bernoulli theory is same as the rotation ψ of the longitudinal axis when in Timoshenko beam that is the difference $\bar{\gamma} = \psi - \theta$ which defines the mean shear deformation. As a result, the second model is more complex but in finite element models are easier to build.

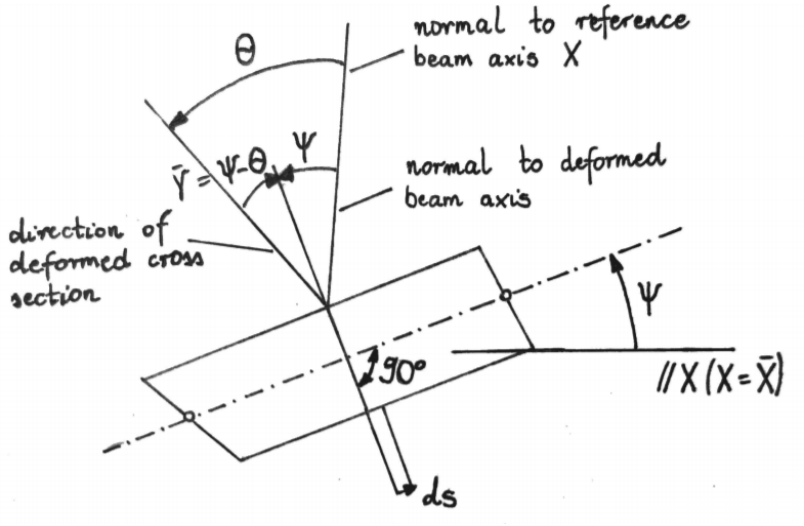

Figure 5: Total section rotation θ and Euler-Bernoulli section rotation ψ in the Timoshenko beam model

The Euler-Bernoulli model is named by C^1 beam due to its continuity attained in the longitudinal direction when Timoshenko model is named by C^0 beam because of transverse displacement and rotation, preserve C^0 continuity. In C^1-continuity conditions, cubic shape functions are used to determine the transverse displacement. The interpolation of the Euler-Bernoulli beam elements uses cubic interpolation functions.

2.3. Assembly of elements

The procedure of assembling the elements is to obtain the equations for the complete set of elements that describes the structure. Each structure node is a connector to which elements are attached. The loads acting at node due to preliminary stress, deformation of the element or external forces produces set of equations which must satisfy the equilibrium.

$$\sum_{i=1}^{N_{els}} \{r\}_i + \sum_{i=1}^{N_{els}} \{r_e\}_i + \{P\} = \{0\} \tag{2.1}$$

Where $\{r\}$ are the loads acting at nodes of the element from element deformation, equal to: $\{r\} = -[k]\{d\}$ and from sources other than element deformation $\{r_e\}$ and external loads $\{P\}$.

2.4. The equation of motion of multi-degree-of-freedom systems

Most of the engineering structures as a continuous system with complex geometry is often for simplicity of analysis approximated as multi-degree-of-freedom system where there is one equation of motion for each degree of freedom. The floating structure dynamic behavior under the environmental loads can be modeled by a system of equation where a force $F(t)$ acts on viscously damped spring-mass system described by the following equation of motion:

$$m\ddot{x} + c\dot{x} + kx = F(t) \tag{2.2}$$

where m represents the structural mass, c and k is the linear damping and spring coefficient, respectively, x is the displacement of the mass and $F(t)$ is the external force applied to the bridge structure.

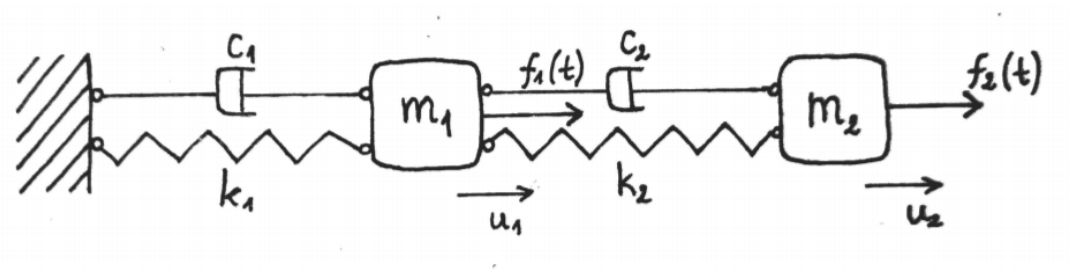

Figure 6: Multi-degree-of-freedom system

The number of eigenvalues is same as the number of degrees of freedom and each of eigenvalue has a corresponding mode shape called the eigenmode. During oscillation of the structure at some frequency, the shape of the deformation is that of the corresponding eigenmode. For damped systems, there is a cross-coupling between eigenmodes so that the transference of energy occurs between various modes during vibration. Furthermore, the orthogonal modes are built when there is a linear combination made up between different modes of vibration. The Rayleigh damping is the most convenient configuration of damping matrix which retains the orthogonality properties.

2.5. Eigenfrequency

Eigenfrequency basically means the “characteristic” frequency in the sense of the frequency that characterizes the system, the frequency that is natural or characteristic of the system. When vibrating at a certain eigenfrequency, a structure deforms into corresponding shape, the

eigenmode. Establishing the eigenfrequencies of a structure is a significant part of structural engineering. Natural frequency at which a system tends to oscillate in the absence of damping force with mass m and spring stiffness k:

$$\omega_n = \sqrt{\frac{k}{m}} \tag{2.3}$$

Resonant frequency occurs when the given system due to external force oscillates at the frequency at which the response amplitude is the highest.

From a study of the damped system, the damped natural frequency is lower than ω_n:

$$\omega_d = \omega_n\sqrt{1-\zeta^2} \tag{2.4}$$

Where ζ is a damping coefficient which is described as the ratio of the damping constant c to the critical damping constant $c_c = 2m\omega_n$:

$$\zeta = \frac{c}{c_c} \tag{2.5}$$

A long beam under tension will behave similarly to vibrating string. Thus, the eigenfrequencies of the individual mode shapes are defined by:

$$\omega_{s,n} = \frac{n\pi}{l}\sqrt{\frac{T}{m}} \qquad where\ n = 1,2,3,\ldots \tag{2.6}$$

where T is the tension in the string, l is the length of it, m is mass per unit length and n is the number of the mode shape.

2.6. Rayleigh damping

The dissipation of energy known as damping is one of the essential aspects in structural engineering which ensures that the system endure stability and prevents the failure of the structure. One of the most common viscous damping mechanisms used to solve finite element problems is Rayleigh damping [1], also called as classical damping. It expresses the damping as a linear combination of mass and stiffness matrices, that is:

$$C = \alpha M + \beta K \tag{27}$$

In given equation M and K are mass and stiffness matrices respectively while α and β represent mass and stiffness proportional damping coefficients.

The damping ratio for the nth mode of system is described as:

$$\xi_n = \frac{\alpha}{2\omega_n} + \beta\frac{\omega_n}{2} \tag{2.8}$$

It can be observed that the achieved damping ratio ξ varies with response frequency. The mass proportional term is inversely proportional to response frequency and is a dominant when lower frequencies occur. While the stiffness proportional damping is linearly proportional term which dominates at the higher frequencies.

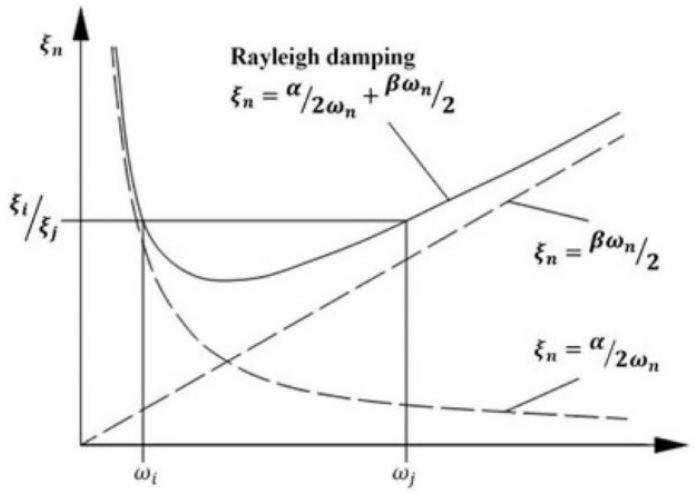

Figure 7: Graphical illustration of Rayleigh damping [1]

In order to obtain α and β coefficients two reference vibration modes are chosen and their damping ratios ξ_1 and ξ_2 at their two eigenfrequencies ω_1 and ω_2:

$$\xi_{1,2} = \frac{\alpha}{2\omega_{1,2}} + \beta\frac{\omega_{1,2}}{2} \Longrightarrow \alpha, \beta \tag{2.9}$$

3. Bridge modeling

Numerical modelling of the bridge is developed in the finite element method software Abaqus. Abaqus allows the user to model the structure using a graphical interface, but one can also create the model by writing an input file (*.inp). This feature gives the user more flexibility, especially when it comes to large structures like Bjørnafjorden bridge where thousands of nodes and elements will be involved. Software MATLAB is used to construct the input file which is presented in the Appendix D.

3.1. Abaqus consistent units

ABAQUS does not have built-in units itself, hence the user has the flexibility to choose a unit system which should be consistently used throughout the modeling process. SI unit system is followed in this thesis:

- Length in m
- Force in N
- Mass in kg
- Density in kg/m^3
- Stress in N/m^2
- Time in s

3.2. Coordinate system

Coordinate of the bridge and forces applied to the model are defined according to the global coordinate system which follows the right-hand rule and is presented in Figure 8.

Origin of the model is located at the southern end of the bridge, hence the first girder node has x- and y-coordinate equal to zero. The x-coordinates of the model are all positive values since the x-axis is pointing to the north while y-coordinate is positive in the west and z-axis is pointing upwards.

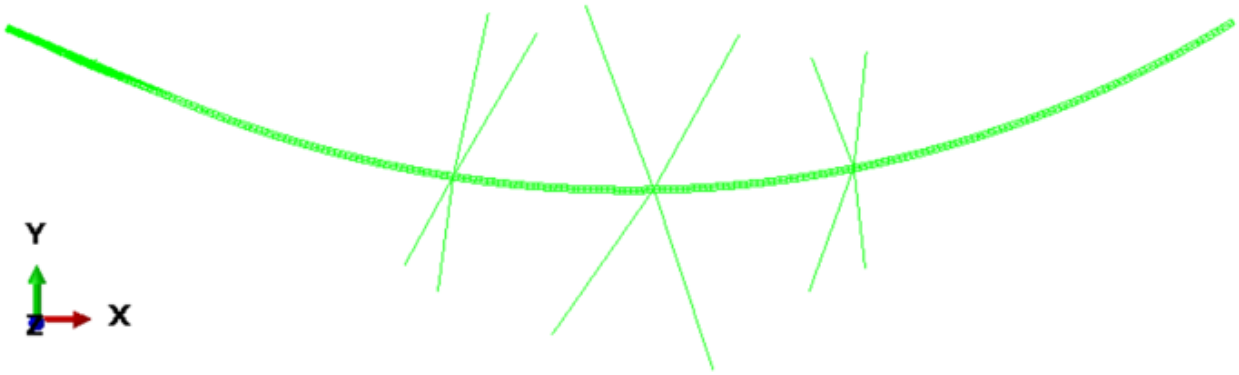

Figure 8: Global coordinate system

3.3. Local orientation

Most of the elements are defined as beam elements. The section orientation of a beam element is specified by a local axis system (t, n_1, n_2), where t represents the tangential axis of the element. The tangential axis is defined when the two nodes of the element are specified. When the n_1-axis is specified by the user, Abaqus will generate the n_2-axis as the cross product of the n_1-axis and t-axis. Abaqus applies default direction (0, 0, -1) if the orientation is not defined.

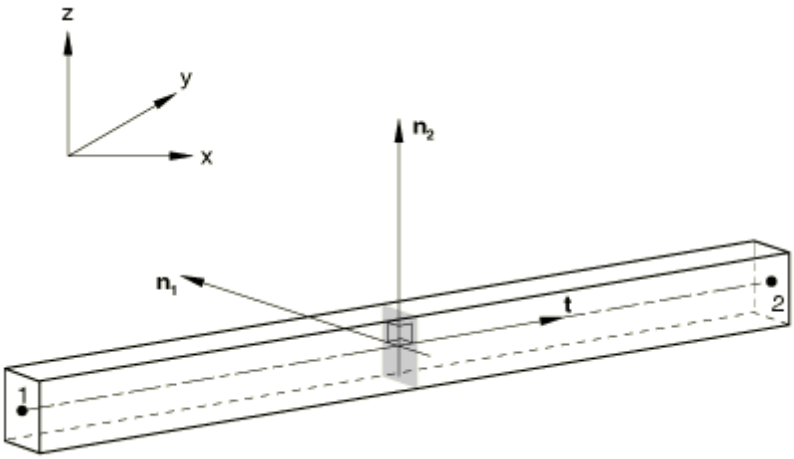

Figure 9: Local axis of a beam element [23]

3.4. General modeling procedure

Modeling starts with defining the number of nodes and the coordinates of nodes according to the geometry of the structure. The nodal coordinates are specified in the input file by using keyword *NODE:

* NODE

Girder node number, x, y, z

The nodes are then connected by elements through using keyword *ELEMENT. Cross sectional properties are assigned using keyword *BEAM SECTION GENERAL:

* ELEMENT, TYPE=xx, ELSET=name of element set

Element number, first node number, second node number

* BEAM SECTION GENERAL, ELSET=name of element set, DENSITY=xx, SECTION=GENERAL

Area, I_{11}, I_{12}, I_{22}, J

The boundary constraints are defined using the command *BOUNDARY. The static and dynamic analysis are performed in the section *Steps. A general procedure of modeling is summarized in the chart below:

Figure 10: Flow chart of modeling general procedure

3.5. Girders

Concrete girder (Figure 11), which has higher torsional stiffness and moment of inertia compared to steel girder (Figure 12), is used to build the first 265 meters of the southern cable-stayed bridge. The remaining girder cross sections are built out of steel.

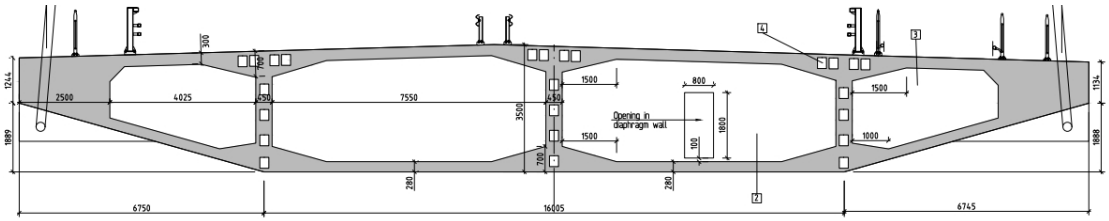

Figure 11: Cross section of concrete box girder [11]

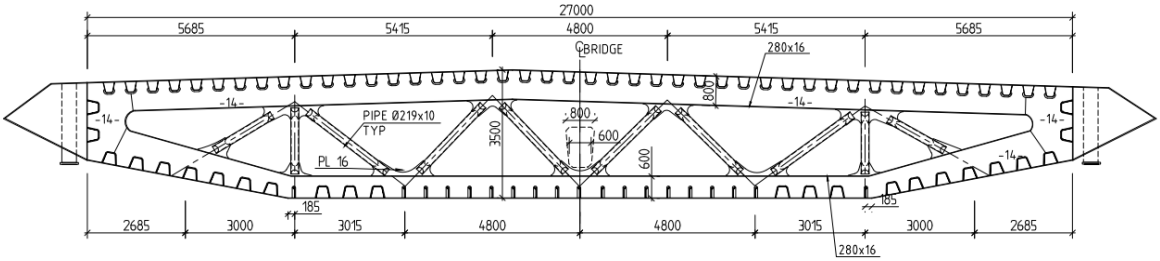

Figure 12: Typical cross section of steel box girder [11]

Each girder cross section is modeled using one girder node and three link nodes. The function of the link nodes is to provide the cross section with right mass moment of the inertia and to take the overturning moment from the wind. The overturning moment is applied to the link element as a pair of parallel forces when using the subroutine *DLOAD, which is explained in detail in Chapter 4.4.2. By connecting the four nodes, each girder cross section is lumped into a rigid body through keyword *RIGID BODY. The reference node which governs the motion of the entire rigid body is defined as the center girder node of the cross section. Girder mass is attached to link nodes as a mass point. To ensure the correct cross-sectional mass moment of inertia, the mass must be distributed to each link node following three criteria:

- correct total mass
- correct cross-sectional mass moment of inertia
- correct location of center of gravity

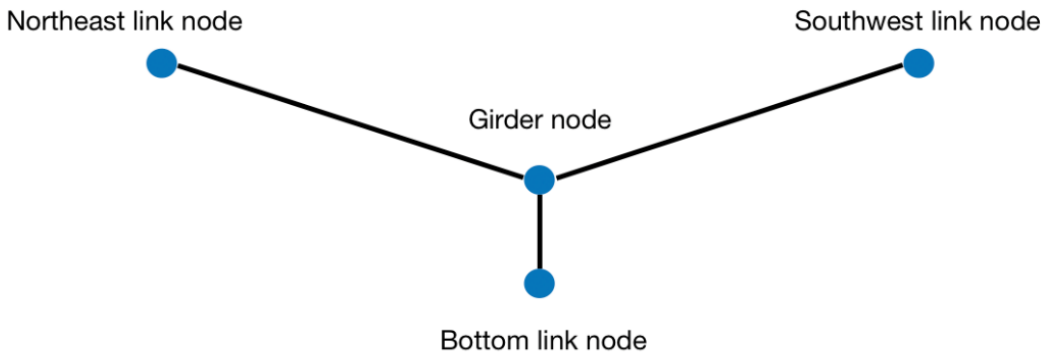

Figure 13: Girder cross section

As it is shown in Figure 14, the length of the girder elements increases along the bridge span. A relatively short element length, 5 meters, is chosen for the first segment considering both the spacing between columns (15 meters) and the spacing between cable anchor points (10 and 20 meters) in the side span of cable-stayed bridge. However, element length of 5 meters is relatively short and will result in more than one thousand girder nodes if adopted for the entire bridge span. This may further give a huge number of data in the analysis stage which will increase the complexity in data processing. Therefore, larger element length is used in the next two segments.

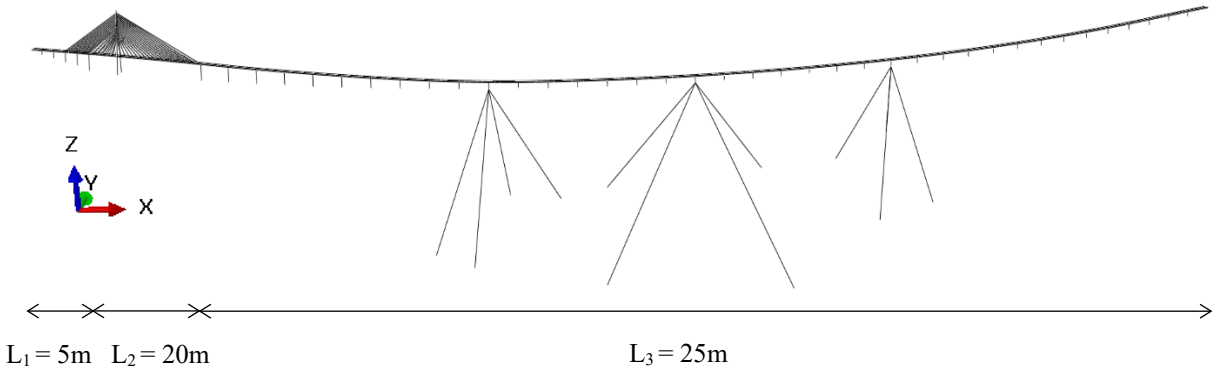

Figure 14: Girder elements length (L_1, L_2, L_3 – element length chosen for the corresponding part of the structure)

The varying curvature and slope of the bridge makes the calculation of the global coordinates of the girder nodes a challenging task. The basic idea is that an arch can be approximated

numerically by straight lines connecting successive points on the arch. Take an arch of radius R for example:

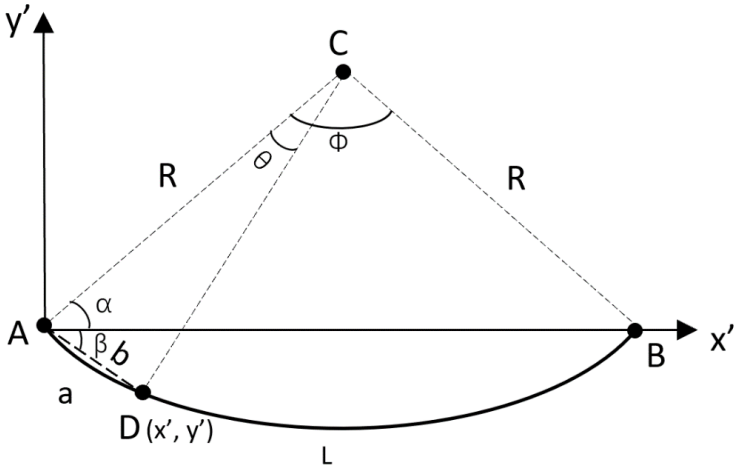

Figure 15: Determination of an arch by numerical method

where:

- L is the arch length of arch AB with radius R
- a is the arch length of arch AD
- b is the length of straight-line AD

Useful relationships:

1. From arch length formula: $L = \Phi * R$, hence angle $\Phi = \frac{L}{R}$
2. Again, from arch length formula: $a = \theta * R$, hence angle $\theta = \frac{a}{R}$
3. For triangle ABC: $2\alpha + \Phi = \pi$
4. For triangle ACD: $2(\alpha + \beta) + \theta = \pi$
5. From relationship 4. and 5. angle β can be calculated as: $\beta = \frac{\Phi - \theta}{2}$
6. For triangle ACD again has: $b = 2R \sin\frac{\theta}{2}$

With this method, nodal coordinates on the curve can be determined by iterative process. Note that these calculated coordinates are local coordinates only, meaning that a transformation from the local coordinate (x', y') to the global coordinate (x, y) is required.

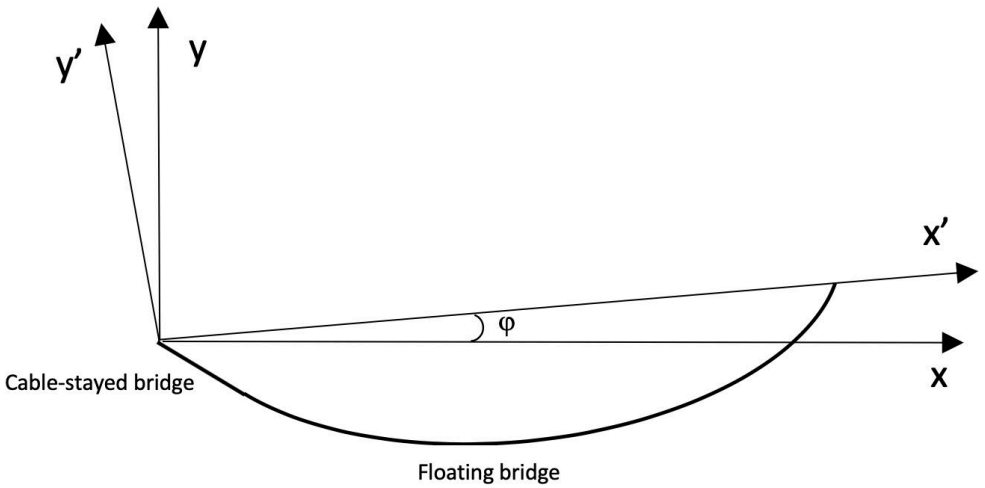

Figure 16: Local coordinate system (x', y') and global coordinate system (x, y)

Bridge side view and plan view, which are constructed using the coordinate results from the MATLAB, are shown in figures below.

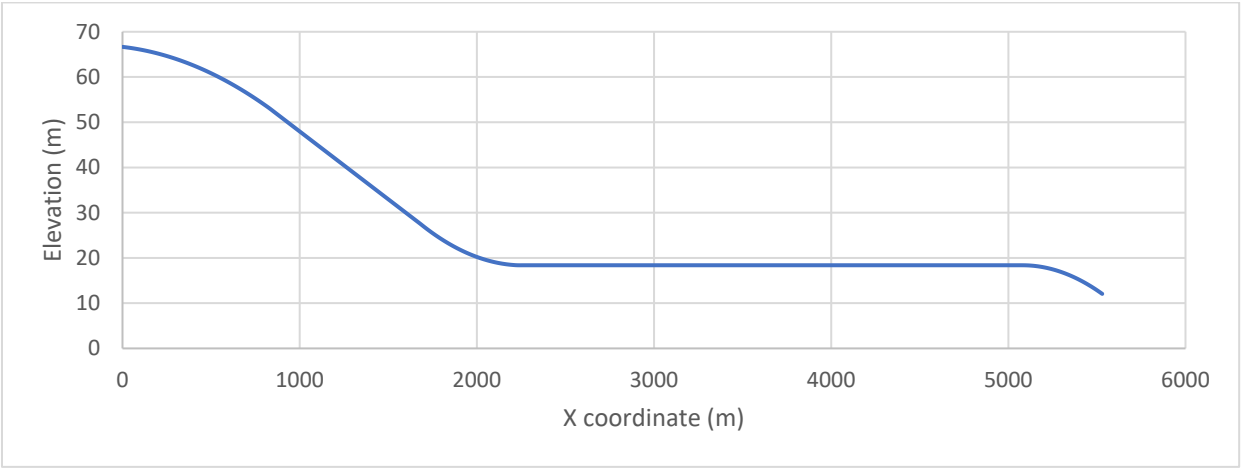

Figure 17: Side view of the bridge

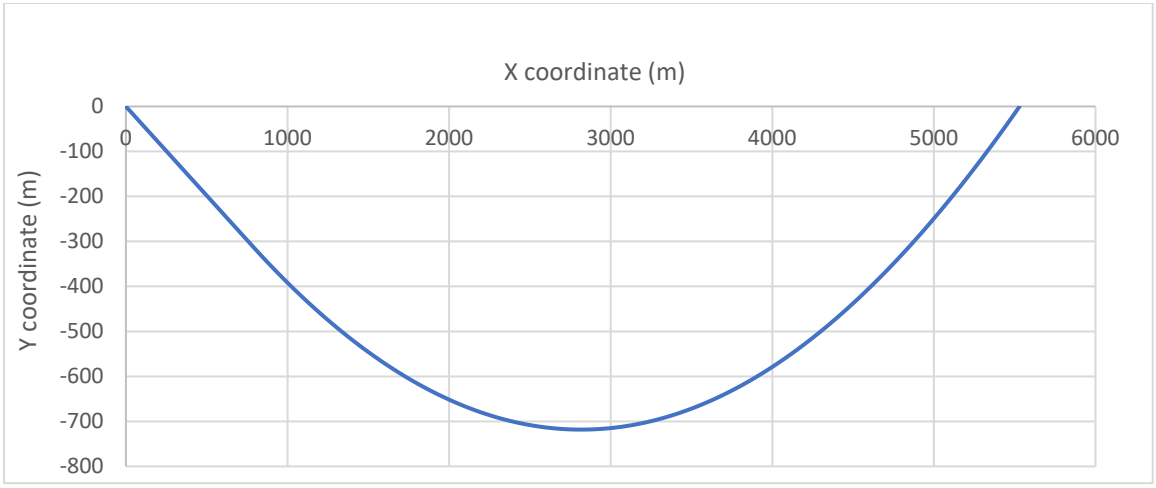

Figure 18: Plan view of the bridge

Girder elements and link elements are modeled as B31 beams. B31 refers to a 3D beam which utilizes linear interpolation. B31 belongs to Timoshenko formulation, which has been discussed in Chapter 2 that the Timoshenko theory takes the shear flexibility into account and can be applied to both thick beams and slender beams. The orientation of the girder elements varies from element to element following the local curvatures and slopes of the bridge. The bending and torsional stiffness are applied to the center beam element. Link elements are modeled with similar properties but with very small Young's modulus and shear modulus and hence will not give additional structural stiffness. The modeled structural properties of the girder element is presented in Table 3.

Table 3: Structural properties of the girder element

	Concrete girder	**Steel girder**
Density (kg/m)	79100	19000
Cross-sectional area (m^2)	27.95	1.88
Moment of inertia about strong axis I_{11} (m^4)	40.50	121.83
Moment of inertia about weak axis I_{22} (m^4)	2138	3.79
Torsional constant J (m^4)	135.40	12
Young's modulus E (Pa)	29 764 000 000	210 000 000

The dummy elements which are created in order to bind each girder cross section into a rigid body are connected by two end link nodes. There are three sets of them: northeastern, southwestern and bottom as it is presented in the Figure 19. Furthermore, the dummy elements

are modeled the same way as girder elements indicating B31 beam as Timoshenko beam formulation, as well as density is set to very small value and hence will not contribute to any additional structural weight. Moment of inertia and torsional constant are set into the high values which provides the element with high bending and torsional resistance:

- Area: 1000 m^2
- Moment of inertia for bending about the 1- and 2-axis: 1000 m^4
- Torsional constant J: 1000 m^4

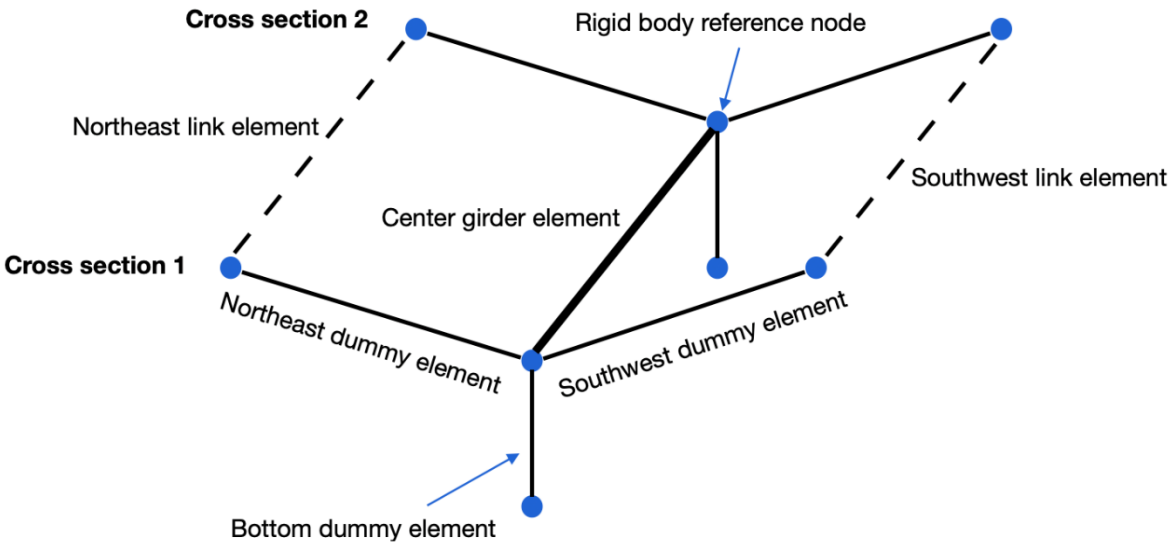

Figure 19: Graphic representation of two girder cross sections

3.6. Cables

There are 36 pairs of steel cables which support the tower and the bridge deck at the cable-stayed bridge. At the back span, the cables are anchored at 10 and 20 meters spacing, and the spacing is 20 meters at the main span side.

Cables composed of multiple strands with diameter 15,7 millimeters each and high tensile strength of 1860 MPa are used in this design where the desired cable cross-sectional area is relatively large. The cables are modeled as B31 elements with individual structural properties each. Area moments of inertia are calculated based on the cross-section diameter information provided by the Norwegian Pubic Roads Administration [11].

The effective Youngs modulus is used due to the variable shape and stress condition of the cables and is evaluated by the Ernst's formula [2]:

$$E_{eff} = E_0 \frac{1}{1 + \frac{\gamma^2 L_h^2 E_0}{12\sigma^3}} \tag{3.1}$$

where E_{eff} is the effective Youngs modulus, E_0 is the elastic modulus without the sag effect, γ is the weight of the cable material, L_h is the projected cable length in a plan and σ is the axial stress of cable.

The cables are pre-tensioned in purpose to carry the dead loads on the high bridge. The tension force in each cable can be verified through a simple equilibrium check that the vertical component of the cable tension balances the self-weight of the corresponding girder segment.

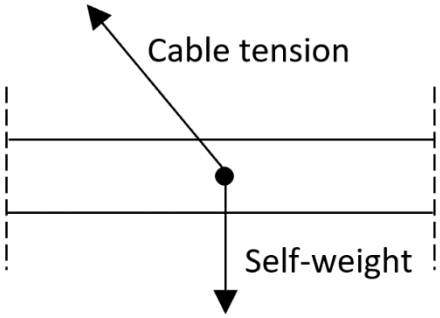

Figure 20: Forces on one girder segment

The cable pre-tension is applied as a temperature load in Abaqus based on the equation:

$$P = E \cdot A \cdot \alpha \cdot \Delta T \tag{3.2}$$

where P is the temperature loading, E is Young's modulus, A is cable cross-sectional area, ΔT is the temperature difference and α is thermal coefficient, which is defined for each cable under the keyword *BEAM SECTION GENERAL:

* BEAM SECTION GENERAL, ELSET=name of element set, DENSITY=xx, SECTION=GENERAL

Area, I_{11}, I_{12}, I_{22}, J

cos<$\overrightarrow{n_1}$, x>, cos<$\overrightarrow{n_1}$, y>, cos<$\overrightarrow{n_1}$, z>

where the three cosine values define the orientation of the beam element and they are calculated by considering the angles between the first local normal axis n_1 and the global axis X, Y and Z respectively.

3.7. Tower

Bridge loads in the cable-stayed part are mainly carried by a concrete tower which has a height of 220 meters. The tower consists of two concrete legs and one concrete cross beam. The cross-sectional area of tower legs decreases gradually from foundation to the top crown. The concrete tower is fixed in all DOF at the foundation. Since the cross-section property of two tower legs varies along the leg span, several nodes are defined at different elevations. The tower elements are modeled using beam B31 elements. The side and front view of the tower is presented in Figure 21.

Tower material properties:

- Density: 2650 kg/m^3
- E-modulus: 29 764 000 000 Pa

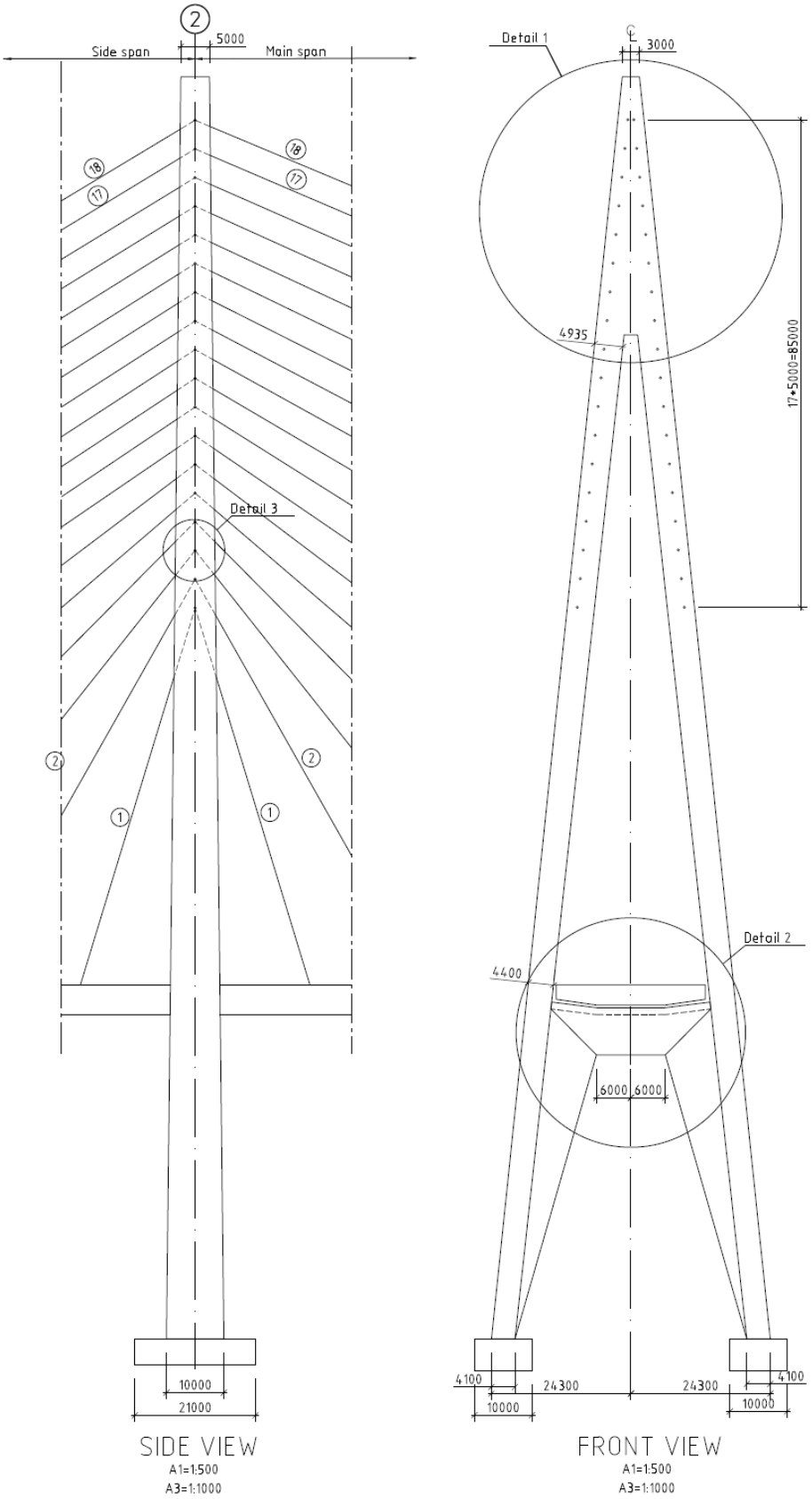

Figure 21: Side and front view of the tower [11]

3.8. Columns and pontoons

The cable-stayed bridge is supported by five concrete columns which are fixed in all DOF at ground. The floating bridge is supported by 38 columns carried by steel pontoons every 125 meters. The pontoons are designed to have a kayak shape which presents good response ability in the 100-year extreme wind condition [2]. The figure below which illustrates the local coordinate of the pontoon structure is provided by Norwegian Public Roads Administration [2].

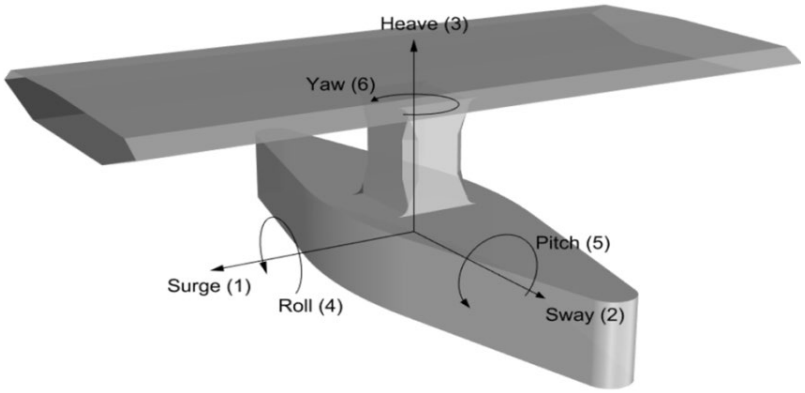

Figure 22: Pontoon with local coordinate system

Columns are modeled as one beam element using two nodes, the top column node shares the same node as the link bottom node. Four nodes are used to create the pontoon structure as shown in the Figure 23. The top pontoon node shares the same node of column bottom. Second node is modeled at the center of gravity. The third node is placed at the center of buoyancy which is calculated based on the value of the draft. The draft for pontoons attached with mooring lines and pontoons without mooring lines are 7.5 meters and 5 meters, respectively.

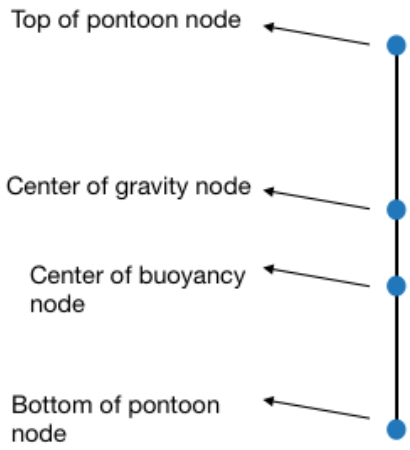

Figure 23: Pontoon nodes

Column nodes in the low bridge as well as pontoon nodes are connected by B31 beam element. Additionally, the pontoons are modeled by beam elements of very small density and the structural weight of them is assigned to the center of pontoon gravity as a point mass through mass element.

The hydrodynamic effects of the environment are of major interest in the analysis of the floating bridge. And a significant aspect in developing the numerical model of the floating structure is to consider the hydrodynamic properties of the pontoons which are intended to be subjected to wave loads. However, only the buoyancy and hydrostatic stiffness are considered in this thesis. The wave excitation force and hydrodynamic damping effect are neglected. Buoyancy was officially documented when Archimedes (287-212 B.C.) discovered that any body submerged in a fluid at rest is acted upon by buoyant force of magnitude equal to the weight of the displaced fluid. Essentially, a structure will not float if the sum of the vertical downward forces is greater than upward buoyancy force. Multiplying the volume of fluid by the density of the fluid, ρ, gives the mass of the displaced fluid.

$$F_b = \rho \cdot V_{disp} \cdot g = m_{disp} \cdot g \tag{3.3}$$

Floating bridge with few fixed supports depends mostly on pontoons and mooring systems, where buoyancy force balances the dead loads such as girder weight, column and pontoons including the ballast. The center of buoyancy, which is the centroid of the displaced volume of the fluid, together with center of gravity define the hydrostatic stability.

The loaded floating object is susceptible for translational and rotational movements and it has following six degrees of freedom:

1. Surge – moving forward and backward on the X-axis
2. Sway – moving left and right on Y-axis
3. Heave – moving up and down on the Z-axis
4. Roll – rotation about longitudinal X-axis
5. Pitch – rotation about transverse Y-axis
6. Yaw – rotation about vertical Z-axis

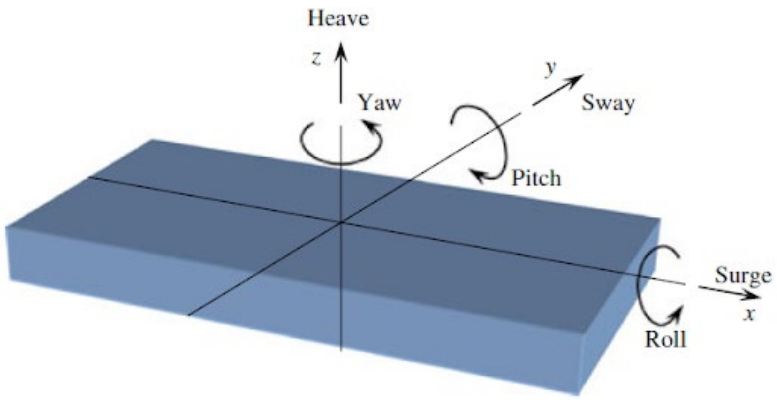

Figure 24: Types of motion of the floating structure [10]

The pontoons act as springs and provide stiffness in the heave, roll and pitch directions. Pontoon stiffness is applied to the center of buoyancy through defining a spring element. The element type SPRING1 means that the element is connected between a node and the ground while SPRING2 should be used if the element connects two nodes. In studied model the type SPRING1 is considered.

* ELEMENT, TYPE=SPRING1, ELSET=name of element set

Element number, node number

Additional mass called ballast is attached to each pontoon to ensure that the floating bridge is in static equilibrium and hence the deflection is controlled. The calculation of the ballast is based on the assumption that each pontoon has the ability to carry the total structural weight of 125 meters span:

$$\rho V = m_{girder} + m_{column} + m_{pontoon} + m_{ballast} \tag{3.4}$$

where ρ is the water density, V is the displaced water volume, m_{girder} is the weight of the girder with span length of 125 meters, m_{column} is the weight of the column, $m_{pontoon}$ is the self weight of the pontoon and $m_{ballast}$ is ballast weight.

Due to the curved geometry of the bridge, a local coordinate system must be defined for each pontoon, this is achieved by using keyword *ORIENTATION. The stiffness could be therefore attached to each pontoon in the correct direction.

* ORIENTATION, NAME=name of the orientation

$x_a, y_a, z_a, x_b, y_b, z_b, x_c, y_c, z_c$

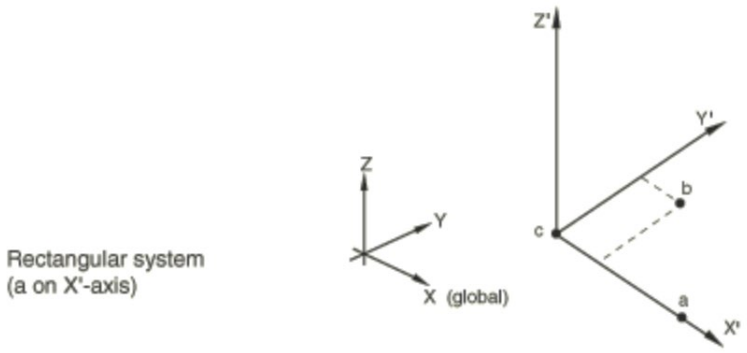

Figure 25: Graphic presentation of system orientation [12]

The pontoon properties are shown in the table below.

Table 4: Pontoon properties

	Moored	**Classical**
Mass (ton)	1540	985
Height (m)	11	8.5
Width (m)	14.9	14.9
Draft (m)	7.5	5
Center of gravity (m)	-2	-0.75
Center of buoyancy (m)	-3.75	-2.5
Stiffness C33 (KN/m)	7460	7459
Stiffness C44 (KN/m)	1559600584	1565995.59
Displaced volume (m^3)	5704.72975	3803.02675
Ixx (ton m^2)	415000	252160
Iyy (ton m^2)	63800	33135
Izz (ton m^2)	430000	252160

3.9. Mooring system

Out of 38 pontoons, three are connected to the four side mooring lines each. The three moored pontoons are the 11th pontoon at arch position 2030 meters, pontoon 18th at 2905 meters and pontoon 25th at 3780 meters. The side mooring lines provide the bridge with improved ability of load capturing, additional restoring stiffness and viscous damping. The horizontal stiffness is effective when the mooring lines are correctly pretensioned. Pretension is applied as temperature load to the mooring lines by the same method used to pretension the cables. The

pretension forces follow the values provided by the Norwegian Public Roads Administration [13] and are listed in Table 5. The bottom end of the mooring lines is anchored to the seafloor while the top chain is connected into the floating pontoons. The mooring line numbering system is shown in the Figure 26.

Table 5: Mooring line pretension

Line number	**1**	**2**	**3**	**4**	**5**	**6**	**7**	**8**	**9**	**10**	**11**	**12**
Pretension (MN)	1.98	2	2.08	1.9	2.59	2.28	2.54	2.63	2.17	1.69	2.09	2.04

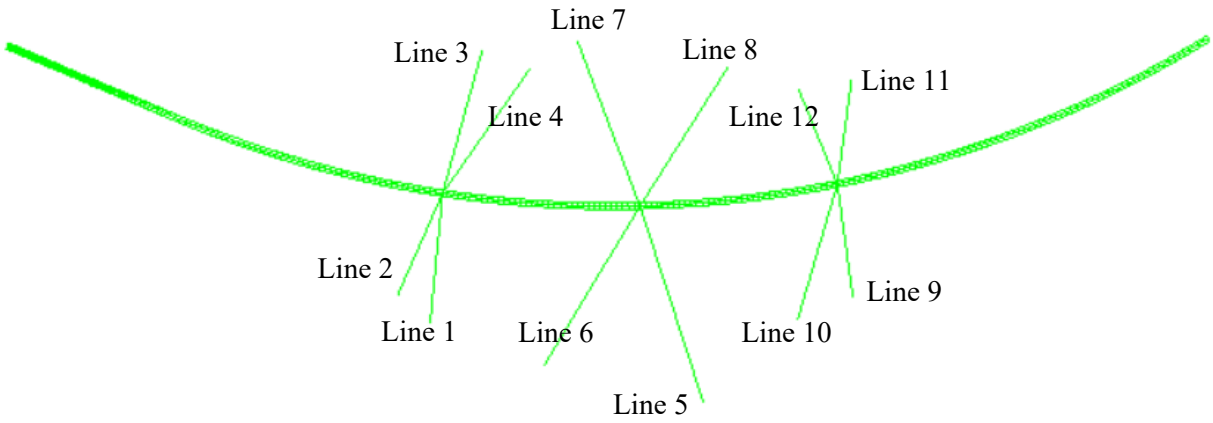

Figure 26: Mooring line numbering

Each mooring line consists of three segments:

- Segment 1: top chain with outer diameter of 0.2641 meter
- Segment 2: middle steel wire with outer diameter of 0.146 meter
- Segment 3: bottom chain with outer diameter of 0.2641 meter

Mooring lines are modeled using B31 elements with structural properties listed in the Table 6.

Table 6: Mooring line parameters

	Outer diameter (m)	Area (m^2)	E (Pa)
Steel wire	0.1449	0.01649	6.1E+10
Chain	0.2641	0.05478	3.15E+10

3.10. Boundary conditions

Boundary conditions applied to the full bridge model are shown in blue and orange colors referring to Figure 27 and Figure 28. Two bridge ends, tower leg and back column foundations as well as mooring lines anchors are fixed in all 6 degree of freedom.

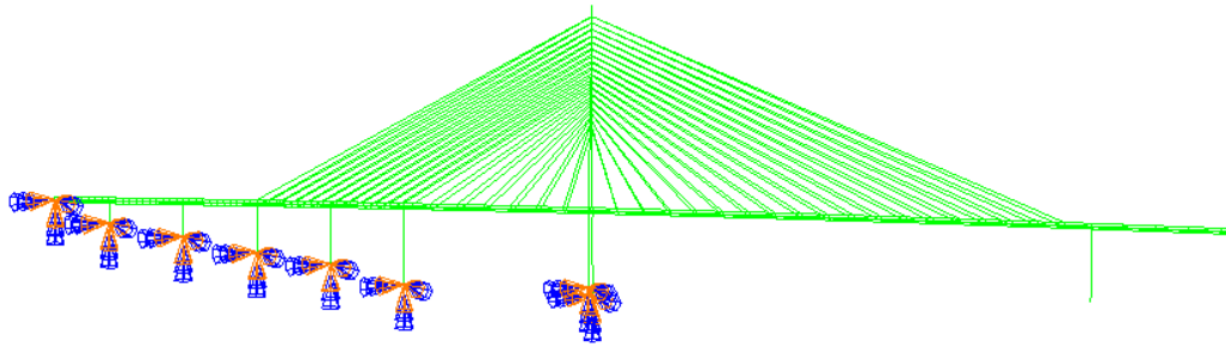

Figure 27: Boundary conditions on cable-stayed bridge model

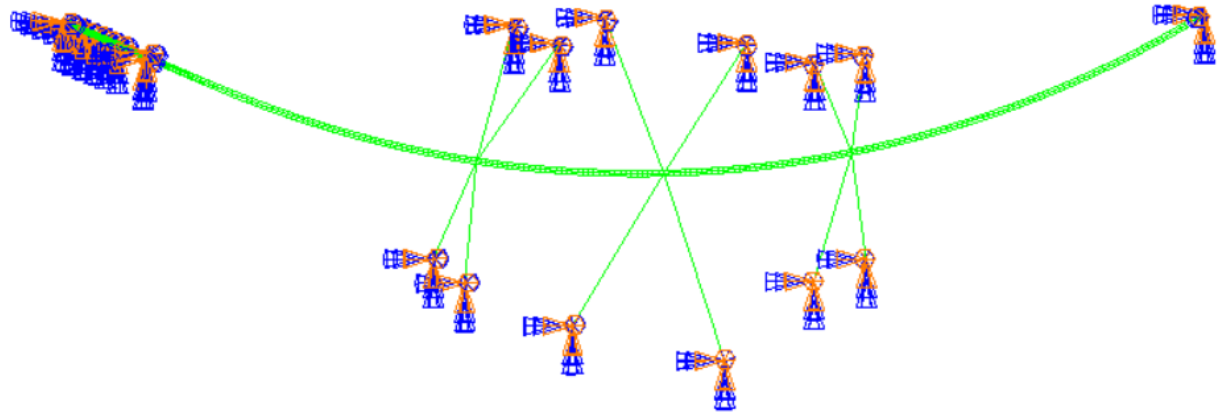

Figure 28: Boundary conditions on plan view

3.11. Steps

The steps and analysis performed are explained as below.

Predefined field: An initial temperature field is defined.

Step 1 (static): The first step is to apply gravitational forces on bridge girders. Cables and mooring lines are removed from the model in this step.

Step 2 (static): Gravitational forces are applied to cables, columns, pontoons and tower. As it is mentioned previously, the pretension is applied to cables and mooring lines by means of a temperature load. This method is followed by a challenge that correct pretension can be achieved only when the structure is in the original undeformed shape before the temperature loading is attached. Therefore, several concentrated loads are introduced to balance the structure. For the cable-stayed bridge, concentrated loads are applied at cable anchor points to balance the gravitational forces, see Table 7. For the low bridge, vertical component of the resultant mooring pretensions is applied to the corresponding pontoon, which are listed in the Table 9.

Step 3 (static): Buoyancy forces are applied to the model. Mooring lines and cables are added back to the model when the model is in the static equilibrium state.

Step 4 (temperature): The temperature difference is considered.

The following analysis are performed in separate runs after the static equilibrium is obtained.

Modal analysis (without aerodynamic load): To obtain eigen-frequencies and mode shapes of the bridge. In this stage, no aerodynamic load is applied.

Static analysis: To examine the bridge response under static wind.

Modal analysis (with static wind load): To obtain eigen-frequencies and mode shapes of the bridge when static wind load is included.

Dynamic analysis: To study the bridge response under dynamic wind load. One-hour simulation is performed with time increment of 0.05 second.

3.12. Static equilibrium check of the bridge model

The cable-stayed bridge model and low bridge model are checked for static equilibrium separately.

Cable-stayed bridge model

Forces applied to the model in the analysis step 1 are listed in the table below. Two ends of the model are fixed at 6 degrees of freedom.

Table 7: Loadings on the cable-stayed bridge

Cable ID (Side span)	***Cload (N)**	**Girder mass (kg/m)**	**Segment length (m)**	**Cable ID (Main span)**	*** Cload (N)**	**Girder mass (kg/m)**	**Segment length (m)**
1	3879855	79100	10	1	1863900	19000	20
2	3879855	79100	10	2	1863900	19000	20
3	3879855	79100	10	3	1863900	19000	20
4	3879855	79100	10	4	1863900	19000	20
5	3879855	79100	10	5	1863900	19000	20
6	3879855	79100	10	6	1863900	19000	20
7	3879855	79100	10	7	1863900	19000	20
8	3879855	79100	10	8	1863900	19000	20
9	3879855	79100	10	9	1863900	19000	20
10	3879855	79100	10	10	1863900	19000	20
11	3879855	79100	10	11	1863900	19000	20
12	2871878	79100	15	12	1863900	19000	20
13	1863900	19000	20	13	1863900	19000	20
14	1863900	19000	20	14	1863900	19000	20
15	1863900	19000	20	15	1863900	19000	20
16	1863900	19000	20	16	1863900	19000	20
17	1863900	19000	20	17	1863900	19000	20
18	1863900	19000	20	18	1863900	19000	20

Table 8: The cable-stayed bridge check for equilibrium

Side span		**Main span**	
Cload (kg)	Girder weight (kg)	Cload (kg)	Girder weight (kg)
11566500	11566500	6840000	6840000

Floating bridge model

The verification of the floating bridge model is performed based on the equation (3.5), which has been explained in the previous section:

$$Buoyancy = (m_{girder} + m_{column} + m_{pontoon} + m_{ballast}) \cdot g \quad (3.5)$$

The listed mooring pretension forces are the sum of the pretension force in four mooring lines in the vertical z direction.

Table 9: Loadings on the low bridge

Pontoon ID	Pontoon self-weight (kg)	Girder weight (kg)	Column weight (kg)	Ballast (kg)	Resultant mooring pretension (kg)	Sum of downward loads (kg)	Buoyancy (kg)
3	985000	1377500	449499	979619		3791618	3791618
4	600000	2375000	416957	399661		3791618	3791618
5	985000	2375000	383312	48305.9		3791618	3791618
6	985000	2375000	349667	81950.7		3791618	3791618
7	985000	2375000	316022	115596		3791618	3791618
8	985000	2375000	201917	229700		3791618	3791618
9	985000	2375000	177859	253759		3791618	3791618
10	985000	2375000	153801	277817		3791618	3791618
11	985000	2375000	130410	301208		3791618	3791618
12	985000	2375000	112079	319538		3791618	3791618
13	1540000	2375000	99202.2	1148749	524663.59	5687616	5687616
14	985000	2375000	91793.2	339824		3791618	3791618
15	985000	2375000	89979	341639		3791618	3791618
16	985000	2375000	89979	341639		3791618	3791618
17	985000	2375000	89979	341639		3791618	3791618
18	985000	2375000	89979	341639		3791618	3791618
19	985000	2375000	89979	341639		3791618	3791618
20	1540000	2375000	89979	1147290	535346.068	5687616	5687616
21	985000	2375000	89979	341639		3791618	3791618
22	985000	2375000	89979	341639		3791618	3791618
23	985000	2375000	89979	341639		3791618	3791618
24	985000	2375000	89979	341639		3791618	3791618
25	985000	2375000	89979	341639		3791618	3791618
26	985000	2375000	89979	341639		3791618	3791618
27	1540000	2375000	89979	1188412	494224.363	5687616	5687616
28	985000	2375000	89979	341639		3791618	3791618
29	985000	2375000	89979	341639		3791618	3791618
30	985000	2375000	89979	341639		3791618	3791618
31	985000	2375000	89979	341639		3791618	3791618
32	985000	2375000	89979	341639		3791618	3791618
33	985000	2375000	89979	341639		3791618	3791618
34	985000	2375000	89979	341639		3791618	3791618

35	985000	2375000	89979	341639		3791618	3791618
36	985000	2375000	89979	341639		3791618	3791618
37	985000	2375000	89979	341639		3791618	3791618
38	985000	2375000	88850.8	342767		3791618	3791618
39	985000	2375000	81956.1	349662		3791618	3791618
40	985000	2375000	68794	362824		3791618	3791618
Sum	38710000	89252500	5191637	1.5E+07	1554234	1.5E+08	1.5E+08

Full bridge

The static analysis, where no wind load is applied, is conducted for the full bridge model after the low bridge and cable-stayed bridge are checked for static equilibrium. The result in Figure 29 shows that the biggest deflection, about 1.1 meters upwards, appears at the cable-stayed main span while the separated cable-stayed bridge model does not present large deflection in the same area. This may because of that the separated cable-stayed bridge model is fixed at the ends. When the corresponding boundary condition is removed in the full bridge model, the load distribution would be affected. Therefore, an attempt to reduce the pretension forces in the main span cables is made.

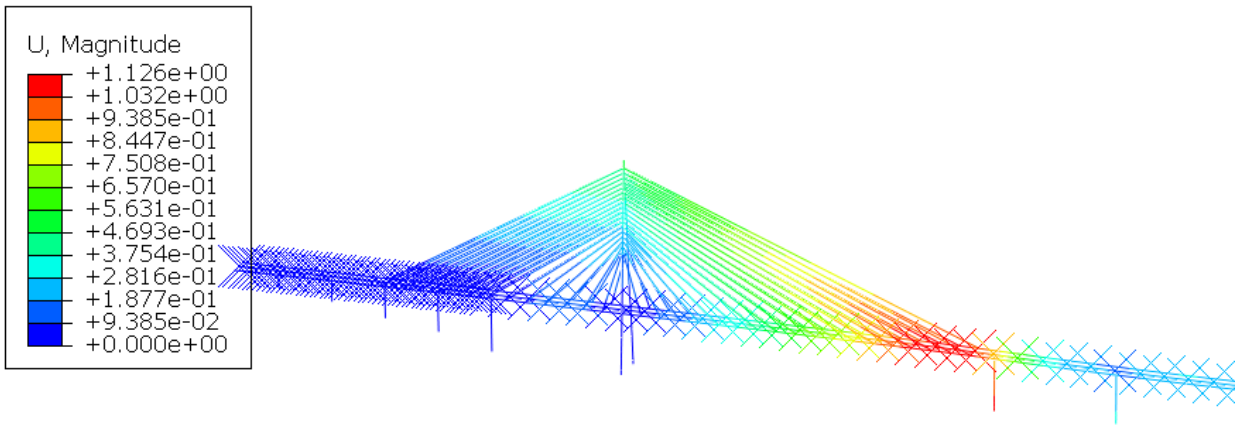

Figure 29: Deflection in Z direction of the cable-stayed bridge model

The modification of the cable pretension requires an iterative process which is performed manually in this thesis study. The best way of accelerating the iterative process and finding the accurate cable pretensions is preferably to create a MATLAB code. The modified cable pretensions are listed in the Table 10. It can be noticed that a relatively large reduction of the pretension force is applied to the last few cables which locate closely to the first pontoon, and higher pretensions are provided to cables which carry the middle part of the main span.

Table 10: Comparison of provided cable pretension and modified cable pretension

Cable ID	Modified cable pretension force (N)	Provided pretension force (N)
Main span-1	1.80E+06	2.40E+06
Main span-2	2.20E+06	2.40E+06
Main span-3	2.40E+06	2.40E+06
Main span-4	2.55E+06	3.00E+06
Main span-5	2.70E+06	3.00E+06
Main span-6	2.85E+06	3.00E+06
Main span-7	3.70E+06	3.00E+06
Main span-8	3.76E+06	4.00E+06
Main span-9	4.00E+06	4.00E+06
Main span-10	4.10E+06	4.00E+06
Main span-11	4.25E+06	4.00E+06
Main span-12	4.50E+06	4.00E+06
Main span-13	4.40E+06	4.00E+06
Main span-14	4.50E+06	5.00E+06
Main span-15	4.50E+06	5.00E+06
Main span-16	4.35E+06	5.00E+06
Main span-17	2.20E+06	5.00E+06
Main span-18	2.20E+06	5.00E+06

After modification, the deflection in the cable-stayed bridge is lowered to a level about few centimeters, referring to Figure 30. The ballast attached to the first pontoon is also been reduced in order to have a minimum possible deflection in the first 125 meters bridge sub-span carried by the first two pontoons. It can be seen in Figure 31 that deflection in vertical direction is also only few centimeters in the full bridge model.

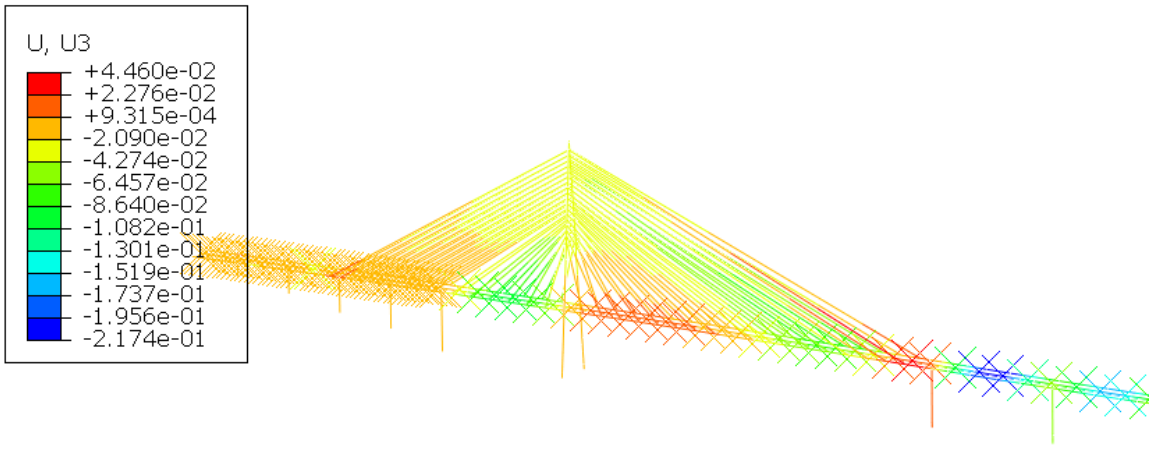

Figure 30: Deflection in vertical direction (global Z) after modification, cable-stayed part

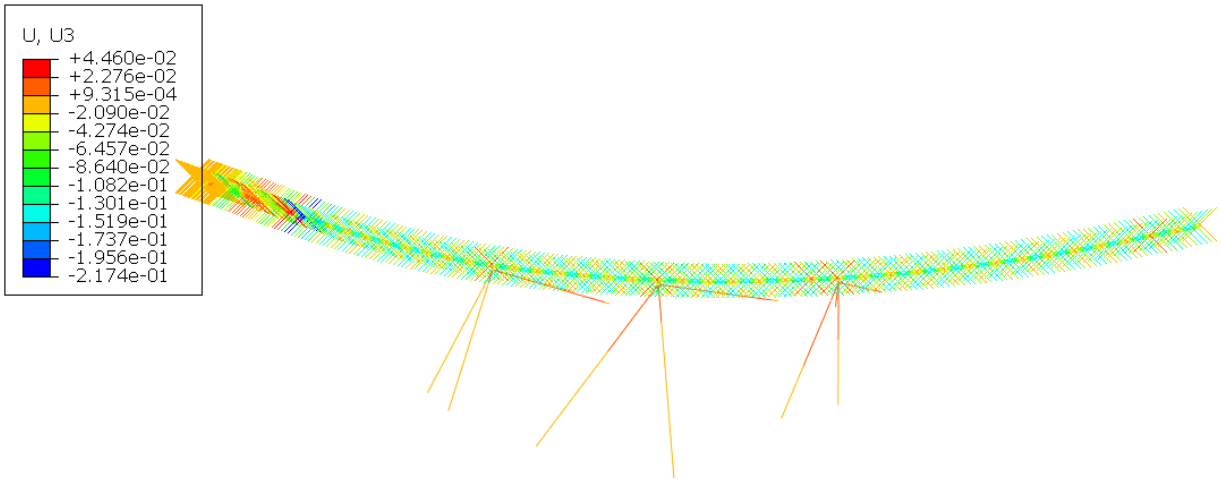

Figure 31: Deflection in vertical direction (global Z) of the full bridge model after modification

The mooring line pretension forces are listed in the table below and are compared with the value found in document provided by the Norwegian Public Roads Administration [13]. It can be seen that the resulted pretensions taken from the ABAQUS model are very close to the provided values.

Table 11: Mooring line pretension

Mooring line ID	Pretension force from Abaqus [MN]	Pretension force provided [MN]
1	2	1.98
2	2	2
3	2	2.08
4	1.9	1.93
5	2.6	2.59
6	2.25	2.28
7	2.5	2.54
8	2.6	2.63
9	2.25	2.17
10	1.75	1.69
11	2	2.09
12	2	2.04

4. Aerodynamic load modelling

The wind is a three-dimensional turbulent flow as a result of shear flow passing through rough surface. A statistical explanation of the wind flow consists of three components: the long-term variation of the mean wind speed, the short-term single point time domain turbulent variation and the short-term spatial distribution of the turbulence ingredients. The representative instantaneous wind velocity profile in along wind direction (u) is presented in the Figure 32 (left column). The mean wind velocity and the turbulence variation with height z_f are illustrated in the middle column and the right column respectively. The aerodynamic theory in the following sections is described based on the book [7].

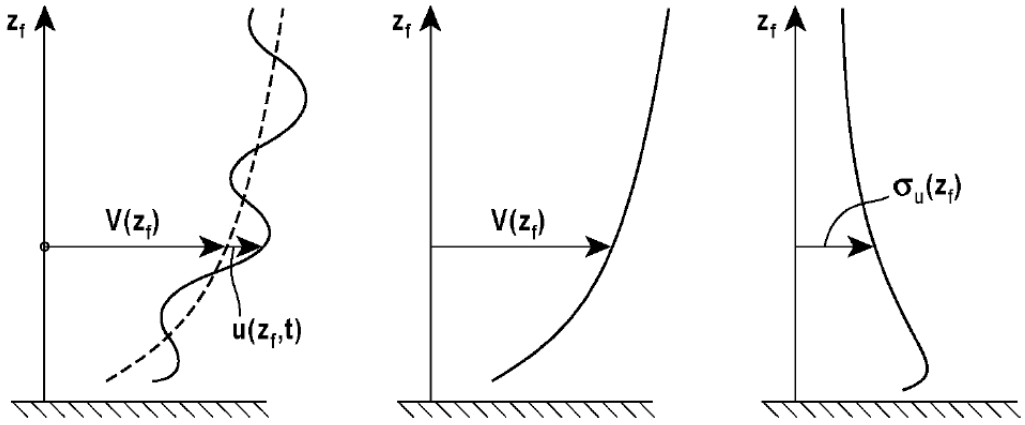

Figure 32: The wind speed and turbulence profiles [7]

4.1.1. Mean wind

The mean wind typically varies with height when the fluctuating parts are stochastic functions of time and space with a zero-mean value. The mean wind profile is normally defined by a constant value at the reference height of 10 m, together with a height dependent wind profile. A typical wind profile is the logarithmic profile in Equation (4.1), governed by the terrain roughness k_T and roughness length z_0 [6]:

$$\frac{V_{10}(z_f)}{V_{10}(10)} = \begin{cases} k_T \cdot \ln\left(\frac{z_f}{z_0}\right) & when\ z_f > z_{min} \\ k_T \cdot \ln\left(\frac{z_{min}}{z_0}\right) & when\ z_f \leq z_{min} \end{cases} \tag{4.1}$$

4.1.2. Wind single point statistics

Typical single point recordings of the fluctuating wind components $u(t)$ - along-wind, $v(t)$ - across wind and $w(t)$ - vertical wind component during the period of T give the source for determination of their time and frequency domain statistical properties. The turbulence components $u(t), v(t)$ and $w(t)$ have zero mean values. The statistics executed on time series recordings of each of these turbulence components will give three zero mean Gaussian probability density distribution with variances defined by:

$$\begin{bmatrix} {\sigma_u}^2 \\ {\sigma_v}^2 \\ {\sigma_w}^2 \end{bmatrix} = \frac{1}{T}\int_0^T \begin{bmatrix} u^2(t) \\ v^2(t) \\ w^2(t) \end{bmatrix} dt \tag{4.2}$$

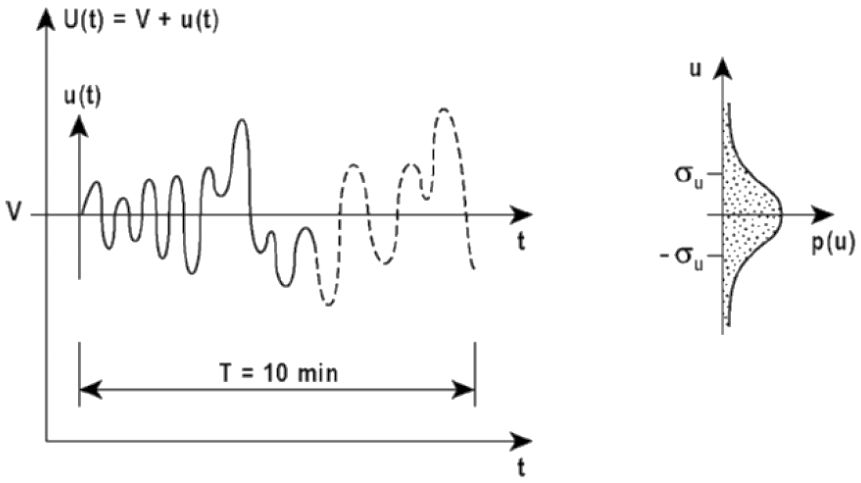

Figure 33: The probability distribution of the along wind u(t) turbulence component [7]

Turbulence intensity and power spectral density give "single point" statistics. The corresponding turbulence intensities are described as the relation between standard deviation σ of respective turbulence component and the mean wind velocity V referring to Equation (4.3). The turbulence intensity reduces gradually with height and increases with surface roughness. Standard deviation expresses an "average" of the variation in wind speed from its mean value. Turbulence intensity is then a non-dimensional measure of this variation.

$$I_n(z_f) = \frac{\sigma_n(z_f)}{V(z_f)} \qquad where\ n = u, v, w \tag{4.3}$$

The turbulence intensity for different wind turbulence components is obtained by:

$$I_u = \frac{\sigma_u}{V} = \begin{cases} c_u \ln\left(\frac{z}{z_1}\right), & if\ z > z_{min} \\ c_u \ln\left(\frac{z_{min}}{z_1}\right), & if\ z \le z_{min} \end{cases} \tag{4.4}$$

$$I_v = \frac{3}{4} I_u \tag{4.5}$$

$$I_v = \frac{1}{2} I_u \tag{4.6}$$

where $c_u$stands for turbulence factor dependent on the terrain category according to [6].

Power spectral density demonstrates the information about turbulence components in the frequency-domain. In other words, it shows the distribution of the wind energy as a function of frequency. Power spectral density of the along wind turbulent component n according to [6] is given in the normalized form:

$$\frac{f \cdot S_n\{f\}}{{\sigma_n}^2} = \frac{A_n \cdot \hat{f}_n}{(1 + 1{,}5 \cdot A_n \cdot \hat{f}_n)^{5/3}} \qquad where\ n = u, v, w \tag{4.7}$$

where $\frac{f \cdot S_n\{f\}}{{\sigma_n}^2}$ is the power spectrum; σ_n is the standard deviation of the wind turbulence component n; u, v, w refers to the along-wind, across-wind and vertical wind component respectively; A_n is the empirical parameter representing the different wind components: $A_u = 6.8$, $A_v = 9.4$ and $A_w = 9.4$ according to the Norwegian bridge design guideline N400; $\hat{f}_n$ is frequency normalized with the mean wind velocity and integral length scale of the turbulence component ${L_n}^x$:

$$\hat{f}_n = f \cdot {L_n}^x / V \tag{4.8}$$

The length scales for different wind turbulence components can be expressed by [9]:

$${L_u}^x = \begin{cases} L_1 (z/z_1)^{0.3}, & if\ z > z_{min} \\ L_1 (z_{min}/z_1)^{0.3}, & if\ z \le z_{min} \end{cases} \tag{4.9}$$

$${L_v}^x = \frac{1}{4} {L_u}^x \tag{4.10}$$

$${L_w}^x = \frac{1}{12} {L_u}^x \tag{4.11}$$

where L_1 stands for the reference length scale of 100 m, z_1 stands for reference height of 10 m and z_{min} stands for an arbitrary minimal height dependent on the terrain category.

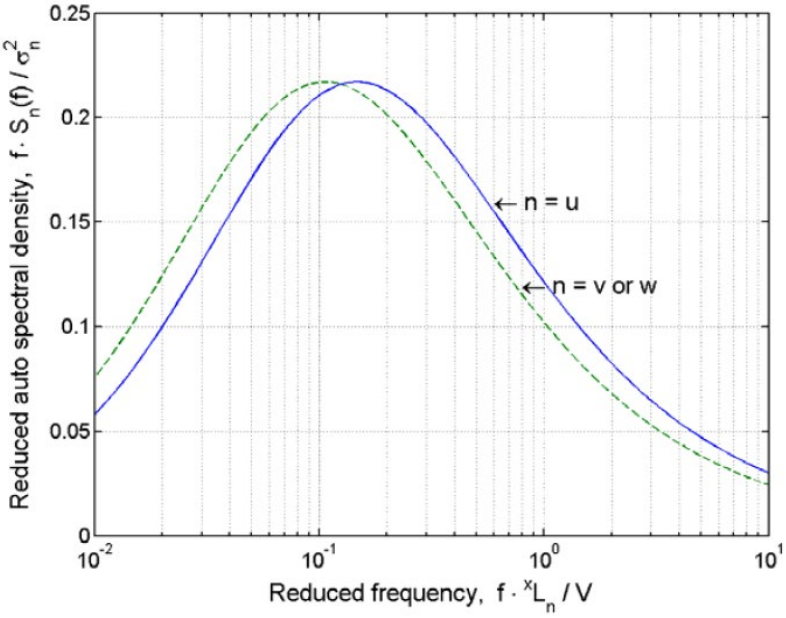

Figure 34: Kaimal auto spectra of turbulence components [7]

4.1.3. Spatial distribution of turbulence components

The other short-term component which is essential to establish the wind load on the entire structure and to determine spatial properties of wind turbulence is the two-point separated data measurement of u, v and w components. The recordings at two different positions separated by distance Δs are expressed in vector form in Equation (4.12)

$$\boldsymbol{u}_a = \begin{bmatrix} u(s,t) \\ v(s,t) \\ w(s,t) \end{bmatrix} \quad and \quad \boldsymbol{u}_b = \begin{bmatrix} u(s+\Delta s, t+\tau) \\ v(s+\Delta s, t+\tau) \\ w(s+\Delta s, t+\tau) \end{bmatrix} \tag{4.12}$$

where τ is a time lag at any step within $\pm T$, s is a distance variable and Δs is separation between the two recordings in three directions.

Hence, the covariance matrix can be defined as:

$$\boldsymbol{Cov}(\Delta s, \tau) = \begin{bmatrix} Cov_{uu} & Cov_{uv} & Cov_{uw} \\ Cov_{vu} & Cov_{vv} & Cov_{vw} \\ Cov_{wu} & Cov_{wv} & Cov_{ww} \end{bmatrix} = E[\boldsymbol{u}_a \cdot \boldsymbol{u}_b{}^T] = \frac{1}{T}\int_0^T (\boldsymbol{u}_a \cdot \boldsymbol{u}_b{}^T) dt \tag{4.13}$$

where the covariance functions may include the spatial separation:

$$Cov_{mn}(\Delta s, \tau) \quad \begin{cases} m, n = u, v, w \\ \Delta s = \Delta x_f, \Delta y_f, \Delta z_f \end{cases} \tag{4.14}$$

The most relevant case for a horizontal structure like a bridge is illustrated in Figure 35 where the u turbulent component along the wind direction is recorded at two different positions a and b. As the separation between the two recordings Δs and time lag τ increase, the covariance properties in the wind field decrease.

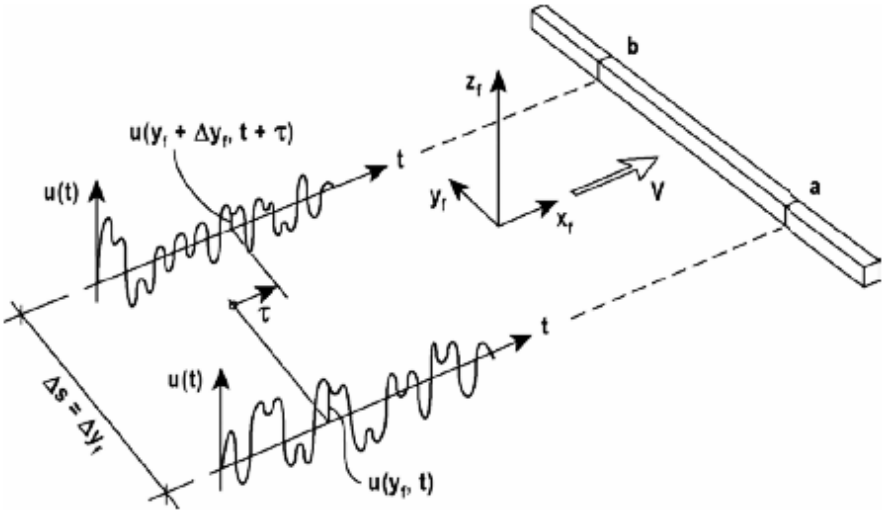

Figure 35: Cross covariance of wind u component for two-point recordings [7]

In this study, the statistical dependence of fluctuating components at two points separated by distance is calculated by Equation (4.15) according to N400 [15]:

$$\gamma(f, d_j) = \frac{Re[S_{i_1,i_2}(f, d_j)]}{\sqrt{S_{i_1}(f) \cdot S_{i_2}(f)}} = \exp\left(-C_{ij} \frac{f d_j}{\overline{U}(z)}\right); \qquad i = u, v, w; j = y, z \tag{4.15}$$

where $\gamma(f, d_j)$ is the co-coherence as a function of the frequency f and Euclidian distance d_j; $S_{i_1}(f)$ and $S_{i_2}(f)$ are the underlying single point power spectral densities of the turbulence i-components; $S_{i_1,i_2}(f, d_j)$ is the co-spectrum of turbulence at two separated points.

The coefficients C_{ij} suggested by N400 [15] that control the co-coherence exponential decay are given as:

$$C_{ux} = C_{wx} = C_{wz} = 3, C_{uy} = C_{uz} = 10,\ C_{vx} = 6,\ C_{vy} = \ C_{vz} = \ C_{wy} = 6.5$$

where: u - along the wind component, v - lateral component, w - vertical component

x - along the wind flow direction, y - lateral wind direction, z - vertical wind direction

4.2. The buffeting theory

The reality is that the real wind field combined with complicated curved geometry of the bridge would result in a complex loading condition where the aerodynamic coefficients are dependent on both angle of attack and the skew wind angle. As a result, the aerodynamic coefficients would be six components for all 6 DOF. However, for the simplicity, in this study the assumption is made that wind acts on 2D girder cross section which results in three load components: drag, lift and overturning moment. These motion-dependent forces are calculated based on the buffeting theory. The theory in this section is described based on the book [7] and is a standard procedure for calculating the buffeting load acting on a straight bridge. The procedure of calculating the buffeting load for a curved bridge considered in this study is explained in Chapter 4.4.1.

According to the standard procedure described in [7], the buffeting wind load consist of the total load created by wind velocity variations in the oncoming flow (Equation (4.16)) and all contributions caused by the structure motion.

$$U(x_f, y_f, z_f) = V(x_f, y_f, z_f) + u(x_f, y_f, z_f), v(x_f, y_f, z_f) \; and \; w(x_f, y_f, z_f) \quad (4.16)$$

The fundamental assumption of the discussed theory is that the instantaneous velocity pressure and load coefficients are used to establish the wind load. Accordingly, the load may be computed from the interpretation of the instantaneous relative velocity vector and flow incidence dependent drag, lift and moment coefficients.

In the theory presented in the [7], the line-like horizontal bridge type of structure is studied where z_f-position in the flow prior to loading is constant along the whole span. The wind field is stationary and homogeneous. Additionally, the theory states that main flow is perpendicular to the span-wise x-axis. Therefore, the fluctuation components of along and across wind vertical directions are considered:

$$U(x,t) = V + u(x,t) \text{ and } w(x,t) \quad (4.17)$$

where U stands for mean wind, $u(x,t)$ for the component of the velocity vector in along wind horizontal direction and $w(x,t)$ for vertical across wind direction.

Furthermore, according to the theory, the structural displacements and rotations of the cross section are small as well as load components $u(x,t)$ and $w(x,t)$ in comparison to V.

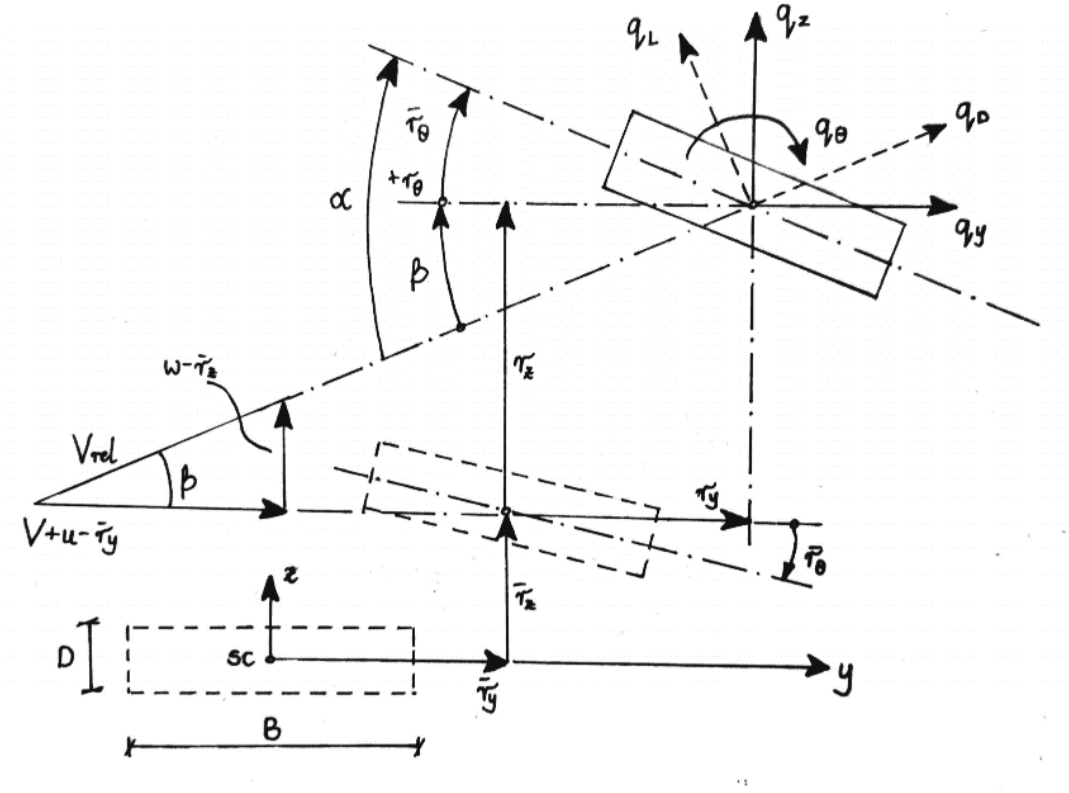

Figure 36: Instantaneous wind flow and displacement quantities [7]

The assumption is that any oscillating quantity consist of time invariant mean component and a zero mean fluctuating component. Therefore, the cross section of the bridge girder is displaced from the initial position by $\bar{r}_y(x), \bar{r}_z(x)$ and $\bar{r}_{y\theta}(x)$ (Figure 36). It is about this position that the structure fluctuates, and the wind velocity vector is $V + u(x,t)$ in the along the horizontal flow direction and $w(x,t)$ across the vertical flow direction. Then also the additional dynamic displacements are given $r_y(x,t), r_z(x,t)$ and $r_{y\theta}(x,t)$ where the instantaneous cross sectional drag, lift and moment forces are described as:

$$\begin{bmatrix} q_D(x,t) \\ q_L(x,t) \\ q_M(x,t) \end{bmatrix} = \frac{1}{2}\rho {V_{rel}}^2 \begin{bmatrix} D \cdot C_D(\alpha) \\ B \cdot C_L(\alpha) \\ B^2 \cdot C_M(\alpha) \end{bmatrix} \tag{4.18}$$

where V_{rel} is the instantaneous relative wind velocity; α the angle of flow incidence; B height and D the width of the cross-section; C_D , C_L , C_M are wind load coefficients. Then the transformation into structural axis is described by:

$$\boldsymbol{q}_{tot}(x,t) = \begin{bmatrix} q_y \\ q_z \\ q_\theta \end{bmatrix}_{tot} = \begin{bmatrix} cos\beta & -sin\beta & 0 \\ sin\beta & cos\beta & 0 \\ 0 & 0 & 1 \end{bmatrix} \cdot \begin{bmatrix} q_D \\ q_L \\ q_M \end{bmatrix} \tag{4.19}$$

where β is the angle as follow: $\beta = \arctan\left(\frac{w-\dot{r}_z}{V+u-\dot{r}_y}\right)$.

The instantaneous relative wind velocity V_{rel} and the angle of attack α according to the Figure 36 are given by:

$$\left.\begin{matrix} {V_{rel}}^2 = \left(V + u - \dot{r}_y\right)^2 + (w - \dot{r}_z)^2 \\ \alpha = \bar{r}_\theta + r_\theta + \beta \end{matrix}\right\} \tag{4.20}$$

Thus, the flow incidence dependent load coefficients are:

$$\begin{bmatrix} C_D(\alpha) \\ C_L(\alpha) \\ C_M(\alpha) \end{bmatrix} = \begin{bmatrix} C_D(\bar{\alpha}) \\ C_L(\bar{\alpha}) \\ C_M(\bar{\alpha}) \end{bmatrix} + \alpha_f \cdot \begin{bmatrix} {C'}_D(\bar{\alpha}) \\ {C'}_L(\bar{\alpha}) \\ {C'}_M(\bar{\alpha}) \end{bmatrix} \tag{4.21}$$

where $\bar{\alpha}$ and α_f are the mean value and the fluctuating part of the angle of incidence, ${C'}_D$, ${C'}_L$ and ${C'}_M$ are the slopes of the load coefficient curves at $\bar{\alpha}$ as on the drawings below.

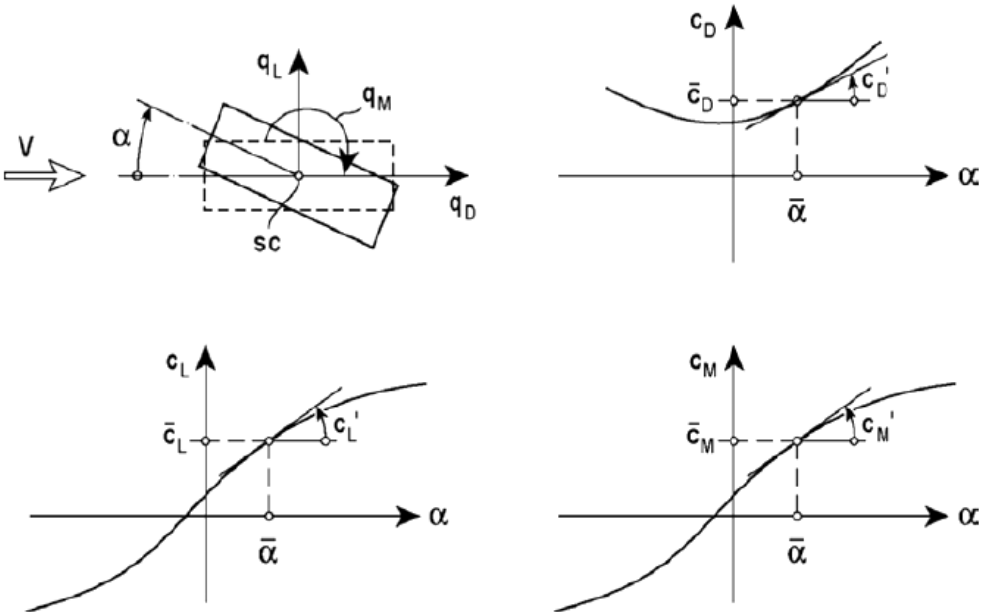

Figure 37: Load coefficients obtained from static tests [7]

By combining above equations and eliminating higher order terms including the product quantities that have been assumed small the following equation is obtained:

$$\boldsymbol{q}_{tot}(x,t) = \begin{bmatrix} \bar{q}_y(x) \\ \bar{q}_z(x) \\ \bar{q}_\theta(x) \end{bmatrix} + \begin{bmatrix} q_y(x,t) \\ q_z(x,t) \\ q_\theta(x,t) \end{bmatrix} = \bar{\boldsymbol{q}} + \boldsymbol{B_q} \cdot \boldsymbol{v} + \boldsymbol{C_{ae}} \cdot \dot{\boldsymbol{r}} + \boldsymbol{K_{ae}} \cdot \boldsymbol{r} \tag{4.22}$$

where $\boldsymbol{B_q} \cdot \boldsymbol{v}$ is the dynamic loading related to turbulence in the oncoming flow, $\boldsymbol{C_{ae}} \cdot \dot{\boldsymbol{r}}$ and $\boldsymbol{K_{ae}} \cdot \boldsymbol{r}$ is the motion induced forces related to velocity of the structure and displacement.

The time invariant mean part:

$$\bar{\boldsymbol{q}}(x,t) = \begin{bmatrix} \bar{q}_y \\ \bar{q}_z \\ \bar{q}_\theta \end{bmatrix} = \frac{1}{2}\rho V^2 B \begin{bmatrix} \bar{C}_D \dfrac{D}{B} \\ \bar{C}_L \\ B\bar{C}_M \end{bmatrix} = \frac{1}{2}\rho V^2 B \cdot \hat{\boldsymbol{b}}_q \tag{4.23}$$

The components of dynamic part:

$$\boldsymbol{V}(x,t) = [u \quad w]^T \tag{4.24}$$

$$\boldsymbol{r}(x,t) = \begin{bmatrix} r_y & r_z & r_\theta \end{bmatrix}^T \tag{4.25}$$

$$\boldsymbol{B}_q(x) = \frac{\rho V B}{2} \begin{bmatrix} 2(D/B)\bar{C}_D & ((D/B)C'_D - \bar{C}_L \\ 2\bar{C}_L & (C'_L + (D/B)\bar{C}_D) \\ 2B\bar{C}_M & BC'_M \end{bmatrix} = \frac{\rho V B}{2} \cdot \hat{\boldsymbol{B}}_q \tag{4.26}$$

$$\boldsymbol{C}_{ae}(x) = -\frac{\rho V B}{2} \begin{bmatrix} 2\left(\dfrac{D}{B}\right)\bar{C}_D & ((D/B)C'_D - \bar{C}_L & 0 \\ 2\bar{C}_L & \left(C'_L + \left(\dfrac{D}{B}\right)\bar{C}_D\right) & 0 \\ 2B\bar{C}_M & BC'_M & 0 \end{bmatrix} \tag{4.27}$$

$$\boldsymbol{K}_{ae}(x) = -\frac{\rho V^2 B}{2} \begin{bmatrix} 0 & 0 & \left(\dfrac{D}{B}\right)C'_D \\ 0 & 0 & C'_L \\ 0 & 0 & BC'_M \end{bmatrix} \tag{4.28}$$

where $\hat{\boldsymbol{b}}_q$ is the buffeting static force coefficient vector, $\boldsymbol{B}_q$ and $\hat{\boldsymbol{B}}_q$ are the buffeting dynamic load coefficient matrices at cross sectional level. $\boldsymbol{C}_{ae}$is the aerodynamic damping matrix and $\boldsymbol{K}_{ae}$ is the aerodynamic stiffness matrix and both the parameters are derived from the buffeting theory.

4.3. Generation of the dynamic wind field

MATLAB code used to generate the wind field in this study was provided by UiS postdoc Etienne Cheynet. The developed code follows N400 [15] and NS-EN 1991-1-4: 2005+NA [6]. The floating bridge is a very long and flexible structure with eigen-period of about 30 sec of the lowest mode. Therefore, in this thesis work one-hour simulation was performed in order to capture the important dynamic features of the bridge. The turbulent wind field is estimated with 100 year return period due to the extreme wind conditions. Furthermore, center beam of the girder is a subject of the interest and the wind field is generated at center of each girder element. In the MATLAB code the wind field data is generated in time series for all the girder elements and in three wind components u, v, w. The time series of turbulent wind is simulated based on mean wind velocity, wind spectra and coherence functions. The established wind field data includes the mean wind part and the turbulent part where the wind velocity components are:

$$V(z) + u(x, y, z, t)$$
$$v(x, y, z, t)$$
$$w(x, y, z, t)$$

where $V(z)$ is the mean wind component; $u(x, y, z, t)$ is the fluctuating wind component in along the wind direction; $v(x, y, z, t)$ - across the wind direction and $w(x, y, z, t)$ – in vertical direction across the wind; z stands for the height above the sea surface.

4.3.1. Mean wind component

The Bjørnafjorden floating bridge is located near wide fjord at relatively flat area with negligible vegetation and without obstacles. According to the Eurocode 1 [6], this type of the terrain is defined as terrain category I. For the reference height at 10 meters above the sea surface and terrain category I, the one-hour fundamental basic wind velocity U_b is 24,3 $\frac{m}{s}$. According to Eurocode 1 [6] and for category I, mean wind speed parameters such as terrain roughness and roughness length are defined as: $k_T = 0{,}17$ and $z_0 = 0{,}01m$. The mean wind velocity at height z above the terrain:

$$V(z) = k_T \cdot U_b \cdot C_{prob} \cdot \ln\left(\frac{z}{z_0}\right) \tag{4.29}$$

The probability factor C_{prob} given by expression:

$$C_{prob} = \left(\frac{1 - 0.2 \cdot ln(-\ln(1-p))}{1 - 0.2 \cdot ln(-\ln(0.98))}\right)^{\frac{1}{2}} \tag{4.30}$$

The probability p for an annual exceedance where T is the return period is determined by:

$$p = 1 - \exp\left(-\frac{1}{T}\right) \tag{4.31}$$

The wind direction is reported based on the direction from where arises and it is measured in degrees from 0° to 360° clockwise from the perfect north. In defining the direction of the wind acting on the structure the tilt of the bridge from the perfect north should be considered. In this study the tilt is equal to 10°.

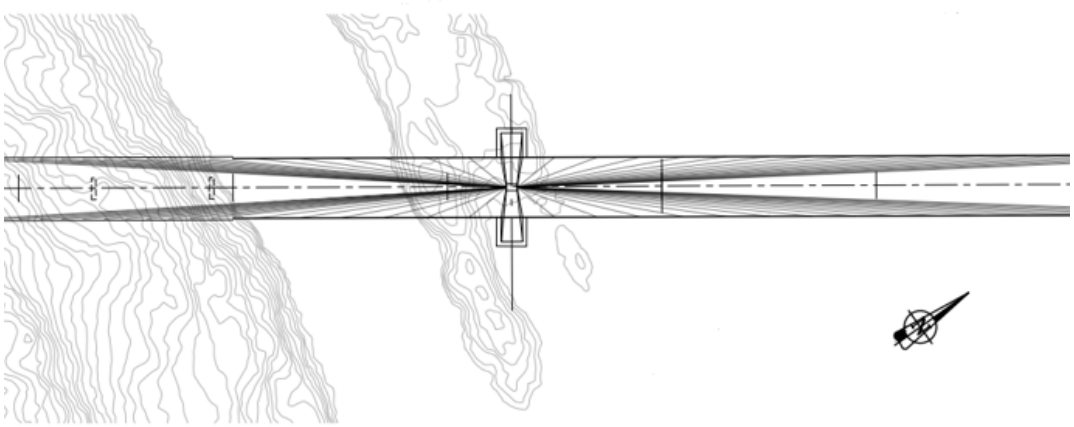

Figure 38: Bridge orientation with respect to cardinal directions [16]

4.3.2. Turbulent wind component

The turbulent part of the wind velocity is obtained by considering the coherence function and the wind spectra. As the bridge is a very long structure, the wind at different locations will not have the same speed at the same time. Therefore, the coherence decay parameters are introduced in the analysis for each wind component and wind direction. The coherence decay parameters vary from 0 to 10 and the lower the parameter is the higher the coherence between elements and increased response. This statistical dependence of fluctuating components at two points is calculated based on Equation (4.15) explained in Chapter 4.1.3. Furthermore, in the MATLAB code the fluctuating wind spectrum which describes the wind energy distribution is computed at each element according to the Equation (4.7) mentioned in Chapter 4.1.2. The energy at specific frequencies is converted into time domain by inversed Fourier transformation. The established wind field data from MATLAB code is further called in the Fortran subroutine in calculations of the load acting on the structure presented in the next chapter.

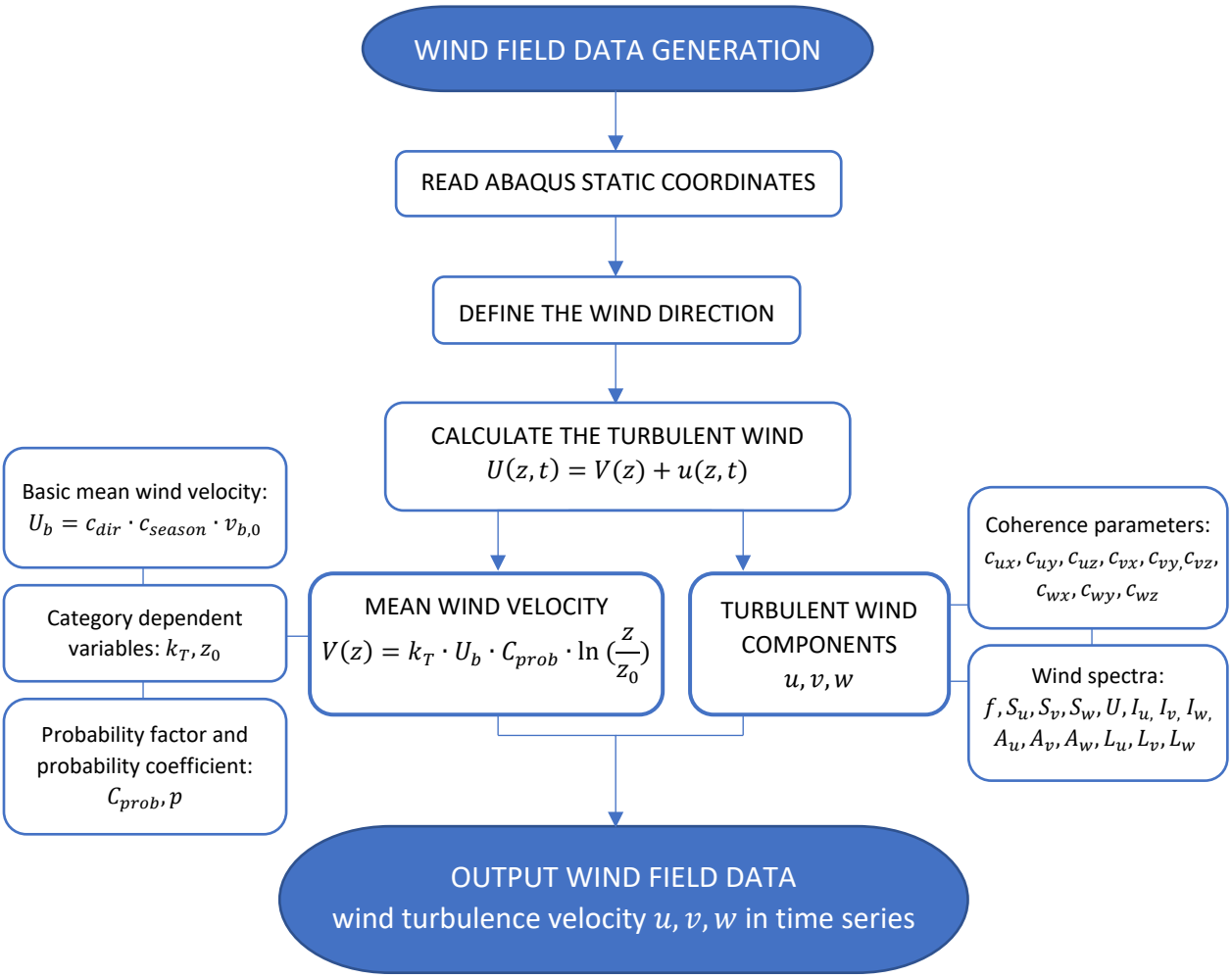

Figure 39: Wind field generation procedure

4.4. Wind load computation

The girder elements and the link elements are subjected to wind loads which are dependent on the instantaneous wind velocity and the velocity of the structure. This characteristic of the wind loads requires that the calculation of these loads should be performed element by element and time step by time step. Fortran subroutines are therefore built in the purpose of calculating the instantaneous wind loads for each of the elements. The DLOAD subroutine is introduced in order to calculate the instantaneous wind loads for each element. According to the buffeting theory, the turbulence induced drag, lift and overturning moment can be calculated from the instantaneous relative wind velocity and the load coefficients that are dependent on the instantaneous angle of attack. The relative wind velocity is the velocity difference between the upcoming wind flow and the structural self-motion, where the wind field is generated by MATLAB code and further imported by the subroutine READDATA. Furthermore, a subroutine called URDFIL is utilized to extract the information of the structural motion from the Abaqus result files. A flow chart shows how the subroutines cooperate is made as Figure 40. The Fortran subroutines are attached in the APPENDIX C.

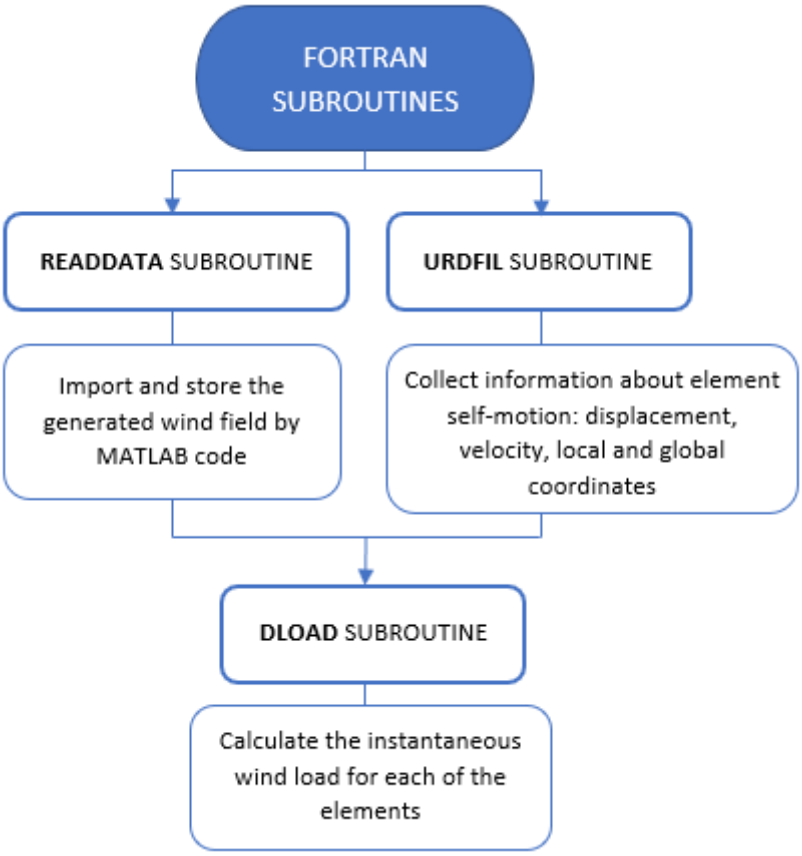

Figure 40: Flow chart of subroutines collaboration

4.4.1. DLOAD subroutine

The DLOAD subroutine can be modified by the user to define a distributed load that varies with time and element position. When the *DLOAD option is specified with a load type label in the input file, the DLOAD subroutine will be called [27]. In this thesis, the wind load is defined as a force per unit length in the global X-, Y- and Z-direction on the girder elements and link elements. The corresponding load type labels used are:

PXNU - Nonuniform force per unit length in global *X*-direction
PYNU - Nonuniform force per unit length in global *Y*-direction
PZNU - Nonuniform force per unit length in global *Z*-direction

The calculation of the wind loads is performed in the element cross-sectional plane, which requires a further decomposition of the resultant wind forces into the global X-, Y- and Z-axis. The magnitude of drag, lift and overturning moment calculated at each time step in the element cross-sectional plane are shown in the equations below:

$$F_D = \frac{1}{2}\rho V_{rel}^2 H(C_D + \alpha C_D') \tag{4.34}$$

$$F_L = \frac{1}{2}\rho V_{rel}^2 B(C_L + \alpha C_L') \tag{4.35}$$

$$M = \frac{1}{2}\rho V_{rel}^2 B^2(C_M + \alpha C_M') \tag{4.36}$$

where ρ is the density of the air, V_{rel} is the instantaneous relative velocity, H is the cross-sectional height of the girder, B is the cross-sectional girder width, α is the instantaneous angle of attack between the instantaneous local wind vector and the instantaneous local normal axis of the girder element. The $C_D, C_L \; and \; C_M$ are load coefficients with the corresponding derivatives denoted as $C_D', C_L' \; and \; C_M'$.

The drag force and lift force are applied to the girder elements, the overturning moment is applied to the link elements as a pair of parallel forces with equal magnitude F_M but oppositely directed:

$$F_M = \frac{M}{B\cos\alpha} \tag{4.37}$$

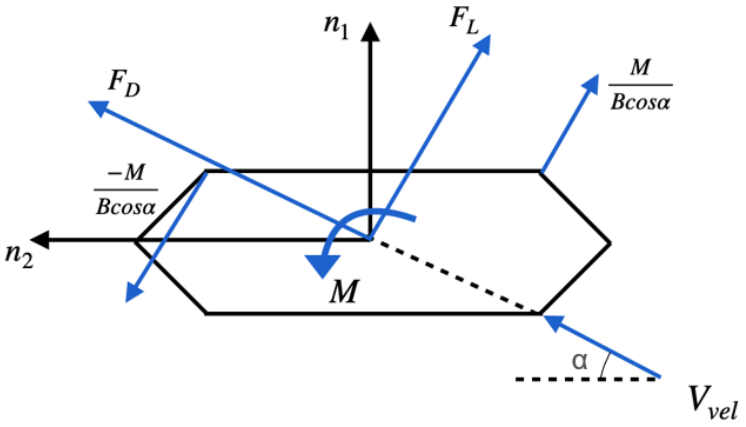

Figure 41: Wind loads on the girder cross section when the wind is coming from west

The instantaneous relative wind velocity in the global plane, $V_{rel}(X,Y,Z)$, is obtained by considering the motion of the girder element together with the instantaneous wind velocity:

$$V_{rel}(X,Y,Z) = V_{wind}(X,Y,Z) - V_{element}(X,Y,Z)$$

The motion of the girder element is collected in the URDFIL subroutine and the wind field is imported by the READDATA subroutine. The wind field imported is originally in the wind coordinate which indicates that a transformation of the wind field from the wind coordinate (U, V, W) to the global coordinate (X, Y, Z) is required.

The transformation from wind coordinate to the global coordinate is performed in the two-dimensional level assumed that the wind W-axis is parallel to the global Z-axis. The rotation angle used in the transformation is the angle between the wind U-axis and the global X-axis, which depends on the direction of the upcoming wind flow, and is calculated as:

Rotation angle = Wind angle + 180°

The zero-wind direction is along the negative direction of the global X-axis.

Table 12: Examples of angle of rotation for different wind directions

Wind direction	**Wind angle**	**Rotation angle**
North	0°	180°
South	180°	0°
West	270°	90°
East	90°	270°

The obtained relative wind velocity in the global plane is further projected to the cross-sectional plane formed by the element local axis n_1 and n_2. The instantaneous angle of attack is identified by this instantaneous wind velocity vector in the cross-sectional plane and the instantaneous local axis of the girder element. The direction of the drag, lift and overturning moment depends on the upcoming wind flow direction. The lift force direction is obtained by the cross product of the drag force vector and the local tangential element axis t:

- Wind coming from the east: $\overrightarrow{F_L} = \vec{t} \times \overrightarrow{F_D}$
- Wind coming from the west: $\overrightarrow{F_L} = \overrightarrow{F_D} \times \vec{t}$

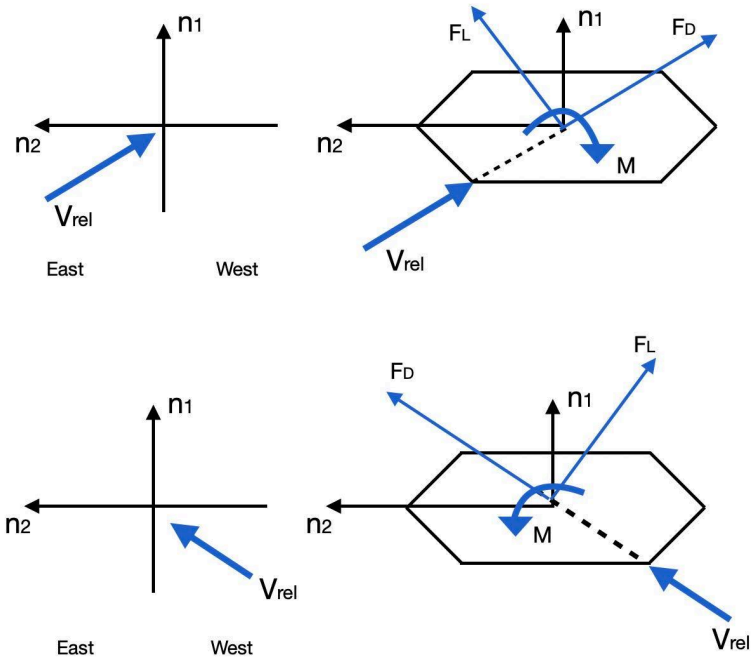

Figure 42: The direction of the wind forces dependent on the wind flow direction

The DLOAD subroutine is summarized in the Figure 44.

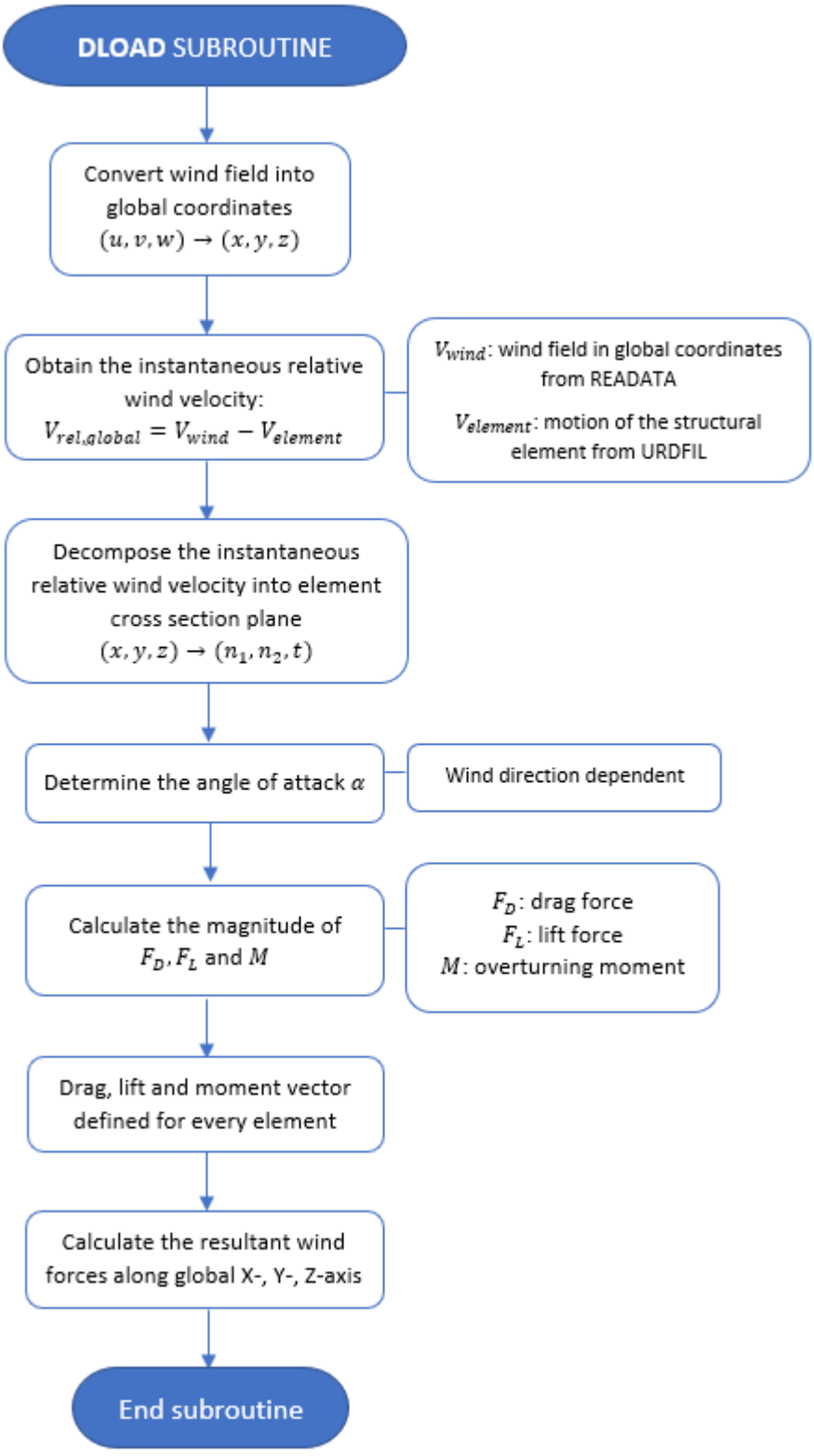

Figure 43: Flowchart of the DLOAD subroutine

4.4.2. READDATA subroutine

The READDATA subroutine is used to import the wind field data generated in MATLAB. A total wind field which consists of three wind components u, v, w will be created in this subroutine. The size of the total wind field should be consistent with the simulation time and the number of elements that will be subjected to the wind load.

4.4.3. URDFIL subroutine

The user subroutine URDFIL is used to obtain the results from Abaqus such as nodal velocity, displacement and the coordinate of local axis as well as the global coordinates. The extracted data from the results file is stored as a COMMON parameter that is shared between the subroutines. The routine which must be called in URDFIL subroutine is DBFILE routine which allows the user to read records from the results file. Also, the routine called POSFIL is introduced to read results from Abaqus at a specified element for a specified time step. It can be used to make decisions such as when to terminate the analysis or whether to overwrite the results of the previous increment. The URDFIL subroutine is summarized in the flowchart below.

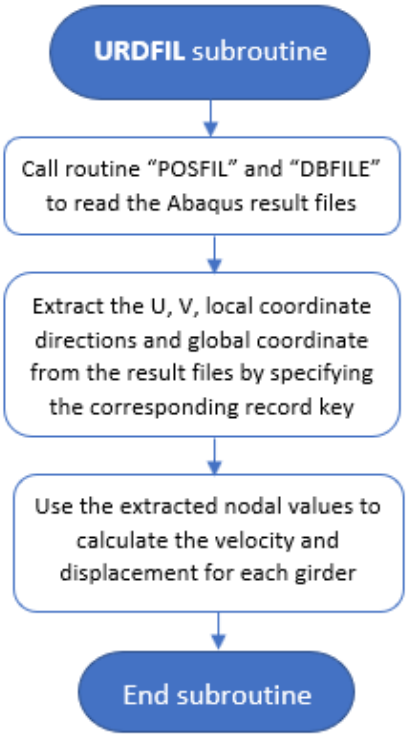

Figure 44: Flowchart of the URDFIL subroutine

5. Modal analysis results

The modal analysis is adopted to describe the real dynamic behavior of the floating structure in the frequency domain by mode shapes when the different degrees of freedom are coupled. In the following section the selected modal responses of the floating structure are presented as well as comparison of the obtained results in terms of eigenfrequencies and eigenmodes of the model of the bridge with and without mooring lines. The eigenfrequencies results can be found in Abaqus software and the user can visualize modal shapes by Abaqus Viewer. Furthermore, this chapter focuses on girder bridge response of the floating part of the structure.

5.1. Mode shapes of the structure

Mode shapes presented in this section represents selection of two representative modes of each motion: horizontal, vertical and torsional that governs the response of the floating structure. Additionally, two modes of symmetrical and asymmetrical horizontal shape are presented as an interesting observation of the modal analysis. The motion in all the directions contribute to each mode, but the dominating motion was a factor to select a representative one for each.

The representative horizontal modes occur at low frequencies starts from mode nr 1 and nr 2 as presented in the Figure 45 and

46. From mode nr 1 to nr 4 there is a great participation of horizontal movement of the structure with vertical and torsional contribution to it.

The dominating vertical contribution can be clearly observed at mode nr 60 where the girder above the middle mooring line deflects upwards and the rest remains close to the initial position (Figure 47). The corresponding eigen-frequency at which vertical modes start to occur is 0.21416 Hz and with period of about 4.67 seconds. The interesting symmetrical mode shape with dominating vertical motion appears at mode nr 65 with the peak above the last span and is shown in the Figure 48.

As it is shown in Figure 49, significant torsional participation occurs at period of 3,7 seconds and mode nr 83, where the vertical and horizontal movement has a great contribution to it as well. The second torsional mode at mode nr 85 with eigen-period of 3,6 seconds presents larger twisting at the middle of the bridge (Figure 51) and it is coupled with other movements as well.

Additionally, two important modes nr 27 and nr 30 were selected where the symmetrical and asymmetrical shape of the girder deck was observed and are presented in the Figure 51 and 52 respectively.

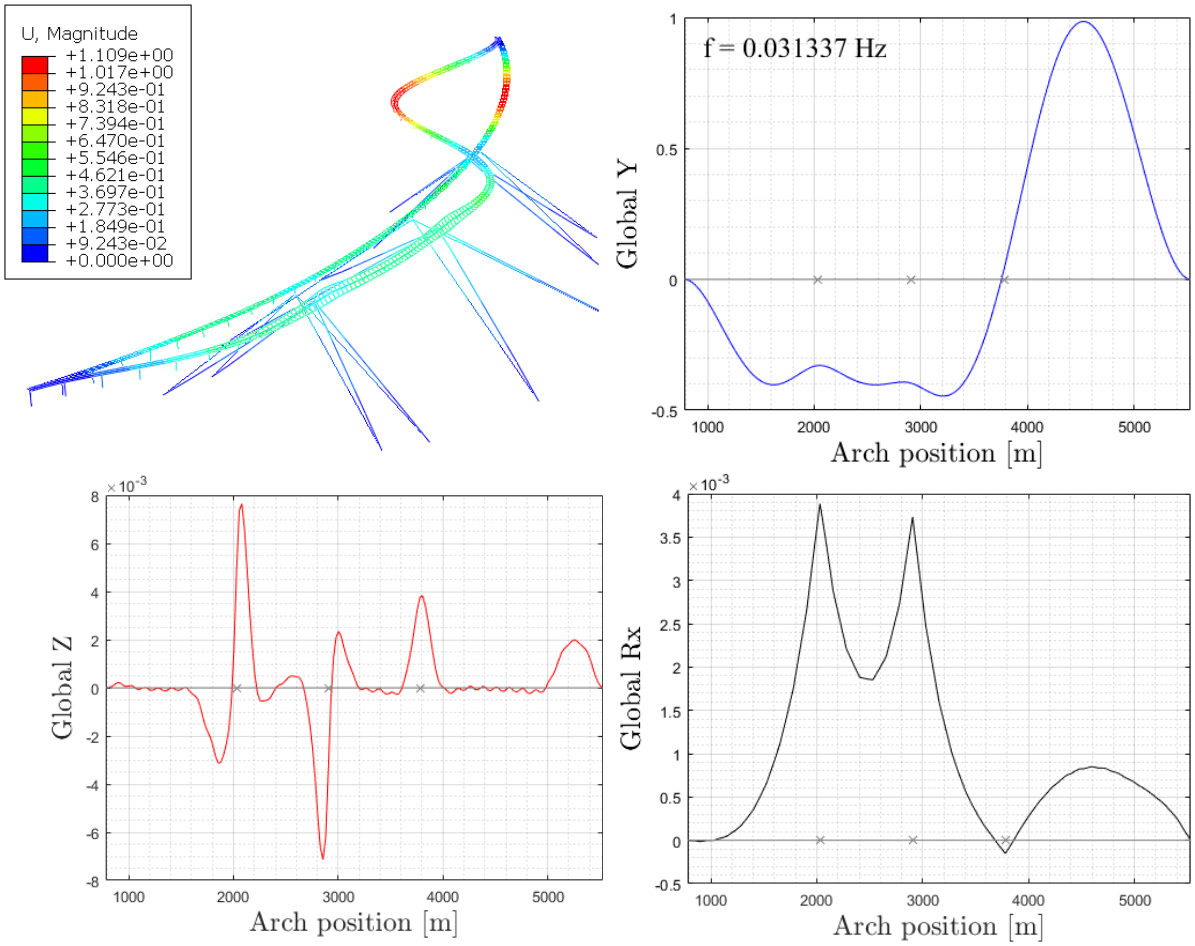

Figure 45: First representative horizontal eigen-mode of the bridge – mode nr 1 (upper left corner: mode shape of the structure; right column and bottom left corner: the corresponding mode shapes in three directions: global Y, global Z and global Rx, the grey line indicates the reference bridge location).

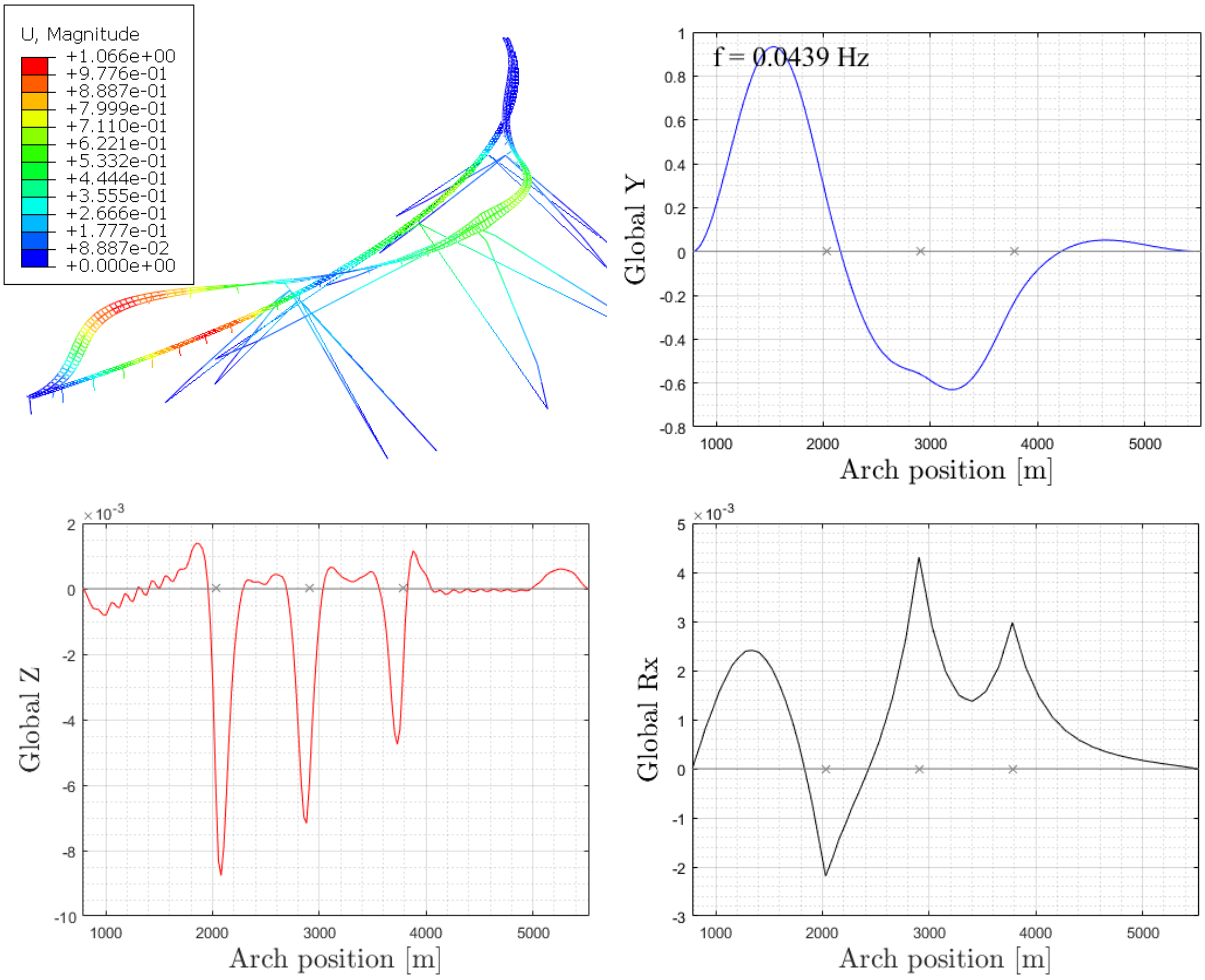

Figure 46: Second representative horizontal eigen-mode of the bridge – mode nr 2 (upper left corner: mode shape of the structure; right column and bottom left corner: the corresponding mode shapes in three directions: global Y, global Z and global Rx, the grey line indicates the reference bridge location).

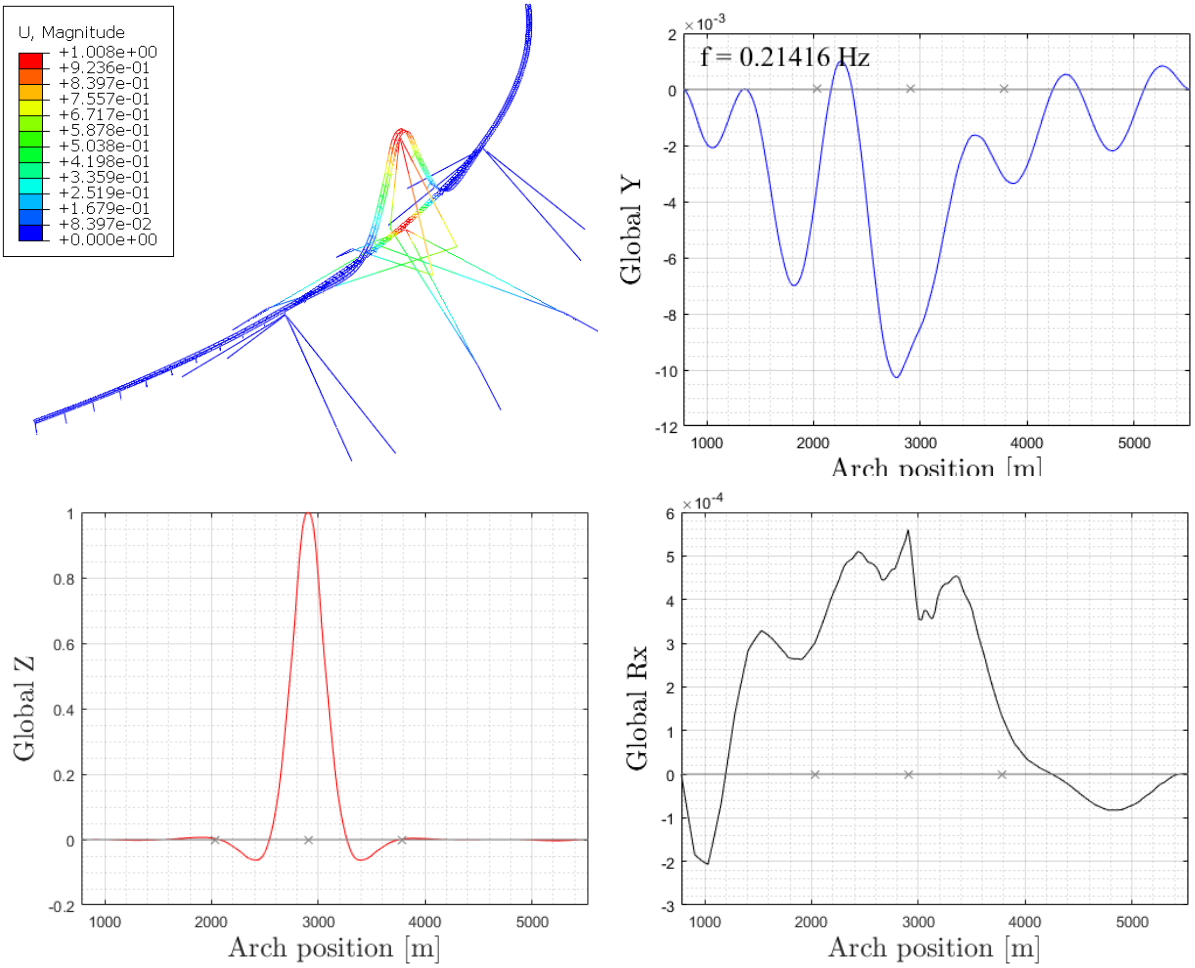

Figure 47: First representative vertical eigen-mode of the bridge – mode nr 60 (upper left corner: mode shape of the structure; right column and bottom left corner: the corresponding mode shapes in three directions: global Y, global Z and global Rx, the grey line indicates the reference bridge location).

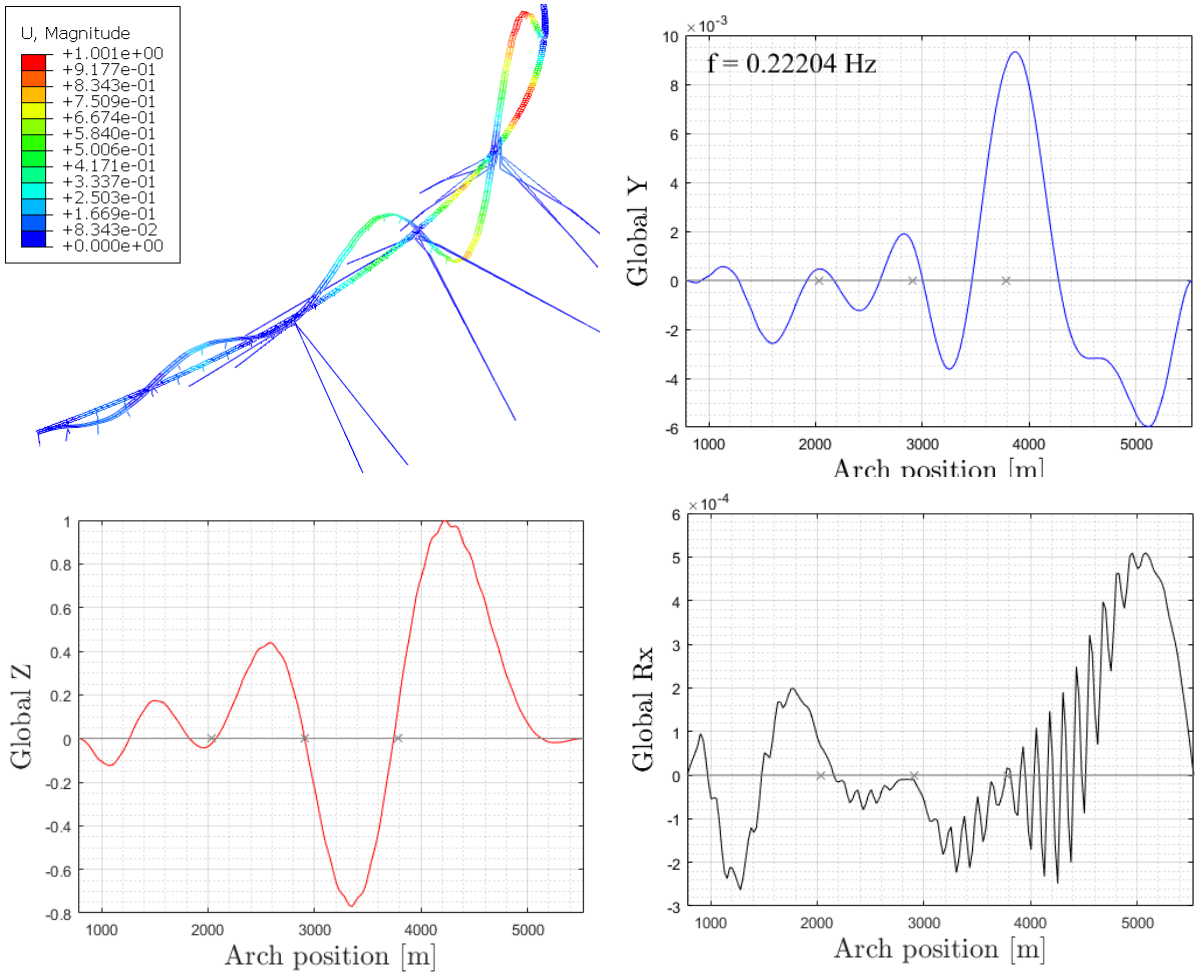

Figure 48: Second representative vertical eigen-mode of the bridge – mode nr 65 (upper left corner: mode shape of the structure; right column and bottom left corner: the corresponding mode shapes in three directions: global Y, global Z and global Rx, the grey line indicates the reference bridge location).

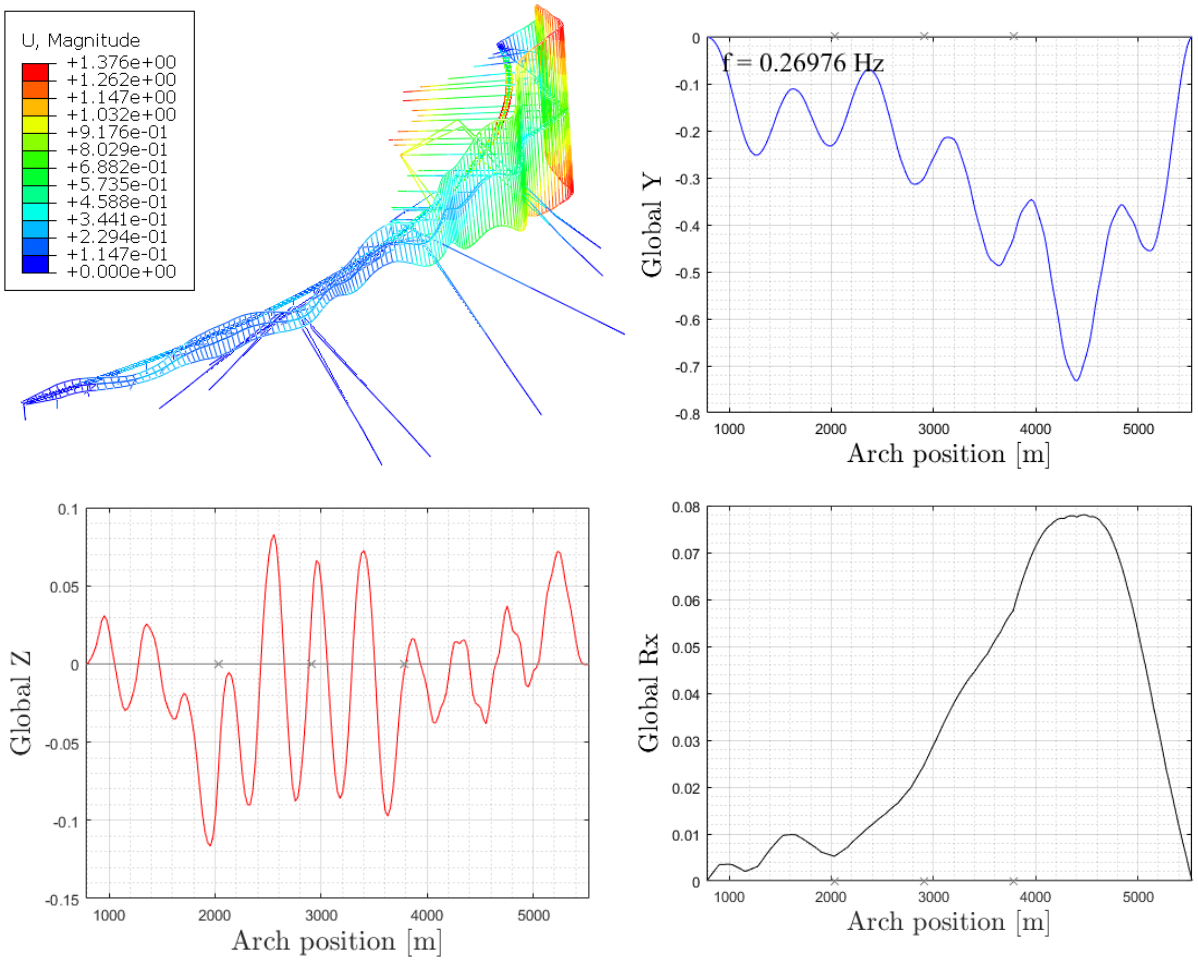

Figure 49: First representative torsional eigen-mode of the bridge – mode nr 83 (upper left corner: mode shape of the structure; right column and bottom left corner: the corresponding mode shapes in three directions: global Y, global Z and global Rx, the grey line indicates the reference bridge location).

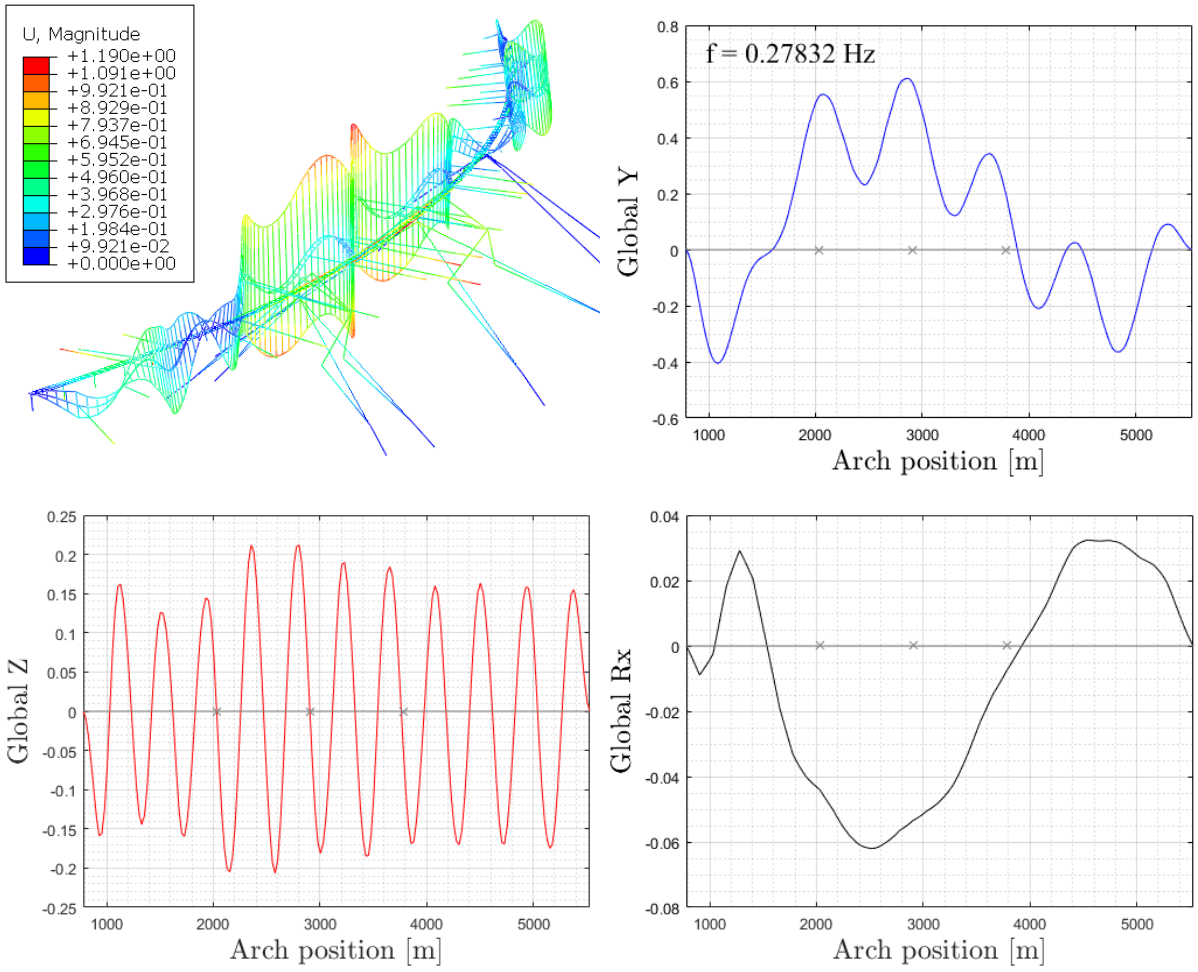

Figure 50: Second representative torsional eigen-mode of the bridge – mode nr 85 (upper left corner: mode shape of the structure; right column and bottom left corner: the corresponding mode shapes in three directions: global Y, global Z and global Rx, the grey line indicates the reference bridge location).

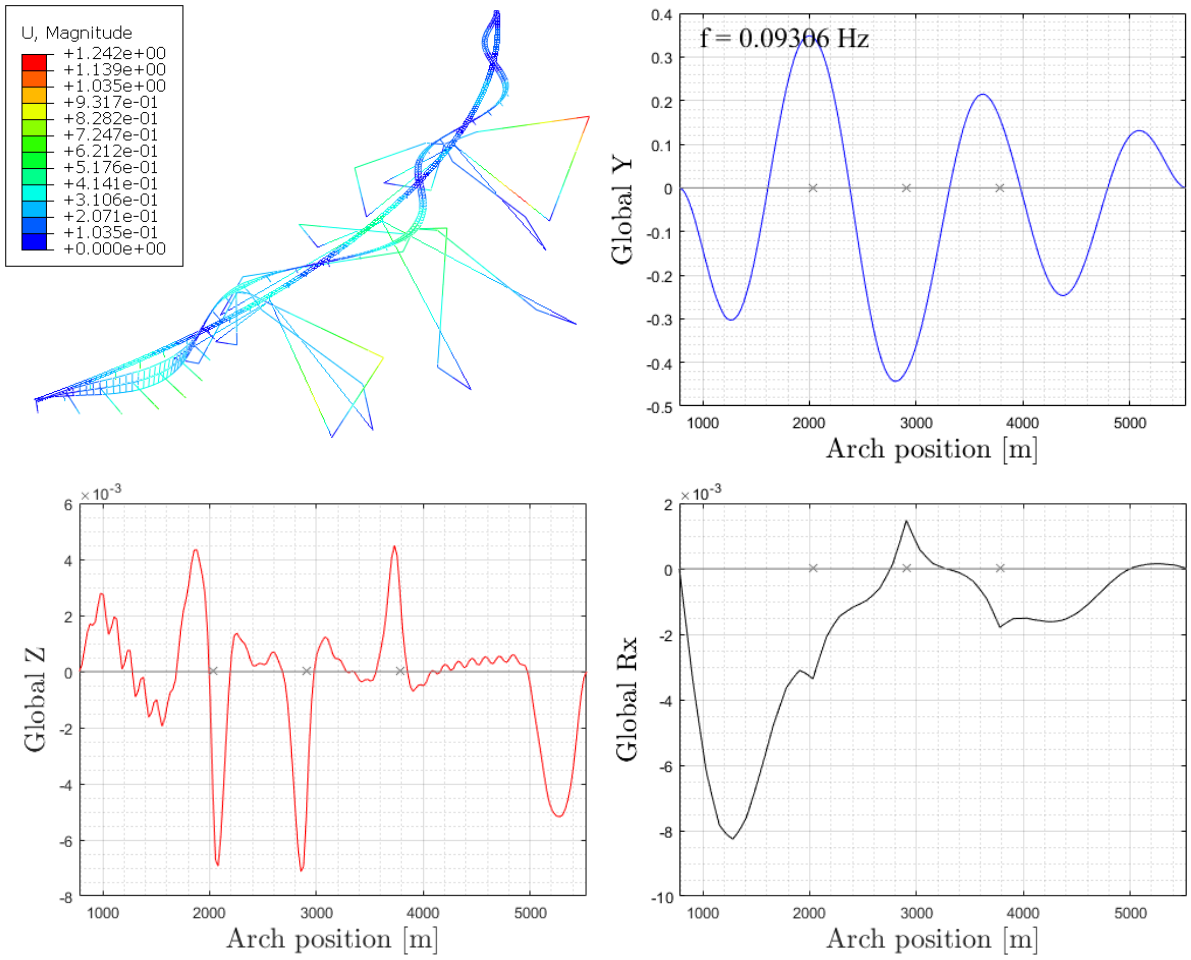

Figure 51: Symmetrical eigen-mode of the bridge girder – mode nr 27 (upper left corner: mode shape of the structure; right column and bottom left corner: the corresponding mode shapes in three directions: global Y, global Z and global Rx, the grey line indicates the reference bridge location).

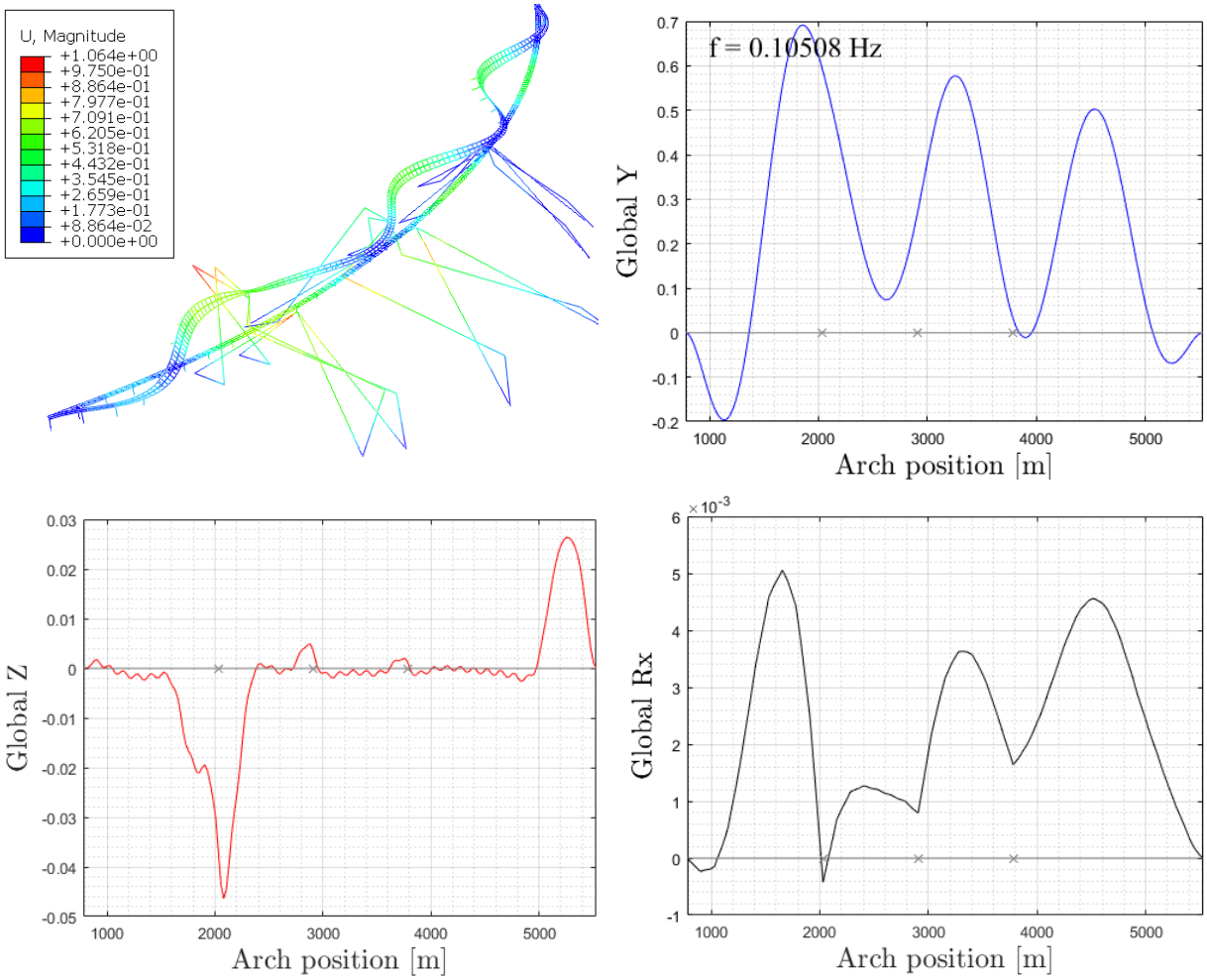

Figure 52: Asymmetrical eigen-mode of the bridge girder – mode nr 30 (upper left corner: mode shape of the structure; right column and bottom left corner: the corresponding mode shapes in three directions: global Y, global Z and global Rx, the grey line indicates the reference bridge location).

The histogram below shows the distribution of the first 100 eigen-frequencies for the low bridge model. The first 100 modes are all below 0.4 Hz. In the range between 0.07 Hz and 0.2 Hz, the mode shapes are governed by the mooring line motion rather than girder motion. The three representative modes in each direction are shown by symbols in the Figure 53.

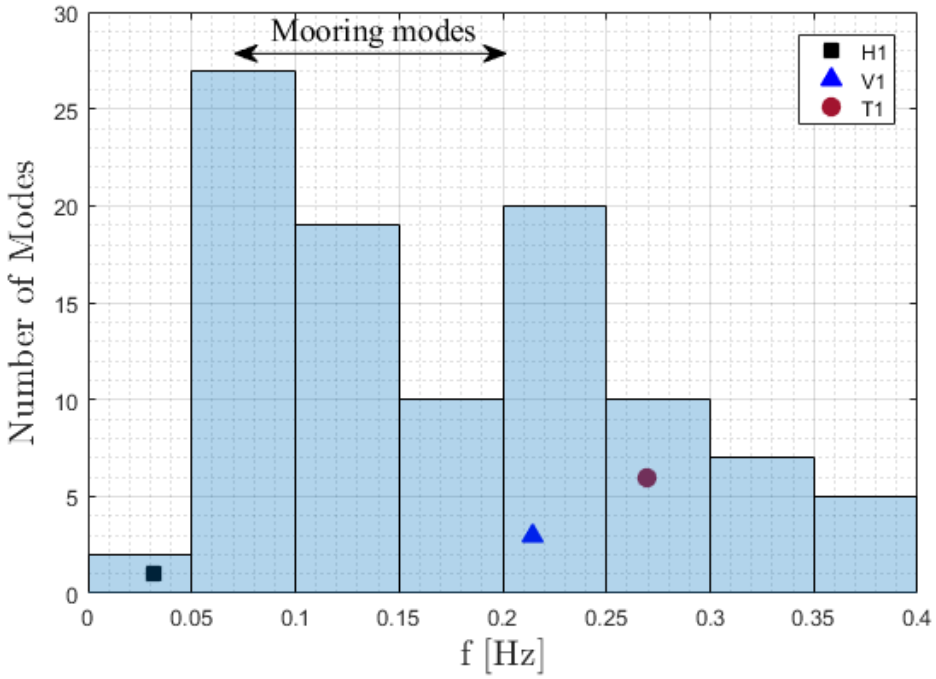

Figure 53: The distribution of the first 100 eigen-frequencies (H1 - first horizontal mode, V1 - first vertical mode, T1 - first torsional mode)

5.2. Eigenfrequency comparison of the low bridge model with and without mooring lines

The mooring lines which provide an additional stiffness mainly in global Y direction were not introduced in the **Concept K11_07** of the bridge where the floating bridge was only anchored at two ends. The following sub-chapter demonstrates the eigenfrequency analysis of the Bjørnafjorden bridge model with and without mooring lines. The first representative modes of each motion for both models are compared and observed to occur earlier in case of the model without mooring lines.

The first dominating horizontal mode appears at the very first mode nr 1 and at low frequency for both models. As it can be evidently observed in the Figure 54, the mode shapes are different and the model without mooring lines presents more horizontal movement. The horizontal

motion in the model with additional stiffness in global Y direction is significantly limited by mooring lines, with a maximum decrease of about 60%.

Table 13: Frequency of the representative first horizontal mode for both models

	Mode no	Frequency [Hz]
Model with mooring lines	1	3.13374E-02
Model without mooring lines	1	1.18992E-02

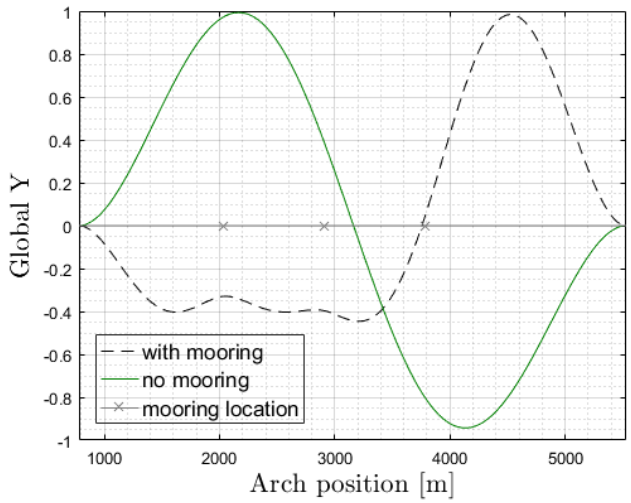

Figure 54: Representative first horizontal mode of both models - mode nr 1

The first dominating vertical mode appears at similar frequency range for both models (Table 14), similarly with the first dominating torsional mode (Table 15). As the mooring lines primarily provide the bridge with horizontal stiffness, the vertical movement and the rotational movement will hence not be decreased remarkably.

Table 14:Frequency of the representative first vertical mode for both models

	Mode no	Frequency [Hz]
Model with mooring lines	60	0.21416
Model without mooring lines	12	0.20568

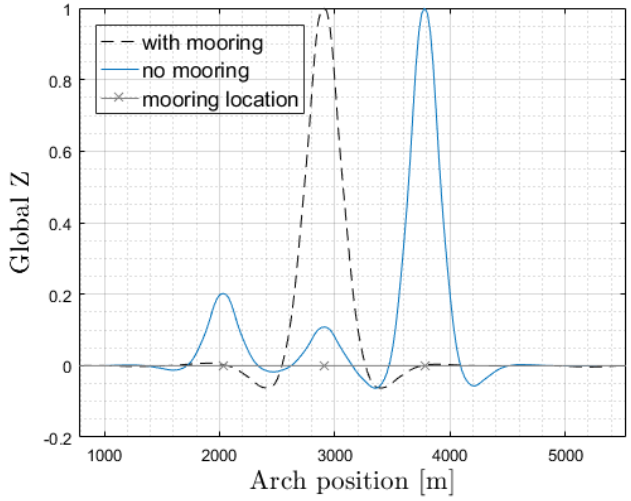

Figure 55: Representative first vertical mode of both models (mode nr 60 in case of the model with mooring lines and mode nr 12 in case of the model without mooring lines)

Table 15: Frequency of the representative first rotational mode for both models

	Mode no	Frequency [Hz]
Model with mooring lines	83	0.26976
Model without mooring lines	34	0.26078

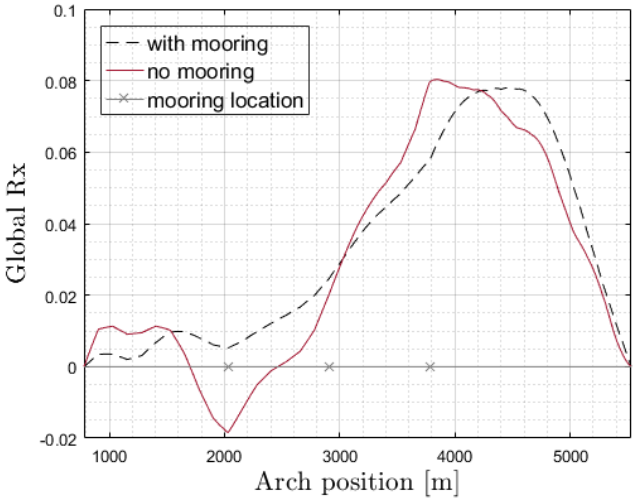

Figure 56: Representative first torsional mode of both models (mode nr 83 in case of the model with mooring lines and mode nr 34 in case of the model without mooring lines)

6. Static analysis under various wind conditions

In this chapter, static response and modal analysis of the low bridge under various static wind conditions are investigated. To compare the bridge response under different static wind loads, various wind directions are considered in the first sub-chapter 6.1. The comparison of mode shape under selected critical wind directions and under no static wind is made for representative modes in sub-chapter 6.2. In the next sub-chapter 6.3, various wind distributions are studied in addition to the constant wind distribution suggested by the Design basis [24]. These different distributions are as follows:

- constant wind distribution V
- distribution case 1a: linearly varying wind distribution from 0,6 · V at south end to V on the north end
- distribution case 1b: linearly varying wind distribution from V at south end to 0,6 · V on the north end
- distribution case 2: linearly varying wind distribution from 0,8 · V at one end to V in the middle of the structure and 0,8 · V at the other end

Moreover, the directional reduction coefficients are considered when generating the static wind speed. The coefficients are suggested by the Design basis [14] and are listed in the Table below.

Table 16: Directional reduction coefficients [14]

Sectors	Reduction coefficients
0° - 75°	0.7
75° - 225°	0.85
225° - 255°	0.9
255° - 285°	1.0
285° - 345°	1.0
345° - 360°	0.7

6.1. The bridge response under different static wind directions with constant wind distribution

In this section, the low bridge response under various wind directions is investigated. The static wind is considered as uniformly distributed. There are 35 wind directions studied in total, from 0° to 350° with a spacing of 10°. It should be pointed out that the wind direction in this thesis is 10° different from the real one due to the 10° tilt of the bridge, and hence 0° wind direction refers to actual wind direction 10°.

Remarkable difference in the maximum horizontal displacement (global Y direction) can be observed even when the wind directions vary just by 20°; 0,1 meter difference between wind direction 20° and 0° referring to Figure 57. The horizontal response is strongest under the wind directions that cause asymmetric static wind load to the girder: 40°, 130°, 220° and 310°. This might be due to the curved bridge shape which has better ability to resist the symmetric wind load. Among these directions, it is the direction 310° which causes the maximum horizontal displacement of about 0,4 meters in the middle of the last span referring to Figure 58.

The vertical displacement is relatively small compared to the horizontal displacement and is under 0,2 meters for all wind directions. Similarly to the case of horizontal direction, the maximum vertical displacement is caused by the wind direction 310° and is about 0,2 meters as it can be seen in Figure 60. It is observed from Figure 59 and 60 that relatively large vertical displacements appear at the middle of each bridge sub-span while the displacement is constrained at pontoon locations.

For the global Rx direction, less displacement is found in the middle of the low bridge under the constraints of the mooring lines as it can be seen in Figure 61 and 62. Larger rotation is observed at two ends of the bridge for all wind directions. The maximum twisting is found to be about 0.69 degrees at the northern end under wind direction 260° and 290°.

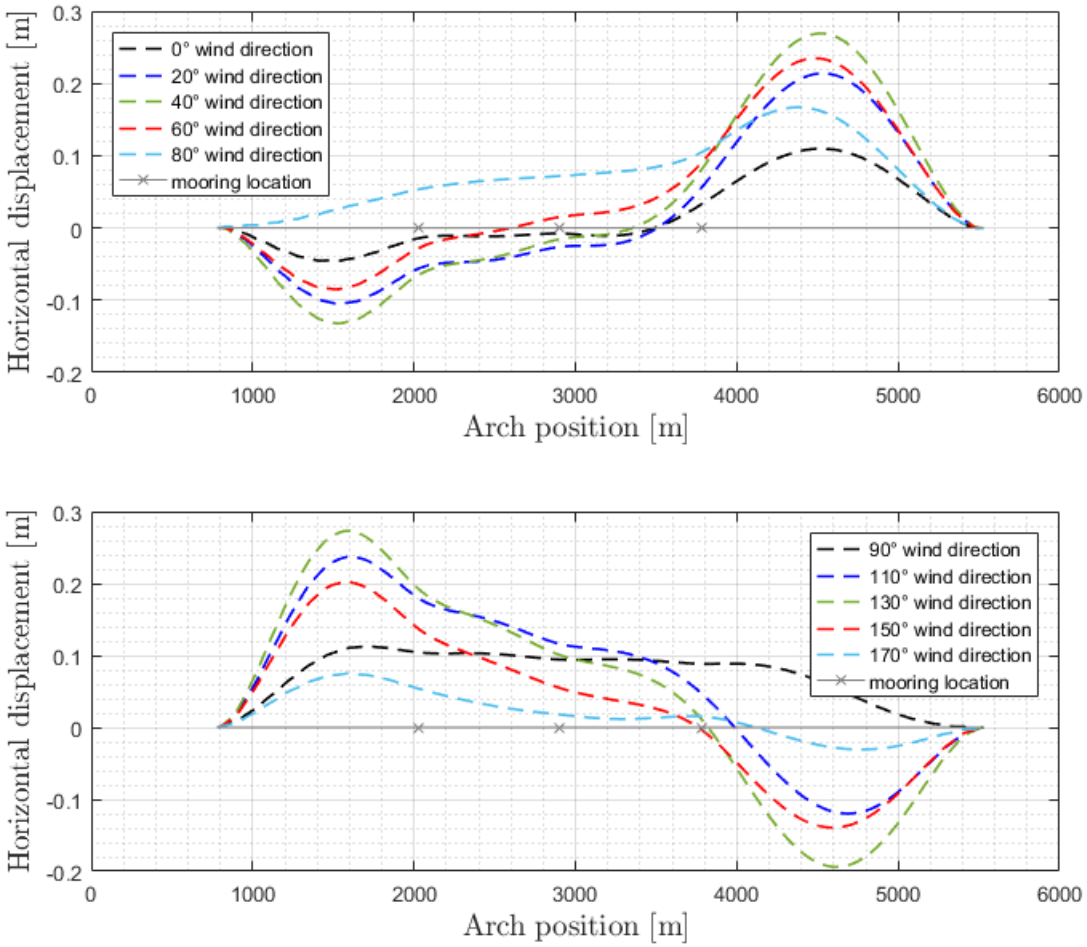

Figure 57: Horizontal displacement in global Y direction of the structure under static wind for selected wind directions from 0° to 170° for constant distribution and considering corresponding reduction coefficients

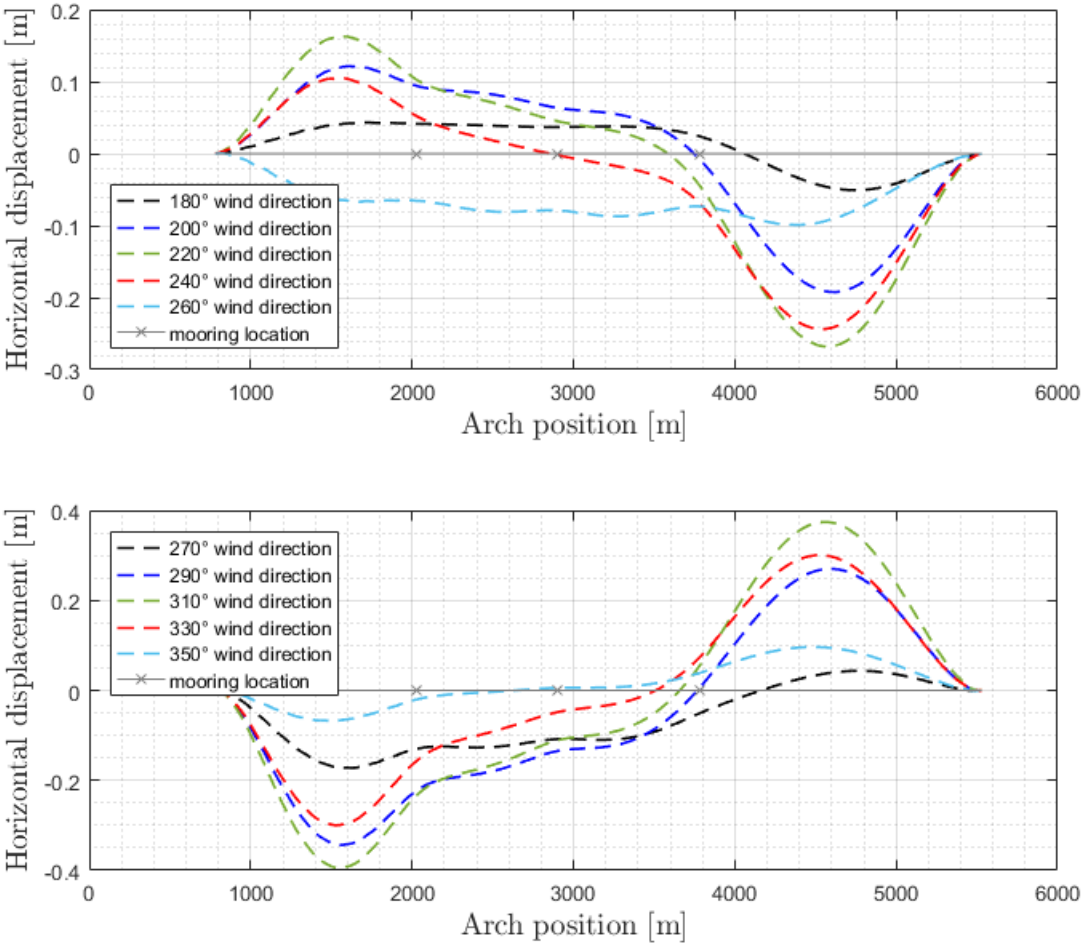

Figure 58: Horizontal displacement in global Y direction of the structure under static wind for selected wind directions from 180° to 350° for constant distribution and considering corresponding reduction coefficients

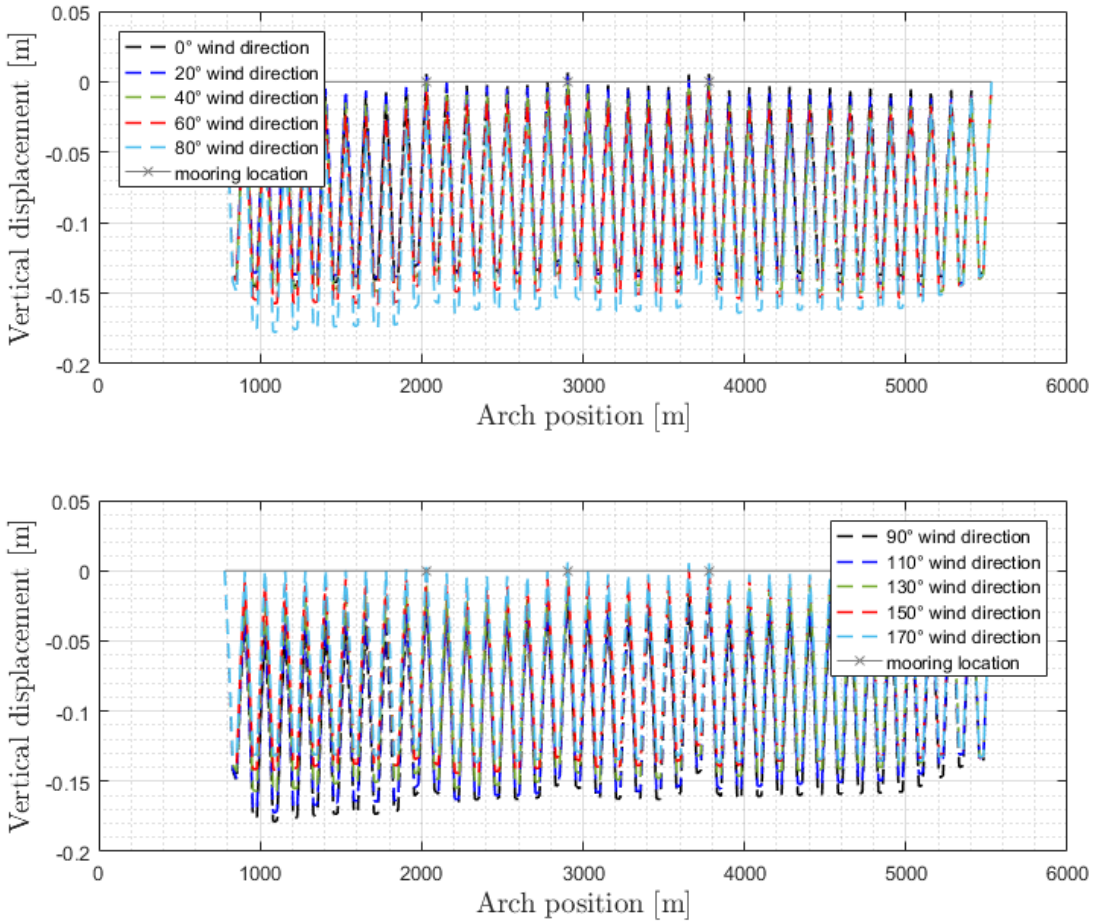

Figure 59: Vertical displacement of the structure under static wind for selected wind directions from 0° to 170° for constant distribution and considering corresponding reduction coefficients

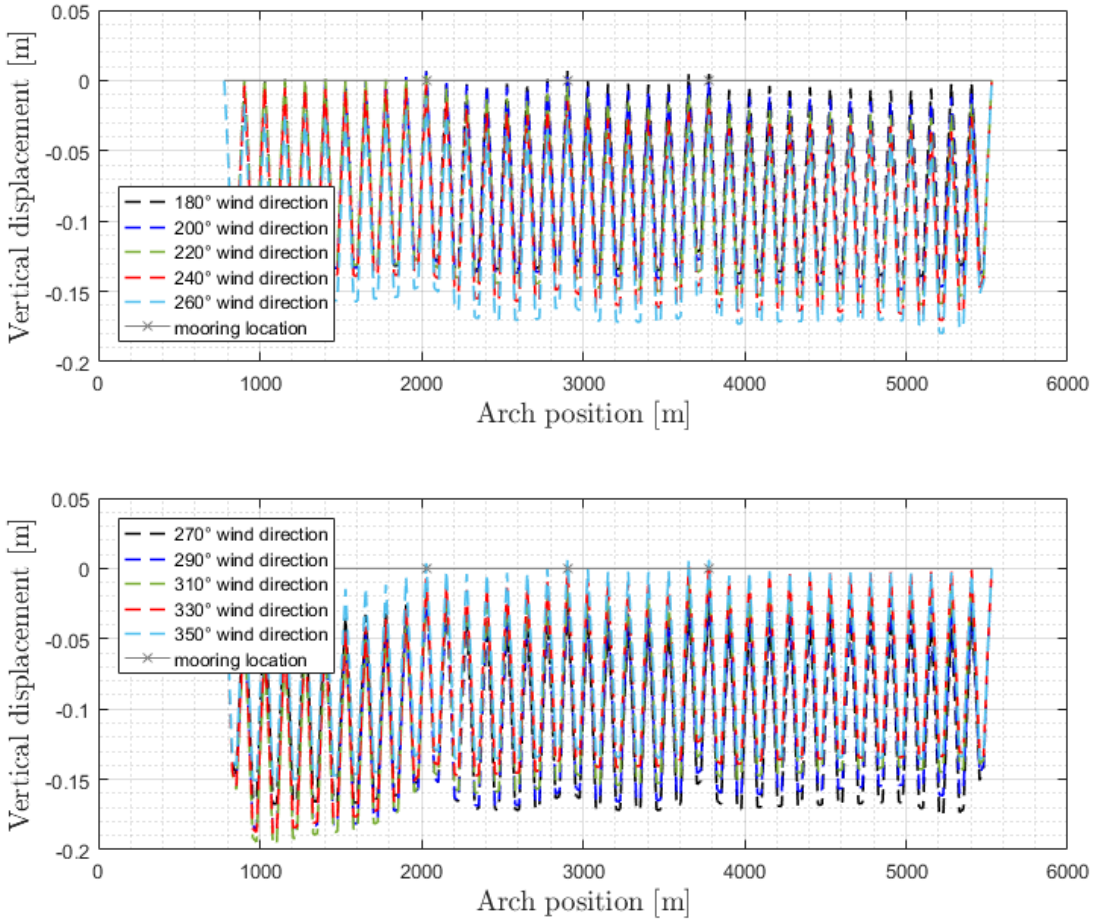

Figure 60: Vertical displacement of the structure under static wind for selected wind directions from 180° to 350° for constant distribution and considering corresponding reduction coefficients

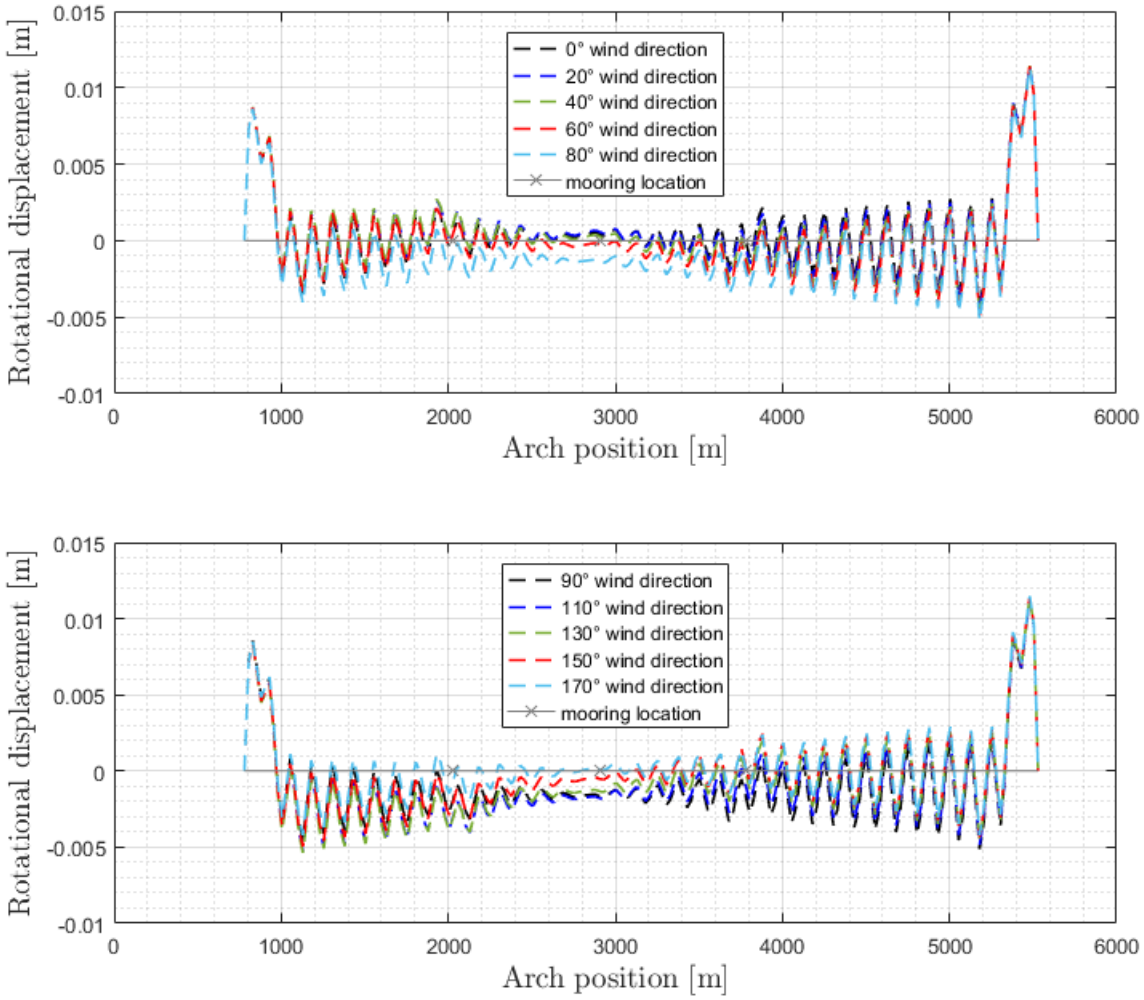

Figure 61: Rotational displacement in global Rx direction of the structure under static wind for selected wind directions from 0° to 170° for constant distribution and considering corresponding reduction coefficients

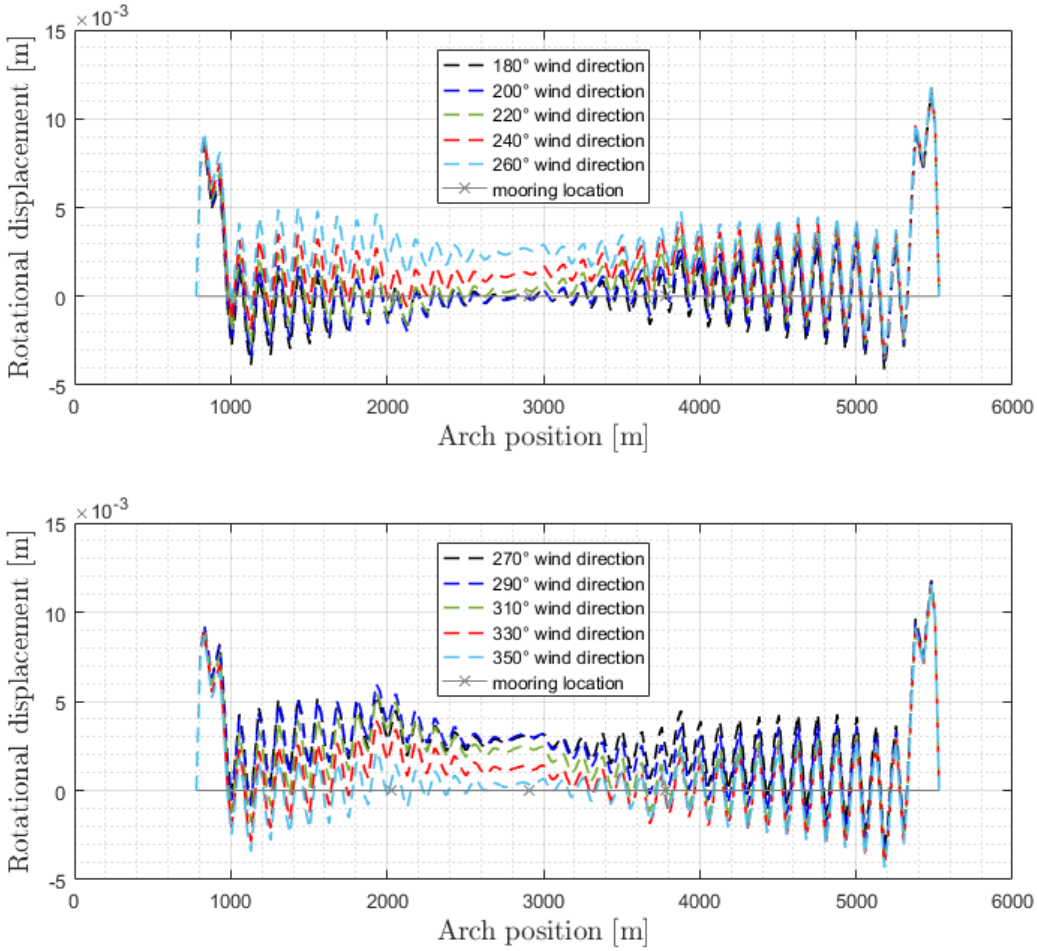

Figure 62: Rotational displacement in global Rx direction of the structure under static wind for selected wind directions from 180° to 350° for constant distribution and considering corresponding reduction coefficients

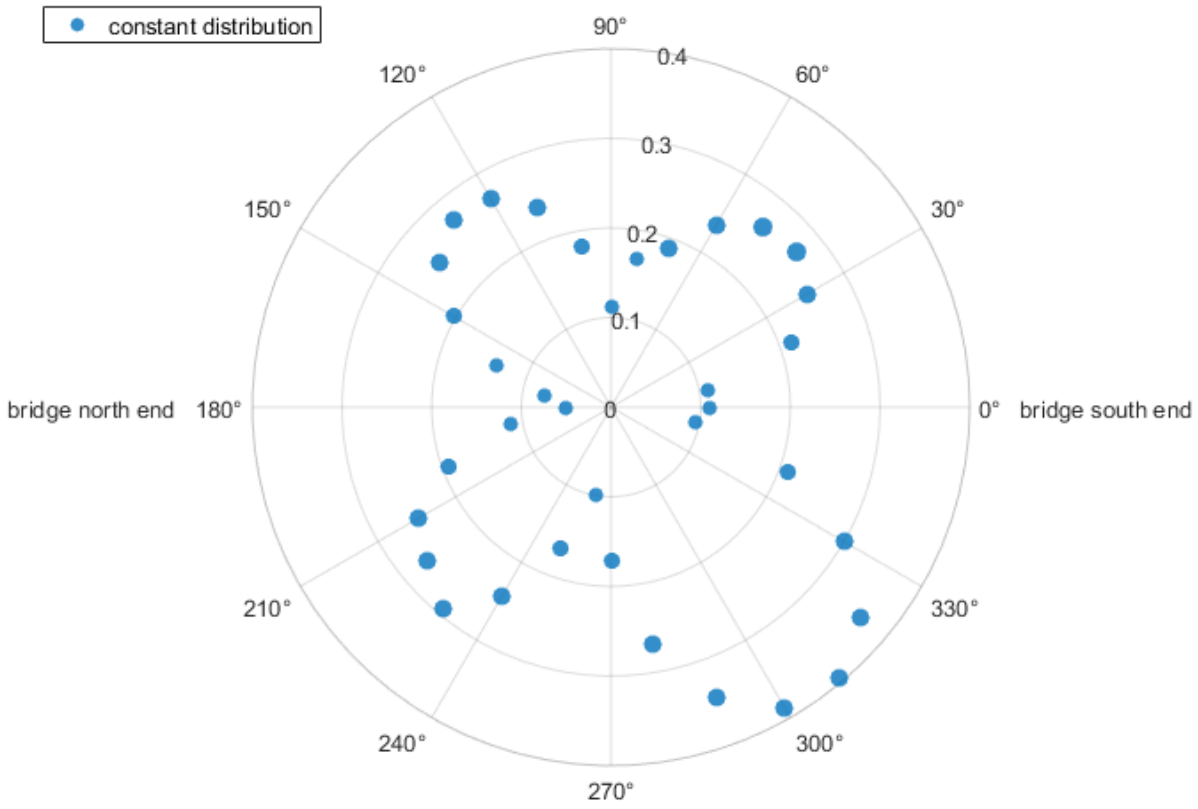

Figure 63: Maximum horizontal displacement under static wind for every 10° from 0° to 350°

6.1. Mode shape comparison

The mode shape is compared with cases without static wind and with selected wind directions for the first horizontal mode, the first vertical mode and the first torsional mode. Wind coming from east (90°) and west (270°) are presented together with critical diagonal wind directions: 40° and 130°. For all wind cases, the first horizontal mode appears at mode number 1, the first vertical mode appears at mode number 60 and mode number 83 for the first torsional mode. The comparison indicates that the mode shapes remain practically the same under various wind directions as under no aerodynamic loads. To get the clear mode shape plots, scaling factors are used to multiply with the displacement. The scaling factor applied to the horizontal displacement is 10^6, while a smaller scaling factor of 10^5 is used for the vertical displacement.

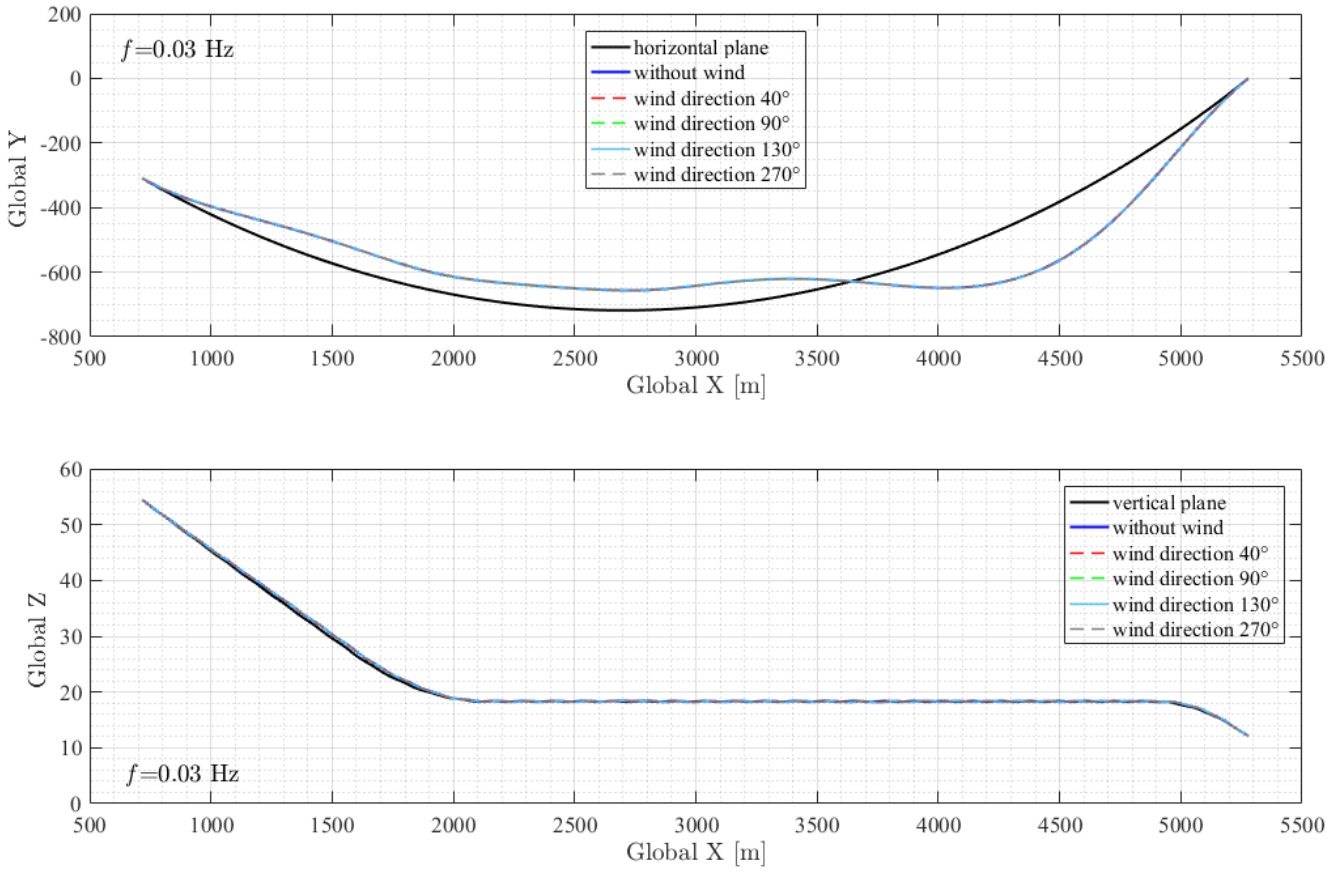

Figure 64: The mode shape of the first horizontal mode (mode nr 1) under static wind for different wind directions and without static wind

Table 17: The comparison of eigen-frequency, the first horizontal mode (mode nr 1)

	No wind	**0°**	**40°**	**90°**	**130°**	**270°**
f [Hz]	0.03134	0.03132	0.03124	0.03117	0.03129	0.031563
T [s]	31.90810	31.92848	32.01024	32.08213	31.95909	31.68267

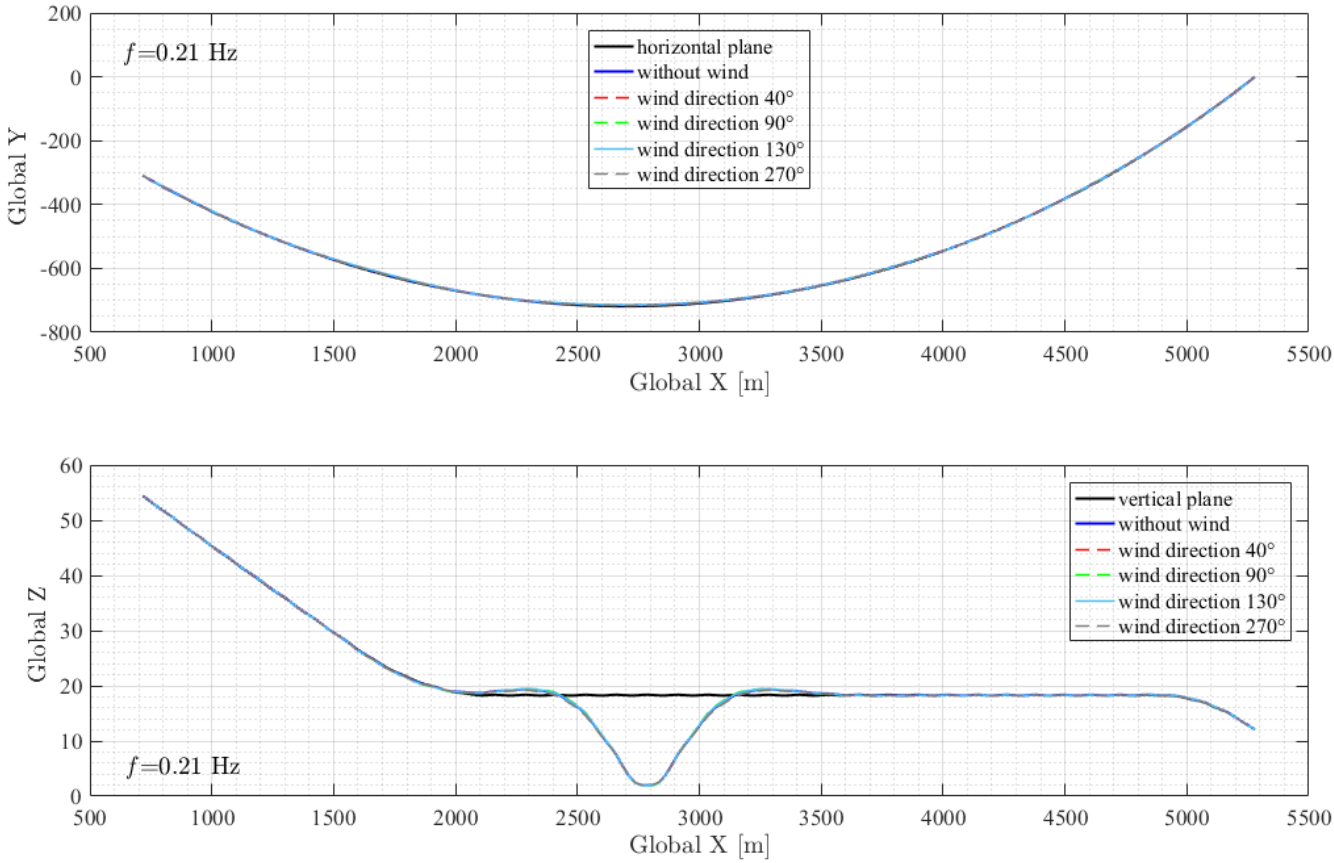

Figure 65: The mode shape of the first vertical mode (mode nr 60) under static wind for different wind directions and without static wind

Table 18: The comparison of eigen-frequency, the first vertical mode (mode nr 60)

	No wind	**0°**	**40°**	**90°**	**130°**	**270°**
f [Hz]	0.21416	0.21415	0.21408	0.21395	0.21406	0.21442
T [s]	4.66941	4.66962	4.67115	4.67399	4.67158	4.66374

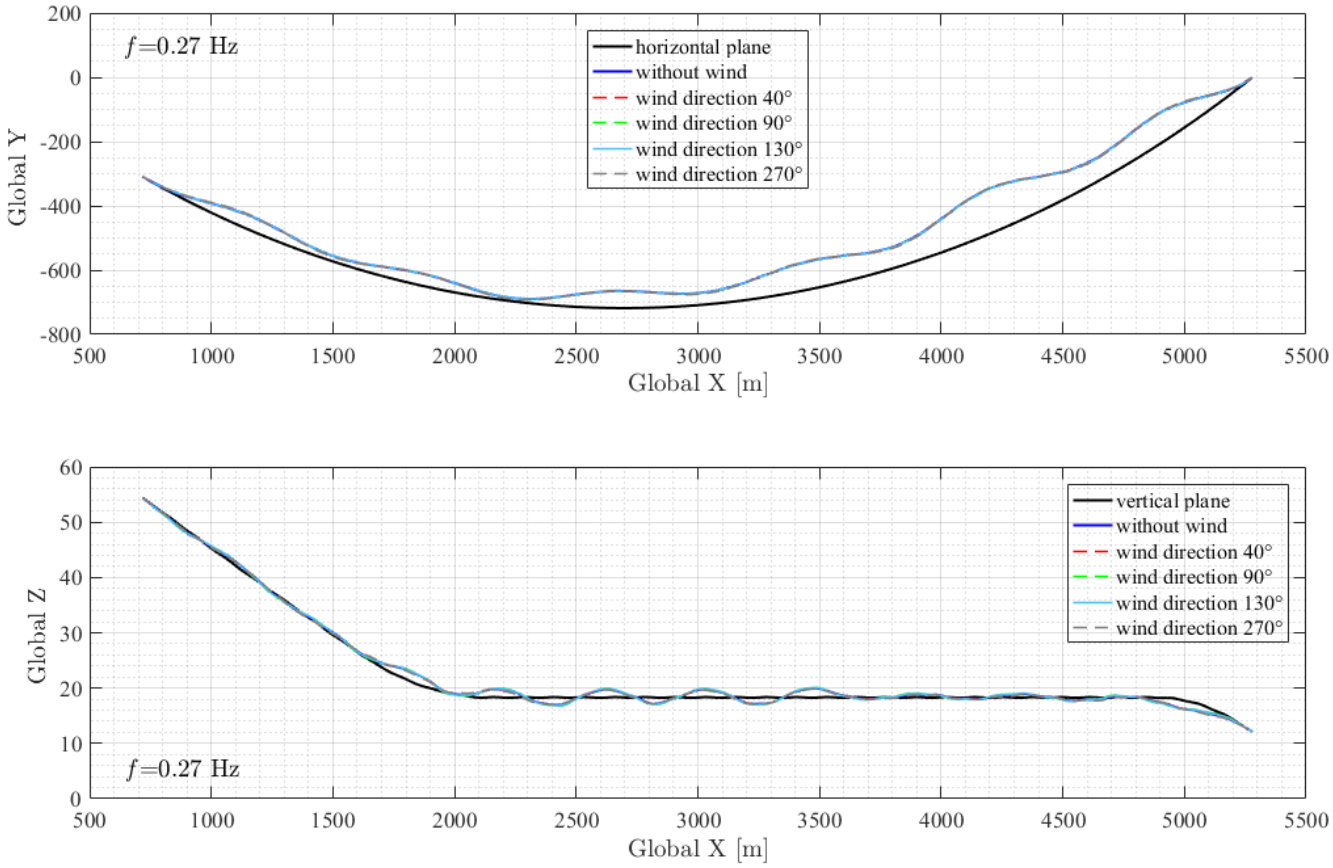

Figure 66: The mode shape of the first torsional mode (mode nr 83) under static wind for different wind directions and without static wind

Table 19: The comparison of eigen-frequency, the first torsional mode (mode nr 83)

	No wind	**0°**	**40°**	**90°**	**130°**	**270°**
f [Hz]	0.26976	0.26973	0.26956	0.26934	0.26959	0.26926
T [s]	3.70699	3.70741	3.70975	3.71278	3.70934	3.71388

6.2. Comparison of wind distributions

The six groups of plots in Figure 68 and 69 illustrate the horizontal, vertical and rotational displacement under the most critical wind directions 40°, 90°, 130°, 220°, 270°, 310° for four different static wind distributions.

The noticeable difference in displacements is observed in global Y direction. The greatest horizontal displacement about 0,4 meter appears in case of wind direction 310° when the uniform distribution and the non-uniform distribution 2 are applied. Under several wind

directions, larger horizontal displacement is caused by non-uniform distributions rather than the uniform distribution as it shows in Figure 68 and 69. It can be seen from the rose plot (Figure 67) that the largest value of the maximum horizontal displacement is given by distribution case 1a when wind direction is in the range 40° – 90°, and 220° –260°. The mentioned two wind direction ranges are close to the wind directions that introduce the symmetric wind load to the girder when uniform distribution is applied. For the distribution 1a, the wind load increases from the bridge south end to the bridge north end and hence the resultant force of the distributed wind load will be moved to the north. Therefore, the resultant wind load given by wind directions near 90° and 270° is no longer symmetric under the non-uniform distribution 1a. For the remaining directions, it is still the constant static wind distribution that gives the largest maximum horizontal displacement. For the vertical and rotational direction, the displacements under three non-uniform distributions remain almost the same as the one caused by the uniform distribution (Figure 68 and 69).

Concluding from the above observation, the safety of the design can be improved by including additional mean wind distributions due to the fact that the uniform wind distribution does not always give the strongest response.

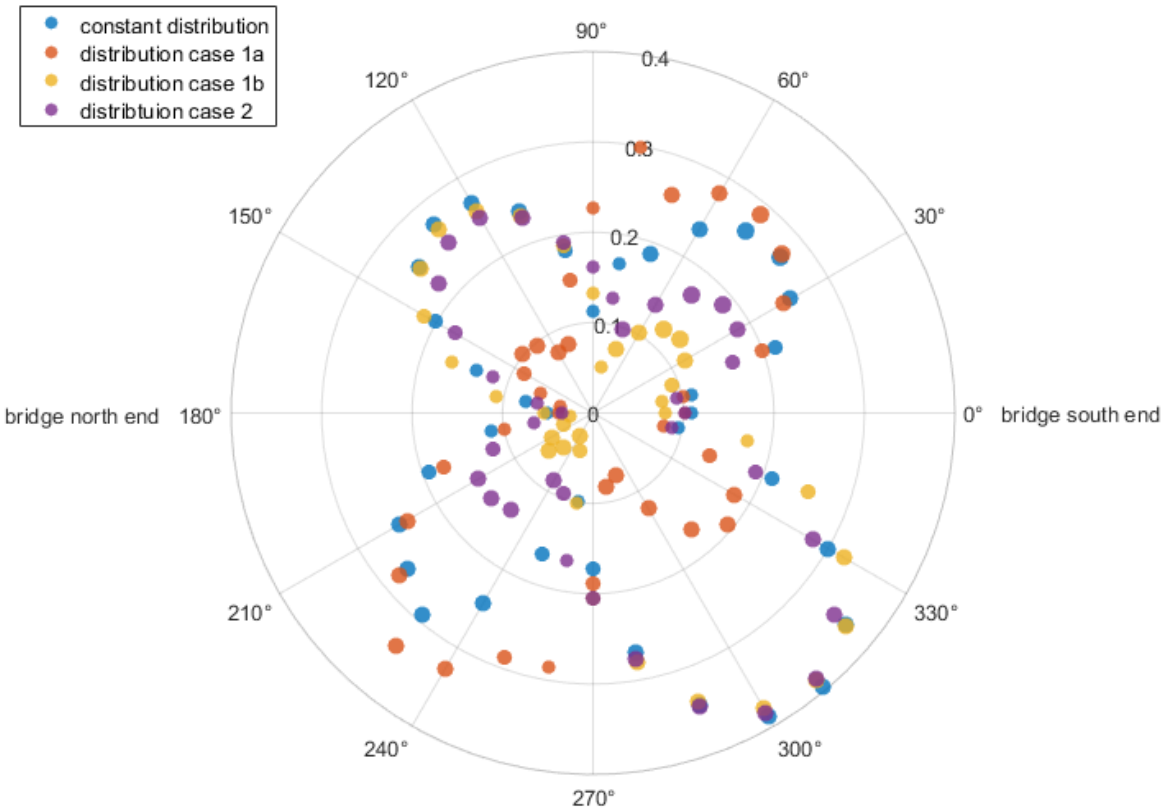

Figure 67: Maximum horizontal displacement (global Y) under static wind for every 10° from 0° to 350° and for four different cases of wind distribution

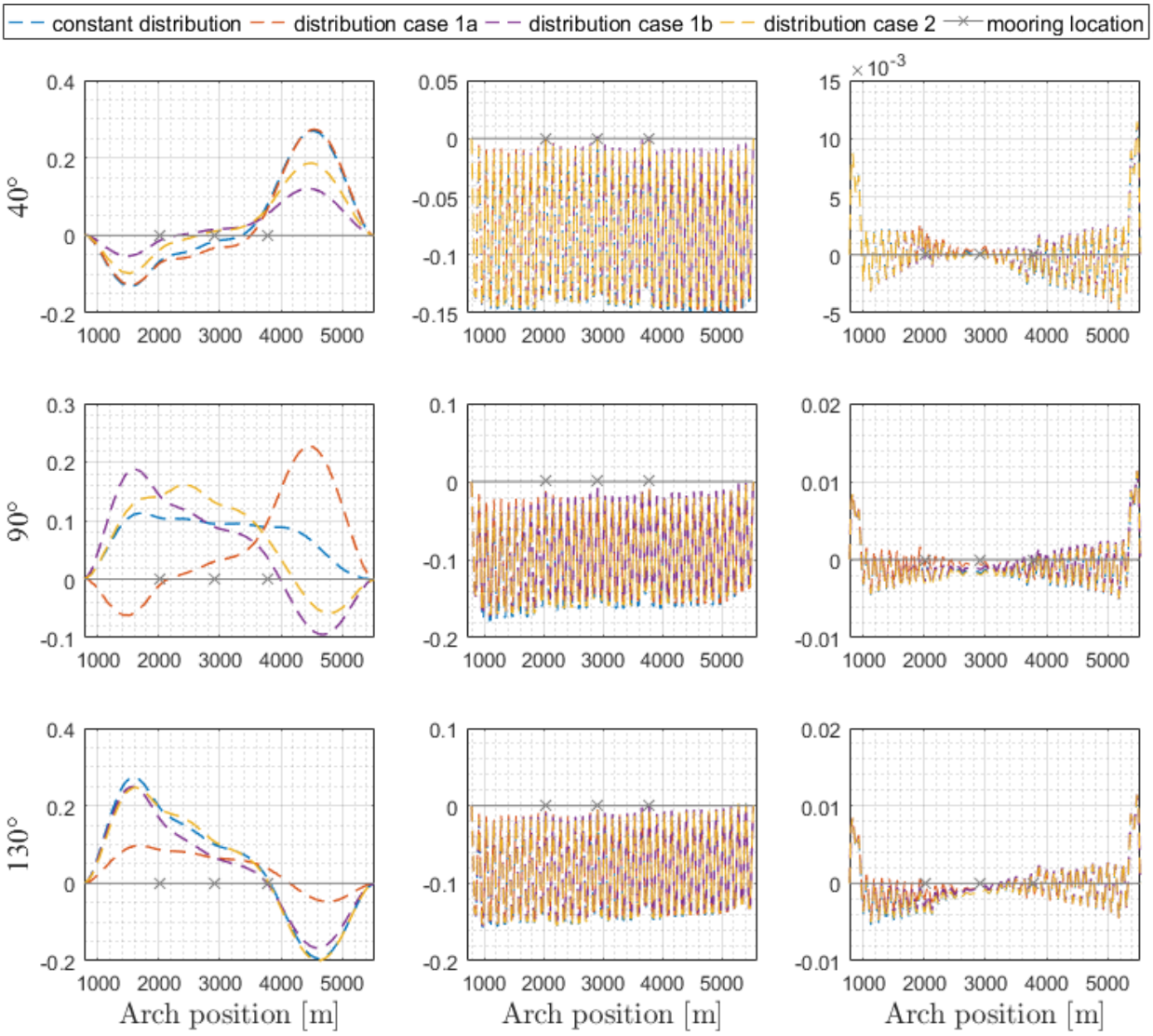

Figure 68: The comparison of four different wind distribution displacements under most critical wind directions: 40°, 90°, 130° (left column: horizontal displacement in global Y direction, middle column: vertical displacement, right column: rotational displacement in global Rx direction)

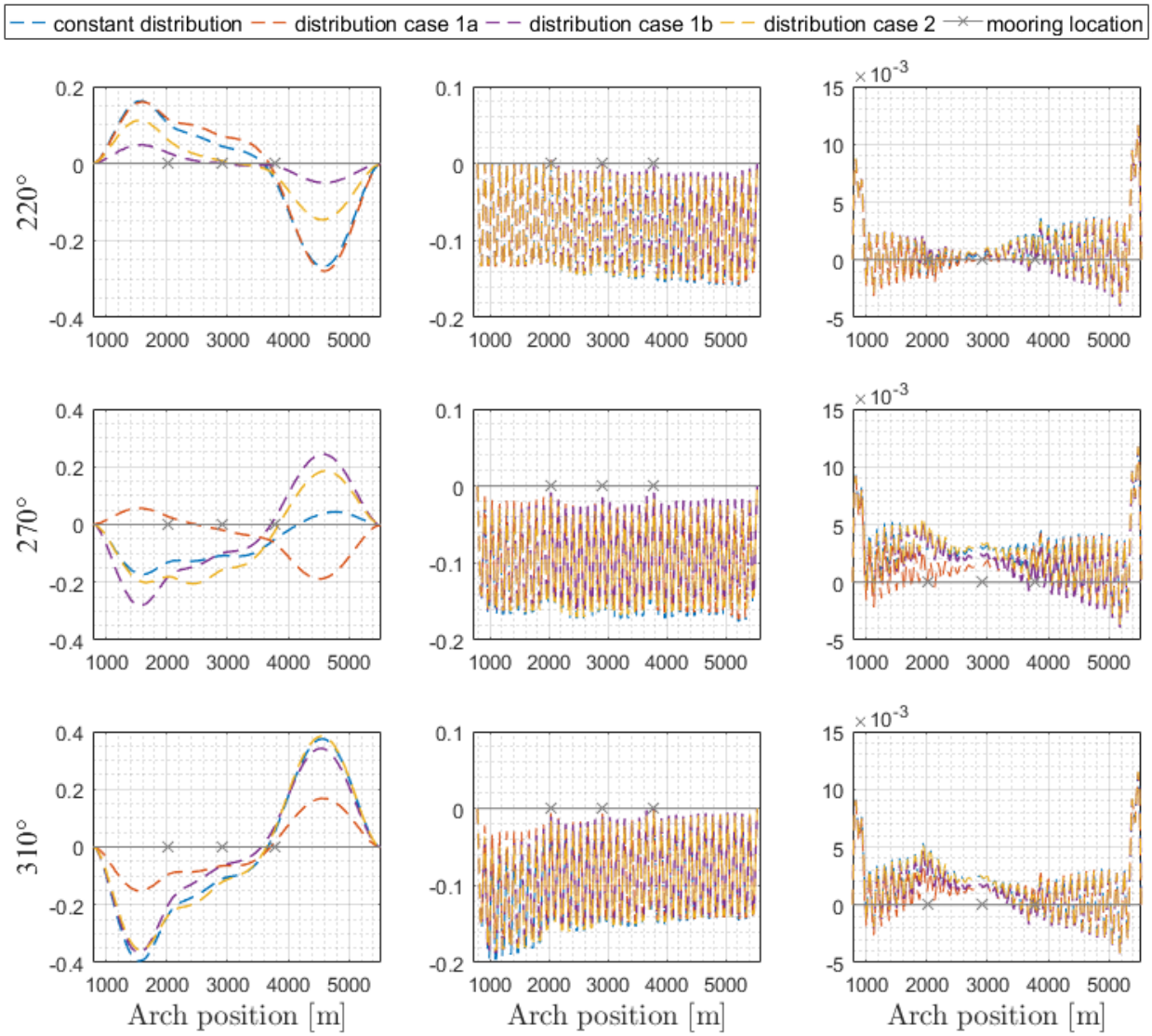

Figure 69: The comparison of four different wind distribution displacements under most critical wind directions: 220°, 270°, 310° (left column: horizontal displacement in global Y direction, middle column: vertical displacement, right column: rotational displacement in global Rx direction)

7. Dynamic analysis

The turbulent wind field was applied on the structure with three groups of coherence parameters. The first group presented in the section 7.1. is a set of spectral and coherence parameters that is recommended in standard N400 [15]. The next two groups consist of representative combination of parameters that are recalculated from the field measurements and provided by the Norwegian Public Roads Administration. The measurements are taken during the storm event at two different points of time: one at 2:00 am and another one at 10:00 am on 1th January 2019 as listed in the table below.

Table 20: Wind parameter groups

	Au	**Av**	**Aw**	**Cux**	**Cuy**	**Cuz**	**Cvx**	**Cvy**	**Cvz**	**Cwx**	**Cwy**	**Cwz**
Standard N400	6.8	9.4	9.4	3	10	10	6	6.5	6.5	3	6.5	3
Group 1 (02:00 am)	4.7	9	7.9	5	6.6	12.4	4	3.4	8.8	5.9	5.4	4.2
Group 2 (10:00 am)	12.8	9	15	3.8	1.15	11	3.1	0.93	8.6	2.8	3.4	3.6

The one-hour wind event simulated based on the standard wind spectral parameters and coherence parameters at height 18.38 meters is presented in the Figure 70. Furthermore, three groups of one-hour wind simulations are compared in the Figure 71.

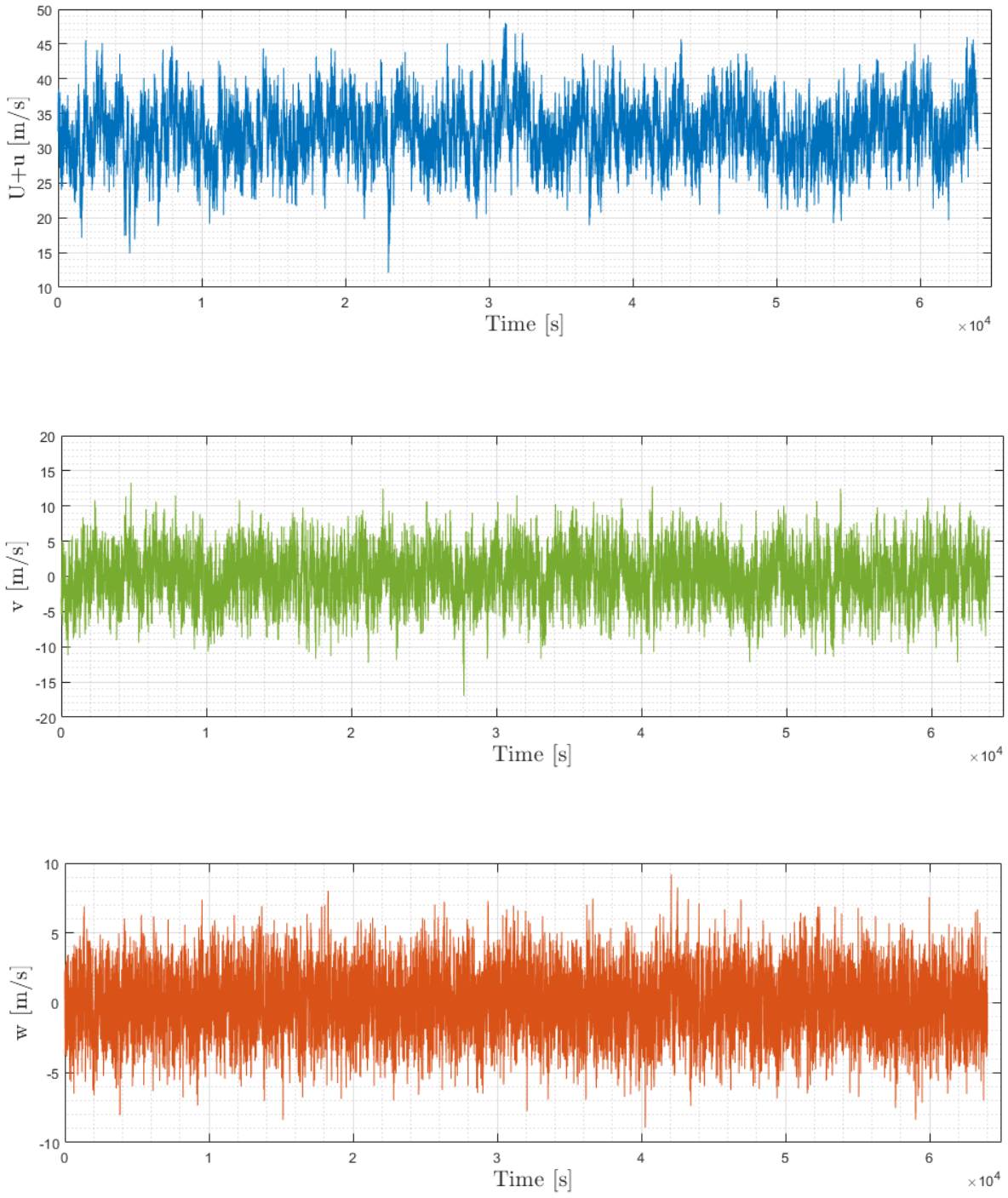

Figure 70: Wind characteristics for one-hour wind simulation at height 18.38 meters with standard wind parameters

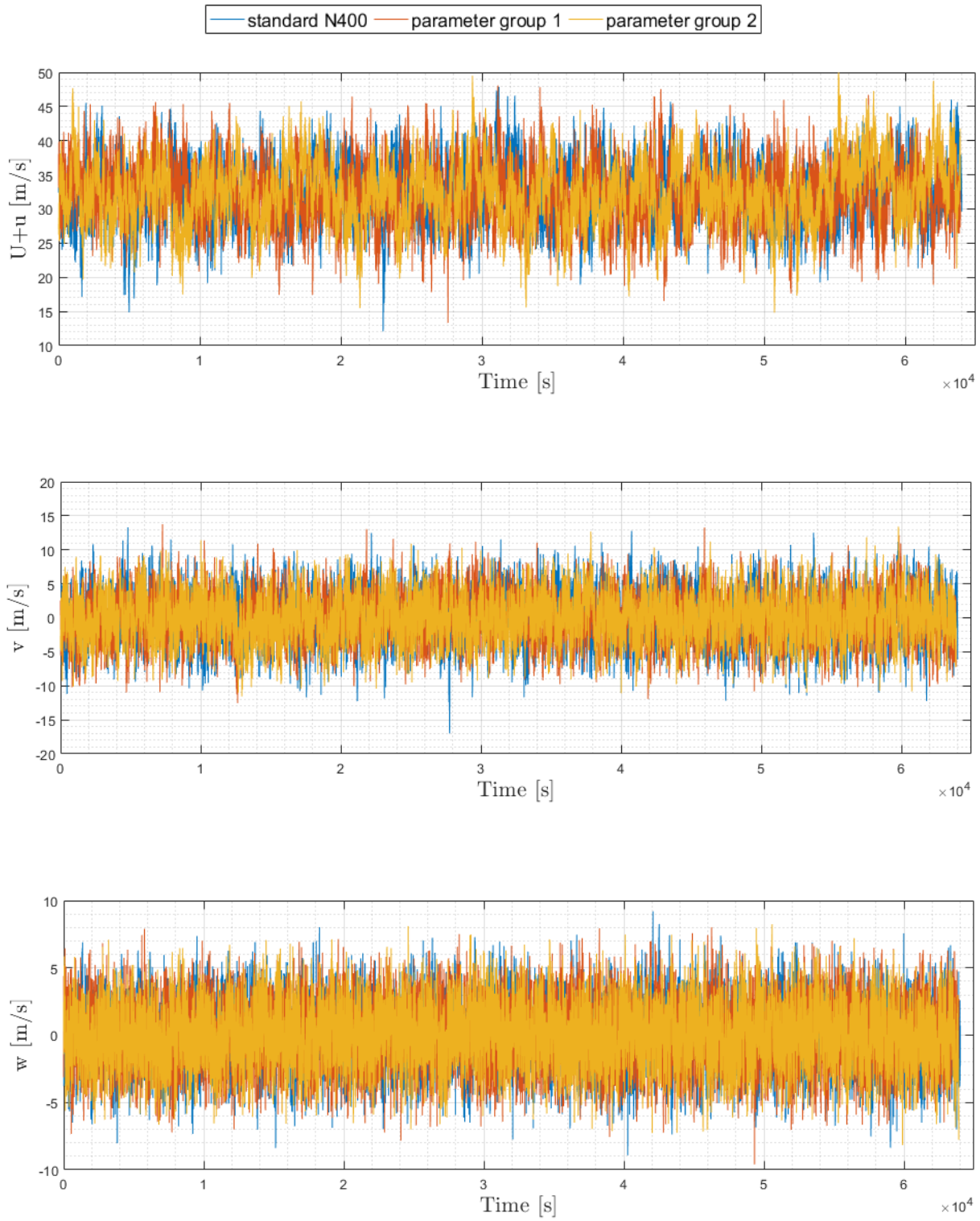

Figure 71: Comparison of wind simulations at height 18.38 meters

7.1. Bridge response under aerodynamic turbulent load

The results in this section presents the low bridge response in three directions: global Y, global Z and global Rx under the wind coming from the east (90°) and west (270°). The plots of the bridge mean displacements and standard deviation are presented based on the averaged results from the six simulated cases. The maximum responses along the bridge in three directions are found among all six realizations and are presented next.

The maximum mean displacement of the girder node in global Y direction is found to be almost 1 meter (Figure 72 (a)) for the wind direction 90° and almost 0,8 meter for the wind direction 270° at 4530 meters distance. It can be clearly observed that the wind direction 90° has a stronger influence on horizontal response of the low bridge and causes about 20% larger displacement at the middle of the last span between last moored pontoon and northern end. The standard deviation of the horizontal displacement (Figure 72 (b)) matches well with the horizontal modal component in the first horizontal mode, referring to Figure 45.

The mean displacement in global Z direction (Figure 72 (c)) of the girder nodes at sub-midspans between pontoons reaches 0,2 meter in negative z downward direction for the wind coming from the east and exceeds 0,2 meter at the last moored pontoon for the wind coming from the west. The comparison of the standard deviation in global Z for both wind directions in Figure 72 (d) shows that the wind coming from the west gives larger standard deviation in global Z with clear rise at the last span between last moored pontoon and end of the bridge.

Furthermore, the Figure 72 (e) indicates that the largest displacements in global Rx direction appear at two ends of the bridge for both wind directions. The rotational motion under the wind coming from the east and west cause the corresponding vertical displacement of the bridge deck edge of about 17 cm. Additionally, the smallest local twisting for both wind direction is observed in the middle of the span between arch position 2500 meters and 3000 meters. The standard deviation plot of the torsional motion is comparable to the torsional mode shape of the first torsional eigen-mode of the bridge what can be seen in Figure 49. The torsional standard deviation in case of wind coming from the wind direction 270° is significantly higher than under the wind coming from the direction 90° what can be seen in Figure 72 (f).

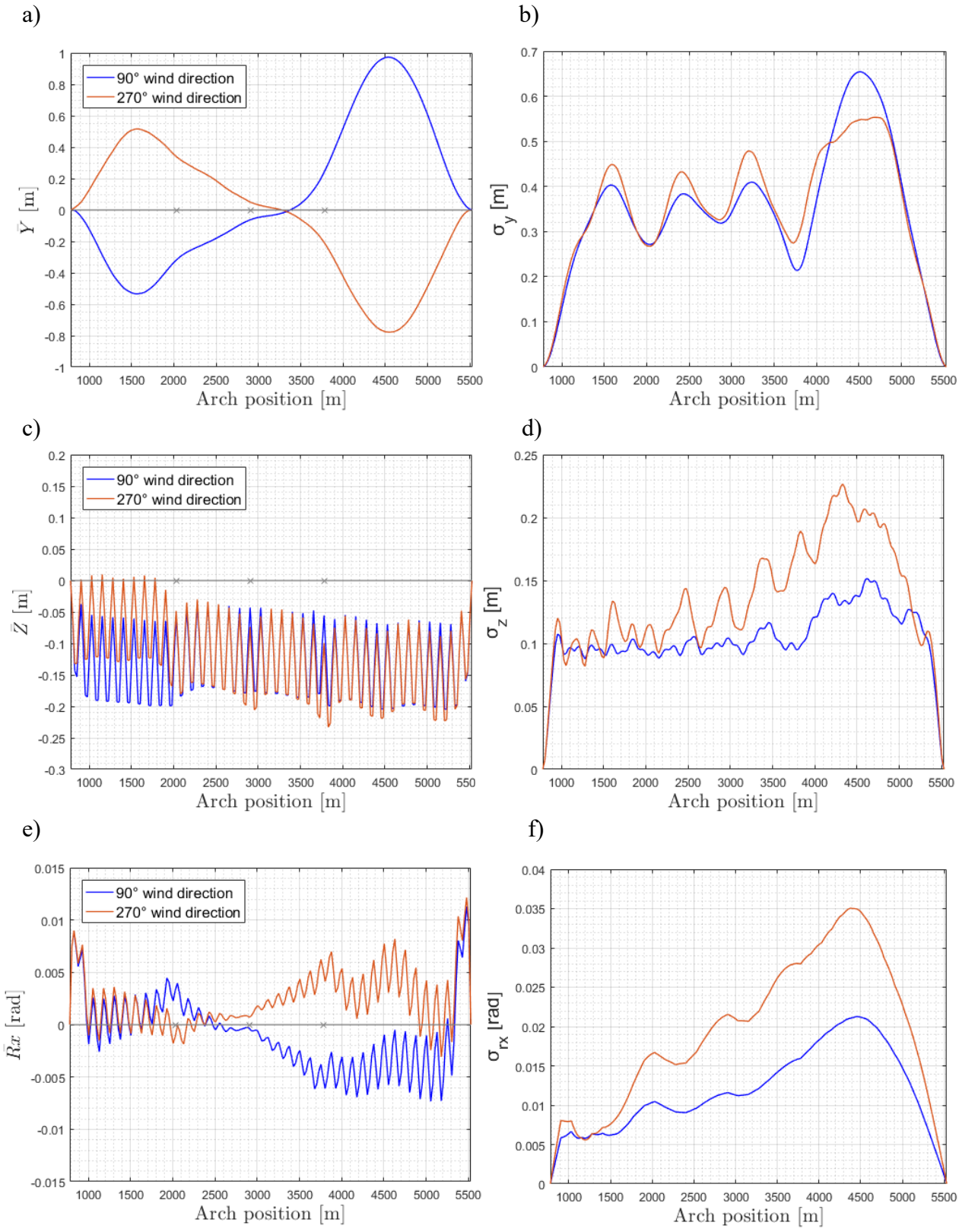

Figure 72: Responses in global Y, global Z and global Rx directions of the Bjørnafjorden bridge under turbulent wind acting from the east (90°) and west (270°) (left column: the mean displacement of the girder, right column: the standard deviation of the girder displacement)

In Figure 73 the maximum response in global Y direction of the low bridge under the wind coming from the east and west is presented. For both wind directions the girder node which displaces the most in global Y direction among all the nodes of the low bridge is node at arch position 4530 meters. Under the wind 90° the mentioned girder (node nr 229) displaces 3,3332 meters in positive global Y direction and 3,2426 meters under the wind 270° in negative global Y direction. The given results indicate that the maximum girder node displacement in global Y direction at arch position 4530 meters is approximately 3% larger under the eastern wind than western wind. Moreover, as can be observed in the Figure 73, the wind direction 270° has more influence on the horizontal response of the southern half of the low bridge.

From the Figure 74 it is clearly observed that the maximum responses in global Z direction of the low bridge girder nodes are noticeably larger under the wind coming from the west (270°) than east (90º). The most displaced girder node under eastern wind is node at arch position 4355 meters indicating downward displacement of 0,9715 meters, while under western wind it is node at arch position 4105 meter with downward displacement of 1,5215 meters.

The Figure 75 demonstrates the maximum girder nodes responses in global Rx direction for both wind directions. The maximum rotational displacements under wind direction 270° are clearly larger with the maximum at arch position 4380 meters equals to 7,1505 degrees. The maximum displacement in global Rx direction is equal to 4,9733 degrees under the wind direction 90° and is found to be at arch position 4430 meters.

It can be concluded from the above results that the wind direction 90° causes larger maximum displacement in global Y direction at the last span of the low bridge and wind direction 270° at the remaining part of the low bridge. Also, that wind direction 270° has stronger influence on displacements in global Z and global Rx directions. Hence the bridge model is more resistant for vertical and torsional displacements when the wind is blowing from 90°.

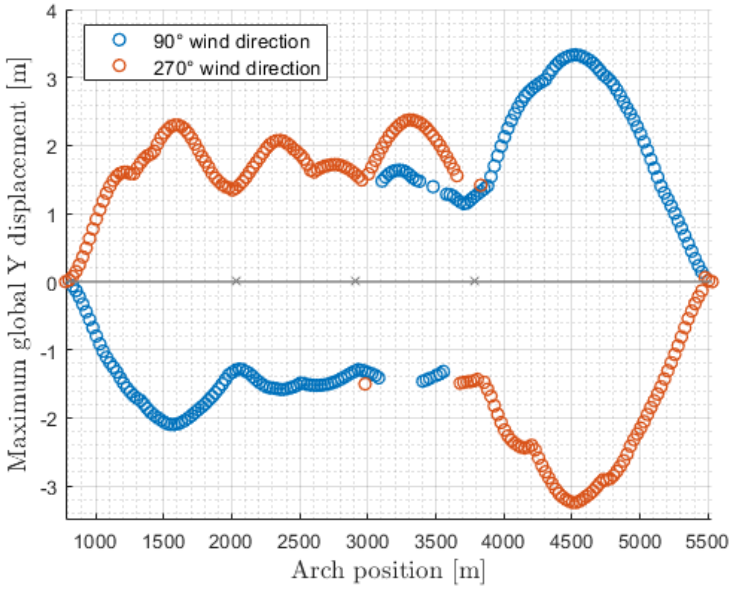

Figure 73: Maximum displacements in global Y direction along the bridge under the wind direction 90° and 270°

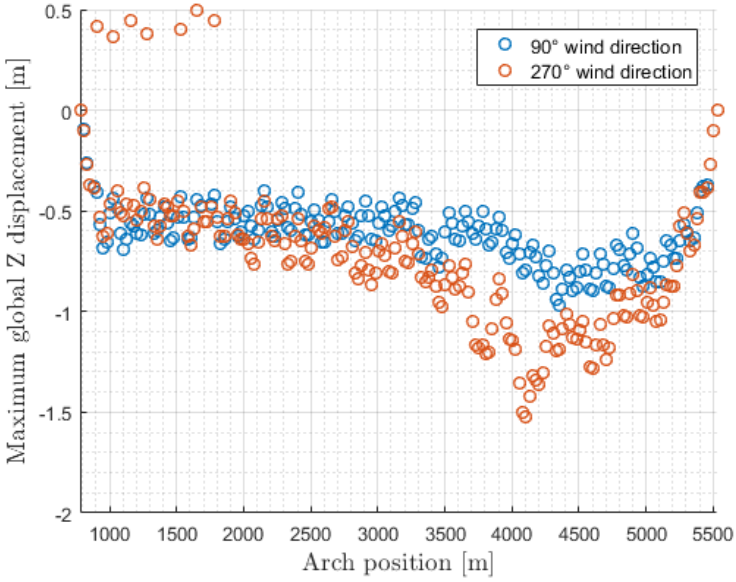

Figure 74: Maximum displacements in global Z direction along the bridge under the wind direction 90° and 270°

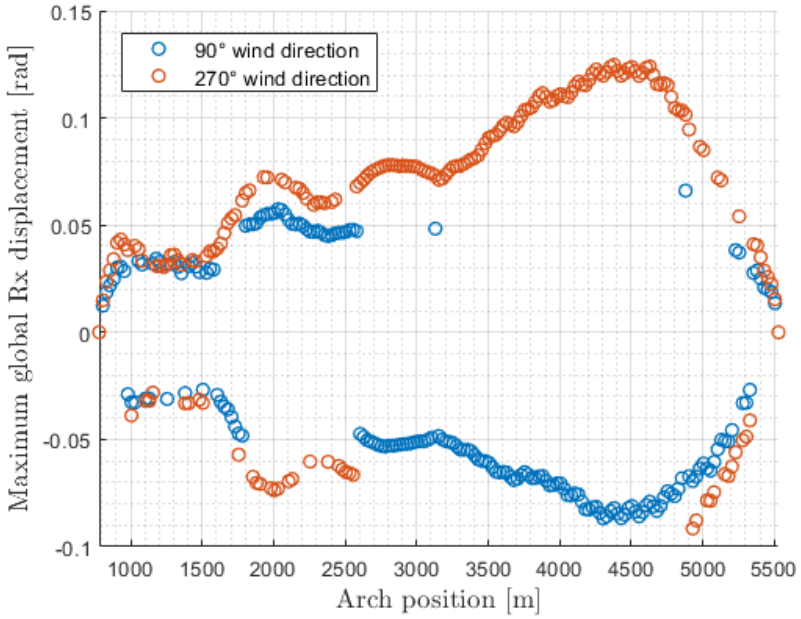

Figure 75: Maximum displacements along the bridge in global Rx direction under the wind direction 90° and 270°

7.2. Coherence parameter groups comparison

Dynamic response under three groups of spectral and coherence parameters is considered in the following section. The mean girder displacements accompanied by standard deviation plots for three directions: global Y, global Z and global Rx are presented first. The maximum responses along the bridge among six realizations for three groups of parameters are found and demonstrated next. At last the mooring line tension forces comparison under two wind directions and for three groups of parameters is presented.

The obtained results imply that the mean displacement in global Y direction for the wind coming from the east (90°) remains nearly the same for all three groups of parameters (Figure 76 (a)). Also, the maximum mean girder node displacement is located at arch position 4530 meters and is found to be the largest in case of standard parameters group. On the other hand, the mean displacement in global Y direction under the wind coming from the west (270°) is largest under parameters group 1 for the low bridge part between arch distance from 2300 to 5500 meters and under standard values for the remaining part (Figure 77 (a)). The maximum response at arch position 4530 meters is the largest in case of group 1. The Figure 77 (b) shows lower horizontal standard deviation for group 1 in comparison to standard values and larger for group 2 for the wind coming from the west. The Figure 76 (b) illustrates the horizontal standard

deviation plot for eastern wind where the differences in standard deviation between groups are smaller.

The mean responses in global Z direction for 90º wind direction are the largest for group 2 with several positions around moored pontoons and at the last span where standard coherence group exceeds these mean values (Figure 76 (c)). In case of 270º wind direction the maximum mean response in global Z appears at last moored pontoon and is the greatest for parameters group 2. As it can be seen in Figure 76 (d) and 77 (d) the standard deviation in global Z in case of the wind blowing from the east 90º and west 270° is larger for standard group for the northern half of the bridge from arch position 3300 meters to 5500 meters. And it is dominated by parameters group 2 for the remaining southern part of the bridge. The smallest standard deviation in global Z is observed for parameters group 1 for both wind directions.

The mean response in global Rx direction is similar among three groups for most of the positions along the bridge with some exceptions where standard group response exceeds other groups responses referring to the Figure 75 (e) and 76 (e). From the Figure 75 (f) and 76 (f) is observed that the torsional standard deviation for the wind coming from the east and west is the largest considering standard parameters and smallest for group 1 of parameters.

Overall, changes in parameters influence the bridge girder response more under the wind direction 270° when the bridge is under tension. The important conclusion from the group comparison is that parameters recommended by standard N400 do not describe the bridge responses under the strong wind conditions accurate enough and hence it is not fully safe to perform the dynamic analysis considering only the values suggested by N400.

a) b)

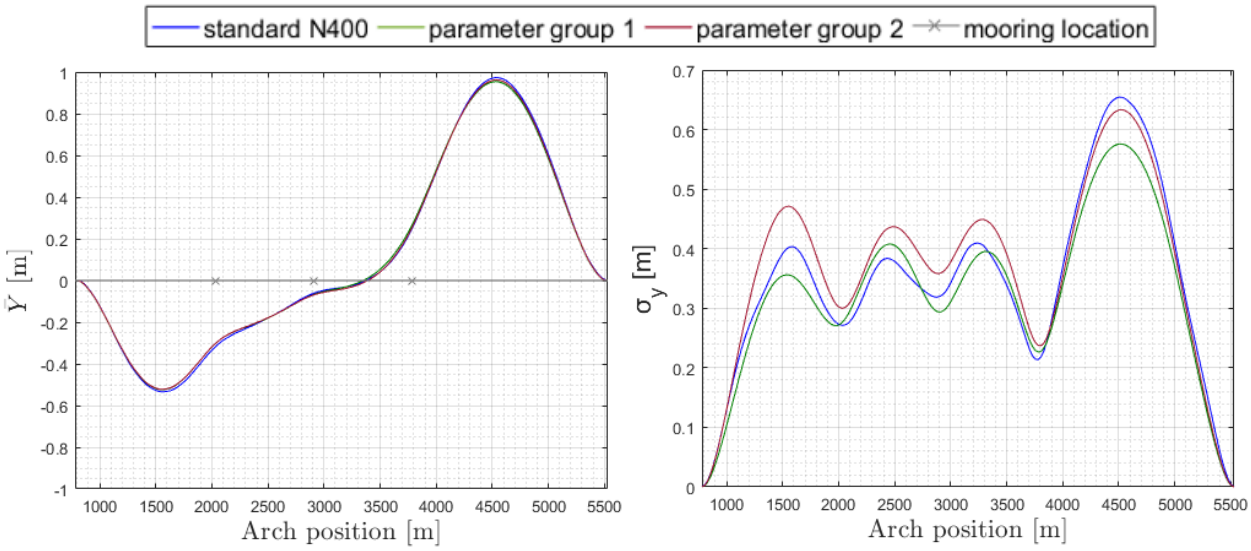

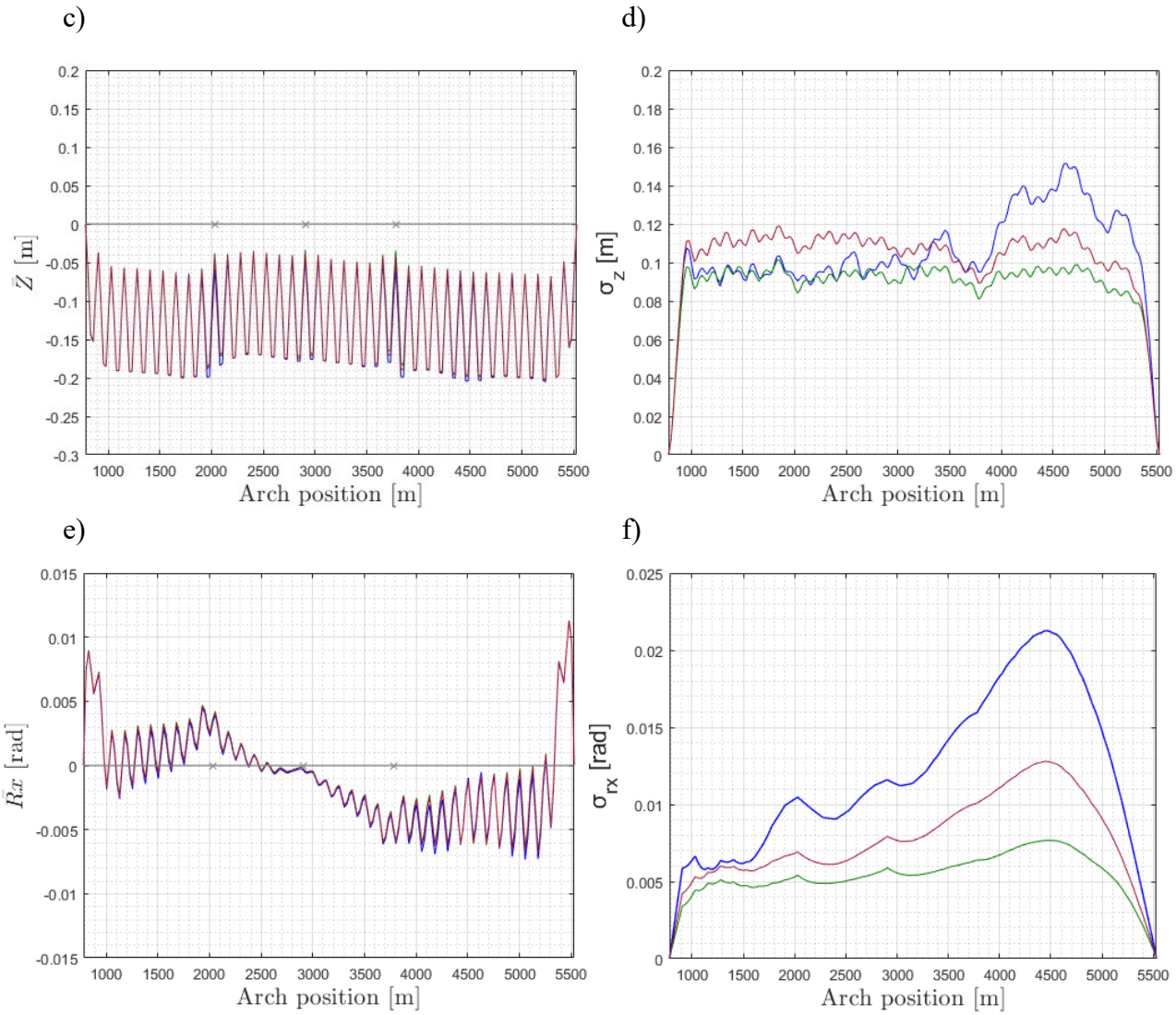

Figure 76: Comparison of responses in global Y, global Z and global Rx of the bridge for three groups of parameters under turbulent wind acting from the east (90°) (left column: the mean displacement of the girder, right column: the standard deviation of the displacement)

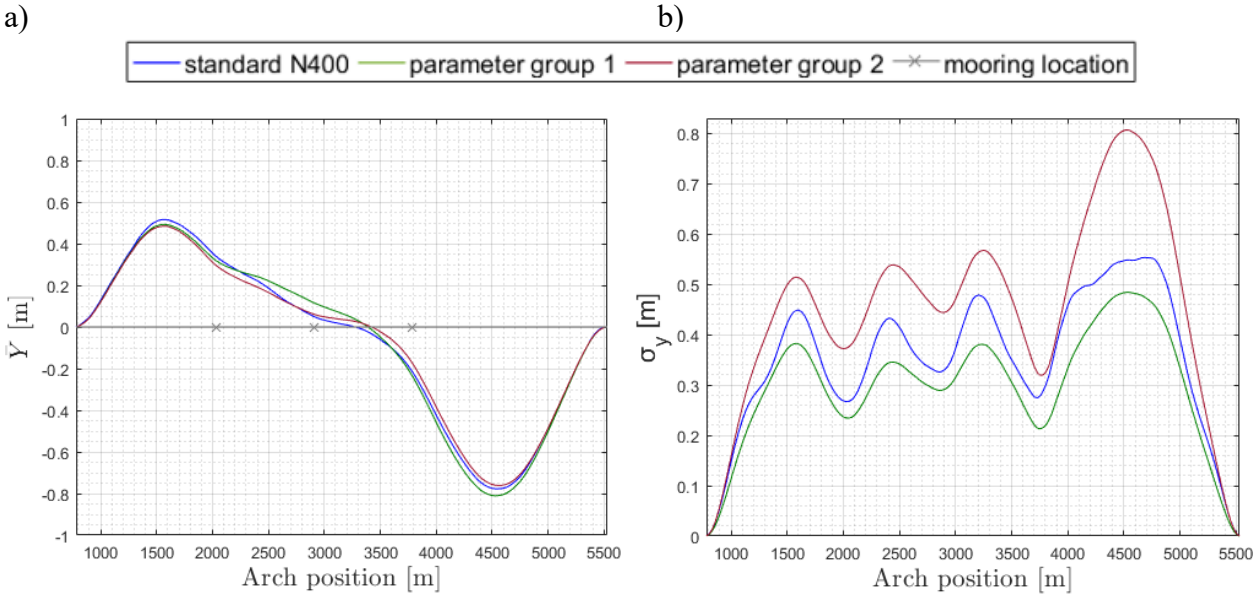

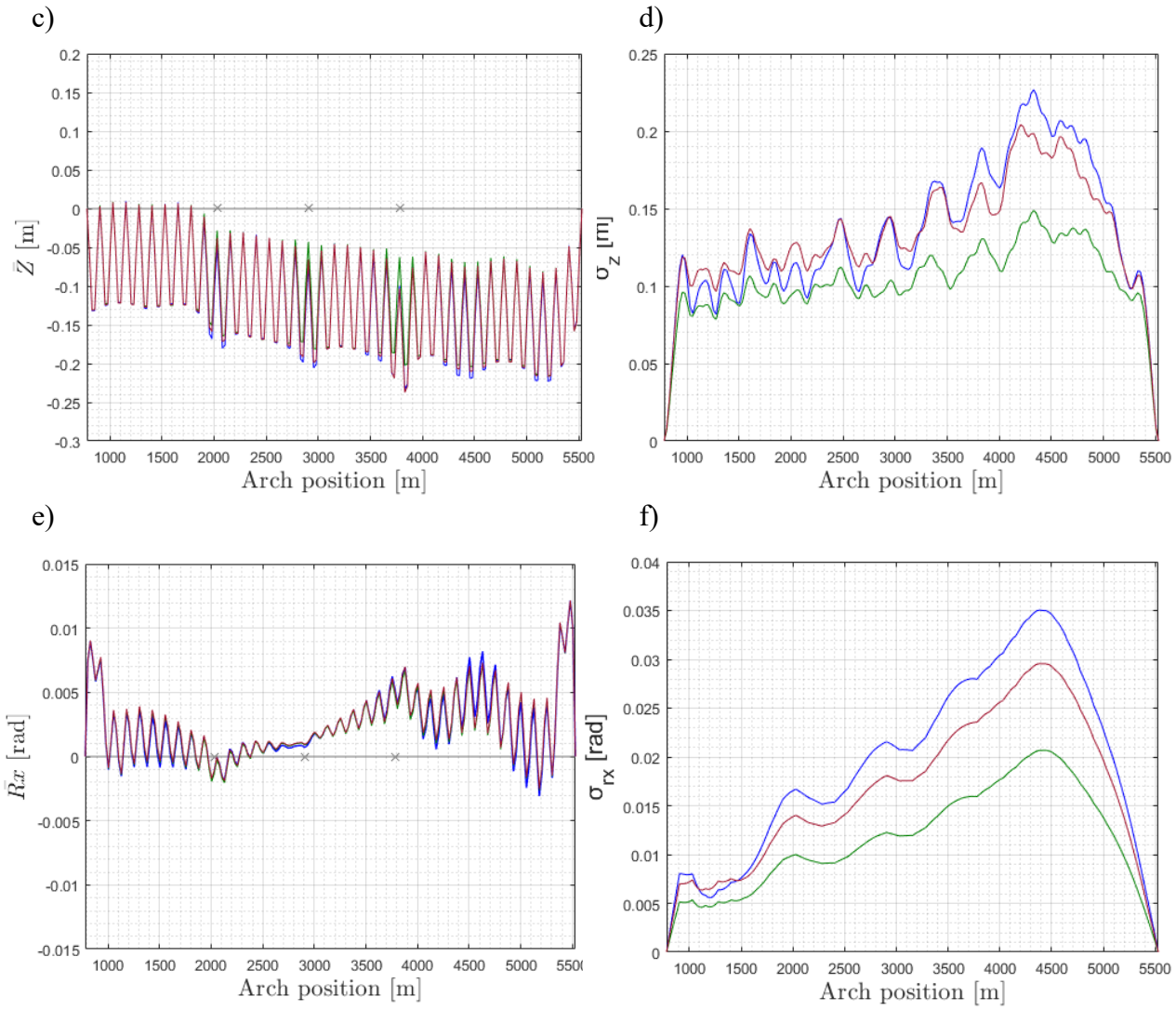

Figure 77: Comparison of responses in global Y, global Z and global Rx of the bridge for three groups of parameters under turbulent wind acting from the west (270°) (left column: the mean displacement of the girder, right column: the standard deviation of the displacement)

The comparison of maximum responses along the bridge for three spectral and coherence parameters groups among six realizations are presented in Figure 78. Figures 78 (a) and (b) show the girder nodes displacements in global Y direction for the wind direction 90° and 270° respectively. It is found that the node which indicates the largest maximum displacement in global Y direction for three groups of parameters under the wind direction 90° is node at arch position 4530 meters. Moreover, two groups of parameters recalculated from field measurements give larger maximum response in global Y direction in comparison to standard values under the eastern wind direction (Figure 78 (a)) with the maximum value of horizontal displacement equals to 3,7475 meters (parameter group 1). For the wind direction 270° the most displaced node in global Y direction along the bridge for standard parameters and parameters

group 2 is node at the same arch position 4530 meters, for group 1 of parameters the most affected node is at arch position 4780 meters. Furthermore, in case of the wind blowing from the west the maximum girder node displacement in global Y direction is equal to 3,3960 meters (parameter group 2). Moreover, from the Figure 78 (b) can be concluded that under the wind direction 270° the group 2 of parameters influences horizontal response more than standard parameters group. Also, that maximum horizontal response is smaller for group 1 of parameters in comparison to standard values.

In the Figure 78 (c) and (d) the maximum responses in global Z direction along the bridge for two wind directions are presented. For the wind coming from the east (90°) the maximum vertical response is found to be 0,9861 meters downwards at arch position 4730 meters for group 1 which is slightly higher than standard maximum response: 0,9715 meters (at arch position 4355 meters). Moreover, the group of standard parameters and group 1 influence the vertical response more at the northern half of the bridge. Also, from the Figure 78 (c) can be observed that the wind with parameters group 2 affects the southern half of the low bridge in vertical direction more than other groups. Further, the maximum vertical response under the wind coming from 270° is at arch position 4105 meters for the wind with standard parameters and is equal to 1,5215 meters downward (Figure 78 (d)).

The maximum torsional displacement when the wind is blowing from the east is the largest for group 1 and equal to 5,1795 degrees at arch position 4555 meters. Among three groups of parameters and under the wind direction 90° the parameters group 1 influences the torsional response more than other groups of parameters what can be seen in Figure 78 (e). Under the wind blowing from the west the standard parameters give the maximum response equals to 7,1505 degrees at arch position 4380 meters and this group influences the reponse the most. Aditionally, the parameters group 2 gives the smallest torsional response for both wind directions.

After the above discussion, it can be concluded that in case of the wind coming from 90° direction the group 1 has the strongest effect at the maximum responses in all three directions. Furthermore, under the wind coming from 270° direction, the parameter group 2 affects the horizontal response the most and standard values give larger displacements in vertical and torsional direction. Hence, performing the analysis by considering only the parameters suggested by standard will not reflect accurate enough the bridge maximum displacements.

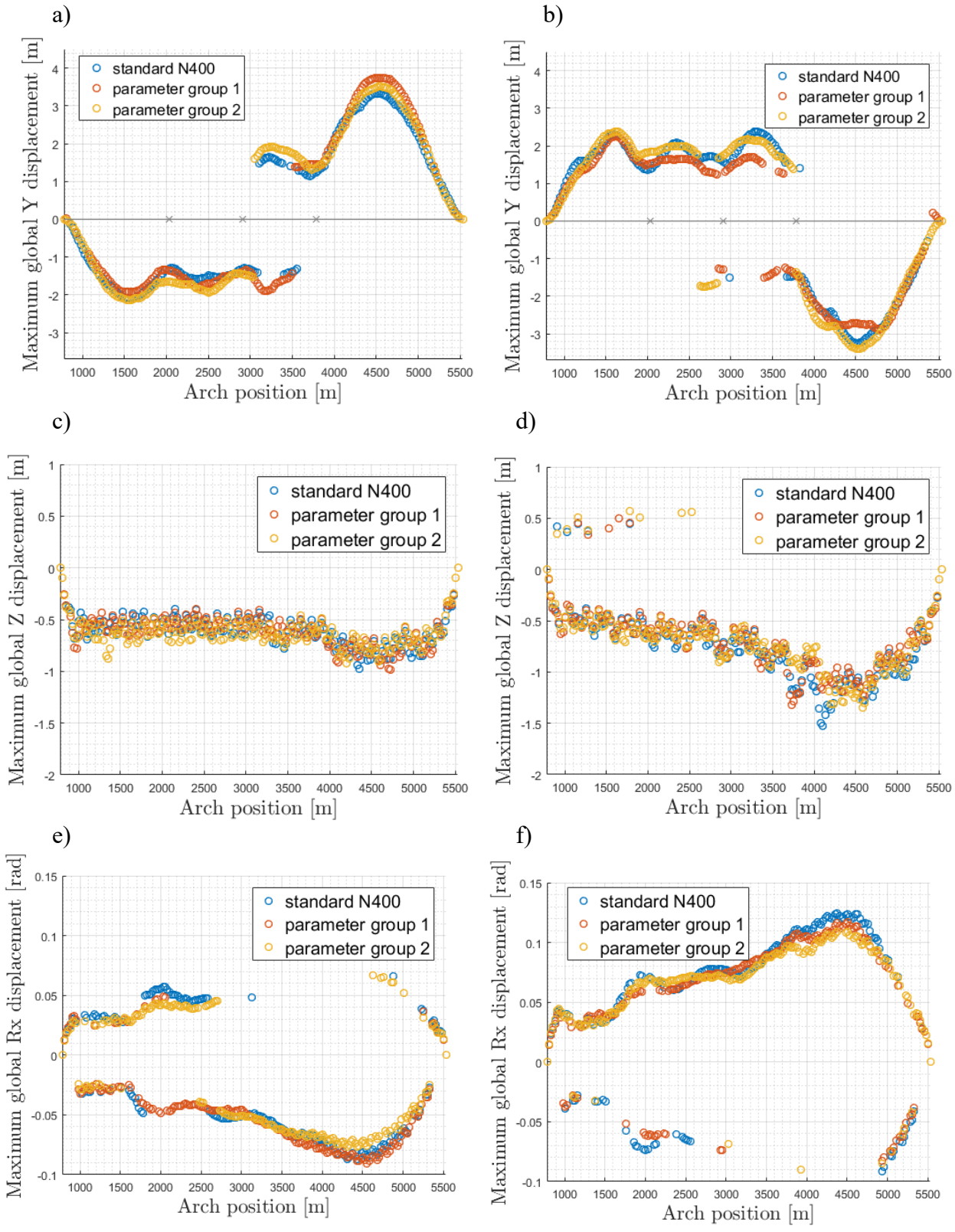

Figure 78: Comparison of maximum responses along the bridge in three directions: global Y, global Z and global Rx for three parameter groups (left column: under the wind coming from the east (90°), right column: under the wind coming from the west (270°))

The mooring line loads under the dynamic wind conditions are presented below. The Figure 79 shows the maximum load for each mooring line when the wind is coming from the east (90°) and west (270°). The presented bar graph clearly shows that the wind direction 270° creates the higher tension in the mooring lines with a strong influence on mooring line nr 11 and 12. The maximum tension force acting on the mooring line nr 11 under 270° wind direction reaches about 6,5 MN as a result of large horizonal displacement which can be seen in Figure 72 (a). The tension forces under the wind coming from the east does not differ significantly and their magnitude is about 4MN which is lower compared to the forces caused by the oppose wind direction.

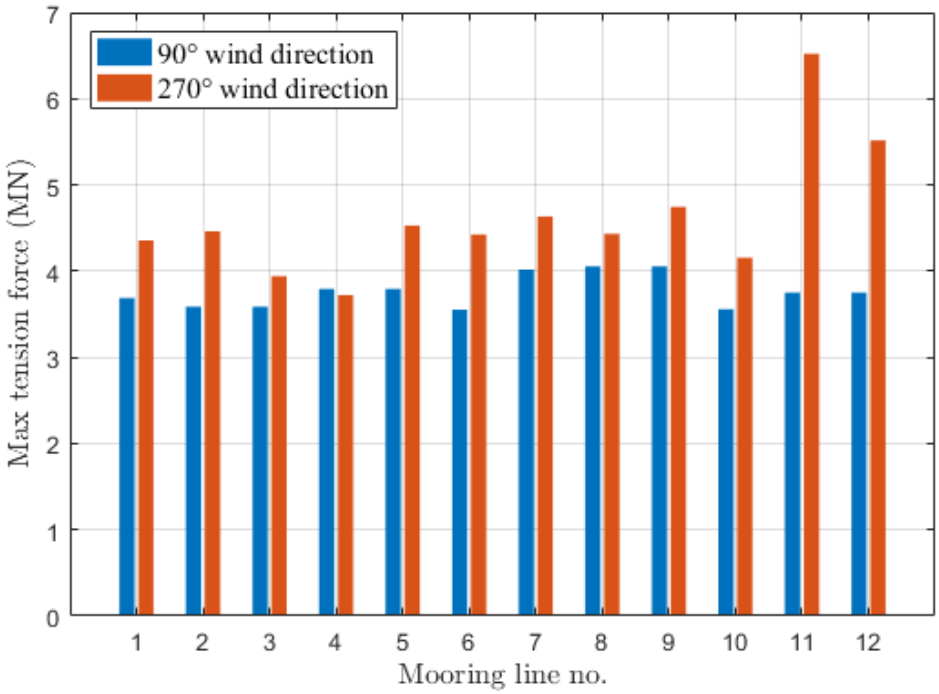

Figure 79: Maximum mooring line tension force comparison for two wind directions

The Figure 80 demonstrates that side mooring lines supporting the floating structure are subjected to lower tension forces under the wind parameter group 1. Furthermore, to the largest tension is subjected mooring line nr 11 on the last pontoon which is confirmed by the persistently larger horizontal displacement of the last span compared to other locations for all wind combinations.

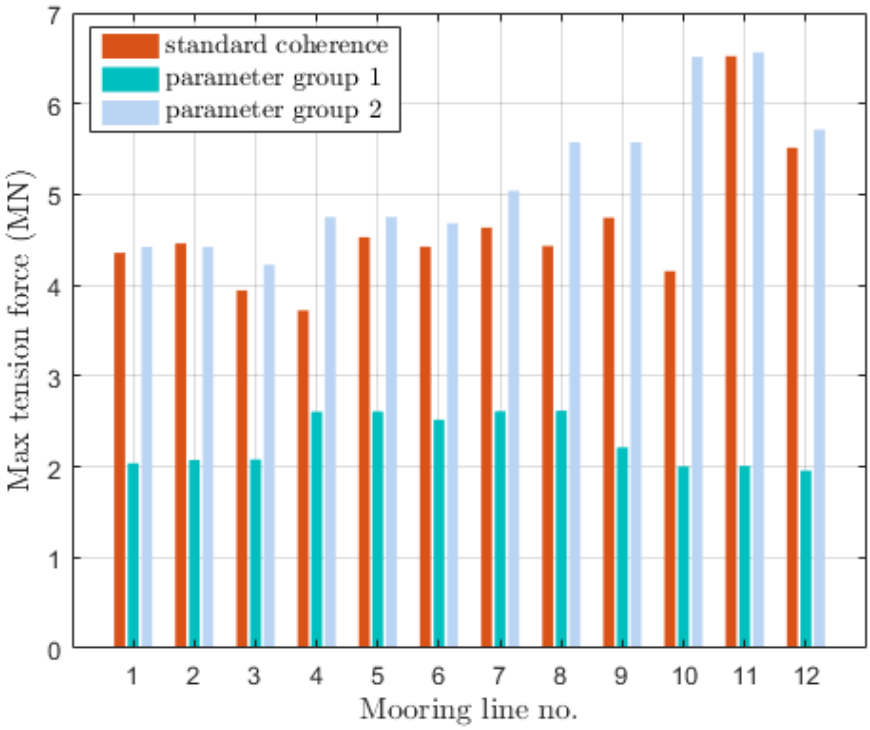

Figure 80: Maximum mooring line tension force comparison of different groups of coherence and wind direction 270°

7.3. Bridge response comparison under different time domain realizations

In order to include the randomness of the generated wind field in time domain analysis, the results of dynamic analysis are concluded based on six simulations. In this section, the mean displacement and standard deviation of each simulation, when the standard wind parameters are used, is compared in the Figure 81 and 82. The comparison of the maximum displacement along the bridge between six simulations is presented in Figure 83. The comparison of simulations is made for two wind directions: 90° and 270°, which in reality are 100° and 280° respectively.

For the global Y direction, the maximum standard deviation of the horizontal displacement appears near the arch position 4530 meters (node nr 229) for all simulation cases in both directions referring to Figure 81 (b) and 82 (b). For the case of wind direction 90°, the largest standard deviation at this node is about 0,77 meters which is 0,22 meters larger than the smallest value given by case 5 (Figure 81 (b)). For the wind direction 270°, the largest standard deviation at this node of 0,66 meters is from case 3 while case 5 gives the smallest standard deviation of 0,46 meters at the same position (Figure 82 (b)).

For the global Z direction, it can be seen from Figure 81 (d) that the peak of standard deviation of case 5 (0,1875 meters) is 1.56 times bigger than the peak of case 4 (0.12 meters). For the wind direction 270°, the largest standard deviation of 0,264 meters is given by case 4 at arch position 4205 meters (Figure 82 (d)). This value is 0,18 meters larger than the results from case 3 at the same position.

For the global Rx direction, twisting is the smallest in the middle of the bridge span for all simulations as it can be seen in Figure 81 (e), 81 (f), 82 (e) and 82 (f). The maximum standard deviation appears near arch position 4400 meters for all cases of 270°. Figure 82 (f) shows that the largest standard deviation of 0,041 radians (2,35 degrees) is from case 4 and the smallest value of 0,031 radians (1,78 degrees) is from case 3.

No significant deviation of mean displacement is found between cases for both wind directions. However, difference between cases can be clearly observed in the standard deviation plots even though the realizations are simulated using the same wind spectral and coherence parameters. Similarly, six realizations introduce different maximum displacements along the bridge in all three DOF as it can been in Figure 83. To include the randomness of the wind field in the time domain analysis, the conclusion of the analysis must be made based on several realizations, and hence to provide a more reliable analysis.

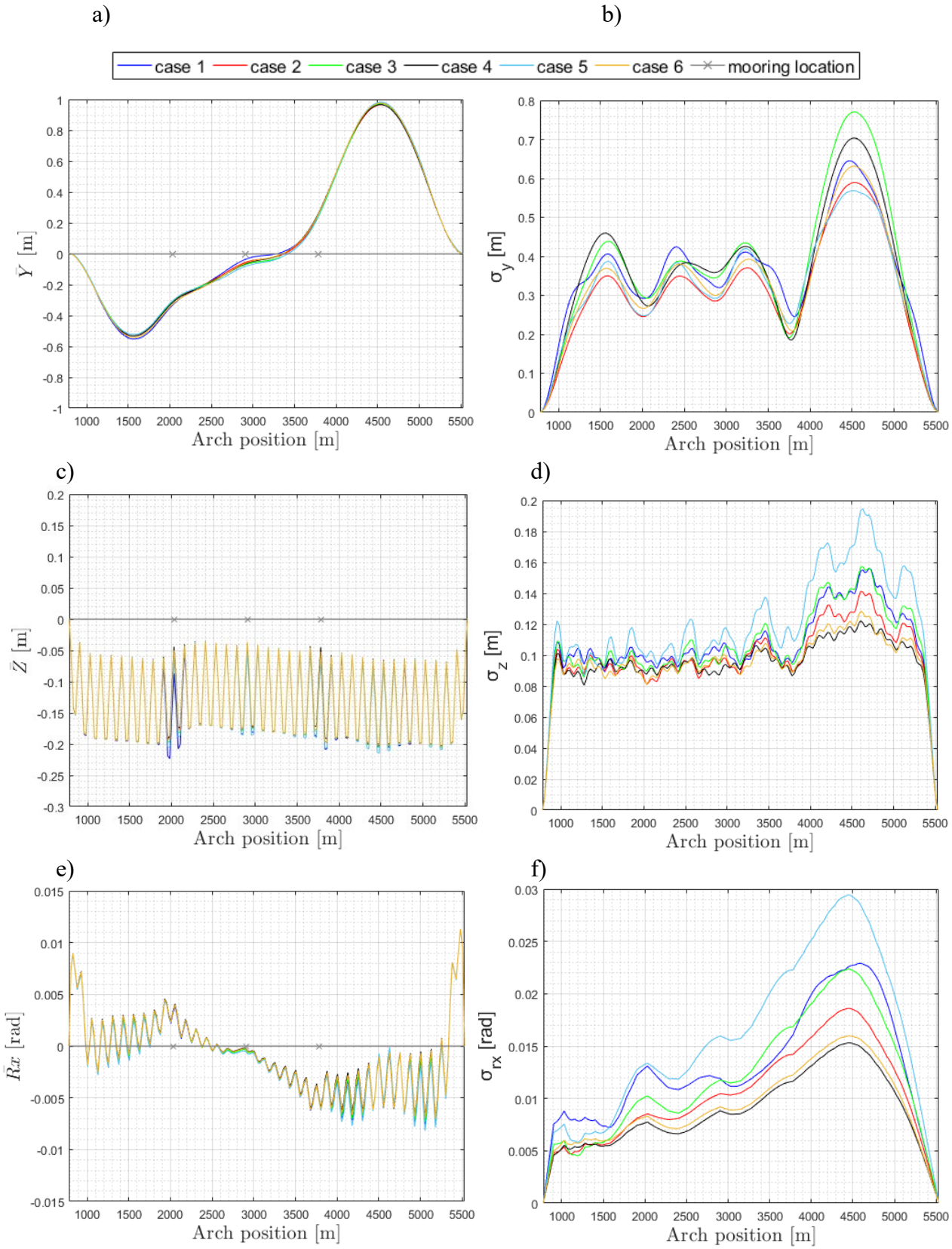

Figure 81: Comparison of the six cases of wind field for standard coherence and wind direction 90° (left column: the mean displacement of the girder, right column: the standard deviation of the displacement)

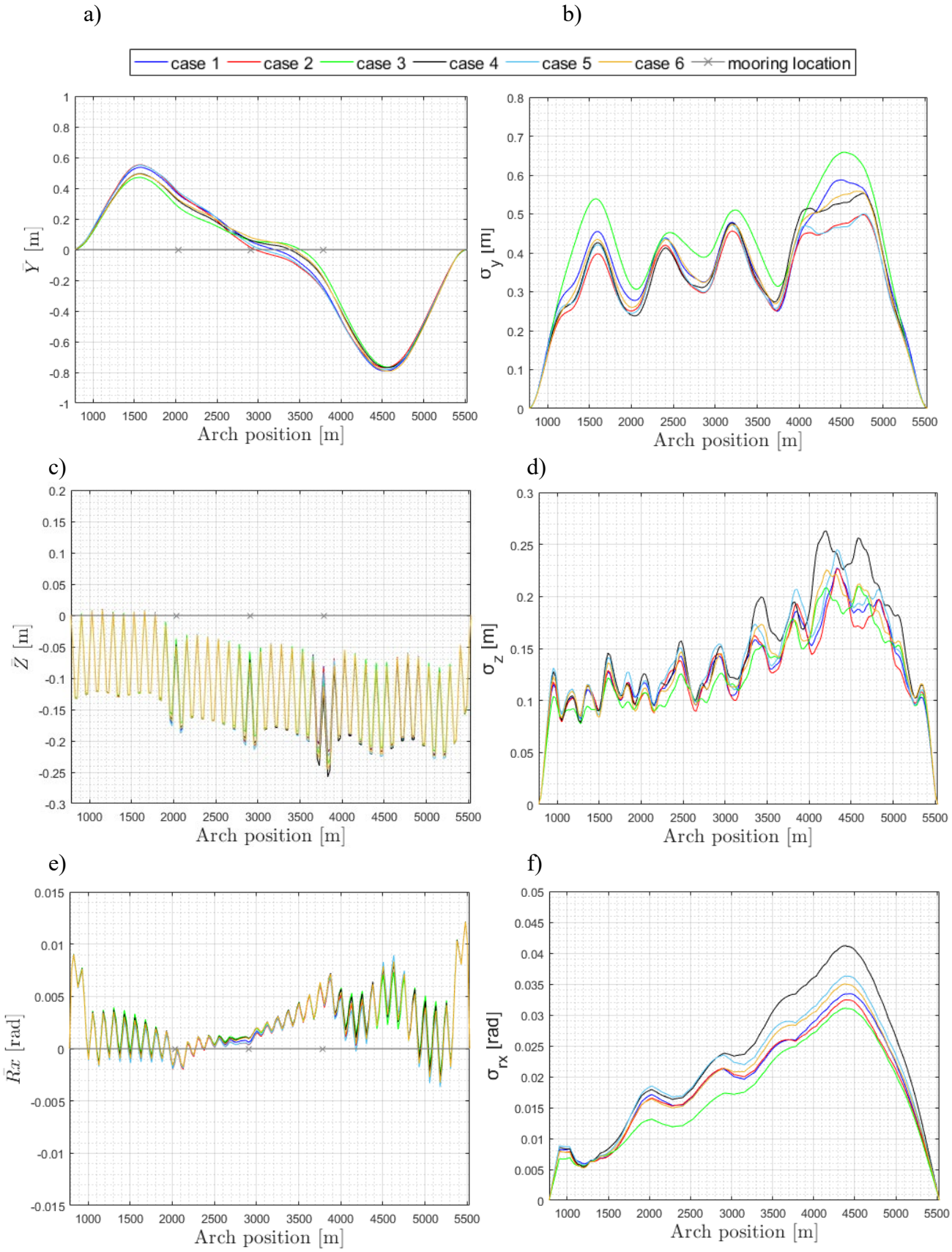

Figure 82: Comparison of the six cases of wind field for standard coherence and wind direction 270° (left column: the mean displacement of the girder, right column: the standard deviation of the displacement)

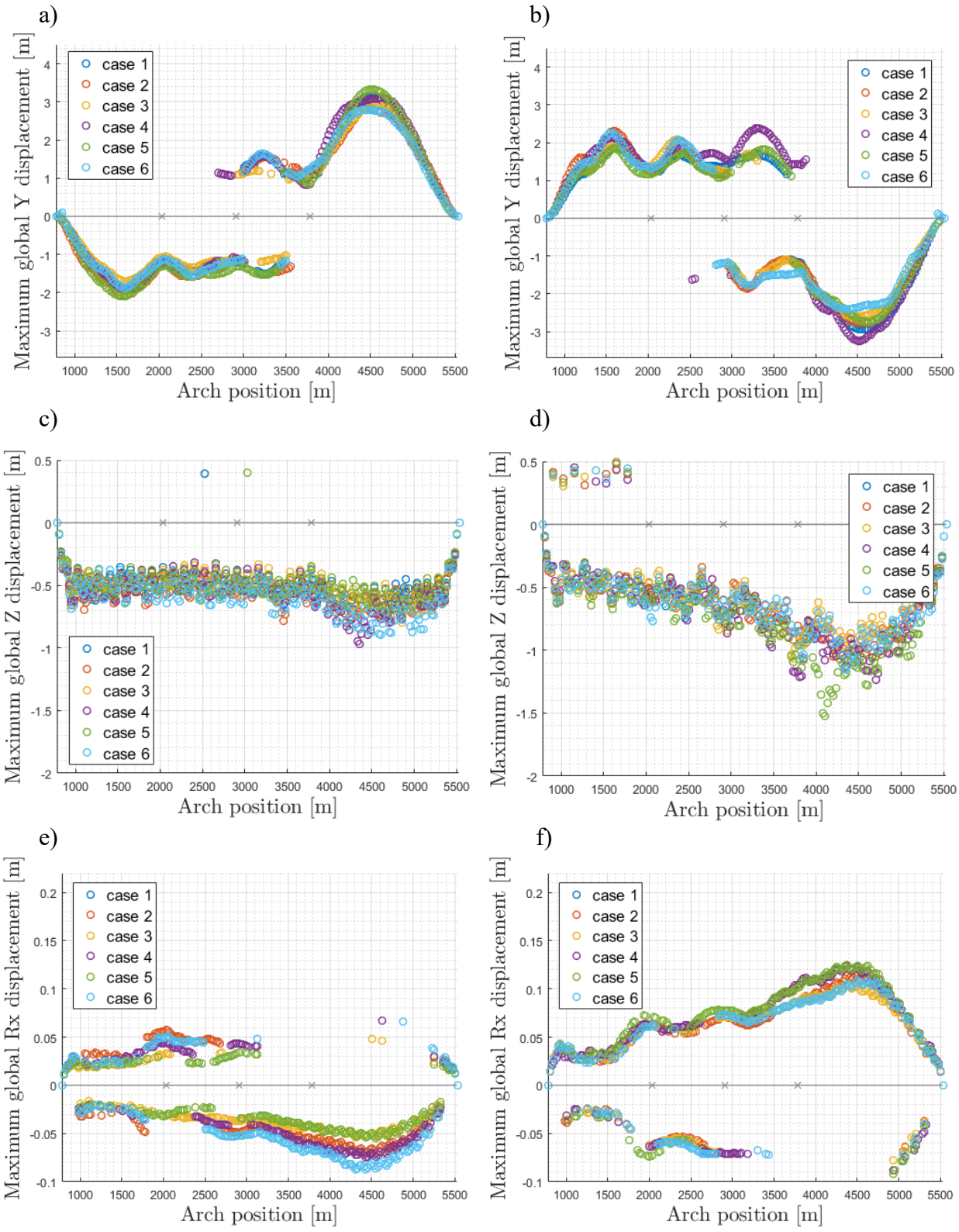

Figure 83: Comparison of maximum responses along the bridge in three directions: global Y, global Z and global Rx for each realization case (left column: under the wind coming from the east (90°), right column: under the wind coming from the west (270°))

7.4. Power spectral density

The plots in the following sections present the power spectral density (PSD) of displacement response of selected girder node under the dynamic wind load. The energy distribution in a turbulent flow field in two wind directions: east (90°) and west (270°) is illustrated based on results from one of the six realizations. The studied point is node at arch position 4530 meters with the largest standard deviation as it is observed in the Figure 72 in the previous section. The power spectral density is estimated using Welch's overlapped segment averaging estimator according to [25]. In the Figure 85, 88 and 90, the following modes are pointed out:

- Group 1
    - H1 – Horizontal 1st mode (mode nr 1)
    - H2 – Horizontal 2nd mode (mode nr 2)
    - H3 – Horizontal 3rd mode (mode nr 3)
- Group 2
    - V1 – Vertical 1st mode (mode nr 60)
- Group 3
    - T1 – Torsional 1st mode (mode nr 83)
- Group 4
    - M1 – Mooring lines mode (mode nr 27)
    - M2 – Mooring lines mode (mode nr 30)
    - M3 – Mooring lines mode (mode nr 31)
    - M4 – Mooring lines mode (mode nr 44)
    - M5 – Mooring lines mode (mode nr 54)

7.4.1. Power spectral density of the girder horizontal response

The Figure 84 below illustrates the energy distribution along the bridge of the horizontal response as a function of frequency. The presented results show that the dominating horizontal response under the dynamic wind load appears at low frequency range.

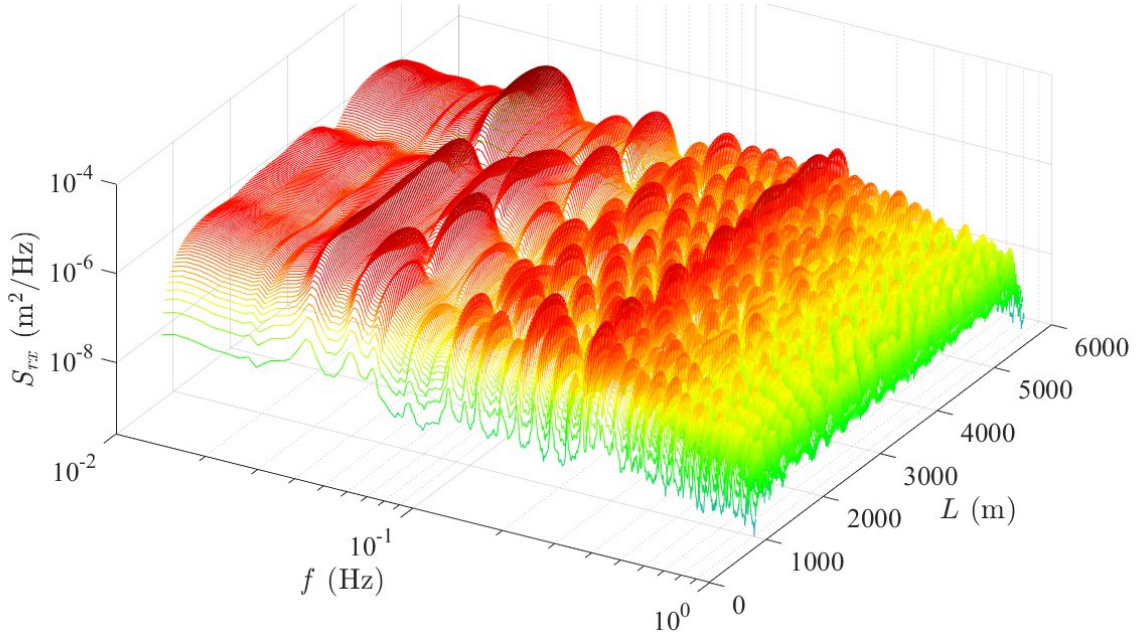

Figure 84: Power spectral density of the girder horizontal response along the structure under turbulent wind direction 90°

The contour plot seen in Figure 85 gives further information to the standard deviation plot in Figure 72 (b). It can be observed in Figure 85 that contribution from 1st horizontal mode and other horizontal modes with low frequencies are all clearly visible. The power spectral density plot at node nr 229 presented in Figure 85 (right column) shows the coupling between the modes and the torsional mode T1 as remarkable peak is clearly identified to be coupled with the horizontal motion.

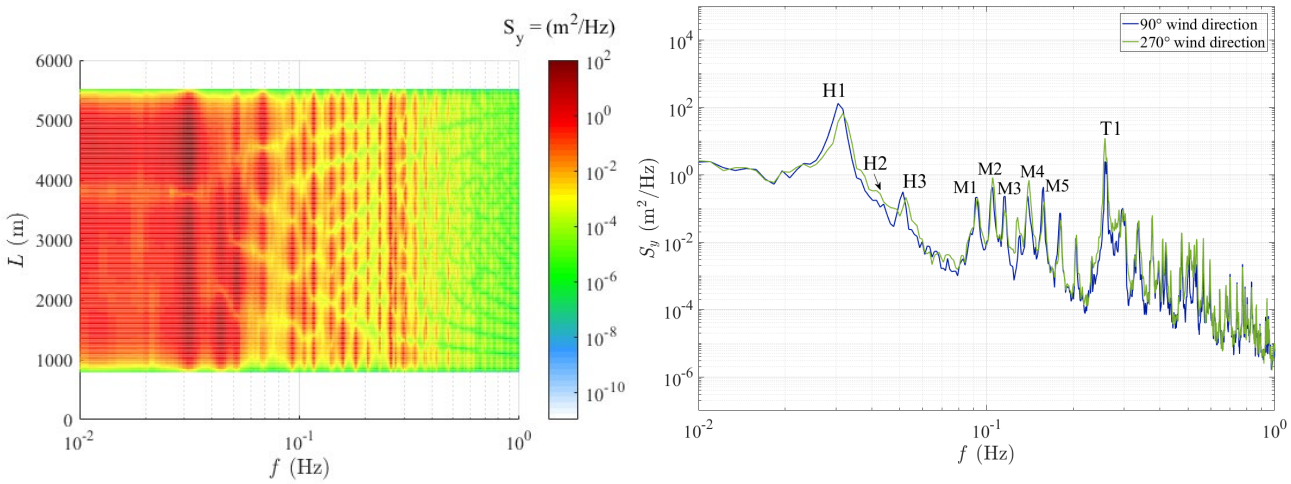

Figure 85: Power spectral density of the girder horizontal response (left column: the contour plot of the power spectral density along the bridge under turbulent wind direction 90°; right column: the power spectral density at node nr 229)

The modes described as mooring line modes M1, M2, M3, M4 and M5 indicate that they are dominated by mooring lines and there is a girder horizontal contribution to it as well. For instance, for the node with largest displacement at mode 30 the relationship between mooring horizontal motion and girder center node is $\frac{1}{0.7752} = 1.29$ which also means that the girder node displacement is 77,5% of the mooring line horizontal displacement.

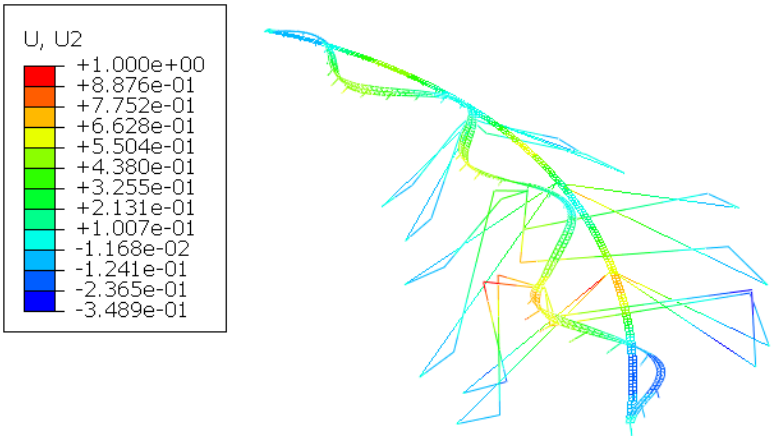

Figure 86: The mode shape of mode nr 30

7.4.2. Power spectral density of the girder vertical response

High energy concentration is observed at the last span of the low bridge as it is shown in Figure 87. This statement is in good agreement with mode shape of the first torsional mode (mode nr 83), where vertical motion of the girder nodes increases towards the north end of the bridge.

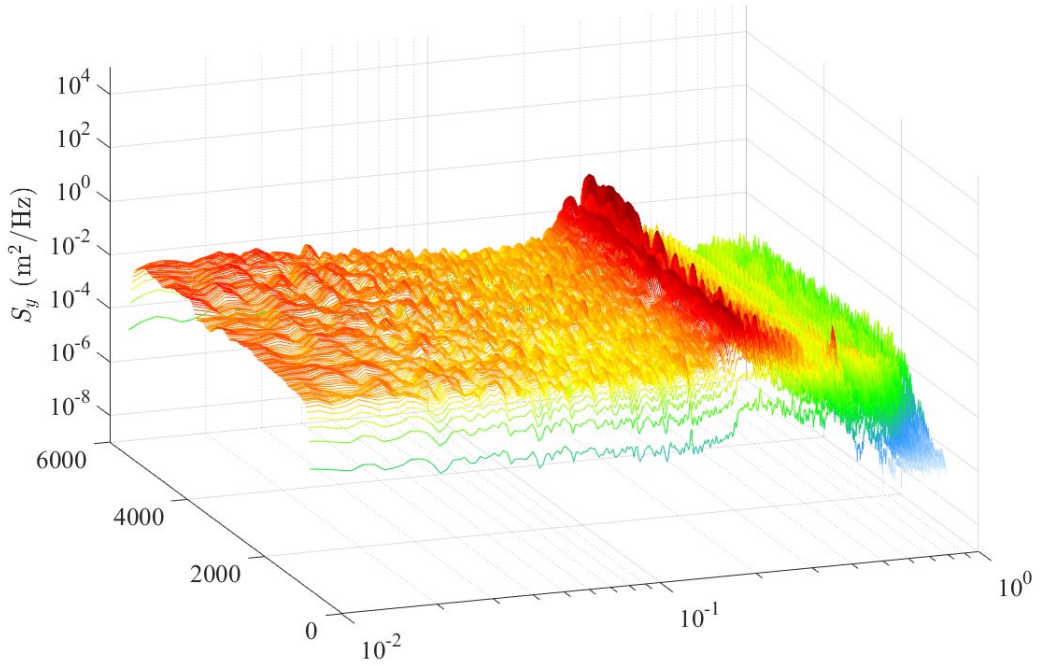

Figure 87: Power spectral density of the girder vertical response along the structure under turbulent wind direction 90°

The power spectral density plot in Figure 88 presents that mode T1 gives the greatest contribution to vertical bridge response at frequency 0,26 Hz. The other spectral peak can be noted at 1st vertical mode V1 and that there is no significant coupling of modes at low frequencies into the vertical response.

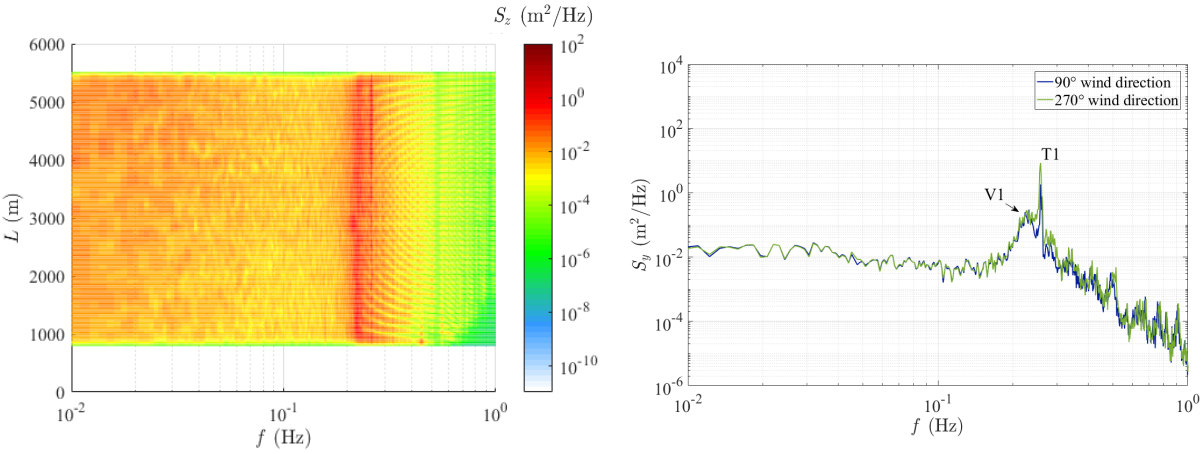

Figure 88: Power spectral density of the girder vertical response (left column: the contour plot of the power spectral density along the bridge under turbulent wind direction 90°; right column: the power spectral density at node nr 229)

7.4.3. Power spectral density of the girder torsional response

The torsional response is highly dominated by the frequency of first torsional mode T1 accompanied with three first representative horizontal modes H1, H2 and H3 (Figure 90).

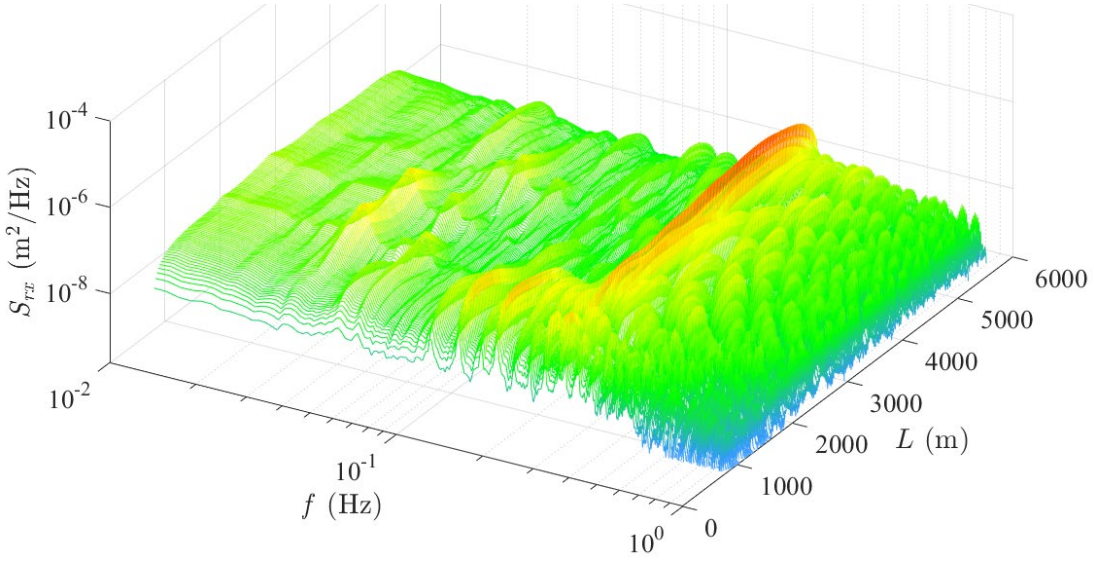

Figure 89: Power spectral density of the girder torsional response along the structure under turbulent wind direction 90°

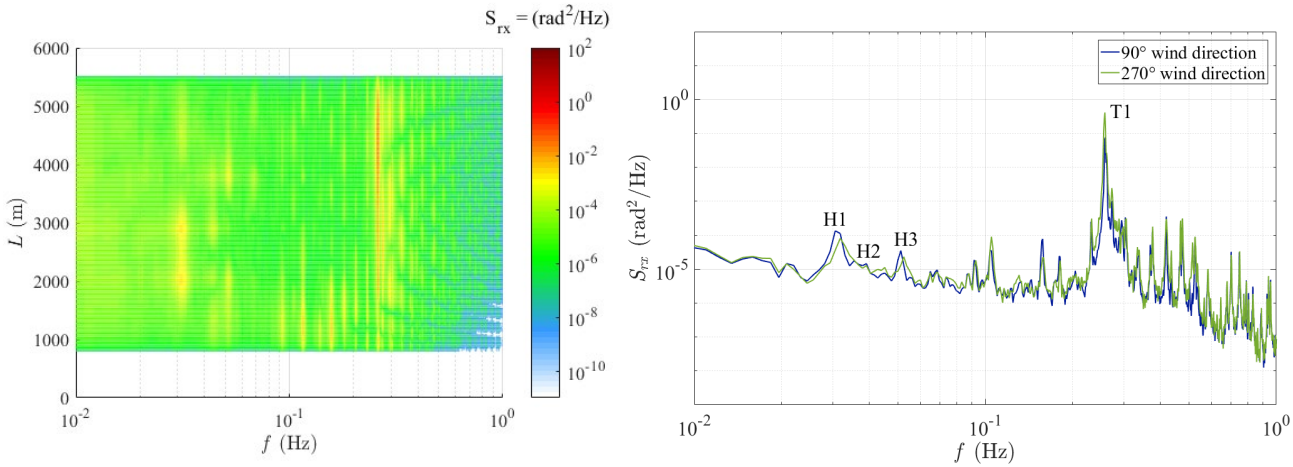

Figure 90: Power spectral density of the girder torsional response (left column: the contour plot of the power spectral density along the bridge under turbulent wind direction 90°; right column: the power spectral density at node nr 229)

7.5. Displacement time histories

The displacement time-histories in three directions: horizontal, vertical and torsional of the girder node at arch position 4530 meters (node nr 229) under wind from the west and from the east are presented in the figures below. Maximum standard deviation can be observed at the selected node, referring to Figure 72. The data is taken from one of the six simulations where the standard wind parameters are applied. It is clearly observed in Figure 91, 92 and 93 that the wind coming from the west gives larger displacement in all three degree of freedom at this selected position.

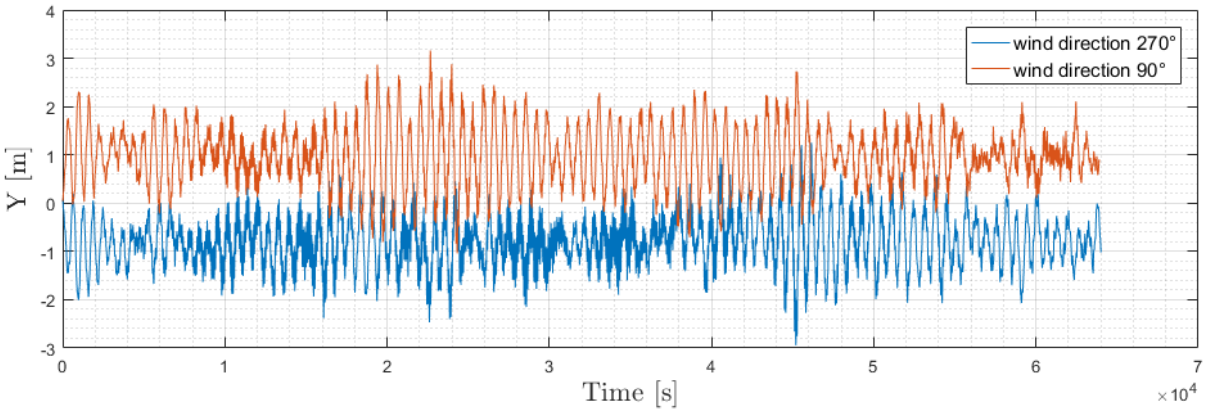

Figure 91: The time-series of horizontal displacement (global Y) at girder node 229

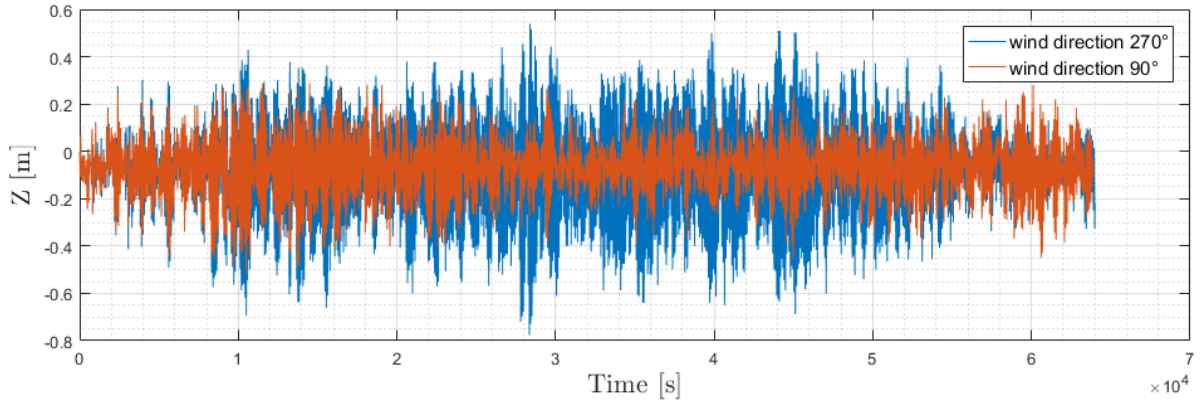

Figure 92: The time-series of vertical displacement (global Z) at girder node 229

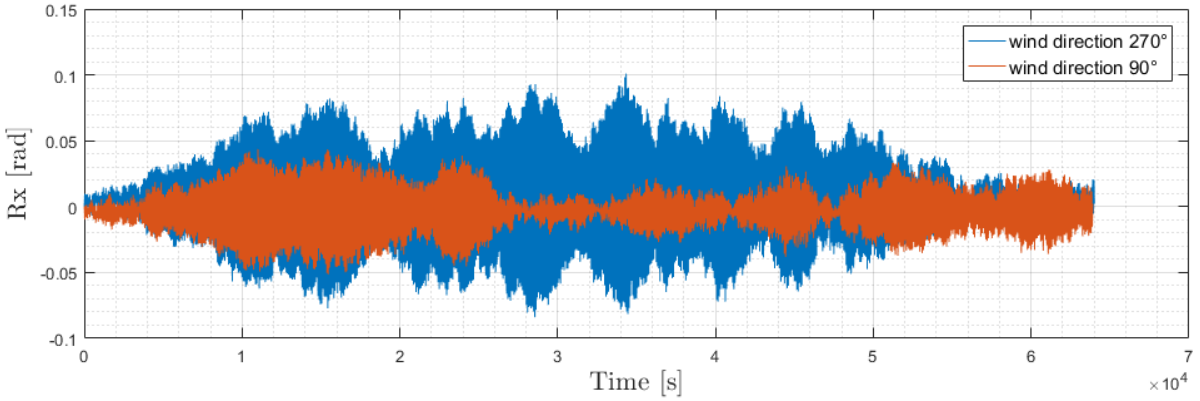

Figure 93: The time-series of rotational displacement (global Rx) at girder node 229

8. Sensitivity check

From the wind parameters comparison made in Chapter 7.2, it is hard to recognise which wind parameter is dominant. In order to investigate the sensitivity of individual wind spectral and coherence parameter on the bridge response, ten additional groups of wind parameters are studied. For all sensitivity simulations, the wind direction 270° (280° in reality) is considered. The results presented in this chapter are averaged over six simulations for each studied group. Ten groups of wind parameters studied are summarized in the table below.

Table 21: Wind parameter groups in sensitivity check

Group no.	Au	Av	Aw	Cux	Cuy	Cuz	Cvx	Cvy	Cvz	Cwx	Cwy	Cwz
1	**4.7**	9.4	9.4	3	10	10	6	6.5	6.5	3	6.5	3
2	**12.8**	9.4	9.4	3	10	10	6	6.5	6.5	3	6.5	3
3	6.8	9.4	**7.9**	3	10	10	6	6.5	6.5	3	6.5	3
4	6.8	9.4	**15**	3	10	10	6	6.5	6.5	3	6.5	3
5	6.8	9.4	9.4	3	**1.15**	10	6	6.5	6.5	3	6.5	3
6	6.8	9.4	9.4	3	**6.6**	10	6	6.5	6.5	3	6.5	3
7	6.8	9.4	9.4	3	10	10	6	6.5	6.5	3	**3.4**	3
8	6.8	9.4	9.4	3	10	10	6	6.5	6.5	3	**5.4**	3
9	6.8	9.4	9.4	3	10	10	6	**3.4**	6.5	3	6.5	3
10	6.8	9.4	9.4	3	10	10	6	**0.93**	6.5	3	6.5	3
Standard N400	6.8	9.4	9.4	3	10	10	6	6.5	6.5	3	6.5	3

8.1. Sensitivity of A parameters in wind spectra

As it is shown in the Table 21, the first four groups of wind parameters studied in this section are with different A_n parameters which can influence the peak location in the wind spectra according to Equation (4.7). The peak of the wind spectra would shift to the left when a higer A parameter is applied.

For the global Y direction, Figure 94 (b) shows that A_u parameter groups (group no.1 and 2) give larger standard deviation along the bridge compared to the standard group. From Figure 95 (b) where A_w parameter is studied, it can be seen that the standard deviation along the bridge is close to the standard results in the case of group 3 ($A_w = 7{,}9$) while group 4 ($A_w = 15$) gives smaller response than the standard group. In comparison with the standard group, all four

A parameter groups give larger mean displement but not along the entire bridge span, referring to Figure 94 (a) and 95 (a). The maximum displacement (Table 24) increases by 52% in the case of group 1 (A_u = 4.7) and 64.9% for the second group (A_u =12.8), comparing to the standard results. As for the A_w parameter, the maximum displacement given by group 3 is also 0,24 meters higher than the standard one (Table 25).

In the global Z direction, remarkable larger mean displacement near the third moored pontoon is observed in A_u parameter groups (group no.1 and 2) referring to Figure 94 (c). It can be also seen for both A_u parameter groups (group no.1 and 2) in Figure 94 (d) that the standard deviation along the bridge is larger than the standard results and the peaks shift to the left. The vertical response under the A_w parameter is not as strong as the one caused by A_u parameter as it shows in Figure 95 (d). When it comes to the maximum displacement, field measured A parameters give larger displacement compared to the standard results except for the A_w parameter group 4, referring to Table 24 and 25.

As for the response in the global Rx direction, two A_u parameter groups no.3 and 4 cause larger standard deviation along the bridge compared to the standard results (Figure 94 (f)) while in the case of A_w parameter only group 3 (A_w = 7.9) gives slightly larger standard deviation in some of the bridge spans (Figure 95 (f)). The maximum twisting caused by both A_u parameter groups (group no. 1 and 2) are two times bigger than the standard values (Table 24). For the A_w parameter, maximum displacement given by group 3 is not as large as the ones of A_u groups but still larger than the standard results (Table 25).

It can be concluded from above observation that larger dynamic response in three DOF will be caused by the change of A_u parameter compared to the parameter A_w. It is reasonable that the A_w parameter does not influence the bridge response as strong as the A_u parameter since the A_u parameter is related to the along wind component while the A_w parameter relates to the vertical wind component. Even though the response under the studied A_w parameter groups are not as strong as under the A_u parameter groups, the field measured A_w parameter (group 3) still causes slightly stronger response compared to the standard result.

Table 22: Wind spectral A parameter group 1 and 2

Group no.	Au	Av	Aw	Cux	Cuy	Cuz	Cvx	Cvy	Cvz	Cwx	Cwy	Cwz
Standard N400	6.8	9.4	9.4	3	10	10	6	6.5	6.5	3	6.5	3
1	**4.7**	9.4	9.4	3	10	10	6	6.5	6.5	3	6.5	3
2	**12.8**	9.4	9.4	3	10	10	6	6.5	6.5	3	6.5	3

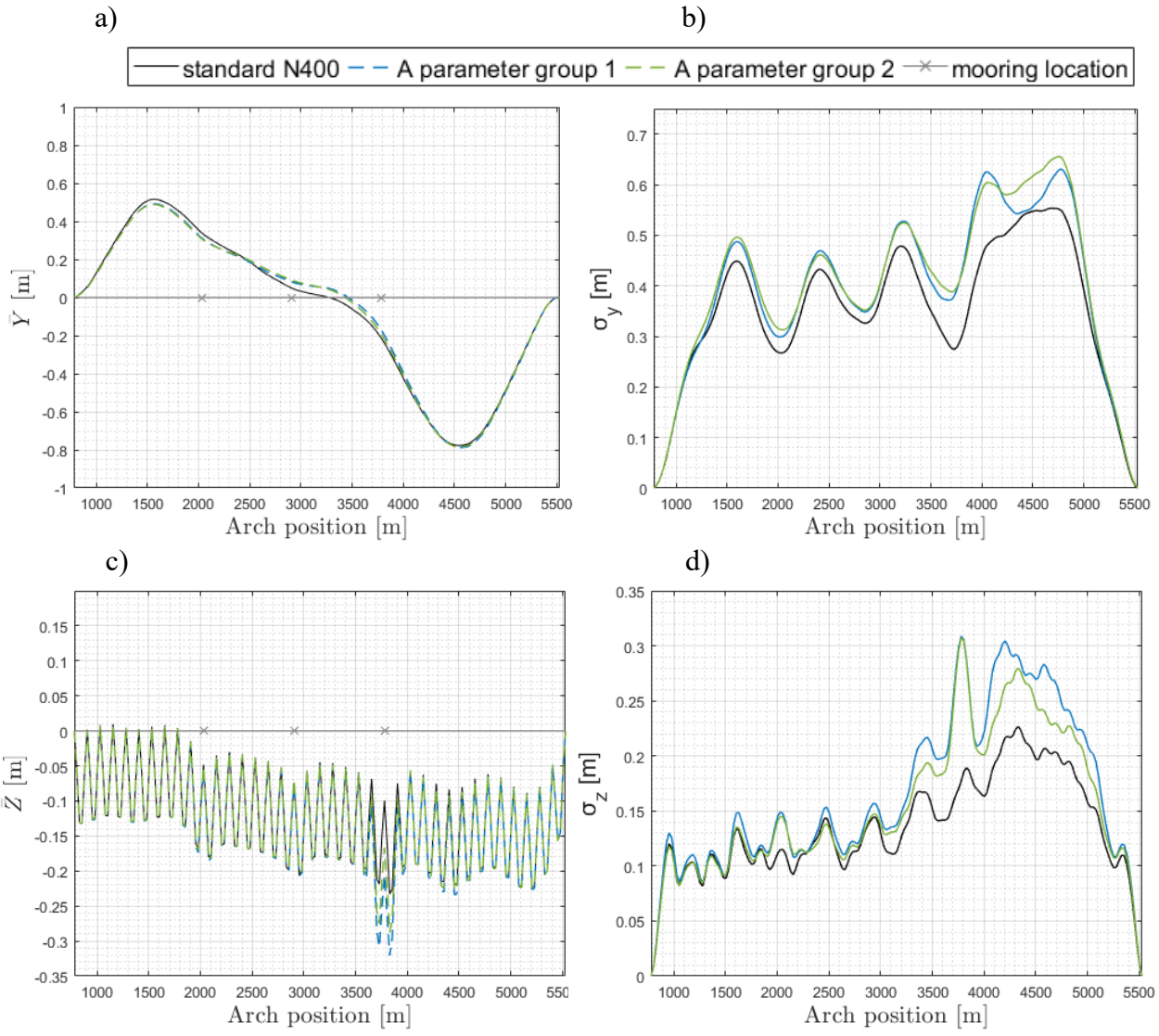

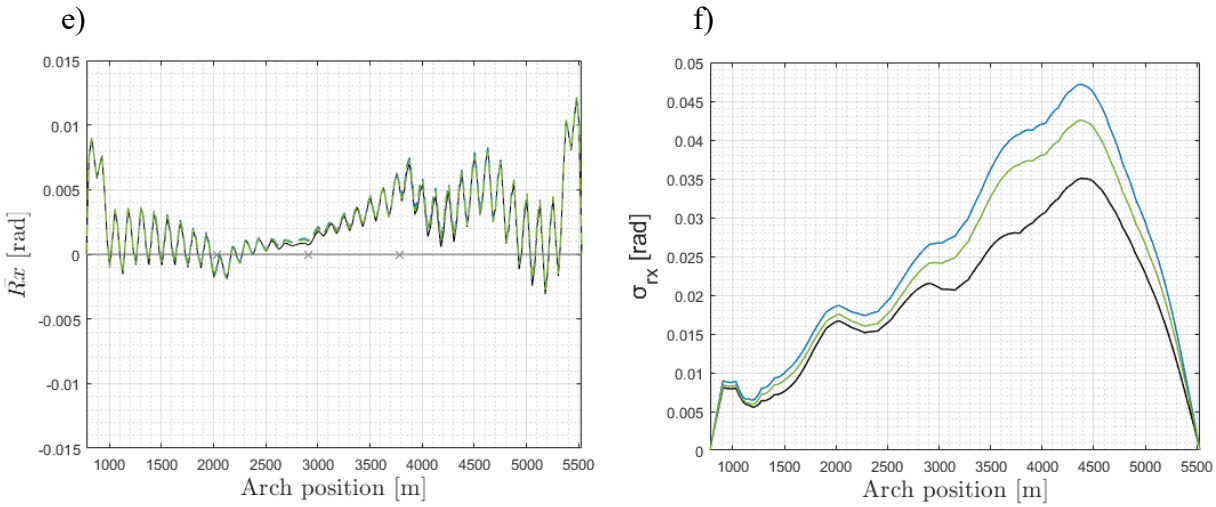

Figure 94: Sensitivity check of the A parameters group 1 and 2 for wind direction 270° (left column: the mean displacement of the girder, right column: the standard deviation of the displacement)

Table 23: Wind spectral A parameter group 3 and 4

Group no.	Au	Av	Aw	Cux	Cuy	Cuz	Cvx	Cvy	Cvz	Cwx	Cwy	Cwz
Standard N400	6.8	9.4	9.4	3	10	10	6	6.5	6.5	3	6.5	3
3	6.8	9.4	**7.9**	3	10	10	6	6.5	6.5	3	6.5	3
4	6.8	9.4	**15**	3	10	10	6	6.5	6.5	3	6.5	3

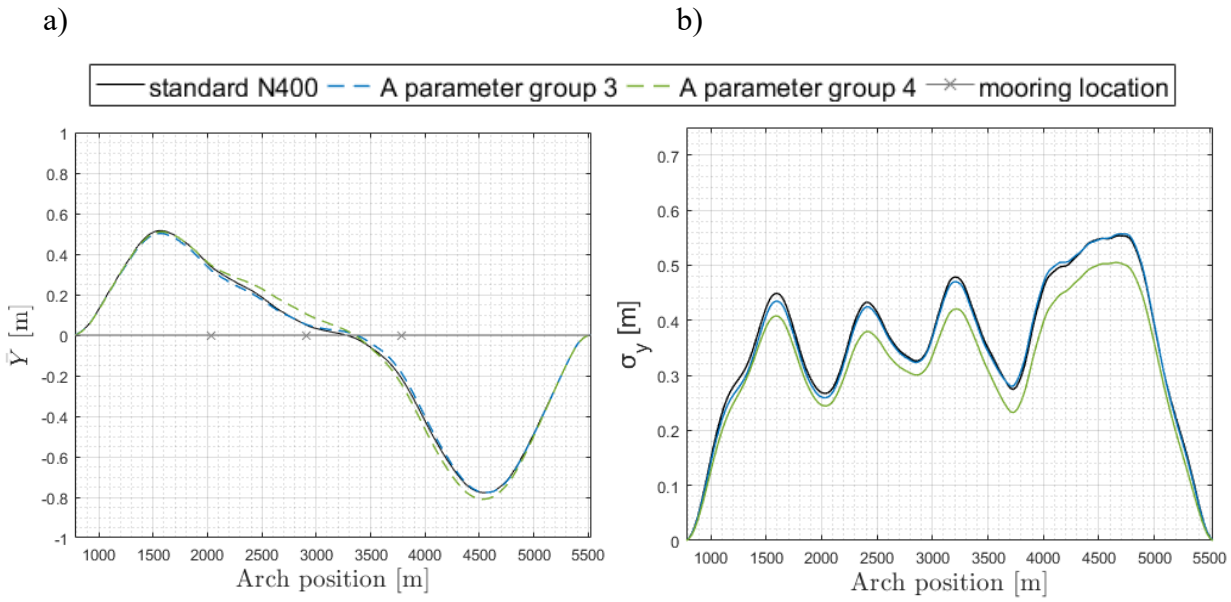

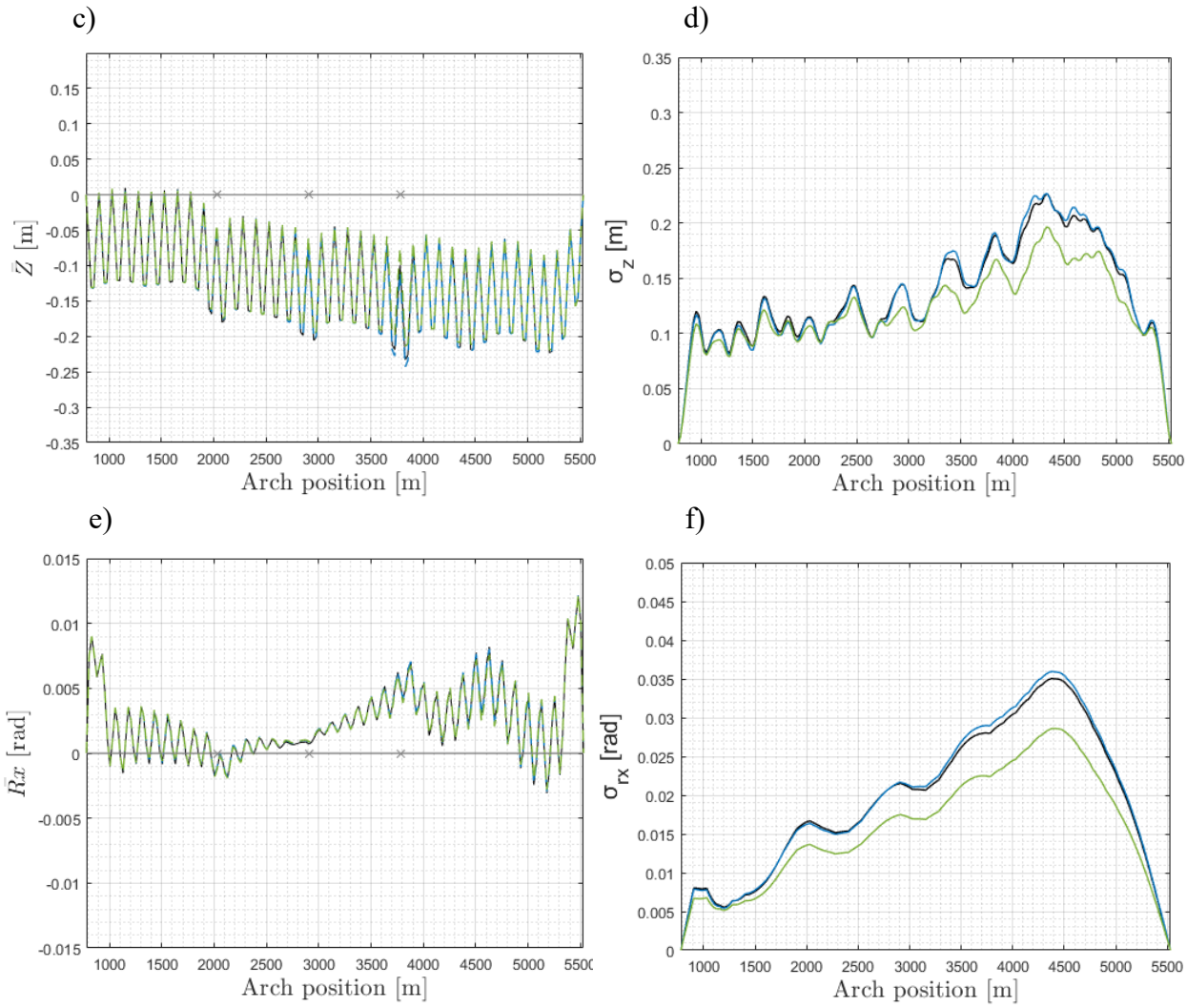

Figure 95: Sensitivity check of the A parameters group 3 and 4 for wind direction 270° (left column: the mean displacement of the girder, right column: the standard deviation of the displacement)

Table 24: Comparison of maximum displacement for A parameter group 1 and 2

Group no.	Y (m)	Z (m)	Rx (deg)
Standard N400	2.3762	0.9581	7.1505
1	3.6228	1.7235	14.5646
2	3.9178	1.5041	14.9198

Table 25: Comparison of maximum displacement for A parameter group 3 and 4

Group no.	Y (m)	Z (m)	Rx (deg)
Standard N400	2.3762	0.9581	7.1505
3	2.5344	1.0699	7.5287
4	2.1050	0.7089	6.2051

8.2. Sensitivity of C parameters in wind coherence

Three types of coherence parameters are studied in this section and they are C_{uy}, C_{vy} and C_{wy}.

For the global Y direction, smaller mean displacement is observed for C_{uy} groups (group no.5 and 6) and C_{wy} groups (group no.9 and 10) compared to the standard results, referring to Figure 96 (a) and Figure 98 (a). The C_{uy} parameters give higher standard deviation along the bridge according to Figure 96 (b) while the standard deviation is close to the standard result under C_{vy} parameter groups (group no.7 and 8) as it can be seen in Figure 97 (b). Figure 98 (b) shows that larger standard deviation is caused by both C_{wy} groups (group no.9 and 10), but not along the entire bridge span. Among all coherence parameter groups, the highest standard deviation of about 0,715 meter appears at arch position 4503 meters when C_{uy} of 6,6 (group 6) is applied. As for the maximum displacement, the largest value of 3,8939 meters is also given by the C_{uy} parameter group (group 6) as observed in Table 29, 30 and 31. Based on the above observation, it can be concluded that it is the parameter C_{uy} that has the biggest influence on the bridge horizontal response among three studied coherence parameter types. A further comparison is made based on Figure 94 (b) and Figure 96 (b), it can be seen that larger standard deviation is given by the coherence parameter C_{uy} rather than the wind spectra parameter A_u.

For the global Z direction, large mean displacement near the third moored pontoon is observed in case of C_{uy} group (group no.6) and C_{vy} groups (group no.8) referring to Figure 96 (c) and 97 (c). Similarly to the case of global Y direction, it is the C_{uy} parameter group (group no.5) gives the largest standard deviation along the bridge by comparing Figure 96 (d), 97 (d) and 98 (d). Furthermore, the stronger response is still caused by C_{uy} parameter group (group no.5) compared to the wind spectra parameter A_u, referring to Figure 94 (d) and Figure 96 (d). Additionally, it can be seen that the largest maximum displacement among all A and C parameter groups is also from the C_{uy} group (group no.6) referring to Table 29, 30 and 31.

Therefore, one can conclude that coherence parameter C_{uy} is the most critical parameter for the bridge vertical response.

For the global Rx direction, it is still the coherence parameter C_{uy} group 6 that gives the largest standard deviation along the bridge shown in Figure 96 (f), 97 (f) and 98 (f). And as expected, the largest value of the maximum rotation among all the coherence parameter groups is from C_{uy} parameter group (group 6) referring to Table 29, 30 and 31. However, larger response is caused by the two A_u parameter groups (group no.1 and 2) rather than the C_{uy} parameter groups (group no.5 and 6) when the results in Figure 94 (f) is compared with the one from Figure 96 (f).

The conclusion can be drawn that the most critical coherence parameter is the C_{uy} parameter among the three types of coherence parameters studied. To be noticed that if it is compared with the standard paramters, larger bridge response is observed not only in the C_{uy} parameter groups but also in other two types of coherence parameter groups. When the C_{uy} parameter is compared with the A_u parameter, parameter C_{uy} generates stronger bridge response in global Y and global Z direction. However, the wind spectra parameter A_u becomes more influential to the bridge response in global Rx direction. The above observation together with the one made in the section 8.1. indicates that the recommended standard wind spectra parameters and coherence parameters are not conservative enough to describe the real wind conditions which the bridge is exposed to during the storm, and it is hence not safe to perform the dynamic analysis only considering the experimental parameters suggested by the standard N400.

Table 26: Coherence parameter group 5 and 6

Group no.	Au	Av	Aw	Cux	Cuy	Cuz	Cvx	Cvy	Cvz	Cwx	Cwy	Cwz
Standard N400	6.8	9.4	9.4	3	10	10	6	6.5	6.5	3	6.5	3
5	6.8	9.4	9.4	3	**1.15**	10	6	6.5	6.5	3	6.5	3
6	6.8	9.4	9.4	3	**6.6**	10	6	6.5	6.5	3	6.5	3

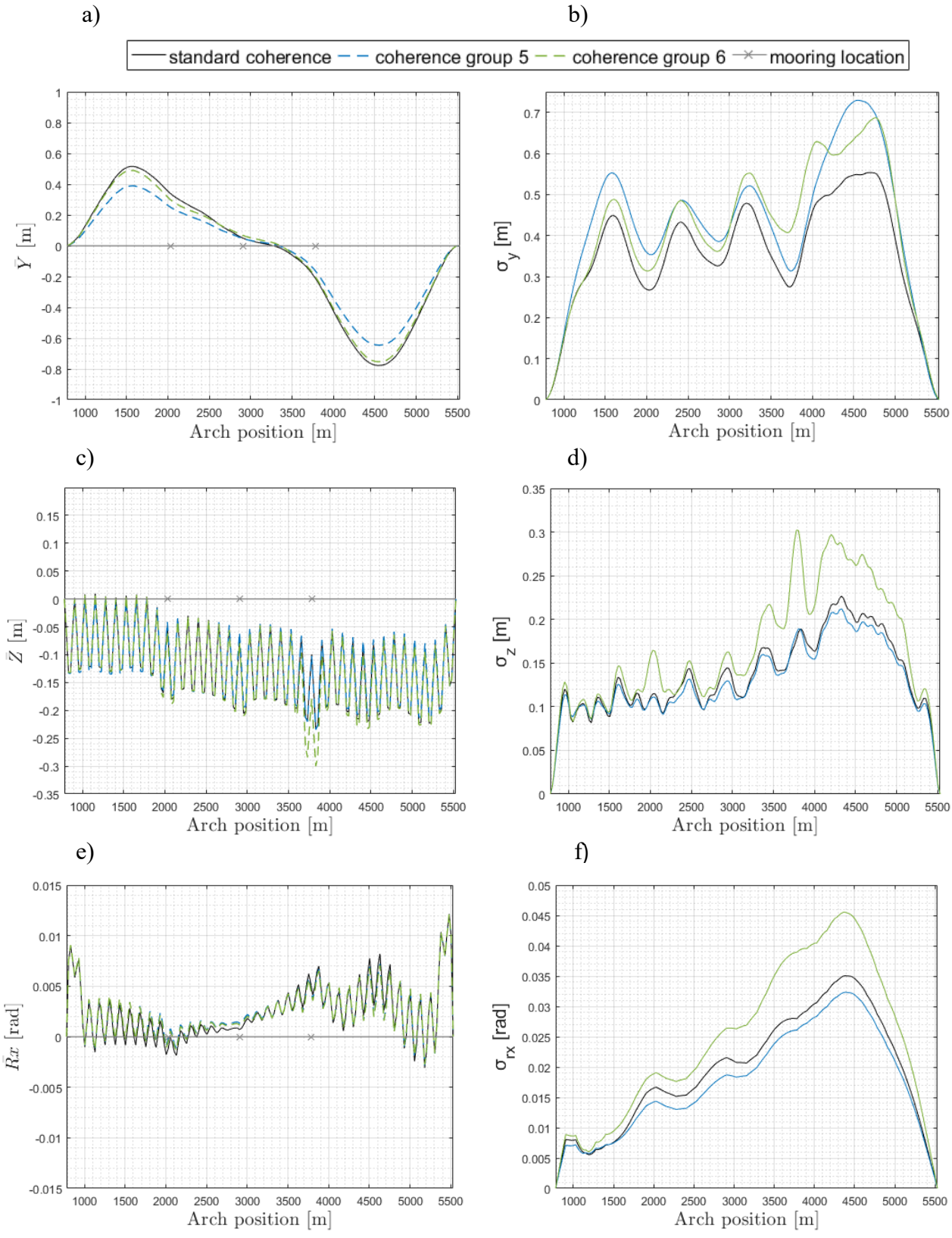

Figure 96: Sensitivity check of the coherence group 5 and 6 for wind direction 270° (left column: the mean displacement of the girder, right column: the standard deviation of the displacement)

Table 27: Coherence parameter group 7 and 8

Group no.	Au	Av	Aw	Cux	Cuy	Cuz	Cvx	Cvy	Cvz	Cwx	Cwy	Cwz
Standard N400	6.8	9.4	9.4	3	10	10	6	6.5	6.5	3	6.5	3
7	6.8	9.4	9.4	3	10	10	6	**3.4**	6.5	3	6.5	3
8	6.8	9.4	9.4	3	10	10	6	**0.93**	6.5	3	6.5	3

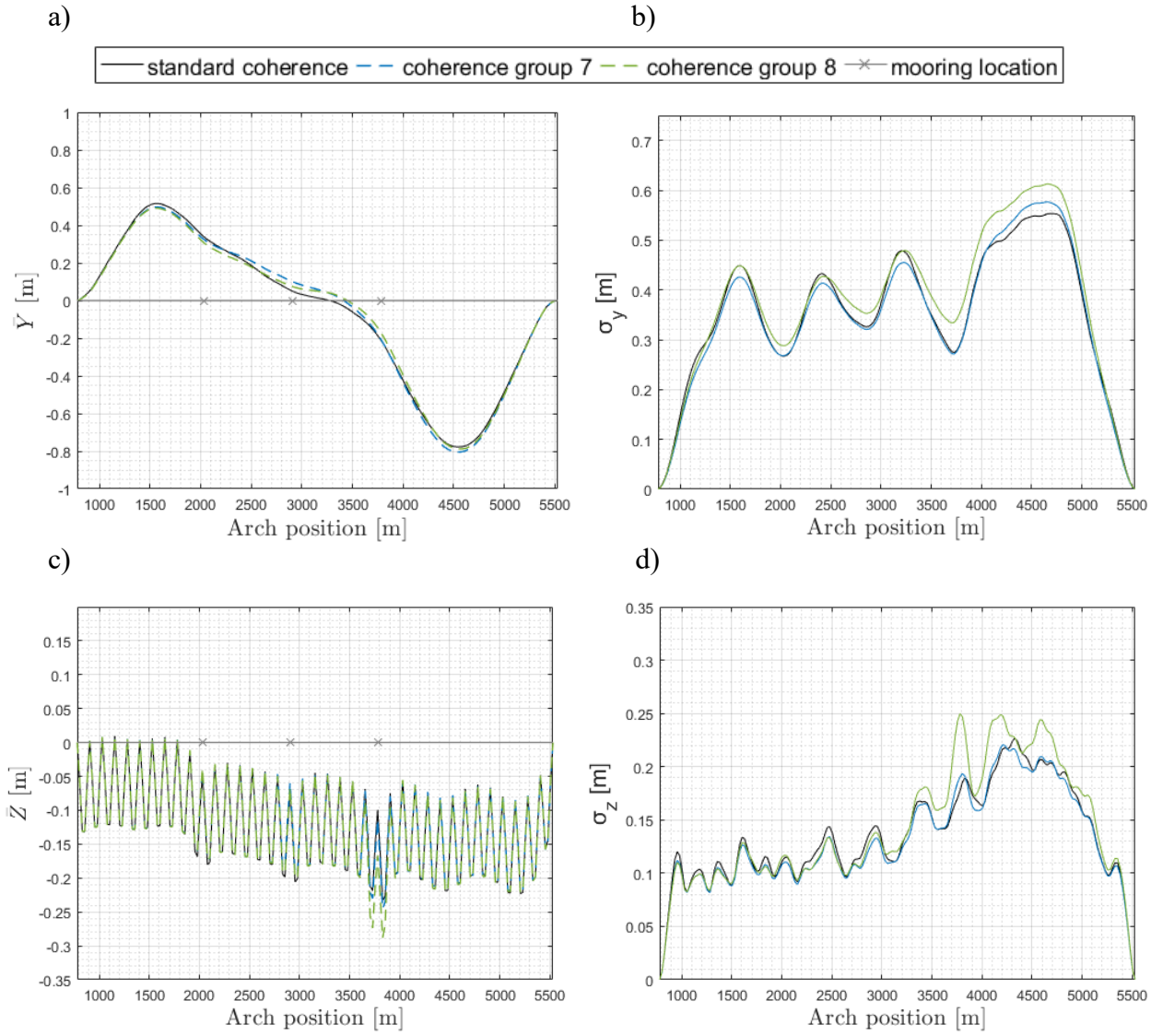

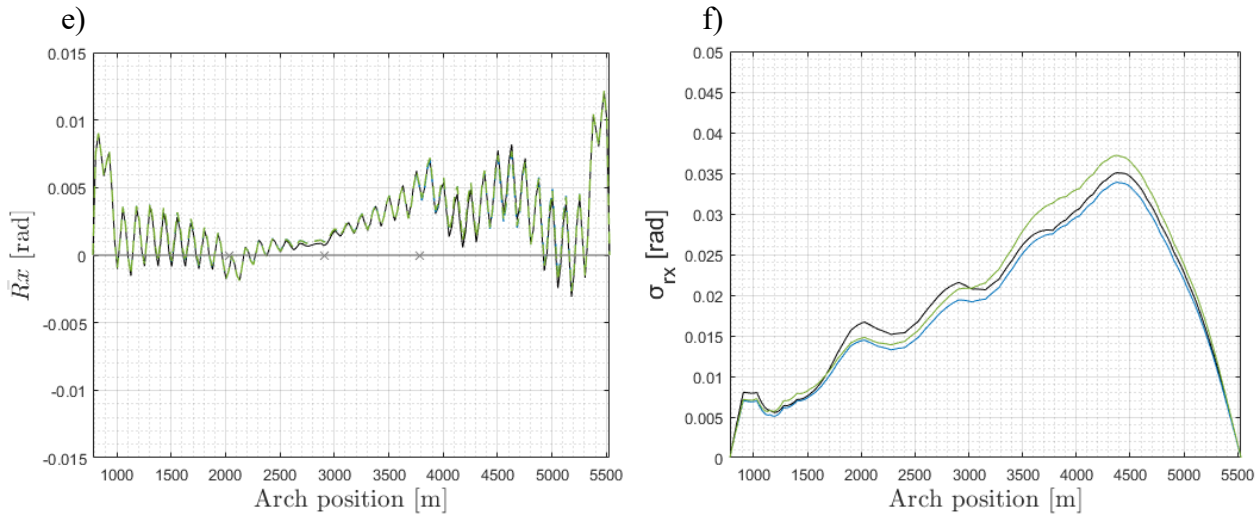

Figure 97: Sensitivity check of the coherence group 7 and 8 for wind direction 270° (left column: the mean displacement of the girder, right column: the standard deviation of the displacement)

Table 28: Coherence parameter group 9 and 10

Group no.	Au	Av	Aw	Cux	Cuy	Cuz	Cvx	Cvy	Cvz	Cwx	Cwy	Cwz
Standard N400	6.8	9.4	9.4	3	10	10	6	6.5	6.5	3	6.5	3
9	6.8	9.4	9.4	3	10	10	6	6.5	6.5	3	**3.4**	3
10	6.8	9.4	9.4	3	10	10	6	6.5	6.5	3	**5.4**	3

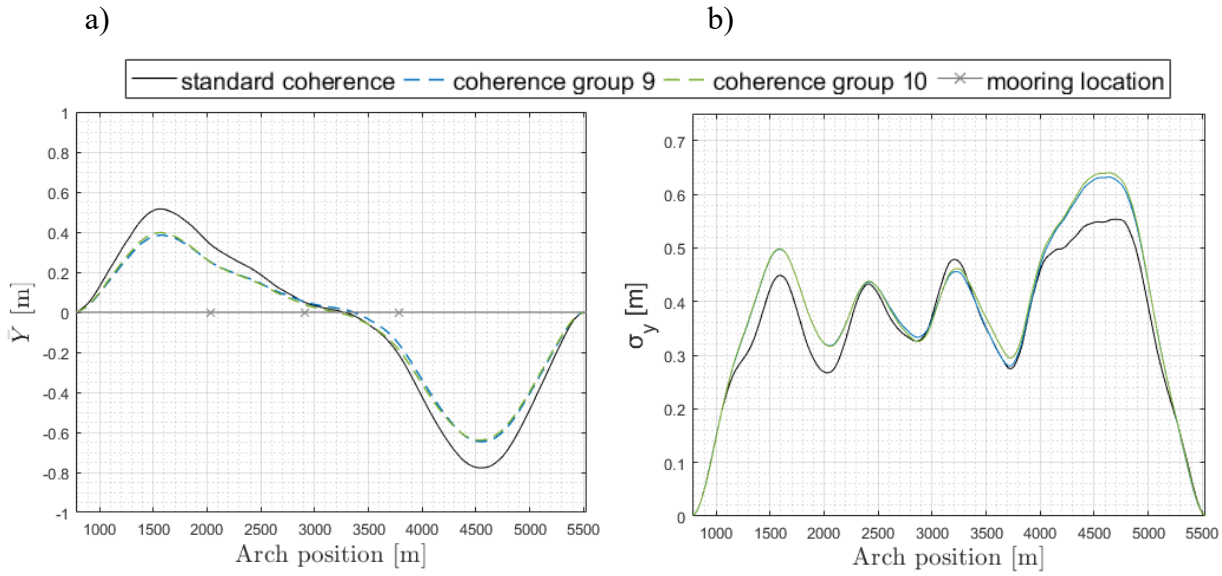

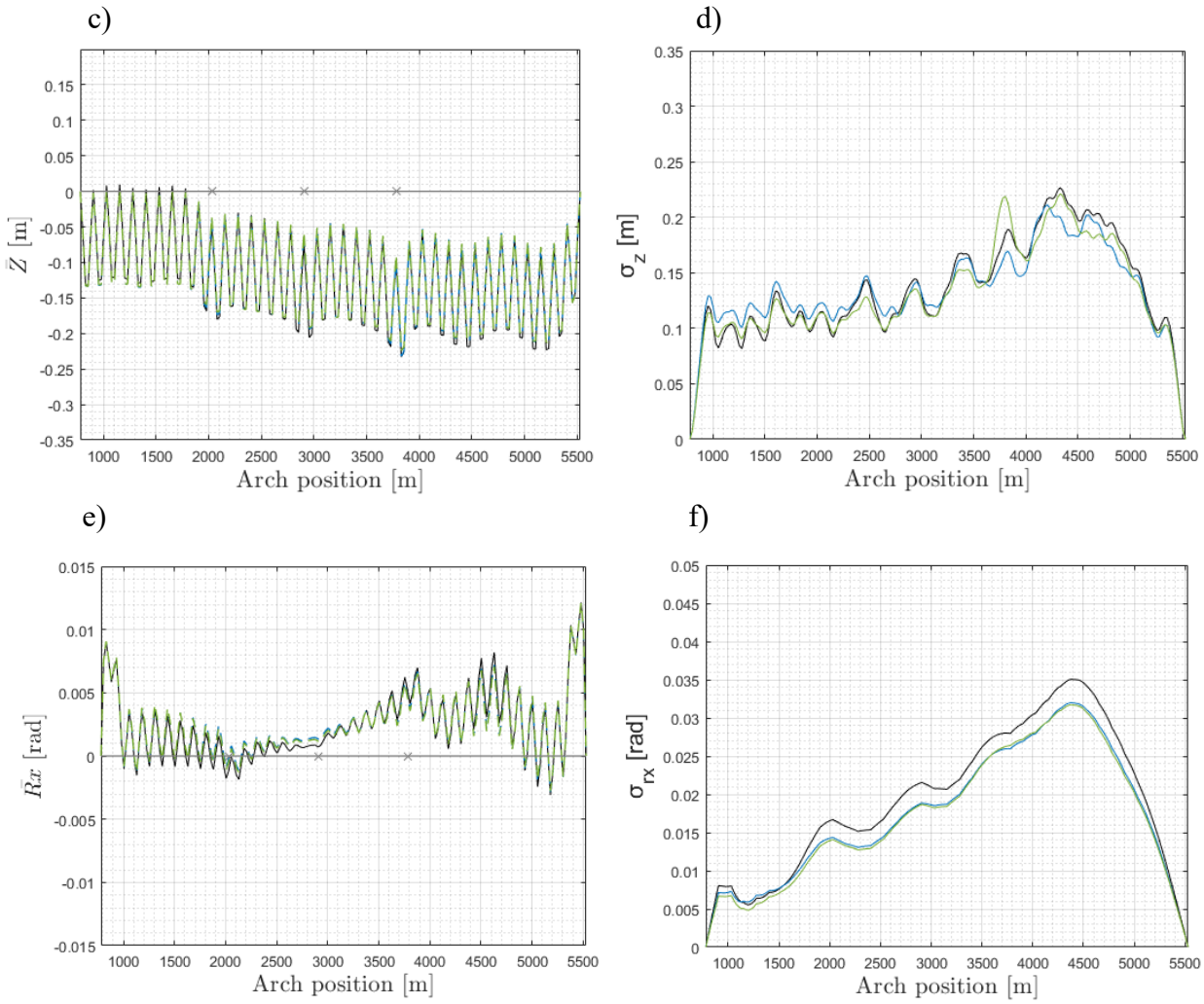

Figure 98: Sensitivity check of the coherence group 9 and 10 for wind direction 270° (left column: the mean displacement of the girder, right column: the standard deviation of the displacement)

Table 29: Comparison of maximum displacement for coherence parameters group 5 and 6

Group no.	Cuy	Y (m)	Z (m)	Rx (deg)
Standard N400	10	2.3762	0.9581	7.1505
5	1.15	2.2803	0.8748	7.7636
6	6.6	3.8939	1.5885	13.9515

Table 30: Comparison of maximum displacement for coherence parameters group 7 and 8

Group no.	Cvy	Y (m)	Z (m)	Rx (deg)
Standard N400	6.5	2.3762	0.9581	7.1505
7	3.4	2.1530	1.0518	7.8381
8	0.93	2.2752	1.1489	8.6459

Table 31: Comparison of maximum displacement for coherence parameters group 9 and 10

Group no.	Cwy	Y (m)	Z (m)	Rx (deg)
Standard N400	6.5	2.3762	0.9581	7.1505
9	3.4	2.3701	0.8818	6.8640
10	5.4	3.8515	1.4943	13.8541

CONCLUSION

In this thesis work the dynamic response of the floating pontoon bridge with side mooring lines under various aerodynamic load conditions is investigated. The finite element model of the structure is developed in Abaqus software. The modal analysis is conducted when there is no aerodynamic loads considered and when there is static wind load applied. The bridge responses under static wind and dynamic wind are studied separately. The time domain analysis is performed in the study of the bridge dynamic response under aerodynamic loads characterized by quasi-steady buffeting theroy. The turbulent wind field with return period of 100 years is simulated in MATLAB considering wind spectral and coherence parameters suggested by the design standard N400 and from field measurements. The motion-dependent instantaneous wind load is calculated in the Fortran subroutines which are developed to integrate with Abaqus.

In the modal analysis, it is found that the horizontal modes are dominated by low-frequencies while the vertical and rotational modes are concentrated in a higher frequency range (after 0,2 Hz). The first horizontal mode has the eigen-period of 31,9 sec, the first vertical mode of 4,7 sec and the first torsional mode of 3,7 sec. Moreover, numbers of mooring lines modes are observed during modal analysis between the first horizontal and vertical mode. Their contribution to horizontal movement can be seen by spectral peaks in Figure 85 of horizontal response power spectral density. The eigenfrequency comparison of the model with and without mooring lines reveals that the mooring lines application can noticeably reduce the dynamic horizontal movement of the bridge. Additionally, the frequency where the first horizontal mode appears in the model without mooring lines is 0,01189 Hz which is almost 40% lower compared to the frequency of the first horizontal mode in model with additional stiffness. No significant difference is observed between the the mode shapes under no aerodynamic loads and the mode shapes under static wind loads.

The study of the bridge response under static wind of various directions shows that the displacement is the largest under wind directions that give assymetric static load to the girder. It is under 320° wind direction that the largest maximum horizontal displacement of the uniform distribution is found and is equal to 0,4 meters. The results reveal that the bridge is more resistant against the symmetric load due to the curved geometry. To improve the design reliability, four possible static wind distributions have been proposed in the Design basis [24] and are investigated in this thesis. It is found in several wind directions that larger displacement

is introduced by the non-uniform static wind distribution when the resultant wind load is moved towards the northern bridge span and becomes assymetric.

The dynamic reponse is performed for the wind coming from the east (90°) and west (270°) and considering several groups of spectral and coherence parameters. Two groups of parameters that are recalculated from the field measurements during the extreme wind conditions are compared to empirical values suggested in standard N400. The important conclusion from the dynamic analysis is that the wind direction 90° has a stronger influence on horizontal response of the low bridge than direction 270° due to the curved geometry of the bridge. It can be seen in Figure 72 (a) that at the last span of the low bridge the eastern wind causes noticeably larger horizontal mean displacement than the western wind. The maximum girder node responses for both wind directions were found to be at the same arch position of 4530 meters distance and equal to 3,3332 meters and 3,2426 meters for eastern and western wind respectively. Furthermore, it is observed that the bridge model is more resistant for displacements in global Z and global Rx direction when the wind is blowing from 90° than from the opposite 270° direction. Moreover, the Figure 79 demonstrates that mooring lines are under higher tension when wind is blowing from the western side and that is due to the fact that curvature to the right side (east) creates initially high tension on mooring lines.

From the spectral and coherence parameters analysis it was concluded that including in the analysis only the parameters suggested by the standard N400 the bridge real dynamic responses under the extreme wind conditions will not be described accurate enough to ensure the safety of the design. It is found through performed results that parameters recalculated from the field measurements result in larger maximum girder nodes responses in all three directions under the eastern wind. It was observed that the field-measured parameters group 1 has stronger influence on maximum girder nodes responses at the northern half of the low bridge. While the field-measured parameters group 2 influences the southern half of the bridge more under the eastern wind. In terms of wind direction 270° the parameters group 2 gives larger horizontal maximum responses along the bridge with the maximum of 3,3960 meters at arch position 4530 meters. The displacements in other directions remain dominated by wind simulated with standard parameters under the western wind. It is also seen in Figure 80 that under wind direction 270° parameters group 2 and standard values cause larger tension forces on mooring lines in comparison to parameters group 1. By considering several realizations in the time domain analysis, the stochasticity of the wind field is included and hence the reliability of the conclusions made in the dynamic analysis is improved.

The power spectral density of the horizontal response (Figure 84) confirms that the horizontal response is governed by low-frequency modes. The modes coupling between horizontal and torsional modes is well captured by the PSD of the horizontal response (Figure 85) and the torsional response (Figure 90). The PSD of the vertical response (Figure 88) indicates that there is a great contribution from the 1st rotational mode.

The result of the sensitivity check reveals that the coherence parameter C_{uy} is the most critical wind parameter to the bridge response in global Y and Z direction, and that the bridge reponse in Rx direction is most influenced by the wind spectra parameter A_u. For both coherence parameter A_n and wind spectra parameter C_n, it is the parameter which associates with the along wind component u that is dominant. The case study also shows that the change of individual wind parameter causes stronger bridge response to varying degrees compared to the results obtained by considering the standard wind parameters.

For the future analyses, the investigation into the aerodynamic effects accompanied by the hydrodynamic loads is recommended. In the modeling of the cable-stayed bridge, more effective solution for performing the iterative processes to obtain the accurate cable pretension forces is suggested and hence ensuring the static equilibrium and the minimum deflection in the structure. Additional mean wind distributions are worth considering due to the complexity and variety of the real wind condition. The bridge dynamic response under asymmetric wind load which is found to be critical in the static analysis is suggested to be studied. The conclusion that field-measured wind parameters cause larger bridge response leads to the recommendation that more sets of wind spectral parameter and coherence parameter can be investigated.

REFERENCES

[1] ResearchGate. Model damping ratio derived from Rayleigh damping. 2017. https://www.researchgate.net/publication/318363169_Studies_on_damping_behavior_of_vertically_mixed_structures_with_upper_steel_and_lower_concrete_substructures.

[2] Statens vegvesen. Concept evaluation – Appendix F. Global analyses – Modelling and assumptions. 31.08.2019.

[3] Statens vegvesen. 21.02.2019.

https://www.vegvesen.no/en/roads/Roads+and+bridges/Road+projects/e39coastalhighwayroute/news/norway-takes-on-its-largest-infrastructure-project-in-modern-history.

[4] Statens vegvesen. 10.2019.

https://www.vegvesen.no/_attachment/2044354/binary/1348188?fast_title=An+overview+-+The+E39+Coastal+Highway+Route.pdf.

[5] Statens vegvesen. 10.2019.

https://www.vegvesen.no/_attachment/2044359/binary/1348191?fast_title=Choice+of+technology+for+fjord+crossings+-+The+E39+Coastal+Highway+Route.pdf.

[6] European Standard. Eurocode 1: Actions on structures – Part 1-4: General actions – Wind actions. 04.2010.

[7] Einar N. Strømmen. Theory of Bridge Aerodynamics. Springer. 2010.

[8] Chapter 9: The TL Timoshenko plane beam element. Available from: http://kis.tu.kielce.pl//mo/COLORADO_NFEM/colorado/NFEM.Ch09.pdf.

[9] Wang J., Cheynet E., Jakobsen J.B., Snæbjörnsson J. Time-domain analysis of wind-induced response of a suspension bridge in comparison with the full-scale measurements. In: ASME 2017 36th International Conference on Ocean, Offshore and Arctic Engineering, American Society of Mechanical Engineering, New York. 2017.

[10] Wang B. Large Floating Structures. Springer. 2018.

[11] Statens vegvesen. Preferred solution, K12– Appendix A. Drawings binder. 15.08.2019.

[12] Abaqus 6.14. Abaqus Analysis User's Guide. Available from: http://ivt-abaqusdoc.ivt.ntnu.no:2080/v6.14/books/usb/default.htm

[13] Statens vegvesen. Concept evaluation– Appendix M. Mooring system. 31.08.2019.

[14] Statens vegvesen. MetOcean Design basis. 2018.

[15] Statens vegvesen. Håndbok N400: Bruprosjektering. 2014.

[16] Sha Y., Amdahl J., Aalberg A., Yu Z. Numerical investigations of the dynamic response of a floating bridge under environmental loadings. Ships and Offshore Structures. Centre for Autonomous Marine Operations and Systems, Department of Marine Technology, Norwegian University of Science and Technology, Trondheim, Norway. 2018.

[17] Cook R.D., Malkus D.S, Plesha M.E., Witt R.J. Concepts and Applications of Finite Element Analysis. Fourth edition. John Wiley. 2002.

[18] Langen I. On dynamic analysis of floating bridges, Division of structural mechanics, The Norwegian Institute of Technology, The University of Trondheim, Norway. 1981.

[19] Rao S.S. Mechanical vibrations, Sixth Edition in SI Units. Pearson Education. 2018.

[20] Wind load on structures, Lecture notes part 1&2, Jasna B. Jakobsen, University of Stavanger. 2019.

[21] Dyrbye C., Hansen S.O., Wind loads on structures. Wiley. 1997.

[22] Writing User Subroutines with Abaqus, Lecture 2: User Subroutine DLOAD. Available from:
https://imechanica.org/files/Writing%20User%20Subroutines%20with%20ABAQUS_0.pdf

[23] Beam element cross-section orientation. Available from:

https://abaqus-docs.mit.edu/2017/English/SIMACAEELMRefMap/simaelm-c-beamcrosssection.htm

[24] Statens vegvesen. Design Basis Bjørnafjorden. Side- and end anchored floating bridge. 07.03.2017.

[25] Welch's power spectral density estimate. Available from:
https://se.mathworks.com/help/signal/ref/pwelch.html

APPENDIX A: Eigenvalue output of the full bridge

E I G E N V A L U E O U T P U T

MODE NO	EIGENVALUE	FREQUENCY (RAD/TIME)	FREQUENCY (CYCLES/TIME)	GENERALIZED MASS	COMPOSITE MODAL
1	2.73259E-02	0.16531	2.63092E-02	1.0000	0.0000
2	5.04869E-02	0.22469	3.57610E-02	1.0000	0.0000
3	0.10327	0.32135	5.11445E-02	1.0000	0.0000
4	0.17776	0.42162	6.71031E-02	1.0000	0.0000
5	0.19564	0.44231	7.03958E-02	1.0000	0.0000
6	0.19566	0.44234	7.04000E-02	1.0000	0.0000
7	0.19940	0.44655	7.10699E-02	1.0000	0.0000
8	0.19948	0.44663	7.10840E-02	1.0000	0.0000
9	0.20049	0.44776	7.12639E-02	1.0000	0.0000
10	0.20104	0.44838	7.13616E-02	1.0000	0.0000
11	0.20124	0.44860	7.13968E-02	1.0000	0.0000
12	0.24089	0.49081	7.81141E-02	1.0000	0.0000
13	0.24090	0.49081	7.81156E-02	1.0000	0.0000
14	0.24443	0.49440	7.86854E-02	1.0000	0.0000
15	0.24446	0.49443	7.86904E-02	1.0000	0.0000
16	0.25292	0.50291	8.00413E-02	1.0000	0.0000
17	0.25294	0.50293	8.00441E-02	1.0000	0.0000
18	0.27417	0.52361	8.33355E-02	1.0000	0.0000
19	0.27423	0.52367	8.33450E-02	1.0000	0.0000
20	0.29044	0.53893	8.57729E-02	1.0000	0.0000
21	0.29050	0.53898	8.57807E-02	1.0000	0.0000
22	0.30838	0.55532	8.83819E-02	1.0000	0.0000
23	0.30844	0.55537	8.83900E-02	1.0000	0.0000
24	0.32446	0.56962	9.06572E-02	1.0000	0.0000
25	0.32457	0.56971	9.06716E-02	1.0000	0.0000
26	0.34504	0.58740	9.34875E-02	1.0000	0.0000
27	0.34513	0.58747	9.34995E-02	1.0000	0.0000
28	0.34997	0.59158	9.41528E-02	1.0000	0.0000
29	0.35004	0.59164	9.41629E-02	1.0000	0.0000
30	0.35480	0.59565	9.48013E-02	1.0000	0.0000
31	0.42670	0.65322	0.10396	1.0000	0.0000
32	0.53505	0.73147	0.11642	1.0000	0.0000
33	0.53592	0.73207	0.11651	1.0000	0.0000
34	0.54545	0.73855	0.11754	1.0000	0.0000
35	0.54611	0.73900	0.11761	1.0000	0.0000
36	0.58950	0.76779	0.12220	1.0000	0.0000
37	0.59075	0.76860	0.12233	1.0000	0.0000
38	0.61622	0.78499	0.12494	1.0000	0.0000
39	0.63944	0.79965	0.12727	1.0000	0.0000
40	0.64087	0.80054	0.12741	1.0000	0.0000
41	0.64769	0.80479	0.12809	1.0000	0.0000
42	0.64870	0.80542	0.12819	1.0000	0.0000
43	0.66043	0.81267	0.12934	1.0000	0.0000
44	0.67172	0.81958	0.13044	1.0000	0.0000
45	0.67175	0.81960	0.13044	1.0000	0.0000
46	0.75187	0.86710	0.13800	1.0000	0.0000
47	0.75318	0.86786	0.13812	1.0000	0.0000
48	0.80593	0.89774	0.14288	1.0000	0.0000
49	0.80680	0.89822	0.14296	1.0000	0.0000
50	0.88621	0.94139	0.14983	1.0000	0.0000
51	0.91017	0.95403	0.15184	1.0000	0.0000
52	0.91094	0.95443	0.15190	1.0000	0.0000
53	0.93171	0.96525	0.15362	1.0000	0.0000
54	0.93280	0.96582	0.15371	1.0000	0.0000
55	0.98658	0.99327	0.15808	1.0000	0.0000
56	0.98769	0.99382	0.15817	1.0000	0.0000
57	1.0338	1.0167	0.16182	1.0000	0.0000
58	1.0352	1.0175	0.16193	1.0000	0.0000
59	1.2519	1.1189	0.17808	1.0000	0.0000

60	1.7320	1.3161	0.20946	1.0000	0.0000
61	1.8112	1.3458	0.21419	1.0000	0.0000
62	1.8380	1.3557	0.21577	1.0000	0.0000
63	1.9135	1.3833	0.22016	1.0000	0.0000
64	1.9181	1.3850	0.22042	1.0000	0.0000
65	1.9348	1.3910	0.22138	1.0000	0.0000
66	1.9375	1.3919	0.22153	1.0000	0.0000
67	1.9451	1.3947	0.22197	1.0000	0.0000
68	1.9469	1.3953	0.22207	1.0000	0.0000
69	1.9493	1.3962	0.22221	1.0000	0.0000
70	1.9532	1.3976	0.22243	1.0000	0.0000
71	1.9622	1.4008	0.22294	1.0000	0.0000
72	1.9742	1.4051	0.22362	1.0000	0.0000
73	2.0045	1.4158	0.22533	1.0000	0.0000
74	2.0260	1.4234	0.22654	1.0000	0.0000
75	2.0654	1.4372	0.22873	1.0000	0.0000
76	2.1067	1.4515	0.23101	1.0000	0.0000
77	2.1690	1.4728	0.23440	1.0000	0.0000
78	2.2443	1.4981	0.23843	1.0000	0.0000
79	2.3064	1.5187	0.24170	1.0000	0.0000
80	2.3236	1.5243	0.24261	1.0000	0.0000
81	2.4232	1.5567	0.24775	1.0000	0.0000
82	2.5344	1.5920	0.25337	1.0000	0.0000
83	2.6639	1.6322	0.25977	1.0000	0.0000
84	2.7792	1.6671	0.26532	1.0000	0.0000
85	2.7929	1.6712	0.26598	1.0000	0.0000
86	2.9573	1.7197	0.27370	1.0000	0.0000
87	2.9632	1.7214	0.27397	1.0000	0.0000
88	3.0890	1.7576	0.27973	1.0000	0.0000
89	3.1187	1.7660	0.28107	1.0000	0.0000
90	3.3117	1.8198	0.28963	1.0000	0.0000
91	3.5369	1.8807	0.29932	1.0000	0.0000
92	3.7166	1.9278	0.30683	1.0000	0.0000
93	3.7855	1.9456	0.30966	1.0000	0.0000
94	3.7917	1.9472	0.30991	1.0000	0.0000
95	4.0793	2.0197	0.32145	1.0000	0.0000
96	4.4122	2.1005	0.33431	1.0000	0.0000
97	4.5619	2.1359	0.33993	1.0000	0.0000
98	4.6260	2.1508	0.34231	1.0000	0.0000
99	4.7742	2.1850	0.34775	1.0000	0.0000
100	4.8698	2.2068	0.35122	1.0000	0.0000
101	5.1739	2.2746	0.36202	1.0000	0.0000
102	5.5876	2.3638	0.37621	1.0000	0.0000
103	5.6245	2.3716	0.37745	1.0000	0.0000
104	5.7750	2.4031	0.38247	1.0000	0.0000
105	6.1501	2.4799	0.39470	1.0000	0.0000
106	6.6006	2.5692	0.40890	1.0000	0.0000
107	6.6209	2.5731	0.40952	1.0000	0.0000
108	6.8301	2.6134	0.41594	1.0000	0.0000
109	6.9500	2.6363	0.41958	1.0000	0.0000
110	7.4046	2.7211	0.43308	1.0000	0.0000
111	7.5615	2.7498	0.43765	1.0000	0.0000
112	8.0529	2.8378	0.45164	1.0000	0.0000
113	8.4862	2.9131	0.46364	1.0000	0.0000
114	8.7196	2.9529	0.46997	1.0000	0.0000
115	8.7972	2.9660	0.47206	1.0000	0.0000
116	8.8327	2.9720	0.47301	1.0000	0.0000
117	9.6809	3.1114	0.49520	1.0000	0.0000
118	10.053	3.1706	0.50461	1.0000	0.0000
119	10.082	3.1752	0.50535	1.0000	0.0000
120	10.366	3.2197	0.51243	1.0000	0.0000
121	10.964	3.3112	0.52700	1.0000	0.0000
122	11.370	3.3719	0.53665	1.0000	0.0000
123	11.857	3.4435	0.54805	1.0000	0.0000
124	12.322	3.5102	0.55867	1.0000	0.0000
125	12.709	3.5650	0.56739	1.0000	0.0000
126	12.792	3.5765	0.56922	1.0000	0.0000
127	13.406	3.6614	0.58273	1.0000	0.0000

128	13.806	3.7157	0.59137	1.0000	0.0000
129	13.861	3.7231	0.59255	1.0000	0.0000
130	14.136	3.7598	0.59839	1.0000	0.0000
131	14.792	3.8461	0.61212	1.0000	0.0000
132	14.925	3.8633	0.61486	1.0000	0.0000
133	15.443	3.9298	0.62544	1.0000	0.0000
134	15.993	3.9991	0.63648	1.0000	0.0000
135	16.419	4.0521	0.64491	1.0000	0.0000
136	16.578	4.0717	0.64802	1.0000	0.0000
137	17.775	4.2160	0.67100	1.0000	0.0000
138	17.924	4.2337	0.67381	1.0000	0.0000
139	18.260	4.2731	0.68009	1.0000	0.0000
140	18.726	4.3273	0.68871	1.0000	0.0000
141	19.460	4.4113	0.70208	1.0000	0.0000
142	20.905	4.5722	0.72769	1.0000	0.0000
143	20.989	4.5813	0.72914	1.0000	0.0000
144	21.657	4.6537	0.74066	1.0000	0.0000
145	21.841	4.6735	0.74381	1.0000	0.0000
146	22.985	4.7943	0.76303	1.0000	0.0000
147	23.174	4.8140	0.76617	1.0000	0.0000
148	23.836	4.8822	0.77703	1.0000	0.0000
149	23.941	4.8930	0.77874	1.0000	0.0000
150	25.306	5.0305	0.80063	1.0000	0.0000
151	26.043	5.1032	0.81220	1.0000	0.0000
152	26.260	5.1245	0.81559	1.0000	0.0000
153	26.827	5.1795	0.82434	1.0000	0.0000
154	28.911	5.3769	0.85575	1.0000	0.0000
155	29.034	5.3883	0.85757	1.0000	0.0000
156	29.842	5.4627	0.86942	1.0000	0.0000
157	30.106	5.4869	0.87326	1.0000	0.0000
158	30.681	5.5390	0.88156	1.0000	0.0000
159	31.655	5.6263	0.89545	1.0000	0.0000
160	32.528	5.7033	0.90771	1.0000	0.0000
161	33.332	5.7733	0.91886	1.0000	0.0000
162	34.713	5.8918	0.93770	1.0000	0.0000
163	35.517	5.9597	0.94851	1.0000	0.0000
164	36.341	6.0283	0.95944	1.0000	0.0000
165	36.592	6.0491	0.96275	1.0000	0.0000
166	37.098	6.0908	0.96938	1.0000	0.0000
167	37.936	6.1592	0.98027	1.0000	0.0000
168	38.091	6.1718	0.98228	1.0000	0.0000
169	39.216	6.2623	0.99668	1.0000	0.0000
170	39.390	6.2761	0.99888	1.0000	0.0000
171	40.659	6.3764	1.0148	1.0000	0.0000
172	41.052	6.4072	1.0197	1.0000	0.0000
173	41.597	6.4495	1.0265	1.0000	0.0000
174	42.356	6.5081	1.0358	1.0000	0.0000
175	42.756	6.5388	1.0407	1.0000	0.0000
176	43.112	6.5660	1.0450	1.0000	0.0000
177	43.994	6.6328	1.0556	1.0000	0.0000
178	44.866	6.6982	1.0661	1.0000	0.0000
179	45.297	6.7303	1.0712	1.0000	0.0000
180	46.600	6.8265	1.0865	1.0000	0.0000
181	48.803	6.9859	1.1118	1.0000	0.0000
182	49.455	7.0324	1.1192	1.0000	0.0000
183	50.497	7.1061	1.1310	1.0000	0.0000
184	51.636	7.1858	1.1437	1.0000	0.0000
185	53.532	7.3166	1.1645	1.0000	0.0000
186	54.545	7.3855	1.1754	1.0000	0.0000
187	57.097	7.5563	1.2026	1.0000	0.0000
188	58.110	7.6230	1.2132	1.0000	0.0000
189	58.499	7.6485	1.2173	1.0000	0.0000
190	60.043	7.7487	1.2332	1.0000	0.0000
191	64.201	8.0126	1.2752	1.0000	0.0000
192	64.455	8.0284	1.2778	1.0000	0.0000
193	65.557	8.0967	1.2886	1.0000	0.0000
194	66.326	8.1441	1.2962	1.0000	0.0000
195	66.497	8.1545	1.2978	1.0000	0.0000

196	66.900	8.1792	1.3018	1.0000	0.0000
197	71.284	8.4430	1.3437	1.0000	0.0000
198	72.631	8.5224	1.3564	1.0000	0.0000
199	75.620	8.6960	1.3840	1.0000	0.0000
200	76.147	8.7262	1.3888	1.0000	0.0000
201	79.441	8.9129	1.4185	1.0000	0.0000
202	79.854	8.9361	1.4222	1.0000	0.0000
203	80.275	8.9596	1.4260	1.0000	0.0000
204	82.122	9.0621	1.4423	1.0000	0.0000
205	82.489	9.0824	1.4455	1.0000	0.0000
206	85.578	9.2508	1.4723	1.0000	0.0000
207	87.269	9.3418	1.4868	1.0000	0.0000
208	93.148	9.6513	1.5361	1.0000	0.0000
209	94.837	9.7384	1.5499	1.0000	0.0000
210	97.907	9.8948	1.5748	1.0000	0.0000
211	101.73	10.086	1.6053	1.0000	0.0000
212	101.94	10.097	1.6069	1.0000	0.0000
213	102.06	10.102	1.6078	1.0000	0.0000
214	103.25	10.161	1.6172	1.0000	0.0000
215	103.34	10.166	1.6179	1.0000	0.0000
216	104.57	10.226	1.6275	1.0000	0.0000
217	105.40	10.266	1.6340	1.0000	0.0000
218	106.61	10.325	1.6433	1.0000	0.0000
219	110.03	10.489	1.6694	1.0000	0.0000
220	110.99	10.535	1.6767	1.0000	0.0000
221	116.32	10.785	1.7165	1.0000	0.0000
222	117.23	10.827	1.7232	1.0000	0.0000
223	117.47	10.838	1.7250	1.0000	0.0000
224	121.92	11.042	1.7573	1.0000	0.0000
225	123.11	11.095	1.7659	1.0000	0.0000
226	125.77	11.215	1.7849	1.0000	0.0000
227	127.26	11.281	1.7954	1.0000	0.0000
228	127.36	11.286	1.7962	1.0000	0.0000
229	127.94	11.311	1.8002	1.0000	0.0000
230	131.23	11.456	1.8232	1.0000	0.0000
231	132.54	11.513	1.8323	1.0000	0.0000
232	135.70	11.649	1.8540	1.0000	0.0000
233	137.91	11.743	1.8690	1.0000	0.0000
234	138.67	11.776	1.8742	1.0000	0.0000
235	139.05	11.792	1.8768	1.0000	0.0000
236	141.50	11.895	1.8932	1.0000	0.0000
237	144.85	12.035	1.9155	1.0000	0.0000
238	146.07	12.086	1.9235	1.0000	0.0000
239	146.70	12.112	1.9277	1.0000	0.0000
240	147.75	12.155	1.9346	1.0000	0.0000
241	153.09	12.373	1.9692	1.0000	0.0000
242	154.43	12.427	1.9778	1.0000	0.0000
243	155.27	12.461	1.9832	1.0000	0.0000
244	155.33	12.463	1.9836	1.0000	0.0000
245	156.00	12.490	1.9879	1.0000	0.0000
246	156.65	12.516	1.9920	1.0000	0.0000
247	157.45	12.548	1.9971	1.0000	0.0000
248	158.15	12.576	2.0015	1.0000	0.0000
249	158.59	12.593	2.0043	1.0000	0.0000
250	159.91	12.645	2.0126	1.0000	0.0000
251	160.65	12.675	2.0173	1.0000	0.0000
252	161.01	12.689	2.0195	1.0000	0.0000
253	162.54	12.749	2.0291	1.0000	0.0000
254	162.74	12.757	2.0303	1.0000	0.0000
255	163.23	12.776	2.0334	1.0000	0.0000
256	164.12	12.811	2.0389	1.0000	0.0000
257	164.28	12.817	2.0399	1.0000	0.0000
258	164.47	12.824	2.0411	1.0000	0.0000
259	165.12	12.850	2.0452	1.0000	0.0000
260	165.64	12.870	2.0483	1.0000	0.0000
261	165.97	12.883	2.0504	1.0000	0.0000
262	166.50	12.904	2.0537	1.0000	0.0000
263	166.83	12.916	2.0557	1.0000	0.0000

264	171.85	13.109	2.0864	1.0000	0.0000
265	173.26	13.163	2.0949	1.0000	0.0000
266	175.91	13.263	2.1109	1.0000	0.0000
267	183.89	13.561	2.1582	1.0000	0.0000
268	184.95	13.600	2.1644	1.0000	0.0000
269	187.34	13.687	2.1784	1.0000	0.0000
270	190.01	13.784	2.1938	1.0000	0.0000
271	197.51	14.054	2.2367	1.0000	0.0000
272	200.94	14.175	2.2561	1.0000	0.0000
273	203.66	14.271	2.2713	1.0000	0.0000
274	208.33	14.434	2.2972	1.0000	0.0000
275	210.19	14.498	2.3074	1.0000	0.0000
276	214.04	14.630	2.3285	1.0000	0.0000
277	224.52	14.984	2.3848	1.0000	0.0000
278	227.43	15.081	2.4002	1.0000	0.0000
279	231.28	15.208	2.4204	1.0000	0.0000
280	241.25	15.532	2.4720	1.0000	0.0000
281	244.27	15.629	2.4875	1.0000	0.0000
282	246.51	15.701	2.4988	1.0000	0.0000
283	251.46	15.857	2.5238	1.0000	0.0000
284	254.74	15.961	2.5402	1.0000	0.0000
285	257.25	16.039	2.5527	1.0000	0.0000
286	266.09	16.312	2.5962	1.0000	0.0000
287	268.84	16.396	2.6096	1.0000	0.0000
288	277.72	16.665	2.6523	1.0000	0.0000
289	277.78	16.667	2.6526	1.0000	0.0000
290	279.11	16.707	2.6589	1.0000	0.0000
291	290.02	17.030	2.7104	1.0000	0.0000
292	299.03	17.293	2.7522	1.0000	0.0000
293	301.87	17.374	2.7652	1.0000	0.0000
294	304.40	17.447	2.7768	1.0000	0.0000
295	310.50	17.621	2.8045	1.0000	0.0000
296	321.73	17.937	2.8547	1.0000	0.0000
297	333.82	18.271	2.9079	1.0000	0.0000
298	337.99	18.384	2.9260	1.0000	0.0000
299	339.65	18.429	2.9331	1.0000	0.0000
300	342.56	18.508	2.9457	1.0000	0.0000
301	344.97	18.573	2.9560	1.0000	0.0000
302	354.59	18.830	2.9970	1.0000	0.0000
303	355.95	18.867	3.0027	1.0000	0.0000
304	357.90	18.918	3.0109	1.0000	0.0000
305	362.53	19.040	3.0304	1.0000	0.0000
306	364.51	19.092	3.0386	1.0000	0.0000
307	374.05	19.340	3.0781	1.0000	0.0000
308	386.83	19.668	3.1302	1.0000	0.0000
309	393.11	19.827	3.1555	1.0000	0.0000
310	401.46	20.036	3.1889	1.0000	0.0000
311	409.05	20.225	3.2189	1.0000	0.0000
312	416.29	20.403	3.2473	1.0000	0.0000
313	425.32	20.623	3.2823	1.0000	0.0000
314	428.94	20.711	3.2962	1.0000	0.0000
315	436.23	20.886	3.3241	1.0000	0.0000
316	443.87	21.068	3.3531	1.0000	0.0000
317	454.30	21.314	3.3923	1.0000	0.0000
318	463.89	21.538	3.4279	1.0000	0.0000
319	465.02	21.564	3.4321	1.0000	0.0000
320	473.66	21.764	3.4638	1.0000	0.0000
321	475.74	21.811	3.4714	1.0000	0.0000
322	481.96	21.954	3.4940	1.0000	0.0000
323	490.54	22.148	3.5250	1.0000	0.0000
324	499.23	22.343	3.5561	1.0000	0.0000
325	509.84	22.580	3.5936	1.0000	0.0000
326	513.20	22.654	3.6055	1.0000	0.0000
327	515.23	22.699	3.6126	1.0000	0.0000
328	525.17	22.917	3.6473	1.0000	0.0000
329	527.61	22.970	3.6557	1.0000	0.0000
330	531.97	23.064	3.6708	1.0000	0.0000
331	534.55	23.120	3.6797	1.0000	0.0000

332	538.82	23.213	3.6944	1.0000	0.0000
333	539.09	23.218	3.6953	1.0000	0.0000
334	541.99	23.281	3.7052	1.0000	0.0000
335	545.65	23.359	3.7177	1.0000	0.0000
336	548.77	23.426	3.7284	1.0000	0.0000
337	550.86	23.470	3.7354	1.0000	0.0000
338	554.90	23.556	3.7491	1.0000	0.0000
339	562.22	23.711	3.7738	1.0000	0.0000
340	564.22	23.753	3.7805	1.0000	0.0000
341	569.13	23.856	3.7969	1.0000	0.0000
342	571.70	23.910	3.8054	1.0000	0.0000
343	573.00	23.937	3.8098	1.0000	0.0000
344	575.44	23.988	3.8179	1.0000	0.0000
345	577.58	24.033	3.8249	1.0000	0.0000
346	579.54	24.074	3.8314	1.0000	0.0000
347	581.88	24.122	3.8392	1.0000	0.0000
348	585.45	24.196	3.8509	1.0000	0.0000
349	592.20	24.335	3.8731	1.0000	0.0000
350	592.94	24.350	3.8755	1.0000	0.0000
351	595.40	24.401	3.8835	1.0000	0.0000
352	598.32	24.461	3.8930	1.0000	0.0000
353	600.40	24.503	3.8998	1.0000	0.0000
354	600.85	24.512	3.9012	1.0000	0.0000
355	601.15	24.518	3.9022	1.0000	0.0000
356	602.61	24.548	3.9069	1.0000	0.0000
357	602.82	24.552	3.9076	1.0000	0.0000
358	605.41	24.605	3.9160	1.0000	0.0000
359	607.60	24.650	3.9231	1.0000	0.0000
360	608.22	24.662	3.9251	1.0000	0.0000
361	609.94	24.697	3.9307	1.0000	0.0000
362	613.10	24.761	3.9408	1.0000	0.0000
363	614.19	24.783	3.9443	1.0000	0.0000
364	616.29	24.825	3.9511	1.0000	0.0000
365	618.81	24.876	3.9591	1.0000	0.0000
366	620.84	24.917	3.9656	1.0000	0.0000
367	621.50	24.930	3.9677	1.0000	0.0000
368	623.49	24.970	3.9741	1.0000	0.0000
369	625.64	25.013	3.9809	1.0000	0.0000
370	628.91	25.078	3.9913	1.0000	0.0000
371	630.03	25.100	3.9949	1.0000	0.0000
372	632.46	25.149	4.0026	1.0000	0.0000
373	634.25	25.184	4.0082	1.0000	0.0000
374	635.39	25.207	4.0118	1.0000	0.0000
375	637.01	25.239	4.0169	1.0000	0.0000
376	639.38	25.286	4.0244	1.0000	0.0000
377	640.37	25.306	4.0275	1.0000	0.0000
378	641.90	25.336	4.0323	1.0000	0.0000
379	642.55	25.349	4.0343	1.0000	0.0000
380	643.21	25.362	4.0364	1.0000	0.0000
381	643.99	25.377	4.0389	1.0000	0.0000
382	644.68	25.391	4.0410	1.0000	0.0000
383	645.54	25.407	4.0437	1.0000	0.0000
384	648.37	25.463	4.0526	1.0000	0.0000
385	659.83	25.687	4.0882	1.0000	0.0000
386	668.74	25.860	4.1158	1.0000	0.0000
387	671.48	25.913	4.1242	1.0000	0.0000
388	679.06	26.059	4.1474	1.0000	0.0000
389	681.79	26.111	4.1557	1.0000	0.0000
390	686.12	26.194	4.1689	1.0000	0.0000
391	689.08	26.250	4.1779	1.0000	0.0000
392	701.62	26.488	4.2157	1.0000	0.0000
393	705.87	26.568	4.2285	1.0000	0.0000
394	715.04	26.740	4.2558	1.0000	0.0000
395	721.48	26.860	4.2750	1.0000	0.0000
396	723.14	26.891	4.2799	1.0000	0.0000
397	724.73	26.921	4.2846	1.0000	0.0000
398	729.78	27.014	4.2995	1.0000	0.0000
399	732.40	27.063	4.3072	1.0000	0.0000

400	736.35	27.136	4.3188	1.0000	0.0000
401	747.10	27.333	4.3502	1.0000	0.0000
402	750.81	27.401	4.3610	1.0000	0.0000
403	757.42	27.521	4.3802	1.0000	0.0000
404	765.52	27.668	4.4035	1.0000	0.0000
405	773.74	27.816	4.4271	1.0000	0.0000
406	781.41	27.954	4.4490	1.0000	0.0000
407	791.21	28.128	4.4768	1.0000	0.0000
408	796.25	28.218	4.4910	1.0000	0.0000
409	812.65	28.507	4.5370	1.0000	0.0000
410	813.11	28.515	4.5383	1.0000	0.0000
411	825.81	28.737	4.5736	1.0000	0.0000
412	836.22	28.918	4.6024	1.0000	0.0000
413	841.36	29.006	4.6165	1.0000	0.0000
414	851.50	29.180	4.6442	1.0000	0.0000
415	851.50	29.180	4.6442	1.0000	0.0000
416	851.98	29.189	4.6455	1.0000	0.0000
417	852.78	29.202	4.6477	1.0000	0.0000
418	858.44	29.299	4.6631	1.0000	0.0000
419	864.69	29.406	4.6801	1.0000	0.0000
420	866.77	29.441	4.6857	1.0000	0.0000
421	878.26	29.635	4.7166	1.0000	0.0000
422	882.42	29.705	4.7278	1.0000	0.0000
423	887.48	29.791	4.7413	1.0000	0.0000
424	892.71	29.878	4.7553	1.0000	0.0000
425	900.88	30.015	4.7770	1.0000	0.0000
426	914.96	30.248	4.8142	1.0000	0.0000
427	963.94	31.047	4.9413	1.0000	0.0000
428	964.64	31.059	4.9432	1.0000	0.0000
429	968.46	31.120	4.9529	1.0000	0.0000
430	968.46	31.120	4.9529	1.0000	0.0000
431	975.23	31.229	4.9702	1.0000	0.0000
432	1011.0	31.797	5.0606	1.0000	0.0000
433	1028.5	32.071	5.1042	1.0000	0.0000
434	1043.1	32.297	5.1402	1.0000	0.0000
435	1069.1	32.698	5.2040	1.0000	0.0000
436	1137.9	33.733	5.3687	1.0000	0.0000
437	1140.3	33.768	5.3744	1.0000	0.0000
438	1156.3	34.005	5.4121	1.0000	0.0000
439	1156.3	34.005	5.4121	1.0000	0.0000
440	1162.9	34.101	5.4274	1.0000	0.0000
441	1165.2	34.135	5.4327	1.0000	0.0000
442	1165.2	34.135	5.4327	1.0000	0.0000
443	1168.4	34.181	5.4401	1.0000	0.0000
444	1168.4	34.181	5.4401	1.0000	0.0000
445	1212.8	34.825	5.5425	1.0000	0.0000
446	1288.6	35.897	5.7133	1.0000	0.0000
447	1294.7	35.982	5.7267	1.0000	0.0000
448	1317.6	36.299	5.7771	1.0000	0.0000
449	1337.2	36.567	5.8199	1.0000	0.0000
450	1366.4	36.965	5.8832	1.0000	0.0000
451	1382.3	37.180	5.9173	1.0000	0.0000
452	1432.8	37.853	6.0244	1.0000	0.0000
453	1469.7	38.337	6.1015	1.0000	0.0000
454	1475.6	38.414	6.1138	1.0000	0.0000
455	1483.7	38.519	6.1305	1.0000	0.0000
456	1483.7	38.519	6.1305	1.0000	0.0000
457	1484.8	38.533	6.1327	1.0000	0.0000
458	1484.8	38.533	6.1327	1.0000	0.0000
459	1489.4	38.593	6.1422	1.0000	0.0000
460	1489.4	38.593	6.1422	1.0000	0.0000
461	1501.2	38.745	6.1664	1.0000	0.0000
462	1505.5	38.800	6.1753	1.0000	0.0000
463	1505.5	38.800	6.1753	1.0000	0.0000
464	1542.4	39.273	6.2505	1.0000	0.0000
465	1553.5	39.414	6.2729	1.0000	0.0000
466	1553.5	39.414	6.2729	1.0000	0.0000
467	1562.1	39.523	6.2903	1.0000	0.0000

468	1609.1	40.114	6.3843	1.0000	0.0000
469	1633.0	40.410	6.4314	1.0000	0.0000
470	1654.4	40.674	6.4735	1.0000	0.0000
471	1712.0	41.376	6.5853	1.0000	0.0000
472	1712.0	41.376	6.5853	1.0000	0.0000
473	1743.2	41.752	6.6450	1.0000	0.0000
474	1744.4	41.767	6.6474	1.0000	0.0000
475	1801.3	42.441	6.7547	1.0000	0.0000
476	1807.6	42.515	6.7665	1.0000	0.0000
477	1836.4	42.853	6.8202	1.0000	0.0000
478	1854.8	43.067	6.8543	1.0000	0.0000
479	1854.8	43.067	6.8543	1.0000	0.0000
480	1871.9	43.265	6.8859	1.0000	0.0000
481	1873.2	43.280	6.8883	1.0000	0.0000
482	1878.6	43.342	6.8982	1.0000	0.0000
483	1883.5	43.399	6.9072	1.0000	0.0000
484	1898.0	43.566	6.9337	1.0000	0.0000
485	1912.2	43.729	6.9596	1.0000	0.0000
486	1919.5	43.812	6.9729	1.0000	0.0000
487	1934.2	43.979	6.9995	1.0000	0.0000
488	1947.0	44.124	7.0226	1.0000	0.0000
489	1959.8	44.269	7.0457	1.0000	0.0000
490	1964.8	44.326	7.0548	1.0000	0.0000
491	1968.6	44.369	7.0615	1.0000	0.0000
492	1978.3	44.478	7.0789	1.0000	0.0000
493	1996.2	44.679	7.1109	1.0000	0.0000
494	2022.7	44.974	7.1579	1.0000	0.0000
495	2025.6	45.007	7.1630	1.0000	0.0000
496	2027.2	45.025	7.1659	1.0000	0.0000
497	2029.0	45.045	7.1691	1.0000	0.0000
498	2038.5	45.150	7.1858	1.0000	0.0000
499	2042.7	45.196	7.1931	1.0000	0.0000
500	2055.8	45.340	7.2162	1.0000	0.0000

APPENDIX B: Eigenvalue output of the low bridge

E I G E N V A L U E O U T P U T

MODE NO	EIGENVALUE	FREQUENCY (RAD/TIME)	FREQUENCY (CYCLES/TIME)	GENERALIZED MASS	COMPOSITE MODAL
1	3.87692E-02	0.19690	3.13374E-02	1.0000	0.0000
2	7.60846E-02	0.27583	4.39004E-02	1.0000	0.0000
3	0.10730	0.32757	5.21348E-02	1.0000	0.0000
4	0.18457	0.42961	6.83749E-02	1.0000	0.0000
5	0.19554	0.44220	7.03777E-02	1.0000	0.0000
6	0.19556	0.44222	7.03818E-02	1.0000	0.0000
7	0.19579	0.44248	7.04230E-02	1.0000	0.0000
8	0.19580	0.44250	7.04257E-02	1.0000	0.0000
9	0.19755	0.44447	7.07394E-02	1.0000	0.0000
10	0.19761	0.44454	7.07500E-02	1.0000	0.0000
11	0.24430	0.49426	7.86645E-02	1.0000	0.0000
12	0.24433	0.49429	7.86692E-02	1.0000	0.0000
13	0.24921	0.49921	7.94524E-02	1.0000	0.0000
14	0.24926	0.49926	7.94591E-02	1.0000	0.0000
15	0.25955	0.50946	8.10830E-02	1.0000	0.0000
16	0.25959	0.50950	8.10888E-02	1.0000	0.0000
17	0.27444	0.52387	8.33761E-02	1.0000	0.0000
18	0.27452	0.52394	8.33883E-02	1.0000	0.0000
19	0.28125	0.53033	8.44040E-02	1.0000	0.0000
20	0.28132	0.53040	8.44154E-02	1.0000	0.0000
21	0.31497	0.56122	8.93217E-02	1.0000	0.0000
22	0.31505	0.56129	8.93323E-02	1.0000	0.0000
23	0.31866	0.56450	8.98432E-02	1.0000	0.0000
24	0.31885	0.56467	8.98698E-02	1.0000	0.0000
25	0.33410	0.57801	9.19935E-02	1.0000	0.0000
26	0.33423	0.57813	9.20121E-02	1.0000	0.0000
27	0.34189	0.58472	9.30603E-02	1.0000	0.0000
28	0.36168	0.60140	9.57159E-02	1.0000	0.0000
29	0.36172	0.60143	9.57203E-02	1.0000	0.0000
30	0.43590	0.66022	0.10508	1.0000	0.0000
31	0.53133	0.72892	0.11601	1.0000	0.0000
32	0.53488	0.73136	0.11640	1.0000	0.0000
33	0.53561	0.73185	0.11648	1.0000	0.0000
34	0.53595	0.73209	0.11652	1.0000	0.0000
35	0.54045	0.73515	0.11700	1.0000	0.0000
36	0.58044	0.76186	0.12125	1.0000	0.0000
37	0.58144	0.76252	0.12136	1.0000	0.0000
38	0.64808	0.80503	0.12812	1.0000	0.0000
39	0.64870	0.80542	0.12819	1.0000	0.0000
40	0.66019	0.81252	0.12932	1.0000	0.0000
41	0.66144	0.81329	0.12944	1.0000	0.0000
42	0.68848	0.82975	0.13206	1.0000	0.0000
43	0.68923	0.83020	0.13213	1.0000	0.0000
44	0.74996	0.86600	0.13783	1.0000	0.0000
45	0.75361	0.86811	0.13816	1.0000	0.0000
46	0.77541	0.88058	0.14015	1.0000	0.0000
47	0.78140	0.88397	0.14069	1.0000	0.0000
48	0.78257	0.88463	0.14079	1.0000	0.0000
49	0.89316	0.94507	0.15041	1.0000	0.0000
50	0.89480	0.94594	0.15055	1.0000	0.0000
51	0.95134	0.97536	0.15523	1.0000	0.0000
52	0.95273	0.97608	0.15535	1.0000	0.0000
53	0.99312	0.99655	0.15861	1.0000	0.0000
54	1.0021	1.0010	0.15932	1.0000	0.0000
55	1.0030	1.0015	0.15939	1.0000	0.0000
56	1.0201	1.0100	0.16075	1.0000	0.0000
57	1.0212	1.0105	0.16083	1.0000	0.0000
58	1.3014	1.1408	0.18156	1.0000	0.0000
59	1.6672	1.2912	0.20550	1.0000	0.0000

60	1.8106	1.3456	0.21416	1.0000	0.0000
61	1.9121	1.3828	0.22008	1.0000	0.0000
62	1.9334	1.3905	0.22130	1.0000	0.0000
63	1.9347	1.3909	0.22137	1.0000	0.0000
64	1.9395	1.3927	0.22165	1.0000	0.0000
65	1.9463	1.3951	0.22204	1.0000	0.0000
66	1.9480	1.3957	0.22213	1.0000	0.0000
67	1.9510	1.3968	0.22230	1.0000	0.0000
68	1.9573	1.3990	0.22266	1.0000	0.0000
69	1.9717	1.4042	0.22348	1.0000	0.0000
70	1.9881	1.4100	0.22441	1.0000	0.0000
71	2.0137	1.4190	0.22585	1.0000	0.0000
72	2.0476	1.4310	0.22774	1.0000	0.0000
73	2.0870	1.4447	0.22992	1.0000	0.0000
74	2.1355	1.4613	0.23258	1.0000	0.0000
75	2.1529	1.4673	0.23352	1.0000	0.0000
76	2.2050	1.4849	0.23633	1.0000	0.0000
77	2.3024	1.5174	0.24150	1.0000	0.0000
78	2.3966	1.5481	0.24639	1.0000	0.0000
79	2.5139	1.5855	0.25234	1.0000	0.0000
80	2.6501	1.6279	0.25909	1.0000	0.0000
81	2.7307	1.6525	0.26300	1.0000	0.0000
82	2.7931	1.6713	0.26599	1.0000	0.0000
83	2.8728	1.6949	0.26976	1.0000	0.0000
84	3.0127	1.7357	0.27625	1.0000	0.0000
85	3.0581	1.7487	0.27832	1.0000	0.0000
86	3.1961	1.7878	0.28453	1.0000	0.0000
87	3.4366	1.8538	0.29504	1.0000	0.0000
88	3.5275	1.8782	0.29892	1.0000	0.0000
89	3.7024	1.9242	0.30624	1.0000	0.0000
90	3.7147	1.9274	0.30675	1.0000	0.0000
91	4.0218	2.0054	0.31917	1.0000	0.0000
92	4.3256	2.0798	0.33101	1.0000	0.0000
93	4.4842	2.1176	0.33702	1.0000	0.0000
94	4.6121	2.1476	0.34180	1.0000	0.0000
95	4.7299	2.1748	0.34613	1.0000	0.0000
96	5.1272	2.2643	0.36038	1.0000	0.0000
97	5.4143	2.3269	0.37033	1.0000	0.0000
98	5.5838	2.3630	0.37608	1.0000	0.0000
99	5.6697	2.3811	0.37897	1.0000	0.0000
100	6.0776	2.4653	0.39236	1.0000	0.0000
101	6.2723	2.5044	0.39860	1.0000	0.0000
102	6.5952	2.5681	0.40873	1.0000	0.0000
103	6.6266	2.5742	0.40970	1.0000	0.0000
104	7.0719	2.6593	0.42324	1.0000	0.0000
105	7.3783	2.7163	0.43231	1.0000	0.0000
106	7.5452	2.7469	0.43718	1.0000	0.0000
107	7.8946	2.8097	0.44718	1.0000	0.0000
108	8.1388	2.8529	0.45405	1.0000	0.0000
109	8.7559	2.9590	0.47094	1.0000	0.0000
110	8.8504	2.9750	0.47348	1.0000	0.0000
111	9.0533	3.0089	0.47888	1.0000	0.0000
112	9.6997	3.1144	0.49568	1.0000	0.0000
113	10.071	3.1736	0.50509	1.0000	0.0000
114	10.120	3.1812	0.50631	1.0000	0.0000
115	11.077	3.3282	0.52970	1.0000	0.0000
116	11.385	3.3742	0.53703	1.0000	0.0000
117	12.243	3.4989	0.55687	1.0000	0.0000
118	12.642	3.5556	0.56589	1.0000	0.0000
119	12.852	3.5850	0.57056	1.0000	0.0000
120	13.589	3.6863	0.58670	1.0000	0.0000
121	13.823	3.7179	0.59172	1.0000	0.0000
122	14.092	3.7540	0.59746	1.0000	0.0000
123	14.603	3.8214	0.60820	1.0000	0.0000
124	15.195	3.8981	0.62041	1.0000	0.0000
125	15.397	3.9239	0.62451	1.0000	0.0000
126	16.216	4.0269	0.64090	1.0000	0.0000
127	16.538	4.0667	0.64723	1.0000	0.0000

128	17.219	4.1496	0.66043	1.0000	0.0000
129	18.141	4.2592	0.67787	1.0000	0.0000
130	18.279	4.2754	0.68045	1.0000	0.0000
131	18.657	4.3193	0.68744	1.0000	0.0000
132	19.453	4.4106	0.70196	1.0000	0.0000
133	19.645	4.4323	0.70542	1.0000	0.0000
134	21.098	4.5933	0.73105	1.0000	0.0000
135	21.646	4.6526	0.74048	1.0000	0.0000
136	21.841	4.6734	0.74379	1.0000	0.0000
137	22.372	4.7299	0.75278	1.0000	0.0000
138	23.118	4.8081	0.76524	1.0000	0.0000
139	23.836	4.8822	0.77703	1.0000	0.0000
140	23.949	4.8938	0.77887	1.0000	0.0000
141	24.874	4.9874	0.79376	1.0000	0.0000
142	25.767	5.0761	0.80789	1.0000	0.0000
143	26.095	5.1084	0.81302	1.0000	0.0000
144	26.802	5.1771	0.82396	1.0000	0.0000
145	27.130	5.2086	0.82898	1.0000	0.0000
146	27.705	5.2636	0.83773	1.0000	0.0000
147	27.902	5.2823	0.84070	1.0000	0.0000
148	28.906	5.3764	0.85568	1.0000	0.0000
149	29.843	5.4629	0.86945	1.0000	0.0000
150	30.647	5.5360	0.88108	1.0000	0.0000
151	31.638	5.6247	0.89521	1.0000	0.0000
152	31.759	5.6355	0.89692	1.0000	0.0000
153	33.334	5.7736	0.91889	1.0000	0.0000
154	34.671	5.8882	0.93714	1.0000	0.0000
155	35.462	5.9550	0.94777	1.0000	0.0000
156	36.383	6.0318	0.96000	1.0000	0.0000
157	36.751	6.0623	0.96484	1.0000	0.0000
158	37.496	6.1234	0.97456	1.0000	0.0000
159	37.955	6.1607	0.98051	1.0000	0.0000
160	39.520	6.2865	1.0005	1.0000	0.0000
161	40.687	6.3786	1.0152	1.0000	0.0000
162	41.293	6.4260	1.0227	1.0000	0.0000
163	42.682	6.5332	1.0398	1.0000	0.0000
164	42.996	6.5572	1.0436	1.0000	0.0000
165	43.276	6.5785	1.0470	1.0000	0.0000
166	44.037	6.6360	1.0562	1.0000	0.0000
167	44.965	6.7056	1.0672	1.0000	0.0000
168	46.549	6.8227	1.0859	1.0000	0.0000
169	48.941	6.9958	1.1134	1.0000	0.0000
170	49.151	7.0108	1.1158	1.0000	0.0000
171	51.598	7.1832	1.1432	1.0000	0.0000
172	53.529	7.3163	1.1644	1.0000	0.0000
173	54.626	7.3909	1.1763	1.0000	0.0000
174	56.229	7.4986	1.1934	1.0000	0.0000
175	58.496	7.6483	1.2173	1.0000	0.0000
176	58.497	7.6483	1.2173	1.0000	0.0000
177	60.101	7.7525	1.2338	1.0000	0.0000
178	64.227	8.0142	1.2755	1.0000	0.0000
179	64.318	8.0199	1.2764	1.0000	0.0000
180	65.558	8.0968	1.2886	1.0000	0.0000
181	66.497	8.1545	1.2978	1.0000	0.0000
182	66.502	8.1549	1.2979	1.0000	0.0000
183	71.301	8.4440	1.3439	1.0000	0.0000
184	73.192	8.5552	1.3616	1.0000	0.0000
185	77.205	8.7866	1.3984	1.0000	0.0000
186	79.441	8.9130	1.4185	1.0000	0.0000
187	79.851	8.9360	1.4222	1.0000	0.0000
188	80.279	8.9598	1.4260	1.0000	0.0000
189	82.139	9.0631	1.4424	1.0000	0.0000
190	84.574	9.1964	1.4637	1.0000	0.0000
191	90.963	9.5374	1.5179	1.0000	0.0000
192	91.597	9.5706	1.5232	1.0000	0.0000
193	95.537	9.7743	1.5556	1.0000	0.0000
194	101.72	10.086	1.6052	1.0000	0.0000
195	101.95	10.097	1.6070	1.0000	0.0000

196	102.06	10.103	1.6079	1.0000	0.0000
197	102.57	10.128	1.6119	1.0000	0.0000
198	103.35	10.166	1.6180	1.0000	0.0000
199	106.60	10.325	1.6433	1.0000	0.0000
200	108.13	10.399	1.6550	1.0000	0.0000
201	108.85	10.433	1.6605	1.0000	0.0000
202	109.98	10.487	1.6691	1.0000	0.0000
203	113.14	10.637	1.6929	1.0000	0.0000
204	117.47	10.838	1.7250	1.0000	0.0000
205	119.35	10.925	1.7387	1.0000	0.0000
206	121.91	11.041	1.7573	1.0000	0.0000
207	123.00	11.090	1.7651	1.0000	0.0000
208	123.81	11.127	1.7709	1.0000	0.0000
209	127.26	11.281	1.7954	1.0000	0.0000
210	127.50	11.292	1.7971	1.0000	0.0000
211	130.43	11.421	1.8176	1.0000	0.0000
212	132.22	11.499	1.8301	1.0000	0.0000
213	135.00	11.619	1.8492	1.0000	0.0000
214	137.90	11.743	1.8690	1.0000	0.0000
215	138.67	11.776	1.8742	1.0000	0.0000
216	140.21	11.841	1.8846	1.0000	0.0000
217	141.26	11.885	1.8916	1.0000	0.0000
218	144.98	12.041	1.9164	1.0000	0.0000
219	146.64	12.110	1.9273	1.0000	0.0000
220	147.71	12.154	1.9343	1.0000	0.0000
221	153.05	12.371	1.9690	1.0000	0.0000
222	153.96	12.408	1.9748	1.0000	0.0000
223	155.29	12.461	1.9833	1.0000	0.0000
224	155.96	12.488	1.9876	1.0000	0.0000
225	156.22	12.499	1.9893	1.0000	0.0000
226	156.75	12.520	1.9926	1.0000	0.0000
227	157.88	12.565	1.9998	1.0000	0.0000
228	157.98	12.569	2.0004	1.0000	0.0000
229	158.44	12.587	2.0033	1.0000	0.0000
230	159.90	12.645	2.0125	1.0000	0.0000
231	160.61	12.673	2.0170	1.0000	0.0000
232	160.82	12.681	2.0183	1.0000	0.0000
233	162.44	12.745	2.0285	1.0000	0.0000
234	162.72	12.756	2.0302	1.0000	0.0000
235	163.23	12.776	2.0334	1.0000	0.0000
236	164.15	12.812	2.0391	1.0000	0.0000
237	164.25	12.816	2.0397	1.0000	0.0000
238	164.33	12.819	2.0402	1.0000	0.0000
239	164.61	12.830	2.0420	1.0000	0.0000
240	165.29	12.856	2.0462	1.0000	0.0000
241	166.00	12.884	2.0506	1.0000	0.0000
242	166.50	12.903	2.0537	1.0000	0.0000
243	166.86	12.917	2.0559	1.0000	0.0000
244	173.11	13.157	2.0940	1.0000	0.0000
245	178.44	13.358	2.1260	1.0000	0.0000
246	184.99	13.601	2.1647	1.0000	0.0000
247	193.58	13.913	2.2143	1.0000	0.0000
248	197.48	14.053	2.2366	1.0000	0.0000
249	200.26	14.151	2.2522	1.0000	0.0000
250	201.05	14.179	2.2567	1.0000	0.0000
251	203.70	14.272	2.2715	1.0000	0.0000
252	208.65	14.445	2.2989	1.0000	0.0000
253	224.42	14.981	2.3843	1.0000	0.0000
254	224.51	14.984	2.3847	1.0000	0.0000
255	227.45	15.081	2.4003	1.0000	0.0000
256	241.26	15.532	2.4721	1.0000	0.0000
257	244.25	15.629	2.4874	1.0000	0.0000
258	248.98	15.779	2.5113	1.0000	0.0000
259	250.80	15.837	2.5205	1.0000	0.0000
260	254.76	15.961	2.5403	1.0000	0.0000
261	266.13	16.313	2.5964	1.0000	0.0000
262	268.86	16.397	2.6097	1.0000	0.0000
263	277.59	16.661	2.6517	1.0000	0.0000

264	277.69	16.664	2.6521	1.0000	0.0000
265	278.75	16.696	2.6572	1.0000	0.0000
266	309.84	17.602	2.8015	1.0000	0.0000
267	319.65	17.879	2.8455	1.0000	0.0000
268	337.97	18.384	2.9259	1.0000	0.0000
269	338.60	18.401	2.9286	1.0000	0.0000
270	342.54	18.508	2.9456	1.0000	0.0000
271	343.18	18.525	2.9484	1.0000	0.0000
272	355.88	18.865	3.0024	1.0000	0.0000
273	357.95	18.920	3.0111	1.0000	0.0000
274	362.55	19.041	3.0304	1.0000	0.0000
275	377.05	19.418	3.0904	1.0000	0.0000
276	387.16	19.676	3.1316	1.0000	0.0000
277	392.35	19.808	3.1525	1.0000	0.0000
278	401.48	20.037	3.1890	1.0000	0.0000
279	417.14	20.424	3.2506	1.0000	0.0000
280	428.85	20.709	3.2959	1.0000	0.0000
281	436.31	20.888	3.3244	1.0000	0.0000
282	447.85	21.163	3.3681	1.0000	0.0000
283	461.47	21.482	3.4189	1.0000	0.0000
284	467.06	21.612	3.4396	1.0000	0.0000
285	471.86	21.722	3.4572	1.0000	0.0000
286	481.91	21.953	3.4939	1.0000	0.0000
287	487.68	22.084	3.5147	1.0000	0.0000
288	495.78	22.266	3.5438	1.0000	0.0000
289	511.23	22.610	3.5985	1.0000	0.0000
290	522.34	22.855	3.6374	1.0000	0.0000
291	524.13	22.894	3.6437	1.0000	0.0000
292	531.51	23.054	3.6692	1.0000	0.0000
293	534.43	23.118	3.6793	1.0000	0.0000
294	536.99	23.173	3.6881	1.0000	0.0000
295	539.90	23.236	3.6981	1.0000	0.0000
296	542.78	23.298	3.7079	1.0000	0.0000
297	546.65	23.380	3.7211	1.0000	0.0000
298	551.85	23.491	3.7388	1.0000	0.0000
299	561.56	23.697	3.7715	1.0000	0.0000
300	562.17	23.710	3.7736	1.0000	0.0000
301	569.33	23.861	3.7976	1.0000	0.0000
302	570.18	23.879	3.8004	1.0000	0.0000
303	572.88	23.935	3.8094	1.0000	0.0000
304	575.79	23.996	3.8190	1.0000	0.0000
305	579.36	24.070	3.8308	1.0000	0.0000
306	580.23	24.088	3.8337	1.0000	0.0000
307	582.65	24.138	3.8417	1.0000	0.0000
308	587.19	24.232	3.8566	1.0000	0.0000
309	592.86	24.349	3.8752	1.0000	0.0000
310	594.92	24.391	3.8819	1.0000	0.0000
311	598.25	24.459	3.8928	1.0000	0.0000
312	600.17	24.498	3.8990	1.0000	0.0000
313	600.89	24.513	3.9014	1.0000	0.0000
314	602.56	24.547	3.9068	1.0000	0.0000
315	604.46	24.586	3.9130	1.0000	0.0000
316	606.45	24.626	3.9194	1.0000	0.0000
317	607.25	24.642	3.9220	1.0000	0.0000
318	608.70	24.672	3.9267	1.0000	0.0000
319	609.46	24.687	3.9291	1.0000	0.0000
320	612.38	24.746	3.9385	1.0000	0.0000
321	613.17	24.762	3.9410	1.0000	0.0000
322	615.31	24.805	3.9479	1.0000	0.0000
323	619.02	24.880	3.9598	1.0000	0.0000
324	621.68	24.934	3.9683	1.0000	0.0000
325	624.39	24.988	3.9769	1.0000	0.0000
326	625.37	25.007	3.9800	1.0000	0.0000
327	627.92	25.058	3.9882	1.0000	0.0000
328	628.84	25.077	3.9911	1.0000	0.0000
329	630.25	25.105	3.9956	1.0000	0.0000
330	632.88	25.157	4.0039	1.0000	0.0000
331	636.07	25.220	4.0140	1.0000	0.0000

332	638.06	25.260	4.0202	1.0000	0.0000
333	639.16	25.282	4.0237	1.0000	0.0000
334	641.14	25.321	4.0299	1.0000	0.0000
335	641.83	25.334	4.0321	1.0000	0.0000
336	643.02	25.358	4.0358	1.0000	0.0000
337	643.91	25.375	4.0386	1.0000	0.0000
338	644.53	25.388	4.0406	1.0000	0.0000
339	645.46	25.406	4.0435	1.0000	0.0000
340	648.22	25.460	4.0521	1.0000	0.0000
341	659.75	25.686	4.0880	1.0000	0.0000
342	659.94	25.689	4.0886	1.0000	0.0000
343	663.69	25.762	4.1002	1.0000	0.0000
344	674.72	25.975	4.1341	1.0000	0.0000
345	685.69	26.186	4.1676	1.0000	0.0000
346	689.07	26.250	4.1778	1.0000	0.0000
347	701.93	26.494	4.2166	1.0000	0.0000
348	715.22	26.744	4.2564	1.0000	0.0000
349	721.60	26.863	4.2753	1.0000	0.0000
350	722.82	26.885	4.2789	1.0000	0.0000
351	725.01	26.926	4.2854	1.0000	0.0000
352	728.42	26.989	4.2955	1.0000	0.0000
353	731.22	27.041	4.3037	1.0000	0.0000
354	737.31	27.153	4.3216	1.0000	0.0000
355	740.32	27.209	4.3304	1.0000	0.0000
356	741.96	27.239	4.3352	1.0000	0.0000
357	752.91	27.439	4.3671	1.0000	0.0000
358	763.22	27.626	4.3969	1.0000	0.0000
359	767.78	27.709	4.4100	1.0000	0.0000
360	781.97	27.964	4.4506	1.0000	0.0000
361	791.96	28.142	4.4789	1.0000	0.0000
362	799.40	28.274	4.4999	1.0000	0.0000
363	802.48	28.328	4.5086	1.0000	0.0000
364	813.71	28.526	4.5400	1.0000	0.0000
365	826.87	28.755	4.5766	1.0000	0.0000
366	839.85	28.980	4.6123	1.0000	0.0000
367	851.12	29.174	4.6432	1.0000	0.0000
368	851.53	29.181	4.6443	1.0000	0.0000
369	851.53	29.181	4.6443	1.0000	0.0000
370	854.65	29.234	4.6528	1.0000	0.0000
371	855.26	29.245	4.6545	1.0000	0.0000
372	859.48	29.317	4.6659	1.0000	0.0000
373	878.85	29.645	4.7182	1.0000	0.0000
374	883.09	29.717	4.7296	1.0000	0.0000
375	887.74	29.795	4.7420	1.0000	0.0000
376	892.71	29.878	4.7553	1.0000	0.0000
377	900.86	30.014	4.7769	1.0000	0.0000
378	910.43	30.173	4.8022	1.0000	0.0000
379	968.46	31.120	4.9529	1.0000	0.0000
380	968.46	31.120	4.9529	1.0000	0.0000
381	977.05	31.258	4.9748	1.0000	0.0000
382	998.57	31.600	5.0293	1.0000	0.0000
383	1049.8	32.400	5.1567	1.0000	0.0000
384	1128.2	33.589	5.3458	1.0000	0.0000
385	1156.3	34.005	5.4121	1.0000	0.0000
386	1156.3	34.005	5.4121	1.0000	0.0000
387	1165.2	34.135	5.4328	1.0000	0.0000
388	1165.2	34.135	5.4328	1.0000	0.0000
389	1168.3	34.181	5.4400	1.0000	0.0000
390	1168.3	34.181	5.4400	1.0000	0.0000
391	1174.2	34.267	5.4537	1.0000	0.0000
392	1211.2	34.802	5.5389	1.0000	0.0000
393	1299.9	36.054	5.7382	1.0000	0.0000
394	1362.8	36.916	5.8753	1.0000	0.0000
395	1392.3	37.313	5.9386	1.0000	0.0000
396	1483.8	38.520	6.1307	1.0000	0.0000
397	1483.8	38.520	6.1307	1.0000	0.0000
398	1484.8	38.532	6.1326	1.0000	0.0000
399	1484.8	38.532	6.1326	1.0000	0.0000

400	1489.4	38.592	6.1421	1.0000	0.0000
401	1489.4	38.592	6.1421	1.0000	0.0000
402	1489.8	38.598	6.1430	1.0000	0.0000
403	1505.4	38.800	6.1752	1.0000	0.0000
404	1505.4	38.800	6.1752	1.0000	0.0000
405	1553.5	39.415	6.2731	1.0000	0.0000
406	1553.5	39.415	6.2731	1.0000	0.0000
407	1574.8	39.683	6.3158	1.0000	0.0000
408	1591.6	39.895	6.3495	1.0000	0.0000
409	1697.7	41.204	6.5577	1.0000	0.0000
410	1712.0	41.377	6.5853	1.0000	0.0000
411	1712.0	41.377	6.5853	1.0000	0.0000
412	1802.2	42.452	6.7564	1.0000	0.0000
413	1803.5	42.468	6.7589	1.0000	0.0000
414	1811.2	42.558	6.7733	1.0000	0.0000
415	1839.0	42.884	6.8252	1.0000	0.0000
416	1854.7	43.066	6.8542	1.0000	0.0000
417	1854.7	43.066	6.8542	1.0000	0.0000
418	1871.8	43.265	6.8858	1.0000	0.0000
419	1883.4	43.398	6.9070	1.0000	0.0000
420	1898.1	43.567	6.9339	1.0000	0.0000
421	1913.2	43.741	6.9615	1.0000	0.0000
422	1923.0	43.852	6.9793	1.0000	0.0000
423	1936.3	44.003	7.0033	1.0000	0.0000
424	1956.8	44.236	7.0403	1.0000	0.0000
425	1967.9	44.361	7.0603	1.0000	0.0000
426	1975.2	44.443	7.0733	1.0000	0.0000
427	1992.3	44.636	7.1040	1.0000	0.0000
428	1999.9	44.720	7.1174	1.0000	0.0000
429	2022.6	44.974	7.1578	1.0000	0.0000
430	2025.4	45.005	7.1627	1.0000	0.0000
431	2027.4	45.026	7.1661	1.0000	0.0000
432	2036.9	45.132	7.1829	1.0000	0.0000
433	2040.0	45.167	7.1885	1.0000	0.0000
434	2045.6	45.228	7.1983	1.0000	0.0000
435	2051.6	45.295	7.2089	1.0000	0.0000
436	2059.1	45.378	7.2221	1.0000	0.0000
437	2060.9	45.397	7.2252	1.0000	0.0000
438	2072.0	45.520	7.2447	1.0000	0.0000
439	2084.9	45.661	7.2671	1.0000	0.0000
440	2097.2	45.796	7.2886	1.0000	0.0000
441	2098.9	45.813	7.2914	1.0000	0.0000
442	2120.4	46.048	7.3288	1.0000	0.0000
443	2127.7	46.127	7.3413	1.0000	0.0000
444	2131.1	46.164	7.3472	1.0000	0.0000
445	2140.8	46.269	7.3640	1.0000	0.0000
446	2156.9	46.442	7.3915	1.0000	0.0000
447	2162.6	46.504	7.4014	1.0000	0.0000
448	2175.3	46.640	7.4230	1.0000	0.0000
449	2188.4	46.780	7.4453	1.0000	0.0000
450	2199.8	46.902	7.4646	1.0000	0.0000
451	2205.3	46.961	7.4740	1.0000	0.0000
452	2220.0	47.117	7.4989	1.0000	0.0000
453	2235.8	47.284	7.5256	1.0000	0.0000
454	2241.5	47.344	7.5350	1.0000	0.0000
455	2262.4	47.565	7.5701	1.0000	0.0000
456	2266.6	47.609	7.5772	1.0000	0.0000
457	2268.8	47.632	7.5808	1.0000	0.0000
458	2282.1	47.772	7.6031	1.0000	0.0000
459	2290.8	47.862	7.6175	1.0000	0.0000
460	2312.1	48.085	7.6529	1.0000	0.0000
461	2314.6	48.111	7.6570	1.0000	0.0000
462	2324.5	48.213	7.6733	1.0000	0.0000
463	2346.5	48.441	7.7096	1.0000	0.0000
464	2350.5	48.482	7.7161	1.0000	0.0000
465	2356.2	48.540	7.7254	1.0000	0.0000
466	2377.2	48.756	7.7598	1.0000	0.0000
467	2380.2	48.788	7.7648	1.0000	0.0000

468	2389.9	48.887	7.7806	1.0000	0.0000
469	2393.3	48.921	7.7860	1.0000	0.0000
470	2408.5	49.077	7.8108	1.0000	0.0000
471	2422.0	49.214	7.8327	1.0000	0.0000
472	2439.0	49.387	7.8601	1.0000	0.0000
473	2450.7	49.505	7.8789	1.0000	0.0000
474	2464.8	49.647	7.9016	1.0000	0.0000
475	2468.1	49.680	7.9069	1.0000	0.0000
476	2480.9	49.808	7.9273	1.0000	0.0000
477	2484.4	49.843	7.9328	1.0000	0.0000
478	2492.9	49.929	7.9465	1.0000	0.0000
479	2496.9	49.969	7.9528	1.0000	0.0000
480	2497.1	49.971	7.9532	1.0000	0.0000
481	2500.3	50.003	7.9582	1.0000	0.0000
482	2502.9	50.029	7.9623	1.0000	0.0000
483	2573.3	50.727	8.0735	1.0000	0.0000
484	2593.1	50.923	8.1046	1.0000	0.0000
485	2612.6	51.114	8.1350	1.0000	0.0000
486	2616.9	51.156	8.1417	1.0000	0.0000
487	2651.3	51.491	8.1950	1.0000	0.0000
488	2687.9	51.845	8.2513	1.0000	0.0000
489	2699.7	51.958	8.2694	1.0000	0.0000
490	2718.8	52.143	8.2988	1.0000	0.0000
491	2757.7	52.514	8.3578	1.0000	0.0000
492	2761.0	52.546	8.3629	1.0000	0.0000
493	2788.5	52.806	8.4043	1.0000	0.0000
494	2814.7	53.054	8.4438	1.0000	0.0000
495	2837.5	53.268	8.4779	1.0000	0.0000
496	2868.9	53.562	8.5247	1.0000	0.0000
497	2870.9	53.580	8.5276	1.0000	0.0000
498	2870.9	53.580	8.5276	1.0000	0.0000
499	2876.8	53.636	8.5364	1.0000	0.0000
500	2910.6	53.950	8.5864	1.0000	0.0000

!This code is written by UiS student Ran Zhao to calculate the instantaneous wind load on Bjørnafjorden bridge

```
!Function of calculating cross product of two matrix
      MODULE crossproduct
      IMPLICIT NONE

      CONTAINS
      Function KCROSS(KA, KB)

       REAL,DIMENSION(3) :: KCROSS
       REAL,DIMENSION(3), INTENT(IN) :: KA, KB !input

      KCROSS(1) = KA(2) * KB(3) - KA(3) * KB(2)
      KCROSS(2) = KA(3) * KB(1) - KA(1) * KB(3)
      KCROSS(3) = KA(1) * KB(2) - KA(2) * KB(1)

      END FUNCTION KCROSS
      END MODULE

      SUBROUTINE DLOAD(F,KSTEP,KINC,TIME,NOEL,NPT,LAYER,KSPT,COORDS,
     1JLTYP,SNAME)

      USE crossproduct
      INCLUDE 'ABA_PARAM.INC'
! TIME     : TIME(1), step time, TIME(2),total time
! COORDS(3): (x,y,z)
      DIMENSION TIME(2), COORDS(3)

      CHARACTER*80 SNAME
      CHARACTER*80 CPNAME

      INTEGER j,k,KFLAG



      REAL KRXG(190),KVXG(190),KVYG(190),KVZG(190),KVE(190,3,2)
      REAL KT(190,3)


      COMMON KRXG,KVXG,KVYG,KVZG,KVE
      COMMON KT



! numn: total wind nodes; nt: total time length;
      INTEGER, PARAMETER :: numn=190,nt=64019
! KWIND : wind field velocity (NOEL(girder),(u v w),TIME)
! KWG: wind velocity in global coordinate
! KWtot: girder velocity is subtracted from the wind velocity in global axis
! KWN1N2: wind velocity projected in structure local coordinate system formed by local axis n1,n2
! KWN2T:  wind velocity projected in structure local coordinate system formed by local axis n2,t
! KWN1N2M: magnitude of KWN1N2

       REAL KWIND(numn,3,nt)
       REAL KWG(3)
       REAL KWtot(3)
```

```
55          REAL KWN1N2(3),KWN2T(3)
56          REAL KWN1N2M
57
58    !KRW:Rotation angle used to rotate the wind coordinate to global coordinate,
        anti-clockwise
59    !First value in KRW is the wind direction in global axis (west is 270 deg)
60    !KALPHA: angle of attack (-90-90)(2D cross section)
61    !KBETA:  Yaw angle with n2(0-90) (3D cross section)
62    !KALPHA: angle of attack (-90-90)(2D cross section)
63    !KWN1,KWN2,KWT:  Angle between 'the wind vector projection on the n1n2 plane'
        and local 'n1, towards east','n2, upwards','t, from south to north'vector

64          REAL, PARAMETER ::  KPI=3.1415926
65          REAL :: KRW
66          REAL :: KWN2,KWN1,KWT,KALPHA,KBETA
67    !rho: air density
68          REAL :: rho
69    !B: girder width; H: girder height
70          REAL :: B,H
71    !CD:drag coefficient, dCD: derivative of drag load coefficient in radians
72    !CL:lift coefficient, dCL: derivative of lift load coefficient in radians
73    !CM:moment forces coefficient, dCM: derivative of moment forces coefficient in
        radians
74          REAL :: CD,dCD,CL,dCL,CM,dCM
75
76    !KFD: drag force magnitude
77    !KFL: lift force magnitude
78    !KM: overturning moment magnitude
79    !KFD_vec: drag force vector
80    !KFL_vec: lift force vector
81    !KFM_vec: force vector used to apply the overturning moment on each link
82    !KFL_dir: lift force direction from cross product
83    !KFL_dir_m: magnitude od the lift force direction vector
84    !KFL_uni: normalized vector of the lift force
85          REAL :: KFD,KFL,KM
86          REAL :: KFD_vec(3)
87          REAL :: KFL_vec(3)
88          REAL :: KFM_vec(3)
89          REAL :: KFL_dir(3)
90          REAL :: KFL_dir_m
91          REAL :: KFL_uni(3)
92    !KFX: total wind load in global x
93    !KFY: total wind load in global y
94    !KFZ: total wind load in global z
95          REAL:: KFX,KFY,KFZ
96
97
98          SAVE KWIND
99          SAVE KFLAG
100   !!!!!!!!!!!!!!!!!!!!!!!!!!!!!!!!!!!!!!!!!!!!!!!!!!!
101   !here to define the wind direction
102         KRW=(270.0*KPI/180.0)+KPI
103   !!!!!!!!!!!!!!!!!!!!!!!!!!!!!!!!!!!!!!!!!!!!!!!!!!!
104         KWN2=0.0;KWN1=0.0;KWT=0.0
105         KALPHA=0.0;KBETA=0.0
106         rho=1.25;B=29.5;H=3.5
```

```
107         CD=0.621073;dCD=-1.163;CL=-0.1219;dCL=3.175
108         CM=0.029;dCM=0.87
109         KFD=0.0;KFL=0.0;KM=0.0
110         KFX=0.0;KFY=0.0;KFZ=0.0
111
112   !To get the part info (NOEL,falg(1 for element),part name, local element
        number,flag)
113         CALL GETPARTINFO(NOEL, 1, CPNAME, LOCNUM, JRCD)
114
115         IF ((KINC==1) .AND. (NOEL==40079) .AND. (NPT==1) .AND. (JLTYP==41)
116        1)   THEN
117                 CALL KREADDATA(KWIND)
118
119             ELSE
120             GOTO 300
121
122             ENDIF
123
124
125   !! TLP1 (FX,FY,FZ)   : LOCNUM(1-2)
126   !! Fw_tot is total force, KF is element line load, should devided by total
        length
127   300   IF ((40079<=NOEL).and.(NOEL<=40269).and.KINC>1)THEN
128           k=NOEL-40078
129   !To transform the wind velocity from wind coordinate to global coordinate
130   !KRW:Rotation angle used to rotate the wind coordinate to global coordinate,
        anti-clockwise
131           KWG(1)= cos(KRW)*KWIND(k,1,KINC)+sin(KRW)*KWIND(k,2,KINC)
132           KWG(2)=-sin(KRW)*KWIND(k,1,KINC)+cos(KRW)*KWIND(k,2,KINC)
133           KWG(3)=    KWIND(k,3,KINC)
134
135   !Girder self motion is subtracted from the wind velocity
136           KWtot(1)=KWG(1)-KVXG(k)
137           KWtot(2)=KWG(2)-KVYG(k)
138           KWtot(3)=KWG(3)-KVZG(k)
139
140
141
142    !To transfer wind velocity to local girder element plane formed by n1 and n2
         (cross section)
143           KWN1N2=KCROSS(KT(k,:),(KCROSS(KWtot,KT(k,:))))
144    !To transfer wind velocity to local girder element plane formed by n2 and t
         (planary section )
145           KWN2T=KCROSS(KVE(k,:,1),(KCROSS(KWtot,KVE(k,:,1))))
146
147   !Magnitude of local wind velocity KWN1N2
148           CALL KVECMAG(KWN1N2,KWN1N2M)
149
150
151   !KWN1 - the angle between local wind velocity(KWN1N2) and local axis N1'

152           CALL KANGLE(KWN1N2,KVE(k,:,1),KWN1)
153   !KALPHA: the angle of attack -- 'pi/2 - the angle between local wind velocity
        (WINDLOC) and local axis n1'
154           KALPHA=KPI/2.0-KWN1
155   !KWN2 - the angle between local wind velocity(KWN2T) and local axis N2'
```

```
        CALL KANGLE(KWN2T,KVE(k,:,2),KWN2)
!KWN2 - the angle between local wind velocity(KWN2T) and local axis T'

        CALL KANGLE(KWN2T,KT(k,:),KWT)

       !KFD:Drag force magnitude
       KFD=0.5*rho*KWN1N2M**2*H*(CD+KALPHA*dCD)
       KFD_vec(:)=KFD*(KWN1N2(:)/KWN1N2M)

       !KFL: Lift force magnitude
       KFL=0.5*rho*KWN1N2M**2*B*(CL+KALPHA*dCL)

       !To calculate the Lift force direction vector
       !The wind is coming from the west(LEFT, KWN2<90deg), lift force direction vector  <drag force x t >
       !If the wind is coming from the east(RIGHT,KWN2>90deg), lift force direction vector  <t x drag force vector >
       IF  (KWN2>KPI/2.0) THEN
           KFL_dir=KCROSS(KT(k,:),KFD_vec)
       ELSE
           KFL_dir=KCROSS(KFD_vec,KT(k,:))
       ENDIF

       !Magnitude of the lift direction vector
       CALL KVECMAG(KFL_dir,KFL_dir_m)
       KFL_uni= KFL_dir/(KFL_dir_m)
       !Lift force vector
       KFL_vec=KFL*KFL_uni

       !Forces in global coordinate
       KFX= KFD_vec(1)+KFL_vec(1)
       KFY= KFD_vec(2)+KFL_vec(2)
       KFZ= KFD_vec(3)+KFL_vec(3)





!!!!!!!!!!!!!!!!!!!!!!!!!!!!!!!!!!!!!!!!!!!!!!!!!!!!!!!!!!!!!!!!!!!!!!!!!!!!!!!!!!
!!!!!!!!!!!!To calculate wind load on the links left side of the girder!!!!!!!!!!!!
       ELSE IF ((41079<=NOEL).and.(NOEL<=41269).and.KINC>1) THEN
         k=NOEL-41078
!To transform the wind velocity from wind coordinate to global coordinate
!KRW:Rotation angle used to rotate the wind coordinate to global coordinate, anti-clockwise
         KWG(1)= cos(KRW)*KWIND(k,1,KINC)+sin(KRW)*KWIND(k,2,KINC)
         KWG(2)=-sin(KRW)*KWIND(k,1,KINC)+cos(KRW)*KWIND(k,2,KINC)
         KWG(3)=    KWIND(k,3,KINC)

!Girder self motion is subtracted from the wind velocity
         KWtot(1)=KWG(1)-KVXG(k)
         KWtot(2)=KWG(2)-KVYG(k)
         KWtot(3)=KWG(3)-KVZG(k)
```

```
205
206
207
208   !To transfer wind velocity to local girder element plane formed by n1 and n2
        (cross section)
209         KWN1N2=KCROSS(KT(k,:),(KCROSS(KWtot,KT(k,:))))
210   !To transfer wind velocity to local girder element plane formed by n2 and t
        (planary section )
211         KWN2T=KCROSS(KVE(k,:,1),(KCROSS(KWtot,KVE(k,:,1))))
212
213   !Magnitude of local wind velocity KWN1N2
214         CALL KVECMAG(KWN1N2,KWN1N2M)
215
216   !KWN1 - the angle between local wind velocity(KWN1N2) and local axis N1'

217         CALL KANGLE(KWN1N2,KVE(k,:,1),KWN1)
218   !KALPHA: the angle of attack -- 'pi/2 - the angle between local wind velocity
        (WINDLOC) and local axis n1'
219         KALPHA=KPI/2.0-KWN1
220   !KWN2 - the angle between local wind velocity(KWN2T) and local axis N2'

221         CALL KANGLE(KWN2T,KVE(k,:,2),KWN2)
222   !KWN2 - the angle between local wind velocity(KWN2T) and local axis T'

223         CALL KANGLE(KWN2T,KT(k,:),KWT)
224
225        KFD_vec(:)=KWN1N2(:)/KWN1N2M
226
227
228        !To calculate the Lift force direction vector
229        !The wind is coming from the west(LEFT, KWN2<90deg), lift force
            direction vector  <drag force x t >
230        !If the wind is coming from the east(RIGHT,KWN2>90deg), lift force
            direction vector  <t x drag force vector >
231        IF  (KWN2>KPI/2.0) THEN
232            KFL_dir=KCROSS(KT(k,:),KFD_vec)
233        ELSE
234            KFL_dir=KCROSS(KFD_vec,KT(k,:))
235        ENDIF
236
237        !Magnitude of the lift direction vector
238        CALL KVECMAG(KFL_dir,KFL_dir_m)
239        KFL_uni= KFL_dir/(KFL_dir_m)
240
241
242   !To calculate the magnitude of the overturning moment
243        KM=0.5*rho*KWN1N2M**2*B**2*(CM+KALPHA*dCM)
244
245   !To calculate the force vector for overturning moment on links
246   !The wind is coming from the west(LEFT, KWN2<90deg), left link vecotr is same
        as lift
247   !The wind is coming from the east(RIGHT,KWN2>90deg), left link vecotr is
        opposite as lift
248
249
250        IF  (KWN2>KPI/2.0) THEN
```

```
            KFM_vec=-(KM/(B*cos(KALPHA)))*KFL_uni
        ELSE
            KFM_vec=(KM/(B*cos(KALPHA)))*KFL_uni
        ENDIF

!Forces in global coordinate
         KFX= KFM_vec(1)
         KFY= KFM_vec(2)
         KFZ= KFM_vec(3)



!!!!!!!!!!!!!!!!!!!!!!!!!!!!!!!!!!!!!!!!!!!!!!!!!!!!!!!!!!!!!!!!!!!!!!!!!!!!!!!!!!!!
!!!!!!!!!!!!To calculate wind load on the links right side of the girder!!!!!!!!!!!!
        ELSE IF ((42079<=NOEL).and.(NOEL<=42269).and.KINC>1) THEN
          k=NOEL-42078
!To transform the wind velocity from wind coordinate to global coordinate
!KRW:Rotation angle used to rotate the wind coordinate to global coordinate, anti-clockwise
          KWG(1)= cos(KRW)*KWIND(k,1,KINC)+sin(KRW)*KWIND(k,2,KINC)
          KWG(2)=-sin(KRW)*KWIND(k,1,KINC)+cos(KRW)*KWIND(k,2,KINC)
          KWG(3)=    KWIND(k,3,KINC)

!Girder self motion is subtracted from the wind velocity
          KWtot(1)=KWG(1)-KVXG(k)
          KWtot(2)=KWG(2)-KVYG(k)
          KWtot(3)=KWG(3)-KVZG(k)



 !To transfer wind velocity to local girder element plane formed by n1 and n2 (cross section)
         KWN1N2=KCROSS(KT(k,:),(KCROSS(KWtot,KT(k,:))))
 !To transfer wind velocity to local girder element plane formed by n2 and t (planary section )
         KWN2T=KCROSS(KVE(k,:,1),(KCROSS(KWtot,KVE(k,:,1))))

!Magnitude of local wind velocity KWN1N2
         CALL KVECMAG(KWN1N2,KWN1N2M)

!KWN1 - the angle between local wind velocity(KWN1N2) and local axis N1'

         CALL KANGLE(KWN1N2,KVE(k,:,1),KWN1)
!KALPHA: the angle of attack -- 'pi/2 - the angle between local wind velocity (WINDLOC) and local axis n1'
         KALPHA=KPI/2.0-KWN1
!KWN2 - the angle between local wind velocity(KWN2T) and local axis N2'

         CALL KANGLE(KWN2T,KVE(k,:,2),KWN2)
!KWN2 - the angle between local wind velocity(KWN2T) and local axis T'

         CALL KANGLE(KWN2T,KT(k,:),KWT)

        KFD_vec(:)=KWN1N2(:)/KWN1N2M
```

```
298
299
300         !To calculate the Lift force direction vector
301         !The wind is coming from the west(LEFT, KWN2<90deg), lift force
              direction vector  <drag force x t >
302         !If the wind is coming from the east(RIGHT,KWN2>90deg), lift force
              direction vector  <t x drag force vector >
303         IF  (KWN2>KPI/2.0) THEN
304             KFL_dir=KCROSS(KT(k,:),KFD_vec)
305         ELSE
306             KFL_dir=KCROSS(KFD_vec,KT(k,:))
307         ENDIF
308
309         !Magnitude of the lift direction vector
310         CALL KVECMAG(KFL_dir,KFL_dir_m)
311         KFL_uni= KFL_dir/(KFL_dir_m)
312
313
314  !To calculate the magnitude of the overturning moment
315         KM=0.5*rho*KWN1N2M**2*B**2*(CM+KALPHA*dCM)
316
317  !To calculate the force vector for overturning moment on links
318  !The wind is coming from the west(LEFT, KWN2<90deg), left link vecotr is
       opposite as lift
319  !The wind is coming from the east(RIGHT,KWN2>90deg), left link vecotr is same
       as lift
320
321
322         IF  (KWN2>KPI/2.0) THEN
323             KFM_vec=(KM/(B*cos(KALPHA)))*KFL_uni
324         ELSE
325             KFM_vec=-(KM/(B*cos(KALPHA)))*KFL_uni
326         ENDIF
327
328  !Forces in global coordinate
329          KFX= KFM_vec(1)
330          KFY= KFM_vec(2)
331          KFZ= KFM_vec(3)
332
333
334
335
336
337
338
339
340
341         ENDIF
342
343  ! To transfer element load
344         IF      (JLTYP==41) THEN
345                 F = KFX
346         ELSEIF (JLTYP==42) THEN
347                 F = KFY
348         ELSEIF (JLTYP==43) THEN
349                 F = KFZ
```

```
350         ENDIF
351
352
353         KFLAG=KINC
354
355
356
357         RETURN
358         END SUBROUTINE
359
360
361
362         SUBROUTINE KREADDATA(KWIND)
363         implicit none
364
365   ! KWIND  : wind field velocity (NOEL(girder),(utot vtur),TIME)
366
367         INTEGER, PARAMETER :: numn=190,nt=64019
368         REAL :: KWIND(numn,3,nt)
369         REAL :: uwind(numn,1),vwind(numn,1), wwind(numn,1)
370         INTEGER i,j
371
372
373         uwind=0.0;vwind=0.0;wwind=0.0
374         KWIND=0.0
375         j=1;i=1
376
377   !READ THE WIND FIELD DATA
378   !KWIND(I,J,K,L)
379   ! I: NOEL ELEMENT NUMBER
380   ! J: 1,along wind velocity, 2,across turbulence velocity, 3, vertical
        turbulence vel
381   ! K: NPT, ELEMENT INTEGRATION NUMBER
382   ! L: time increments
383   ! When wind not cohering, we need to add one more loop
384         OPEN(UNIT=102,FILE='C:\temp\RP100_1_u.dat')
385         OPEN(UNIT=103,FILE='C:\temp\RP100_1_v.dat')
386         OPEN(UNIT=104,FILE='C:\temp\RP100_1_w.dat')
387
388
389         DO j=1,nt
390             READ(102,*) (uwind(i,1),i=1,numn)
391             READ(103,*) (vwind(i,1),i=1,numn)
392             READ(104,*) (wwind(i,1),i=1,numn)
393
394             KWIND(1:numn,1,j)=uwind(1:numn,1)
395             KWIND(1:numn,2,j)=vwind(1:numn,1)
396             KWIND(1:numn,3,j)=wwind(1:numn,1)
397
398
399
400         END DO
401         CLOSE(102)
402         CLOSE(103)
403         CLOSE(104)
404
```

```
405
406
407
408         RETURN
409         END SUBROUTINE
410
411
412   ! Subroutine to obtain the girder rotation and element velocity
413         SUBROUTINE URDFIL(LSTOP,LOVRWRT,KSTEP,KINC,DTIME,TIME)
414         USE crossproduct
415         INCLUDE 'ABA_PARAM.INC'
416
417         DIMENSION ARRAY(513),JRRAY(NPRECD,513),TIME(2),LRUNIT(2,1)
418
419         EQUIVALENCE (ARRAY(1),JRRAY(1,1))
420         INTEGER num,KELM,KINTP,KNNUM
421         INTEGER i,j,k,kk,kkk
422
423         REAL KCOORD(40000,3)
424         REAL KD(40000,6),KV(40000,6),KVEC(40000,6)
425         REAL KRXG(190),KVXG(190),KVYG(190),KVZG(190),KVE(190,3,2)
426         REAL KT(190,3)
427
428         COMMON KRXG,KVXG,KVYG,KVZG,KVE
429         COMMON KT
430
431
432   !num (results record, all nodes*number of contents (SEE NODEFILE))
433
434         num=40000;KIELM=0; KINTP=0 ; KNNUM=0
435         i=1;j=1;k=1;kk=1;kkk=1
436
437         KCOORD=0.0
438         KD=0.0;KV=0.0;KVEC=0.0
439         KRXG=0.0;KVYG=0.0;KVZG=0.0;KVE=0.0
440         KTX=0.0; KTY=0.0;KTZ=0.0
441         KT(:,1)=1;KT(:,2)=0;KT(:,3)=0
442
443
444
445
446   !We need to overwrite the data from last time increment if LOVRWRT=1
447         LOVRWRT=1
448   !Call POSTFIL and DBFIL to read results
449   !JCRD: return code, 0 found increment, 1 not
450
451         CALL POSFIL(KSTEP,KINC,ARRAY,JRCD)
452
453
454   ! i loop till num because we need to loop all the file record
        (num_nodes*num_cont)
455         DO i=1,num
456           CALL DBFILE(0,ARRAY,JRCD)
457
458           IF (JRCD.NE.0) THEN
459           GO TO 110
```

```
460         END IF
461
462         KEY=JRRAY(1,2)
463
464 ! REAL attributes of ARRAY starts from location 3, 1 is record length, 2 is
      type key
465 ! see>Abaqus > Output > File Output Format > Results file output format >
      Results file > Label record
466 ! KEY=101, ARRAY is U disp and rotation (4,5,6,7,8,9)
467 ! ARRAY(7) is rx, based on right hang rule, node rotation is -
468 ! rotation is in radian
469 ! HERE,transfer the displacement file to KD
470         IF (KEY==101) THEN
471         KD(j,1)=ARRAY(4)
472         KD(j,2)=ARRAY(5)
473         KD(j,3)=ARRAY(6)
474         KD(j,4)=ARRAY(7)
475         KD(j,5)=ARRAY(8)
476         KD(j,6)=ARRAY(9)
477         j=j+1
478 ! KEY=102, ARRAY is V velocity (4,5,6,7,8,9)
479         ELSE IF (KEY==102) THEN
480 ! HERE,transfer the velocity file to KV
481         !KNUM(k) =ARRAY(3)
482         KV(k,1)=ARRAY(4)
483         KV(k,2)=ARRAY(5)
484         KV(k,3)=ARRAY(6)
485         KV(k,4)=ARRAY(7)
486         KV(k,5)=ARRAY(8)
487         KV(k,6)=ARRAY(9)
488         k=k+1
489 ! KEY=85, ARRAY is Local coordinate directions (3,4,5,6,7,8)
490         ELSE IF (KEY .EQ. 85) THEN
491 ! HERE,transfer the local coordinate direction file to KVEC
492         KVEC(kk,1)=ARRAY(3)
493         KVEC(kk,2)=ARRAY(4)
494         KVEC(kk,3)=ARRAY(5)
495         KVEC(kk,4)=ARRAY(6)
496         KVEC(kk,5)=ARRAY(7)
497         KVEC(kk,6)=ARRAY(8)
498         kk=kk+1
499         END IF
500
501         END DO
502
503  110  CONTINUE
504
505 ! To get the angle, velocity and local coordinate directions at GIRDER element

506 ! Rotation in Abaqus is opposite to the load definition
507       DO i=1,190
508           KRXG(i) =-0.5*(KD(i,4)+KD(i+1,4))
509           KVXG(i) = 0.5*(KV(i,1)+KV(i+1,1))
510           KVYG(i) = 0.5*(KV(i,2)+KV(i+1,2))
511           KVZG(i) = 0.5*(KV(i,3)+KV(i+1,3))
512
```

```
513             KVE(i,1:3,1) = KVEC(i,1:3)
514             KVE(i,1:3,2) = KVEC(i,4:6)
515
516             KT(i,:)=KCROSS(KVE(i,:,1),KVE(i,:,2))
517          END DO
518
519
520
521         CLOSE(20)
522         RETURN
523         END
524
525
526
527
528
529         SUBROUTINE KROSSPRODUCT(KA,KB,KC)
530
531         !calculating cross product of two vectors
532         REAL :: KA(3),KB(3)
533         REAL :: KC(3)
534
535         KC(1) = KA(2) * KB(3) - KA(3) * KB(2)
536         KC(2) = KA(3) * KB(1) - KA(1) * KB(3)
537         KC(3) = KA(1) * KB(2) - KA(2) * KB(1)
538
539         RETURN
540         END SUBROUTINE
541
542         SUBROUTINE KANGLE(KA,KB,KANG)
543
544         !calculating angle between two vectors (0-180deg)
545         REAL :: KA(3),KB(3)
546         REAL :: KANG
547
548          KANG= ACOS(DOT_PRODUCT(KA,KB)/(
549        1    sqrt(KA(1)**2+KA(2)**2+KA(3)**2)
550        2   *sqrt(KB(1)**2+KB(2)**2+KB(3)**2)))
551
552         RETURN
553         END SUBROUTINE
554
555
556         SUBROUTINE KVECMAG(KA,KVMAG)
557
558         !calculating cross product of two vectors
559         REAL :: KA(3)
560         REAL :: KVMAG
561
562          KVMAG= sqrt(KA(1)**2+KA(2)**2+KA(3)**2)
563
564         RETURN
565         END SUBROUTINE
```

APPENDIX D: Matlab code for Abaqus input file (full bridge model)

```
%This code is written by two UiS master students: Joanna Syper and Ran Zhao
%to generate the Abaqus input file of the Bjørnafjorden bridge
clc
clear all


%Import data
girdernode='girdernode.xlsx';
girder_node=xlsread(girdernode);

coumnnode='column.xlsx';
column_node=xlsread(coumnnode);

towernode='tower.xlsx';
tower_node=xlsread(towernode);

pontoonnode='pontoon.xlsx';
pontoon_node=xlsread(pontoonnode);

mooringlinenode='mooringnode.xlsx';
mooring_node=xlsread(mooringlinenode);

mooringele='mooringele.xlsx';
mooring_ele=xlsread(mooringele);

girderele='girderelement.xlsx';
girder_ele=xlsread(girderele);

dummyele='dummy.xlsx';
dummy_ele=xlsread(dummyele);

cableele='cable.xlsx';
cable_ele=xlsread(cableele);

cablecload='cable_cload.xlsx';
cable_cl=xlsread(cablecload);


pontoonconnector='pontoonconnector.xlsx';
pontoon_connector=xlsread(pontoonconnector);

pontoonori='pontoon_orientation.xlsx';
pontoon_orien=xlsread(pontoonori);

pontoonspring='spring.xlsx';
pon_spring=xlsread(pontoonspring);

pontoonmass='pontoonmass.xlsx';
pon_mass=xlsread(pontoonmass);

massele='massele.xlsx';
mass_ele=xlsread(massele);
```

```
format long
formatSpec='%d, %10.4f, %10.4f, %10.4f\n';
formatSpec1='%s\n';
formatSpec2='%d, %d, %d\n';
```

```
formatSpec3='%d, %d\n';
formatSpec4='%d\n';
formatSpec5='%d, %d, %d, %d, %d\n';
formatSpec6='%d, %d, %d, %d\n';
formatSpec7='%s%d%s\n';
formatSpec8='%s%d\n';
formatSpec9='%s%d%s%d%s\n';
formatSpec10='%s, %d, %d\n';
formatSpec11='%d, %d, %d, %d, %d, %d\n';
formatSpec12='%s%d%s%s%d\n';
formatSpec13='%s%d%s%d\n';

fileID = fopen('C:\temp\Matlab input\fullbridge.inp','w');
fprintf(fileID,formatSpec1,'**');
fprintf(fileID,formatSpec1,'**');

% NODES
% girder_nodes
fprintf(fileID,formatSpec1,'************************************');
fprintf(fileID,formatSpec1,'*Node');
fprintf(fileID,formatSpec1,'**girder_node');
for i=1:length(girder_node);

fprintf(fileID,formatSpec,girder_node(i,2),girder_node(i,3),girder_node(i,4),girder_node(i,5))
;
end
%line node
fprintf(fileID,formatSpec1,'************************************');
fprintf(fileID,formatSpec1,'**link_ne_node');
for i=1:length(girder_node);

fprintf(fileID,formatSpec,girder_node(i,2+5),girder_node(i,3+5),girder_node(i,4+5),girder_node
(i,5+5));
end
fprintf(fileID,formatSpec1,'************************************');
fprintf(fileID,formatSpec1,'**link_sw_node');
for i=1:length(girder_node);

fprintf(fileID,formatSpec,girder_node(i,2+2*5),girder_node(i,3+2*5),girder_node(i,4+2*5),girde
r_node(i,5+2*5));
end
fprintf(fileID,formatSpec1,'************************************');
fprintf(fileID,formatSpec1,'**link_b_node');
for i=1:length(girder_node);

fprintf(fileID,formatSpec,girder_node(i,2+3*5),girder_node(i,3+3*5),girder_node(i,4+3*5),girde
r_node(i,5+3*5));
end
%column node
fprintf(fileID,formatSpec1,'************************************');
fprintf(fileID,formatSpec1,'**column_node');
for i=1:length(column_node);

fprintf(fileID,formatSpec,column_node(i,1),column_node(i,2),column_node(i,3),column_node(i,4))
;
end
%tower leg node
```

```
fprintf(fileID,formatSpec1,'************************************');
fprintf(fileID,formatSpec1,'**leg_sw_towernode');
for i=1:length(tower_node);

fprintf(fileID,formatSpec,tower_node(i,1),tower_node(i,2),tower_node(i,3),tower_node(i,4));
end
fprintf(fileID,formatSpec1,'************************************');
fprintf(fileID,formatSpec1,'**leg_ne_towernode');
for i=1:length(tower_node)-1;

fprintf(fileID,formatSpec,tower_node(i,1+5),tower_node(i,2+5),tower_node(i,3+5),tower_node(i,4
+5));
end
%pontoon nodes
fprintf(fileID,formatSpec1,'************************************');
fprintf(fileID,formatSpec1,'**pontoon_COG_node');
for i=1:length(pontoon_node);

fprintf(fileID,formatSpec,pontoon_node(i,1),pontoon_node(i,2),pontoon_node(i,3),pontoon_node(i
,4));
end
fprintf(fileID,formatSpec1,'************************************');
fprintf(fileID,formatSpec1,'**pontoon_COB_node');
for i=1:length(pontoon_node);

fprintf(fileID,formatSpec,pontoon_node(i,1+5),pontoon_node(i,2+5),pontoon_node(i,3+5),pontoon_
node(i,4+5));
end
fprintf(fileID,formatSpec1,'************************************');
fprintf(fileID,formatSpec1,'**pontoon_bottom_node');
for i=1:length(pontoon_node);

fprintf(fileID,formatSpec,pontoon_node(i,1+5*2),pontoon_node(i,2+5*2),pontoon_node(i,3+5*2),po
ntoon_node(i,4+5*2));
end
fprintf(fileID,formatSpec1,'************************************');
fprintf(fileID,formatSpec1,'**mooringline_node');
for i=1:length(mooring_node);

fprintf(fileID,formatSpec,mooring_node(i,1),mooring_node(i,2),mooring_node(i,3),mooring_node(i
,4));
end
fprintf(fileID,formatSpec1,'************************************');
```

```
%Element
fprintf(fileID,formatSpec1,'**');
fprintf(fileID,formatSpec1,'**');
fprintf(fileID,formatSpec1,'************************************');
% girder_elements
fprintf(fileID,formatSpec1,'**girder_ele_concrete');
for i=1:52;
    fprintf(fileID,formatSpec8,'*Element, type=B31, Elset=girder_concrete_',i);
    fprintf(fileID,formatSpec2,girder_ele(i,1),girder_ele(i,2),girder_ele(i,3));
end

fprintf(fileID,formatSpec1,'**');
fprintf(fileID,formatSpec1,'**girder_ele_steel');
```

```
for i=53:80;
     fprintf(fileID,formatSpec8,'*Element, type=B31, Elset=girder_steel_',i);
    fprintf(fileID,formatSpec2,girder_ele(i,1),girder_ele(i,2),girder_ele(i,3));
end
fprintf(fileID,formatSpec1,'**');
for i=81:115
    fprintf(fileID,formatSpec8,'*Element, type=B31, Elset=girder_transition_',i);
    fprintf(fileID,formatSpec2,girder_ele(i,1),girder_ele(i,2),girder_ele(i,3));
end
fprintf(fileID,formatSpec1,'**');
     fprintf(fileID,formatSpec1,'*Element, type=B31, Elset=girder_steel_2');
for i=116:268;
    fprintf(fileID,formatSpec2,girder_ele(i,1),girder_ele(i,2),girder_ele(i,3));
end
fprintf(fileID,formatSpec1,'**********************************');

% link_ne_elements
fprintf(fileID,formatSpec1,'**link_ne_concrete');
for i=1:52;
    fprintf(fileID,formatSpec8,'*Element, type=B31, Elset=link_ne_concrete_',i);
    fprintf(fileID,formatSpec2,girder_ele(i,5),girder_ele(i,6),girder_ele(i,7));
end
fprintf(fileID,formatSpec1,'**');
fprintf(fileID,formatSpec1,'**link_ne_ele_steel');
for i=53:80;
     fprintf(fileID,formatSpec8,'*Element, type=B31, Elset=link_ne_steel_',i);
    fprintf(fileID,formatSpec2,girder_ele(i,5),girder_ele(i,6),girder_ele(i,7));
end
fprintf(fileID,formatSpec1,'**');
for i=81:115
    fprintf(fileID,formatSpec8,'*Element, type=B31, Elset=link_ne_transition_',i);
    fprintf(fileID,formatSpec2,girder_ele(i,5),girder_ele(i,6),girder_ele(i,7));
end
fprintf(fileID,formatSpec1,'**');
fprintf(fileID,formatSpec1,'*Element, type=B31, Elset=link_ne_steel_2');
for i=116:268;
    fprintf(fileID,formatSpec2,girder_ele(i,5),girder_ele(i,6),girder_ele(i,7));
end
fprintf(fileID,formatSpec1,'**********************************');

% link_sw_elements
fprintf(fileID,formatSpec1,'**link_sw_concrete');
for i=1:52;
    fprintf(fileID,formatSpec8,'*Element, type=B31, Elset=link_sw_concrete_',i);
    fprintf(fileID,formatSpec2,girder_ele(i,9),girder_ele(i,10),girder_ele(i,11));
end
fprintf(fileID,formatSpec1,'**');
fprintf(fileID,formatSpec1,'**link_sw_ele_steel');
for i=53:80;
     fprintf(fileID,formatSpec8,'*Element, type=B31, Elset=link_sw_steel_',i);
    fprintf(fileID,formatSpec2,girder_ele(i,9),girder_ele(i,10),girder_ele(i,11));
end
fprintf(fileID,formatSpec1,'**');
for i=81:115
    fprintf(fileID,formatSpec8,'*Element, type=B31, Elset=link_sw_transition_',i);
    fprintf(fileID,formatSpec2,girder_ele(i,9),girder_ele(i,10),girder_ele(i,11));
end
```

```
fprintf(fileID,formatSpec1,'**');
     fprintf(fileID,formatSpec1,'*Element, type=B31, Elset=link_sw_steel_2');
for i=116:268;
    fprintf(fileID,formatSpec2,girder_ele(i,9),girder_ele(i,10),girder_ele(i,11));
end
fprintf(fileID,formatSpec1,'************************************');
%link bottom element
fprintf(fileID,formatSpec1,'**link_bottom_concrete');
for i=1:52;
    fprintf(fileID,formatSpec8,'*Element, type=B31, Elset=link_bottom_concrete_',i);
    fprintf(fileID,formatSpec2,girder_ele(i,13),girder_ele(i,14),girder_ele(i,15));
end
fprintf(fileID,formatSpec1,'**');
fprintf(fileID,formatSpec1,'**link_bottom_steel');
for i=53:80;
     fprintf(fileID,formatSpec8,'*Element, type=B31, Elset=link_bottom_steel_',i);
    fprintf(fileID,formatSpec2,girder_ele(i,13),girder_ele(i,14),girder_ele(i,15));
end
fprintf(fileID,formatSpec1,'**');
for i=81:115
    fprintf(fileID,formatSpec8,'*Element, type=B31, Elset=link_bottom_transition_',i);
    fprintf(fileID,formatSpec2,girder_ele(i,13),girder_ele(i,14),girder_ele(i,15));
end
fprintf(fileID,formatSpec1,'**');
     fprintf(fileID,formatSpec1,'*Element, type=B31, Elset=link_bottom_steel_2');
for i=116:268;
    fprintf(fileID,formatSpec2,girder_ele(i,13),girder_ele(i,14),girder_ele(i,15));
end
fprintf(fileID,formatSpec1,'************************************');

%dummy element
fprintf(fileID,formatSpec1,'**dummy_ne_ele');
for i=1:269
    fprintf(fileID,formatSpec8,'*Element, type=B31, Elset=dummy_ne_',i);
    fprintf(fileID,formatSpec2,dummy_ele(i,1),dummy_ele(i,2),dummy_ele(i,3));
end

fprintf(fileID,formatSpec1,'************************************');
fprintf(fileID,formatSpec1,'**dummy_sw_ele');
for i=1:269
    fprintf(fileID,formatSpec8,'*Element, type=B31, Elset=dummy_sw_',i);
    fprintf(fileID,formatSpec2,dummy_ele(i,1+4),dummy_ele(i,2+4),dummy_ele(i,3+4));
end

fprintf(fileID,formatSpec1,'************************************');
fprintf(fileID,formatSpec1,'**dummy_b_ele');
for i=1:269
    fprintf(fileID,formatSpec8,'*Element, type=B31, Elset=dummy_b_',i);
    fprintf(fileID,formatSpec2,dummy_ele(i,1+4*2),dummy_ele(i,2+4*2),dummy_ele(i,3+4*2));
end
fprintf(fileID,formatSpec1,'************************************');
%column element
fprintf(fileID,formatSpec1,'**column_ele');
fprintf(fileID,formatSpec1,'*Element, type=B31, Elset=back_column');
for i=1:5
    fprintf(fileID,formatSpec2,column_node(i,1+5),column_node(i,2+5),column_node(i,3+5));
end
```

```
fprintf(fileID,formatSpec1,'*Element, type=B31, Elset=column_A1');

for i=6:10;
    fprintf(fileID,formatSpec2,column_node(i,1+5),column_node(i,2+5),column_node(i,3+5));
end

fprintf(fileID,formatSpec1,'*Element, type=B31, Elset=column_A1_2');

for i=11;
    fprintf(fileID,formatSpec2,column_node(i,1+5),column_node(i,2+5),column_node(i,3+5));
end
fprintf(fileID,formatSpec1,'*Element, type=B31, Elset=column_A2');

for i=12:length(column_node);
    fprintf(fileID,formatSpec2,column_node(i,1+5),column_node(i,2+5),column_node(i,3+5));
end
fprintf(fileID,formatSpec1,'**********************************');

%tower element
fprintf(fileID,formatSpec1,'**tower_elements');
for i=1:23;
    fprintf(fileID,formatSpec8,'*Element, type=B31, Elset=leg_sw_tower_',i);
    fprintf(fileID,formatSpec2,tower_node(i,11),tower_node(i,11+1),tower_node(i,11+2));
end
for i=24;
    fprintf(fileID,formatSpec8,'*Element, type=B31, Elset=leg_sw_tower_',i);
    fprintf(fileID,formatSpec2,tower_node(i,11),tower_node(i,11+1),tower_node(i,11+2));
    fprintf(fileID,formatSpec2,tower_node(i+1,11),tower_node(i+1,11+1),tower_node(i+1,11+2));
    fprintf(fileID,formatSpec2,tower_node(i+2,11),tower_node(i+2,11+1),tower_node(i+2,11+2));
end
for i=27:34;
    fprintf(fileID,formatSpec8,'*Element, type=B31, Elset=leg_sw_tower_',i-2);
    fprintf(fileID,formatSpec2,tower_node(i,11),tower_node(i,11+1),tower_node(i,11+2));
end
fprintf(fileID,formatSpec1,'**********************************');
for i=1:23;
    fprintf(fileID,formatSpec8,'*Element, type=B31, Elset=leg_ne_tower_',i);
    fprintf(fileID,formatSpec2,tower_node(i,11+4),tower_node(i,11+5),tower_node(i,11+6));
end
for i=24;
    fprintf(fileID,formatSpec8,'*Element, type=B31, Elset=leg_ne_tower_',i);
    fprintf(fileID,formatSpec2,tower_node(i,11+4),tower_node(i,11+5),tower_node(i,11+6));

fprintf(fileID,formatSpec2,tower_node(i+1,11+4),tower_node(i+1,11+5),tower_node(i+1,11+6));

fprintf(fileID,formatSpec2,tower_node(i+2,11+4),tower_node(i+2,11+5),tower_node(i+2,11+6));
end
for i=27:34;
    fprintf(fileID,formatSpec8,'*Element, type=B31, Elset=leg_ne_tower_',i-2);
    fprintf(fileID,formatSpec2,tower_node(i,11+4),tower_node(i,11+5),tower_node(i,11+6));
end
fprintf(fileID,formatSpec1,'**********************************');

%cross beam element
fprintf(fileID,formatSpec1,'**crossbeam_elements');

fprintf(fileID,formatSpec1,'*Element, type=B31, Elset=crossbeam');
```

```
fprintf(fileID,formatSpec2,tower_node(1,11+8),tower_node(1,11+9),tower_node(1,11+10));
fprintf(fileID,formatSpec2,tower_node(2,11+8),tower_node(2,11+9),tower_node(2,11+10));
fprintf(fileID,formatSpec1,'**********************************');

%cable element
fprintf(fileID,formatSpec1,'**cable_ne_sidespan');
for i=1:18;
    fprintf(fileID,formatSpec8,'*Element, type=B31, Elset=cable_ne_side_A',i);
    fprintf(fileID,formatSpec2,cable_ele(i,1),cable_ele(i,2),cable_ele(i,3));
end
fprintf(fileID,formatSpec1,'**********************************');
fprintf(fileID,formatSpec1,'**cable_sw_sidespan');
for i=1:18;
    fprintf(fileID,formatSpec8,'*Element, type=B31, Elset=cable_sw_side_A',i);
    fprintf(fileID,formatSpec2,cable_ele(i,1+4),cable_ele(i,2+4),cable_ele(i,3+4));
end
fprintf(fileID,formatSpec1,'**********************************');
fprintf(fileID,formatSpec1,'**cable_ne_mainspan');
for i=1:18;
    fprintf(fileID,formatSpec8,'*Element, type=B31, Elset=cable_ne_main_A',i);
    fprintf(fileID,formatSpec2,cable_ele(i,1+4*2),cable_ele(i,2+4*2),cable_ele(i,3+4*2));
end
fprintf(fileID,formatSpec1,'**********************************');
fprintf(fileID,formatSpec1,'**cable_sw_mainspan');
for i=1:18;
    fprintf(fileID,formatSpec8,'*Element, type=B31, Elset=cable_sw_main_A',i);
    fprintf(fileID,formatSpec2,cable_ele(i,1+4*3),cable_ele(i,2+4*3),cable_ele(i,3+4*3));
end
fprintf(fileID,formatSpec1,'**********************************');

%pontoon connector
fprintf(fileID,formatSpec1,'**pontoon_connectors');
for i=1:3:length(pontoon_connector);
    fprintf(fileID,formatSpec8,'*Element, type=B31, Elset=pontoon_connector_',i);

fprintf(fileID,formatSpec2,pontoon_connector(i,1),pontoon_connector(i,2),pontoon_connector(i,3
));

fprintf(fileID,formatSpec2,pontoon_connector(i+1,1),pontoon_connector(i+1,2),pontoon_connector
(i+1,3));

fprintf(fileID,formatSpec2,pontoon_connector(i+2,1),pontoon_connector(i+2,2),pontoon_connector
(i+2,3));
end
%mooring line element
fprintf(fileID,formatSpec1,'**********************************');
fprintf(fileID,formatSpec1,'**mooring_ele');
%%connect pontoon13
fprintf(fileID,formatSpec1,'*Element, type=B31, Elset=mooring_element_13_line1b');
fprintf(fileID,formatSpec2,mooring_ele(1,1),mooring_ele(1,2),mooring_ele(1,3));
fprintf(fileID,formatSpec1,'*Element, type=B31, Elset=mooring_element_13_line1w');
fprintf(fileID,formatSpec2,mooring_ele(2,1),mooring_ele(2,2),mooring_ele(2,3));
fprintf(fileID,formatSpec1,'*Element, type=B31, Elset=mooring_element_13_line1t');
fprintf(fileID,formatSpec2,mooring_ele(3,1),mooring_ele(3,2),mooring_ele(3,3));
fprintf(fileID,formatSpec1,'*Element, type=B31, Elset=mooring_element_13_line2b');
fprintf(fileID,formatSpec2,mooring_ele(4,1),mooring_ele(4,2),mooring_ele(4,3));
fprintf(fileID,formatSpec1,'*Element, type=B31, Elset=mooring_element_13_line2w');
```

```
fprintf(fileID,formatSpec2,mooring_ele(5,1),mooring_ele(5,2),mooring_ele(5,3));
fprintf(fileID,formatSpec1,'*Element, type=B31, Elset=mooring_element_13_line2t');
fprintf(fileID,formatSpec2,mooring_ele(6,1),mooring_ele(6,2),mooring_ele(6,3));
fprintf(fileID,formatSpec1,'*Element, type=B31, Elset=mooring_element_13_line3b');
fprintf(fileID,formatSpec2,mooring_ele(7,1),mooring_ele(7,2),mooring_ele(7,3));
fprintf(fileID,formatSpec1,'*Element, type=B31, Elset=mooring_element_13_line3w');
fprintf(fileID,formatSpec2,mooring_ele(8,1),mooring_ele(8,2),mooring_ele(8,3));
fprintf(fileID,formatSpec1,'*Element, type=B31, Elset=mooring_element_13_line3t');
fprintf(fileID,formatSpec2,mooring_ele(9,1),mooring_ele(9,2),mooring_ele(9,3));
fprintf(fileID,formatSpec1,'*Element, type=B31, Elset=mooring_element_13_line4b');
fprintf(fileID,formatSpec2,mooring_ele(10,1),mooring_ele(10,2),mooring_ele(10,3));
fprintf(fileID,formatSpec1,'*Element, type=B31, Elset=mooring_element_13_line4w');
fprintf(fileID,formatSpec2,mooring_ele(11,1),mooring_ele(11,2),mooring_ele(11,3));
fprintf(fileID,formatSpec1,'*Element, type=B31, Elset=mooring_element_13_line4t');
fprintf(fileID,formatSpec2,mooring_ele(12,1),mooring_ele(12,2),mooring_ele(12,3));
fprintf(fileID,formatSpec1,'*Element, type=B31, Elset=mooring_element_20_line5b');
fprintf(fileID,formatSpec2,mooring_ele(13,1),mooring_ele(13,2),mooring_ele(13,3));

fprintf(fileID,formatSpec1,'*Element, type=B31, Elset=mooring_element_20_line5w');
fprintf(fileID,formatSpec2,mooring_ele(14,1),mooring_ele(14,2),mooring_ele(14,3));
fprintf(fileID,formatSpec1,'*Element, type=B31, Elset=mooring_element_20_line5t');
fprintf(fileID,formatSpec2,mooring_ele(15,1),mooring_ele(15,2),mooring_ele(15,3));
fprintf(fileID,formatSpec1,'*Element, type=B31, Elset=mooring_element_20_line6b');
fprintf(fileID,formatSpec2,mooring_ele(16,1),mooring_ele(16,2),mooring_ele(16,3));
fprintf(fileID,formatSpec1,'*Element, type=B31, Elset=mooring_element_20_line6w');
fprintf(fileID,formatSpec2,mooring_ele(17,1),mooring_ele(17,2),mooring_ele(17,3));
fprintf(fileID,formatSpec1,'*Element, type=B31, Elset=mooring_element_20_line6t');
fprintf(fileID,formatSpec2,mooring_ele(18,1),mooring_ele(18,2),mooring_ele(18,3));
fprintf(fileID,formatSpec1,'*Element, type=B31, Elset=mooring_element_20_line7b');
fprintf(fileID,formatSpec2,mooring_ele(19,1),mooring_ele(19,2),mooring_ele(19,3));
fprintf(fileID,formatSpec1,'*Element, type=B31, Elset=mooring_element_20_line7w');
fprintf(fileID,formatSpec2,mooring_ele(20,1),mooring_ele(20,2),mooring_ele(20,3));
fprintf(fileID,formatSpec1,'*Element, type=B31, Elset=mooring_element_20_line7t');
fprintf(fileID,formatSpec2,mooring_ele(21,1),mooring_ele(21,2),mooring_ele(21,3));
fprintf(fileID,formatSpec1,'*Element, type=B31, Elset=mooring_element_20_line8b');
fprintf(fileID,formatSpec2,mooring_ele(22,1),mooring_ele(22,2),mooring_ele(22,3));
fprintf(fileID,formatSpec1,'*Element, type=B31, Elset=mooring_element_20_line8w');
fprintf(fileID,formatSpec2,mooring_ele(23,1),mooring_ele(23,2),mooring_ele(23,3));
fprintf(fileID,formatSpec1,'*Element, type=B31, Elset=mooring_element_20_line8t');
fprintf(fileID,formatSpec2,mooring_ele(24,1),mooring_ele(24,2),mooring_ele(24,3));
fprintf(fileID,formatSpec1,'*Element, type=B31, Elset=mooring_element_27_line9b');
fprintf(fileID,formatSpec2,mooring_ele(25,1),mooring_ele(25,2),mooring_ele(25,3));
fprintf(fileID,formatSpec1,'*Element, type=B31, Elset=mooring_element_27_line9w');
fprintf(fileID,formatSpec2,mooring_ele(26,1),mooring_ele(26,2),mooring_ele(26,3));
fprintf(fileID,formatSpec1,'*Element, type=B31, Elset=mooring_element_27_line9t');
fprintf(fileID,formatSpec2,mooring_ele(27,1),mooring_ele(27,2),mooring_ele(27,3));
fprintf(fileID,formatSpec1,'*Element, type=B31, Elset=mooring_element_27_line10b');
fprintf(fileID,formatSpec2,mooring_ele(28,1),mooring_ele(28,2),mooring_ele(28,3));
fprintf(fileID,formatSpec1,'*Element, type=B31, Elset=mooring_element_27_line10w');
fprintf(fileID,formatSpec2,mooring_ele(29,1),mooring_ele(29,2),mooring_ele(29,3));
fprintf(fileID,formatSpec1,'*Element, type=B31, Elset=mooring_element_27_line10t');
fprintf(fileID,formatSpec2,mooring_ele(30,1),mooring_ele(30,2),mooring_ele(30,3));
fprintf(fileID,formatSpec1,'*Element, type=B31, Elset=mooring_element_27_line11b');
fprintf(fileID,formatSpec2,mooring_ele(31,1),mooring_ele(31,2),mooring_ele(31,3));
fprintf(fileID,formatSpec1,'*Element, type=B31, Elset=mooring_element_27_line11w');
fprintf(fileID,formatSpec2,mooring_ele(32,1),mooring_ele(32,2),mooring_ele(32,3));
fprintf(fileID,formatSpec1,'*Element, type=B31, Elset=mooring_element_27_line11t');
```

```
fprintf(fileID,formatSpec2,mooring_ele(33,1),mooring_ele(33,2),mooring_ele(33,3));
fprintf(fileID,formatSpec1,'*Element, type=B31, Elset=mooring_element_27_line12b');
fprintf(fileID,formatSpec2,mooring_ele(34,1),mooring_ele(34,2),mooring_ele(34,3));
fprintf(fileID,formatSpec1,'*Element, type=B31, Elset=mooring_element_27_line12w');
fprintf(fileID,formatSpec2,mooring_ele(35,1),mooring_ele(35,2),mooring_ele(35,3));
fprintf(fileID,formatSpec1,'*Element, type=B31, Elset=mooring_element_27_line12t');
fprintf(fileID,formatSpec2,mooring_ele(36,1),mooring_ele(36,2),mooring_ele(36,3));

%%Orientation, pontoon
fprintf(fileID,formatSpec1,'**********************************');
for i=1:length(pontoon_orien)
    fprintf(fileID,formatSpec8,'*ORIENTATION, NAME=pontoon',i+2);

fprintf(fileID,formatSpec11,pontoon_orien(i,1),pontoon_orien(i,2),pontoon_orien(i,3),pontoon_o
rien(i,4),pontoon_orien(i,5),pontoon_orien(i,6));
end
%Pontoon spring
fprintf(fileID,formatSpec1,'**********************************');
for i=1:length(pon_spring)
    fprintf(fileID,formatSpec7,'*ELEMENT, TYPE=SPRING1, Elset=pontoon',i+2,'_spring_Z');
    fprintf(fileID,formatSpec3,pon_spring(i,2),pon_spring(i,5));
    fprintf(fileID,formatSpec7,'*ELEMENT, TYPE=SPRING1, Elset=pontoon',i+2,'_spring_RX');
    fprintf(fileID,formatSpec3,pon_spring(i,3),pon_spring(i,5));
    fprintf(fileID,formatSpec7,'*ELEMENT, TYPE=SPRING1, Elset=pontoon',i+2,'_spring_RY');
    fprintf(fileID,formatSpec3,pon_spring(i,4),pon_spring(i,5));
    fprintf(fileID,formatSpec12,'*Spring,
elset=pontoon',i+2,'_spring_Z',',Orientation=pontoon',i+2);
    fprintf(fileID,formatSpec1,'3');
    fprintf(fileID,formatSpec4,pon_spring(i,6));
    fprintf(fileID,formatSpec12,'*Spring,
elset=pontoon',i+2,'_spring_RX',',Orientation=pontoon',i+2);
    fprintf(fileID,formatSpec1,'4');
    fprintf(fileID,formatSpec4,pon_spring(i,7));
    fprintf(fileID,formatSpec12,'*Spring,
elset=pontoon',i+2,'_spring_RY',',Orientation=pontoon',i+2);
    fprintf(fileID,formatSpec1,'5');
    fprintf(fileID,formatSpec4,pon_spring(i,8));
    fprintf(fileID,formatSpec1,'**********************************');
end

%pontoon mass
for i=1:length(pon_mass)
  fprintf(fileID,formatSpec8,'*ELEMENT, TYPE=MASS, ELSET=pontoon_mass_',i+2);
  fprintf(fileID,formatSpec3,pon_mass(i,2),pon_mass(i,3));
  fprintf(fileID,formatSpec8,'*MASS, ELSET=pontoon_mass_',i+2);
  fprintf(fileID,formatSpec4,pon_mass(i,4));
end

%girder mass
fprintf(fileID,formatSpec1,'**********************************');
fprintf(fileID,formatSpec1,'**mass_ne_5');
fprintf(fileID,formatSpec1,'*Element, type=MASS, Elset=mass_ne_5');
for i=1:52;
    fprintf(fileID,formatSpec3,mass_ele(i,1),mass_ele(i,2));
end
fprintf(fileID,formatSpec1,'**mass_ne_20');
fprintf(fileID,formatSpec1,'*Element, type=MASS, Elset=mass_ne_20');
```

```
for i=53:78;
    fprintf(fileID,formatSpec3,mass_ele(i,1),mass_ele(i,2));
end
fprintf(fileID,formatSpec1,'**mass_ne_25');
fprintf(fileID,formatSpec1,'*Element, type=MASS, Elset=mass_ne_25');
for i=79:268;
    fprintf(fileID,formatSpec3,mass_ele(i,1),mass_ele(i,2));
end

fprintf(fileID,formatSpec1,'**mass_sw_5');
fprintf(fileID,formatSpec1,'*Element, type=MASS, Elset=mass_sw_5');
for i=1:52;
    fprintf(fileID,formatSpec3,mass_ele(i,1+3),mass_ele(i,2+3));
end
fprintf(fileID,formatSpec1,'**mass_sw_20');
fprintf(fileID,formatSpec1,'*Element, type=MASS, Elset=mass_sw_20');
for i=53:78;
    fprintf(fileID,formatSpec3,mass_ele(i,1+3),mass_ele(i,2+3));
end
fprintf(fileID,formatSpec1,'**mass_sw_25');
fprintf(fileID,formatSpec1,'*Element, type=MASS, Elset=mass_sw_25');
for i=79:268;
    fprintf(fileID,formatSpec3,mass_ele(i,1+3),mass_ele(i,2+3));
end

fprintf(fileID,formatSpec1,'**mass_b_5');
fprintf(fileID,formatSpec1,'*Element, type=MASS, Elset=mass_b_5');
for i=1:52;
    fprintf(fileID,formatSpec3,mass_ele(i,1+3*2),mass_ele(i,2+3*2));
end
fprintf(fileID,formatSpec1,'**mass_b_20');
fprintf(fileID,formatSpec1,'*Element, type=MASS, Elset=mass_b_20');
for i=53:78;
    fprintf(fileID,formatSpec3,mass_ele(i,1+3*2),mass_ele(i,2+3*2));
end
fprintf(fileID,formatSpec1,'**mass_b_25');
fprintf(fileID,formatSpec1,'*Element, type=MASS, Elset=mass_b_25');
for i=79:268;
    fprintf(fileID,formatSpec3,mass_ele(i,1+3*2),mass_ele(i,2+3*2));
end
%mass
fprintf(fileID,formatSpec1,'**********************************');
fprintf(fileID,formatSpec1,'**girder_mass');
fprintf(fileID,formatSpec1,'*MASS, elset=mass_ne_5');
fprintf(fileID,formatSpec1,'57735');
fprintf(fileID,formatSpec1,'*MASS, elset=mass_sw_5');
fprintf(fileID,formatSpec1,'57735');
fprintf(fileID,formatSpec1,'*MASS, elset=mass_b_5');
fprintf(fileID,formatSpec1,'280030');
fprintf(fileID,formatSpec1,'*MASS, elset=mass_ne_20');
fprintf(fileID,formatSpec1,'46100');
fprintf(fileID,formatSpec1,'*MASS, elset=mass_sw_20');
fprintf(fileID,formatSpec1,'46100');
fprintf(fileID,formatSpec1,'*MASS, elset=mass_b_20');
fprintf(fileID,formatSpec1,'287800');
fprintf(fileID,formatSpec1,'*MASS, elset=mass_ne_25');
fprintf(fileID,formatSpec1,'57625');
```

```
fprintf(fileID,formatSpec1,'*MASS, elset=mass_sw_25');
fprintf(fileID,formatSpec1,'57625');
fprintf(fileID,formatSpec1,'*MASS, elset=mass_b_25');
fprintf(fileID,formatSpec1,'359750');
fprintf(fileID,formatSpec1,'**********************************');
```

```
fprintf(fileID,formatSpec1,'**');
fprintf(fileID,formatSpec1,'**********************************');
fprintf(fileID,formatSpec1,'**Defining Cross Sections');
% girder elememt
%girder with concrete cross section
for i=1:52
fprintf(fileID,formatSpec7,'*Beam General Section, elset=girder_concrete_',i, ',density=1E-16,
section=GENERAL');
fprintf(fileID,formatSpec5,girder_ele(i,1+4*4),girder_ele(i,2+4*4),0,girder_ele(i,3+4*4),girde
r_ele(i,4+4*4));
fprintf(fileID,formatSpec2,girder_ele(i,7+4*4),girder_ele(i,8+4*4),girder_ele(i,9+4*4));
fprintf(fileID,formatSpec3,girder_ele(i,5+4*4),girder_ele(i,6+4*4));
fprintf(fileID,formatSpec1,'*DAMPING, ALPHA=0.00196185717187488, BETA=0.000184063576686462');
fprintf(fileID,formatSpec1,'*SECTION POINTS');
fprintf(fileID,formatSpec1,'0,0');
fprintf(fileID,formatSpec1,'**********************************');
end
fprintf(fileID,formatSpec1,'**********************************');
%girder with steel cross section in transition
for i=53:80
fprintf(fileID,formatSpec7,'*Beam General Section, elset=girder_steel_',i, ',density=1E-16,
section=GENERAL');
fprintf(fileID,formatSpec5,girder_ele(i,1+4*4),girder_ele(i,2+4*4),0,girder_ele(i,3+4*4),girde
r_ele(i,4+4*4));
fprintf(fileID,formatSpec2,girder_ele(i,7+4*4),girder_ele(i,8+4*4),girder_ele(i,9+4*4));
fprintf(fileID,formatSpec3,girder_ele(i,5+4*4),girder_ele(i,6+4*4));
fprintf(fileID,formatSpec1,'*DAMPING, ALPHA=0.00196185717187488, BETA=0.000184063576686462');
fprintf(fileID,formatSpec1,'*SECTION POINTS');
fprintf(fileID,formatSpec1,'0,0');
fprintf(fileID,formatSpec1,'**********************************');
end
for i=81:115
fprintf(fileID,formatSpec7,'*Beam General Section, elset=girder_transition_',i, ',density=1E-
16, section=GENERAL');
fprintf(fileID,formatSpec5,girder_ele(i,1+4*4),girder_ele(i,2+4*4),0,girder_ele(i,3+4*4),girde
r_ele(i,4+4*4));
fprintf(fileID,formatSpec2,girder_ele(i,7+4*4),girder_ele(i,8+4*4),girder_ele(i,9+4*4));
fprintf(fileID,formatSpec3,girder_ele(i,5+4*4),girder_ele(i,6+4*4));
fprintf(fileID,formatSpec1,'*DAMPING, ALPHA=0.00196185717187488, BETA=0.000184063576686462');
fprintf(fileID,formatSpec1,'*SECTION POINTS');
fprintf(fileID,formatSpec1,'0,0');
fprintf(fileID,formatSpec1,'**********************************');
end
for i=116
fprintf(fileID,formatSpec1,'*Beam General Section, elset=girder_steel_2, density=1E-16,
section=GENERAL');
fprintf(fileID,formatSpec5,girder_ele(i,1+4*4),girder_ele(i,2+4*4),0,girder_ele(i,3+4*4),girde
r_ele(i,4+4*4));
```

```
fprintf(fileID,formatSpec2,girder_ele(i,7+4*4),girder_ele(i,8+4*4),girder_ele(i,9+4*4));
fprintf(fileID,formatSpec3,girder_ele(i,5+4*4),girder_ele(i,6+4*4));
fprintf(fileID,formatSpec1,'*DAMPING, ALPHA=0.00196185717187488, BETA=0.000184063576686462');
fprintf(fileID,formatSpec1,'*SECTION POINTS');
fprintf(fileID,formatSpec1,'0,0');
fprintf(fileID,formatSpec1,'**********************************');
end
% LINK NE ELEMENT
%link with concrete cross section
for i=1:52
fprintf(fileID,formatSpec7,'*Beam General Section, elset=link_ne_concrete_',i, ',density=1E-
16, section=GENERAL');
fprintf(fileID,formatSpec1,'27.9510Oe+00, 2.1380Oe+03, 0, 4.050Oe+01, 1.3540Oe+02');
fprintf(fileID,formatSpec2,girder_ele(i,7+4*4),girder_ele(i,8+4*4),girder_ele(i,9+4*4));
fprintf(fileID,formatSpec1,'10, 5');
fprintf(fileID,formatSpec1,'*DAMPING, ALPHA=0.00196185717187488, BETA=0.000184063576686462');
fprintf(fileID,formatSpec1,'**********************************');
end
fprintf(fileID,formatSpec1,'**********************************');
%girder with steel cross section in transition
for i=53:80
fprintf(fileID,formatSpec7,'*Beam General Section, elset=link_ne_steel_',i, ',density=1E-16,
section=GENERAL');
fprintf(fileID,formatSpec1,'1.8830Oe+00, 12.1830Oe+01, 0, 3.785000e+00, 12.010Oe+00');
fprintf(fileID,formatSpec2,girder_ele(i,7+4*4),girder_ele(i,8+4*4),girder_ele(i,9+4*4));
fprintf(fileID,formatSpec1,'10, 5');
fprintf(fileID,formatSpec1,'*DAMPING, ALPHA=0.00196185717187488, BETA=0.000184063576686462');
fprintf(fileID,formatSpec1,'**********************************');
end
for i=81:115
fprintf(fileID,formatSpec7,'*Beam General Section, elset=link_ne_transition_',i, ',density=1E-
16, section=GENERAL');
fprintf(fileID,formatSpec1,'1.8830Oe+00, 12.1830Oe+01, 0, 3.785000e+00, 12.010Oe+00');
fprintf(fileID,formatSpec2,girder_ele(i,7+4*4),girder_ele(i,8+4*4),girder_ele(i,9+4*4));
fprintf(fileID,formatSpec1,'10, 5');
fprintf(fileID,formatSpec1,'*DAMPING, ALPHA=0.00196185717187488, BETA=0.000184063576686462');
fprintf(fileID,formatSpec1,'**********************************');
end
fprintf(fileID,formatSpec1,'*Beam General Section, elset=link_ne_steel_2, density=1E-16,
section=GENERAL');
for i=116
fprintf(fileID,formatSpec1,'1.8830Oe+00, 12.1830Oe+01, 0, 3.785000e+00, 12.010Oe+00');
fprintf(fileID,formatSpec2,girder_ele(i,7+4*4),girder_ele(i,8+4*4),girder_ele(i,9+4*4));
fprintf(fileID,formatSpec1,'10, 5');
fprintf(fileID,formatSpec1,'*DAMPING, ALPHA=0.00196185717187488, BETA=0.000184063576686462');
fprintf(fileID,formatSpec1,'**********************************');
end

% LINK sw ELEMENT
%link with concrete cross section
for i=1:52
fprintf(fileID,formatSpec7,'*Beam General Section, elset=link_sw_concrete_',i, ',density=1E-
16, section=GENERAL');
fprintf(fileID,formatSpec1,'27.9510Oe+00, 2.1380Oe+03, 0, 4.050Oe+01, 1.3540Oe+02');
fprintf(fileID,formatSpec2,girder_ele(i,7+4*4),girder_ele(i,8+4*4),girder_ele(i,9+4*4));
fprintf(fileID,formatSpec1,'10, 5');
fprintf(fileID,formatSpec1,'*DAMPING, ALPHA=0.00196185717187488, BETA=0.000184063576686462');
```

```
fprintf(fileID,formatSpec1,'************************************');
end
fprintf(fileID,formatSpec1,'************************************');
%girder with steel cross section in transition
for i=53:80
fprintf(fileID,formatSpec7,'*Beam General Section, elset=link_sw_steel_',i, ',density=1E-16,
section=GENERAL');
fprintf(fileID,formatSpec1,'1.88300e+00, 12.18300e+01, 0, 3.785000e+00, 12.0100e+00');
fprintf(fileID,formatSpec2,girder_ele(i,7+4*4),girder_ele(i,8+4*4),girder_ele(i,9+4*4));
fprintf(fileID,formatSpec1,'10, 5');
fprintf(fileID,formatSpec1,'*DAMPING, ALPHA=0.00196185717187488, BETA=0.000184063576686462');
fprintf(fileID,formatSpec1,'************************************');
end
for i=81:115
fprintf(fileID,formatSpec7,'*Beam General Section, elset=link_sw_transition_',i, ',density=1E-
16, section=GENERAL');
fprintf(fileID,formatSpec1,'1.88300e+00, 12.18300e+01, 0, 3.785000e+00, 12.0100e+00');
fprintf(fileID,formatSpec2,girder_ele(i,7+4*4),girder_ele(i,8+4*4),girder_ele(i,9+4*4));
fprintf(fileID,formatSpec1,'10, 5');
fprintf(fileID,formatSpec1,'*DAMPING, ALPHA=0.00196185717187488, BETA=0.000184063576686462');
fprintf(fileID,formatSpec1,'************************************');
end
fprintf(fileID,formatSpec1,'*Beam General Section, elset=link_sw_steel_2, density=1E-16,
section=GENERAL');
for i=116
fprintf(fileID,formatSpec1,'1.88300e+00, 12.18300e+01, 0, 3.785000e+00, 12.0100e+00');
fprintf(fileID,formatSpec2,girder_ele(i,7+4*4),girder_ele(i,8+4*4),girder_ele(i,9+4*4));
fprintf(fileID,formatSpec1,'10, 5');
fprintf(fileID,formatSpec1,'*DAMPING, ALPHA=0.00196185717187488, BETA=0.000184063576686462');
fprintf(fileID,formatSpec1,'************************************');
end
% LINK BOTTON ELEMENT
%link with concrete cross section
for i=1:52
fprintf(fileID,formatSpec7,'*Beam General Section, elset=link_bottom_concrete_',i,
',density=1E-16, section=GENERAL');
fprintf(fileID,formatSpec1,'27.95100e+00, 2.13800e+03, 0, 4.0500e+01, 1.35400e+02');
fprintf(fileID,formatSpec2,girder_ele(i,7+4*4),girder_ele(i,8+4*4),girder_ele(i,9+4*4));
fprintf(fileID,formatSpec1,'10, 5');
fprintf(fileID,formatSpec1,'*DAMPING, ALPHA=0.00196185717187488, BETA=0.000184063576686462');
fprintf(fileID,formatSpec1,'************************************');
end
fprintf(fileID,formatSpec1,'************************************');
%girder with steel cross section in transition
for i=53:80
fprintf(fileID,formatSpec7,'*Beam General Section, elset=link_bottom_steel_',i, ',density=1E-
16, section=GENERAL');
fprintf(fileID,formatSpec1,'1.88300e+00, 12.18300e+01, 0, 3.785000e+00, 12.0100e+00');
fprintf(fileID,formatSpec2,girder_ele(i,7+4*4),girder_ele(i,8+4*4),girder_ele(i,9+4*4));
fprintf(fileID,formatSpec1,'10, 5');
fprintf(fileID,formatSpec1,'*DAMPING, ALPHA=0.00196185717187488, BETA=0.000184063576686462');
fprintf(fileID,formatSpec1,'************************************');
end
for i=81:115
fprintf(fileID,formatSpec7,'*Beam General Section, elset=link_bottom_transition_',i,
',density=1E-16, section=GENERAL');
fprintf(fileID,formatSpec1,'1.88300e+00, 12.18300e+01, 0, 3.785000e+00, 12.0100e+00');
```

```
fprintf(fileID,formatSpec2,girder_ele(i,7+4*4),girder_ele(i,8+4*4),girder_ele(i,9+4*4));
fprintf(fileID,formatSpec1,'10, 5');
fprintf(fileID,formatSpec1,'*DAMPING, ALPHA=0.00196185717187488, BETA=0.000184063576686462');
fprintf(fileID,formatSpec1,'**********************************');
end
fprintf(fileID,formatSpec1,'*Beam General Section, elset=link_bottom_steel_2, density=1E-16,
section=GENERAL');
for i=270
fprintf(fileID,formatSpec1,'1.88300e+00, 12.18300e+01, 0, 3.785000e+00, 12.0100e+00');
fprintf(fileID,formatSpec1,'0, 0, 1');
fprintf(fileID,formatSpec1,'10, 5');
fprintf(fileID,formatSpec1,'*DAMPING, ALPHA=0.00196185717187488, BETA=0.000184063576686462');
fprintf(fileID,formatSpec1,'**********************************');
end
```

```
%dummy elements
fprintf(fileID,formatSpec1,'**');
for i=1:269
fprintf(fileID,formatSpec7,'*Beam General Section, elset=dummy_ne_',i, ',density=1E-16,
section=GENERAL');
fprintf(fileID,formatSpec5,dummy_ele(i,1+4*5),dummy_ele(i,2+4*5),dummy_ele(i,3+4*5),dummy_ele(
i,4+4*5),dummy_ele(i,5+4*5));
fprintf(fileID,formatSpec2,dummy_ele(i,1+3*4),dummy_ele(i,2+3*4),dummy_ele(i,3+3*4));
fprintf(fileID,formatSpec3,dummy_ele(i,1+5*5),dummy_ele(i,2+5*5));
fprintf(fileID,formatSpec1,'*DAMPING, ALPHA=0.00196185717187488, BETA=0.000184063576686462');
fprintf(fileID,formatSpec1,'**********************************');

end
for i=1:269
fprintf(fileID,formatSpec7,'*Beam General Section, elset=dummy_sw_',i, ',density=1E-16,
section=GENERAL');
fprintf(fileID,formatSpec5,dummy_ele(i,1+4*5),dummy_ele(i,2+4*5),dummy_ele(i,3+4*5),dummy_ele(
i,4+4*5),dummy_ele(i,5+4*5));
fprintf(fileID,formatSpec2,dummy_ele(i,1+3*4),dummy_ele(i,2+3*4),dummy_ele(i,3+3*4));
fprintf(fileID,formatSpec3,dummy_ele(i,1+5*5),dummy_ele(i,2+5*5));
fprintf(fileID,formatSpec1,'*DAMPING, ALPHA=0.00196185717187488, BETA=0.000184063576686462');
fprintf(fileID,formatSpec1,'**********************************');

end
for i=1:269
fprintf(fileID,formatSpec7,'*Beam General Section, elset=dummy_b_',i, ',density=1E-16,
section=GENERAL');
fprintf(fileID,formatSpec5,dummy_ele(i,1+4*5),dummy_ele(i,2+4*5),dummy_ele(i,3+4*5),dummy_ele(
i,4+4*5),dummy_ele(i,5+4*5));
fprintf(fileID,formatSpec2,dummy_ele(i,1+3*4),dummy_ele(i,2+3*4),dummy_ele(i,3+3*4));
fprintf(fileID,formatSpec3,dummy_ele(i,1+5*5),dummy_ele(i,2+5*5));
fprintf(fileID,formatSpec1,'*DAMPING, ALPHA=0.00196185717187488, BETA=0.000184063576686462');
fprintf(fileID,formatSpec1,'**********************************');

end

%cable element
for i=1:18
fprintf(fileID,formatSpec7,'*Beam General Section, elset=cable_ne_side_A',i,
',density=7.83e+03, section=GENERAL');
fprintf(fileID,formatSpec5,cable_ele(i,17),cable_ele(i,17+1),0,cable_ele(i,17+1),cable_ele(i,1
7+2));
fprintf(fileID,formatSpec2,cable_ele(i,17+3),cable_ele(i,17+4),cable_ele(i,17+5));
```

```
fprintf(fileID,formatSpec2,cable_ele(i,32),cable_ele(i,34),cable_ele(i,35));
fprintf(fileID,formatSpec1,'*DAMPING, ALPHA=0.00196185717187488, BETA=0.000184063576686462');
fprintf(fileID,formatSpec1,'**********************************');

end

for i=1:18
fprintf(fileID,formatSpec7,'*Beam General Section, elset=cable_sw_side_A',i,
',density=7.83e+03, section=GENERAL');
fprintf(fileID,formatSpec5,cable_ele(i,17),cable_ele(i,17+1),0,cable_ele(i,17+1),cable_ele(i,1
7+2));
fprintf(fileID,formatSpec2,cable_ele(i,23),cable_ele(i,24),cable_ele(i,25));
fprintf(fileID,formatSpec2,cable_ele(i,32),cable_ele(i,34),cable_ele(i,35));
fprintf(fileID,formatSpec1,'*DAMPING, ALPHA=0.00196185717187488, BETA=0.000184063576686462');
fprintf(fileID,formatSpec1,'**********************************');

end

for i=1:18
fprintf(fileID,formatSpec7,'*Beam General Section, elset=cable_ne_main_A',i,
',density=7.83e+03, section=GENERAL');
fprintf(fileID,formatSpec5,cable_ele(i,17),cable_ele(i,17+1),0,cable_ele(i,17+1),cable_ele(i,1
7+2));
fprintf(fileID,formatSpec2,cable_ele(i,26),cable_ele(i,27),cable_ele(i,28));
fprintf(fileID,formatSpec2,cable_ele(i,33),cable_ele(i,34),cable_ele(i,36));
fprintf(fileID,formatSpec1,'*DAMPING, ALPHA=0.00196185717187488, BETA=0.000184063576686462');
fprintf(fileID,formatSpec1,'**********************************');

end

for i=1:18
fprintf(fileID,formatSpec7,'*Beam General Section, elset=cable_sw_main_A',i,
',density=7.83e+03, section=GENERAL');
fprintf(fileID,formatSpec5,cable_ele(i,17),cable_ele(i,17+1),0,cable_ele(i,17+1),cable_ele(i,1
7+2));
fprintf(fileID,formatSpec2,cable_ele(i,29),cable_ele(i,30),cable_ele(i,31));
fprintf(fileID,formatSpec2,cable_ele(i,33),cable_ele(i,34),cable_ele(i,36));
fprintf(fileID,formatSpec1,'*DAMPING, ALPHA=0.00196185717187488, BETA=0.000184063576686462');
fprintf(fileID,formatSpec1,'**********************************');

end

%tower element
for i=1:32
fprintf(fileID,formatSpec7,'*Beam General Section, leg_sw_tower_',i, ',density=2.65e+03,
section=GENERAL');
fprintf(fileID,formatSpec5,tower_node(i,23),tower_node(i,25),0,tower_node(i,26),tower_node(i,2
7));
fprintf(fileID,formatSpec2,tower_node(i,28),tower_node(i,29),tower_node(i,30));
fprintf(fileID,formatSpec3,tower_node(i,34),tower_node(i,35));
fprintf(fileID,formatSpec1,'*DAMPING, ALPHA=0.00196185717187488, BETA=0.000184063576686462');
fprintf(fileID,formatSpec1,'**********************************');

end

for i=1:32
fprintf(fileID,formatSpec7,'*Beam General Section, leg_ne_tower_',i, ',density=2.65e+03,
```

```
section=GENERAL');
fprintf(fileID,formatSpec5,tower_node(i,24),tower_node(i,25),0,tower_node(i,26),tower_node(i,2
7));
fprintf(fileID,formatSpec2,tower_node(i,31),tower_node(i,32),tower_node(i,33));
fprintf(fileID,formatSpec3,tower_node(i,34),tower_node(i,35));
fprintf(fileID,formatSpec1,'*DAMPING, ALPHA=0.00196185717187488, BETA=0.000184063576686462');
fprintf(fileID,formatSpec1,'************************************');

end

%mooring line cs
for i=1:3:10
fprintf(fileID,formatSpec9,'*Beam General Section,
elset=mooring_element_13_line',mooring_ele(i,5), 'b,density=',mooring_ele(i,6),
',section=GENERAL');
fprintf(fileID,formatSpec5,mooring_ele(i,7),mooring_ele(i,8),0,mooring_ele(i,9),mooring_ele(i,
10));
fprintf(fileID,formatSpec2,mooring_ele(i,1+3*4),mooring_ele(i,2+3*4),mooring_ele(i,3+3*4));
fprintf(fileID,formatSpec2,mooring_ele(i,2+3*3),mooring_ele(i,1+5*3),mooring_ele(i,3+3*3));
fprintf(fileID,formatSpec1,'*DAMPING, ALPHA=0.00196185717187488, BETA=0.000184063576686462');
fprintf(fileID,formatSpec1,'************************************');

end
for i=2:3:11
fprintf(fileID,formatSpec9,'*Beam General Section,
elset=mooring_element_13_line',mooring_ele(i,5), 'w,density=',mooring_ele(i,6),
',section=GENERAL');
fprintf(fileID,formatSpec5,mooring_ele(i,7),mooring_ele(i,8),0,mooring_ele(i,9),mooring_ele(i,
10));
fprintf(fileID,formatSpec2,mooring_ele(i,1+3*4),mooring_ele(i,2+3*4),mooring_ele(i,3+3*4));
fprintf(fileID,formatSpec2,mooring_ele(i,2+3*3),mooring_ele(i,1+5*3),mooring_ele(i,3+3*3));
fprintf(fileID,formatSpec1,'*DAMPING, ALPHA=0.00196185717187488, BETA=0.000184063576686462');
fprintf(fileID,formatSpec1,'************************************');

end
for i=3:3:12
fprintf(fileID,formatSpec9,'*Beam General Section,
elset=mooring_element_13_line',mooring_ele(i,5), 't,density=',mooring_ele(i,6),
',section=GENERAL');
fprintf(fileID,formatSpec5,mooring_ele(i,7),mooring_ele(i,8),0,mooring_ele(i,9),mooring_ele(i,
10));
fprintf(fileID,formatSpec2,mooring_ele(i,1+3*4),mooring_ele(i,2+3*4),mooring_ele(i,3+3*4));
fprintf(fileID,formatSpec2,mooring_ele(i,2+3*3),mooring_ele(i,1+5*3),mooring_ele(i,3+3*3));
fprintf(fileID,formatSpec1,'*DAMPING, ALPHA=0.00196185717187488, BETA=0.000184063576686462');
fprintf(fileID,formatSpec1,'************************************');

end

%
for i=13:3:22
fprintf(fileID,formatSpec9,'*Beam General Section,
elset=mooring_element_20_line',mooring_ele(i,5), 'b,density=',mooring_ele(i,6),
',section=GENERAL');
fprintf(fileID,formatSpec5,mooring_ele(i,7),mooring_ele(i,8),0,mooring_ele(i,9),mooring_ele(i,
10));
fprintf(fileID,formatSpec2,mooring_ele(i,1+3*4),mooring_ele(i,2+3*4),mooring_ele(i,3+3*4));
fprintf(fileID,formatSpec2,mooring_ele(i,2+3*3),mooring_ele(i,1+5*3),mooring_ele(i,3+3*3));
```

```
fprintf(fileID,formatSpec1,'*DAMPING, ALPHA=0.00196185717187488, BETA=0.000184063576686462');
fprintf(fileID,formatSpec1,'************************************');

end
for i=14:3:23
fprintf(fileID,formatSpec9,'*Beam General Section,
elset=mooring_element_20_line',mooring_ele(i,5), 'w,density=',mooring_ele(i,6),
',section=GENERAL');
fprintf(fileID,formatSpec5,mooring_ele(i,7),mooring_ele(i,8),0,mooring_ele(i,9),mooring_ele(i,
10));
fprintf(fileID,formatSpec2,mooring_ele(i,1+3*4),mooring_ele(i,2+3*4),mooring_ele(i,3+3*4));
fprintf(fileID,formatSpec2,mooring_ele(i,2+3*3),mooring_ele(i,1+5*3),mooring_ele(i,3+3*3));
fprintf(fileID,formatSpec1,'*DAMPING, ALPHA=0.00196185717187488, BETA=0.000184063576686462');
fprintf(fileID,formatSpec1,'************************************');

end
for i=15:3:24
fprintf(fileID,formatSpec9,'*Beam General Section,
elset=mooring_element_20_line',mooring_ele(i,5), 't,density=',mooring_ele(i,6),
',section=GENERAL');
fprintf(fileID,formatSpec5,mooring_ele(i,7),mooring_ele(i,8),0,mooring_ele(i,9),mooring_ele(i,
10));
fprintf(fileID,formatSpec2,mooring_ele(i,1+3*4),mooring_ele(i,2+3*4),mooring_ele(i,3+3*4));
fprintf(fileID,formatSpec2,mooring_ele(i,2+3*3),mooring_ele(i,1+5*3),mooring_ele(i,3+3*3));
fprintf(fileID,formatSpec1,'*DAMPING, ALPHA=0.00196185717187488, BETA=0.000184063576686462');
fprintf(fileID,formatSpec1,'************************************');

end
%
for i=25:3:34
fprintf(fileID,formatSpec9,'*Beam General Section,
elset=mooring_element_27_line',mooring_ele(i,5), 'b,density=',mooring_ele(i,6),
',section=GENERAL');
fprintf(fileID,formatSpec5,mooring_ele(i,7),mooring_ele(i,8),0,mooring_ele(i,9),mooring_ele(i,
10));
fprintf(fileID,formatSpec2,mooring_ele(i,1+3*4),mooring_ele(i,2+3*4),mooring_ele(i,3+3*4));
fprintf(fileID,formatSpec2,mooring_ele(i,2+3*3),mooring_ele(i,1+5*3),mooring_ele(i,3+3*3));
fprintf(fileID,formatSpec1,'*DAMPING, ALPHA=0.00196185717187488, BETA=0.000184063576686462');
fprintf(fileID,formatSpec1,'************************************');

end
for i=26:3:35
fprintf(fileID,formatSpec9,'*Beam General Section,
elset=mooring_element_27_line',mooring_ele(i,5), 'w,density=',mooring_ele(i,6),
',section=GENERAL');
fprintf(fileID,formatSpec5,mooring_ele(i,7),mooring_ele(i,8),0,mooring_ele(i,9),mooring_ele(i,
10));
fprintf(fileID,formatSpec2,mooring_ele(i,1+3*4),mooring_ele(i,2+3*4),mooring_ele(i,3+3*4));
fprintf(fileID,formatSpec2,mooring_ele(i,2+3*3),mooring_ele(i,1+5*3),mooring_ele(i,3+3*3));
fprintf(fileID,formatSpec1,'*DAMPING, ALPHA=0.00196185717187488, BETA=0.000184063576686462');
fprintf(fileID,formatSpec1,'************************************');

end
for i=27:3:36
fprintf(fileID,formatSpec9,'*Beam General Section,
elset=mooring_element_27_line',mooring_ele(i,5), 't,density=',mooring_ele(i,6),
',section=GENERAL');
```

```
fprintf(fileID,formatSpec5,mooring_ele(i,7),mooring_ele(i,8),0,mooring_ele(i,9),mooring_ele(i,
10));
fprintf(fileID,formatSpec2,mooring_ele(i,1+3*4),mooring_ele(i,2+3*4),mooring_ele(i,3+3*4));
fprintf(fileID,formatSpec2,mooring_ele(i,2+3*3),mooring_ele(i,1+5*3),mooring_ele(i,3+3*3));
fprintf(fileID,formatSpec1,'*DAMPING, ALPHA=0.00196185717187488, BETA=0.000184063576686462');
fprintf(fileID,formatSpec1,'**********************************');

end

%pontoon connector element
fprintf(fileID,formatSpec1,'**pontoon_connectors');
for i=1:3:length(pontoon_connector);
    fprintf(fileID,formatSpec7,'*Beam General Section, Elset=pontoons_',i,'_connector,
density=1E-16, section=GENERAL');
    fprintf(fileID,formatSpec1,'4, 135, 0, 135, 135');
    fprintf(fileID,formatSpec1,'1, 0, 0');
    fprintf(fileID,formatSpec1,'2.10E+11');
    fprintf(fileID,formatSpec1,'*DAMPING, ALPHA=0.00196185717187488,
BETA=0.000184063576686462');
    fprintf(fileID,formatSpec1,'**********************************');
end
```

```
%Defining node set
%nodeset for rigid body
fprintf(fileID,formatSpec1,'**nodeset_rigid_body');
for i=1:length(girder_node)
    fprintf(fileID,formatSpec8,'*NSET,NSET=girder_node_',i);
    fprintf(fileID,formatSpec4,girder_node(i,2));
end
fprintf(fileID,formatSpec1,'**********************************');

%nodeset for cable
for i=1:18
    fprintf(fileID,formatSpec7,'*NSET,NSET=cable_',i,'_side_ne');
    fprintf(fileID,formatSpec4,cable_ele(i,3));
end
for i=1:18
    fprintf(fileID,formatSpec7,'*NSET,NSET=cable_',i,'_side_sw');
    fprintf(fileID,formatSpec4,cable_ele(i,3+4));
end
for i=1:18
    fprintf(fileID,formatSpec7,'*NSET,NSET=cable_',i,'_main_ne');
    fprintf(fileID,formatSpec4,cable_ele(i,3+4*2));
end
for i=1:18
    fprintf(fileID,formatSpec7,'*NSET,NSET=cable_',i,'_main_sw');
    fprintf(fileID,formatSpec4,cable_ele(i,3+4*3));
end
fprintf(fileID,formatSpec1,'**********************************');

%element set
fprintf(fileID,formatSpec1,'*ELSET, ELSET=tower     ');
for i=1:32
    fprintf(fileID,formatSpec8,'leg_sw_tower_',i);
    fprintf(fileID,formatSpec8,'leg_ne_tower_',i);
end
fprintf(fileID,formatSpec1,'crossbeam');
```

```
fprintf(fileID,formatSpec1,'***********************************');

%nodeset for buoyancy
 fprintf(fileID,formatSpec1,'*NSET,NSET=buoyancy_pontoon3,GENERATE');
 fprintf(fileID,formatSpec2,pontoon_node(1,16),pontoon_node(1,17),pontoon_node(1,18));
 fprintf(fileID,formatSpec1,'*NSET,NSET=buoyancy_pontoons1,GENERATE       ');
for i=2:5;
   fprintf(fileID,formatSpec2,pontoon_node(i,16),pontoon_node(i,17),pontoon_node(i,18));
end
 fprintf(fileID,formatSpec1,'*NSET,NSET=buoyancy_pontoon13_mooring,GENERATE');
 fprintf(fileID,formatSpec2,pontoon_node(1,21),pontoon_node(1,22),pontoon_node(1,23));
 fprintf(fileID,formatSpec1,'*NSET,NSET=buoyancy_pontoon20_mooring,GENERATE');
 fprintf(fileID,formatSpec2,pontoon_node(2,21),pontoon_node(2,22),pontoon_node(2,23));
 fprintf(fileID,formatSpec1,'*NSET,NSET=buoyancy_pontoon27_mooring,GENERATE');
 fprintf(fileID,formatSpec2,pontoon_node(3,21),pontoon_node(3,22),pontoon_node(3,23));
 fprintf(fileID,formatSpec1,'***********************************');

%Nodeset for temperature
fprintf(fileID,formatSpec1,'*NSET,NSET=temperature, GENERATE');
fprintf(fileID,formatSpec1,'41031, 41051, 2');
fprintf(fileID,formatSpec1,'41053, 41059, 1');
fprintf(fileID,formatSpec1,'42031, 42051, 2');
fprintf(fileID,formatSpec1,'42053, 42059, 1');
fprintf(fileID,formatSpec1,'30039, 30056, 1');
fprintf(fileID,formatSpec1,'30004, 30021, 1');
fprintf(fileID,formatSpec1,'41061, 41078, 1');
fprintf(fileID,formatSpec1,'42061, 42078, 1 ');
fprintf(fileID,formatSpec1,'70087, 70087, 0');
fprintf(fileID,formatSpec1,'70094, 70094, 0');
fprintf(fileID,formatSpec1,'70101, 70101, 0');
fprintf(fileID,formatSpec1,'80001, 80036, 1');
%Nodeset for mooring line cload
fprintf(fileID,formatSpec1,'*NSET,NSET=mooringpontoon13,GENERATE');
fprintf(fileID,formatSpec1,'70087, 70087, 0');
fprintf(fileID,formatSpec1,'*NSET,NSET=mooringpontoon20,GENERATE');
fprintf(fileID,formatSpec1,'70094, 70094, 0');
fprintf(fileID,formatSpec1,'*NSET,NSET=mooringpontoon27,GENERATE');
fprintf(fileID,formatSpec1,'70101, 70101, 0');
%Nodeset for cable
fprintf(fileID,formatSpec1,'*NSET,NSET=cable,GENERATE');
fprintf(fileID,formatSpec1,'30004, 30021,1');
fprintf(fileID,formatSpec1,'30039,30056,1');
fprintf(fileID,formatSpec1,'41031,41053,2');
fprintf(fileID,formatSpec1,'41054,41059,1');
fprintf(fileID,formatSpec1,'42031,42053,2');
fprintf(fileID,formatSpec1,'42054,42059,1');
fprintf(fileID,formatSpec1,'41061, 41078,1');
fprintf(fileID,formatSpec1,'42061, 42078,1');

fprintf(fileID,formatSpec1,'***********************************');
```

```
fprintf(fileID,formatSpec1,'**GIRDER Cross Section rigid body');
for i=1:269;
    fprintf(fileID,formatSpec8,'*NSET,NSET=girder_cs',i);
```

```
    fprintf(fileID,formatSpec2,girder_ele(i,30),girder_ele(i,1+30),girder_ele(i,2+30));
    fprintf(fileID,formatSpec9,'*Rigid Body, ref node=girder_node_',i,', TIE
NSET=girder_cs',i,', position=INPUT');
end
fprintf(fileID,formatSpec1,'**');
fprintf(fileID,formatSpec1,'************************************');
```

```
%Define pontoon as rigid body
for i=1:length(pontoon_node);
    fprintf(fileID,formatSpec8,'*NSET,NSET=pontoon_COG_',i+2);
    fprintf(fileID,formatSpec4,pontoon_node(i,1));
end
fprintf(fileID,formatSpec1,'************************************');
for i=1:38;
    fprintf(fileID,formatSpec8,'*ELSET,ELSET=pontoon_',i+2);
    fprintf(fileID,formatSpec2,pontoon_node(i,29),pontoon_node(i,30),pontoon_node(i,31));
    fprintf(fileID,formatSpec9,'*Rigid Body, ref node=pontoon_COG_',i+2,',
elset=pontoon_',i+2,', position=INPUT');
end
fprintf(fileID,formatSpec1,'************************************');
```

```
fprintf(fileID,formatSpec1,'**PREDEFINED FIELDS');
fprintf(fileID,formatSpec1,'** Name: TEMP   Type: Temperature');
fprintf(fileID,formatSpec1,'*Initial Conditions, type=TEMPERATURE ');
fprintf(fileID,formatSpec1,'TEMPERATURE, 30.');
% girder weight
fprintf(fileID,formatSpec1,'**STEP1: girder weight');
fprintf(fileID,formatSpec1,'*Step, name=girder weight, nlgeom=NO, inc=1000000');
fprintf(fileID,formatSpec1,'*Static');
fprintf(fileID,formatSpec1,'1.000000e-07, 1, 1.000000e-16, 1');
fprintf(fileID,formatSpec1,'**');
fprintf(fileID,formatSpec1,'************************************');
fprintf(fileID,formatSpec1,'*MODEL CHANGE, remove, type=element');
for i=1:18;
    fprintf(fileID,formatSpec8,'cable_ne_side_A',i);
    fprintf(fileID,formatSpec8,'cable_sw_side_A',i);
    fprintf(fileID,formatSpec8,'cable_ne_main_A',i);
    fprintf(fileID,formatSpec8,'cable_sw_main_A',i);
end
for i=1:4;
    fprintf(fileID,formatSpec7,'mooring_element_13_line',i,'b');
    fprintf(fileID,formatSpec7,'mooring_element_13_line',i,'w');
    fprintf(fileID,formatSpec7,'mooring_element_13_line',i,'t');
end

for i=5:8;
    fprintf(fileID,formatSpec7,'mooring_element_20_line',i,'b');
    fprintf(fileID,formatSpec7,'mooring_element_20_line',i,'w');
    fprintf(fileID,formatSpec7,'mooring_element_20_line',i,'t');
end

for i=9:12;
    fprintf(fileID,formatSpec7,'mooring_element_27_line',i,'b');
    fprintf(fileID,formatSpec7,'mooring_element_27_line',i,'w');
```

```
    fprintf(fileID,formatSpec7,'mooring_element_27_line',i,'t');
end
fprintf(fileID,formatSpec1,'**********************************');
fprintf(fileID,formatSpec1,'*BOUNDARY, OP=NEW');
fprintf(fileID,formatSpec1,'40001,   1,      6,      0');
fprintf(fileID,formatSpec1,'40269,   1,      6,      0');
fprintf(fileID,formatSpec1,'30035,   1,      6,      0');
fprintf(fileID,formatSpec1,'30070,   1,      6,      0');
fprintf(fileID,formatSpec1,'60001,   1,      6,      0');
fprintf(fileID,formatSpec1,'60003,   1,      6,      0');
fprintf(fileID,formatSpec1,'60005,   1,      6,      0');
fprintf(fileID,formatSpec1,'60007,   1,      6,      0');
fprintf(fileID,formatSpec1,'60009,   1,      6,      0');
fprintf(fileID,formatSpec1,'70001,  1,      6,      0');

fprintf(fileID,formatSpec1,'*Dload');
fprintf(fileID,formatSpec1,'mass_ne_5, GRAV, 9.81, 0., 0., -1.');
fprintf(fileID,formatSpec1,'mass_sw_5, GRAV, 9.81, 0., 0., -1.');
fprintf(fileID,formatSpec1,'mass_b_5, GRAV, 9.81, 0., 0., -1.');
fprintf(fileID,formatSpec1,'mass_ne_20, GRAV, 9.81, 0., 0., -1.');
fprintf(fileID,formatSpec1,'mass_sw_20, GRAV, 9.81, 0., 0., -1.');
fprintf(fileID,formatSpec1,'mass_b_20, GRAV, 9.81, 0., 0., -1.');
fprintf(fileID,formatSpec1,'mass_ne_25, GRAV, 9.81, 0., 0., -1.');
fprintf(fileID,formatSpec1,'mass_sw_25, GRAV, 9.81, 0., 0., -1.');
fprintf(fileID,formatSpec1,'mass_b_25, GRAV, 9.81, 0., 0., -1.');

fprintf(fileID,formatSpec1,'*Cload, OP=NEW');
for i=1:18;
    fprintf(fileID,formatSpec13,'cable_',i,'_side_sw, 3,',cable_cl(i,2));
end
for i=1:18;
    fprintf(fileID,formatSpec13,'cable_',i,'_side_ne, 3,',cable_cl(i,3));
end
for i=1:18;
    fprintf(fileID,formatSpec13,'cable_',i,'_main_sw, 3,',cable_cl(i,4));

end
for i=1:18;
    fprintf(fileID,formatSpec13,'cable_',i,'_main_ne, 3,',cable_cl(i,5));
end
fprintf(fileID,formatSpec1,'** OUTPUT REQUESTS');
fprintf(fileID,formatSpec1,'*Restart, write, frequency=0');
fprintf(fileID,formatSpec1,'*Output, field, frequency=1');
fprintf(fileID,formatSpec1,'*Node Output');
fprintf(fileID,formatSpec1,'CF, COORD, RF, U');
fprintf(fileID,formatSpec1,'*Output, field, frequency=1');
fprintf(fileID,formatSpec1,'*Element Output, directions=YES');
fprintf(fileID,formatSpec1,'S');
fprintf(fileID,formatSpec1,'*End Step');
fprintf(fileID,formatSpec1,'**');
fprintf(fileID,formatSpec1,'**********************************');

%step 2: gravity(pontoon, column,tower)
fprintf(fileID,formatSpec1,'**STEP2: gravity');
fprintf(fileID,formatSpec1,'*Step, name=pontoon gravity, nlgeom=YES, inc=1000000');
fprintf(fileID,formatSpec1,'*Static');
fprintf(fileID,formatSpec1,'1.000000e-07, 1, 1.000000e-16, 1');
```

```
fprintf(fileID,formatSpec1,'**');
fprintf(fileID,formatSpec1,'**********************************');
fprintf(fileID,formatSpec1,'*Temperature');
fprintf(fileID,formatSpec1,'temperature, 30.');
fprintf(fileID,formatSpec1,'*BOUNDARY, OP=NEW');
fprintf(fileID,formatSpec1,'40001,   1,     6,     0');
fprintf(fileID,formatSpec1,'40269,   1,     6,     0');
fprintf(fileID,formatSpec1,'30035,   1,     6,     0');
fprintf(fileID,formatSpec1,'30070,   1,     6,     0');
fprintf(fileID,formatSpec1,'60001,   1,     6,     0');
fprintf(fileID,formatSpec1,'60003,   1,     6,     0');
fprintf(fileID,formatSpec1,'60005,   1,     6,     0');
fprintf(fileID,formatSpec1,'60007,   1,     6,     0');
fprintf(fileID,formatSpec1,'60009,   1,     6,     0');
fprintf(fileID,formatSpec1,'*Dload');
fprintf(fileID,formatSpec1,'back_column, GRAV, 9.81, 0., 0., -1.');
fprintf(fileID,formatSpec1,'column_A1, GRAV, 9.81, 0., 0., -1.');
fprintf(fileID,formatSpec1,'column_A1_2, GRAV, 9.81, 0., 0., -1.');
fprintf(fileID,formatSpec1,'column_A2, GRAV, 9.81, 0., 0., -1.');
fprintf(fileID,formatSpec1,'tower, GRAV, 9.81, 0., 0., -1.');
for i=3:40;
    fprintf(fileID,formatSpec7,'pontoon_mass_',i,', GRAV, 9.81, 0., 0., -1.');
end
fprintf(fileID,formatSpec1,'*Cload, OP=NEW');
for i=1:18;
    fprintf(fileID,formatSpec13,'cable_',i,'_side_sw, 3,',cable_cl(i,2));
end
for i=1:18;
    fprintf(fileID,formatSpec13,'cable_',i,'_side_ne, 3,',cable_cl(i,3));
end
for i=1:18;
    fprintf(fileID,formatSpec13,'cable_',i,'_main_sw, 3,',cable_cl(i,4));

end
for i=1:18;
    fprintf(fileID,formatSpec13,'cable_',i,'_main_ne, 3,',cable_cl(i,5));
end
fprintf(fileID,formatSpec1,'mooringpontoon13, 3, -5146949.81');
fprintf(fileID,formatSpec1,'mooringpontoon20, 3, -5251744.93');
fprintf(fileID,formatSpec1,'mooringpontoon27, 3, -4848341');
fprintf(fileID,formatSpec1,'** OUTPUT REQUESTS');
fprintf(fileID,formatSpec1,'*Restart, write, frequency=0');
fprintf(fileID,formatSpec1,'*Output, field, frequency=1');
fprintf(fileID,formatSpec1,'*Node Output');
fprintf(fileID,formatSpec1,'CF, COORD, RF, U');
fprintf(fileID,formatSpec1,'*Output, field, frequency=1');
fprintf(fileID,formatSpec1,'*Element Output, directions=YES');
fprintf(fileID,formatSpec1,'S');
fprintf(fileID,formatSpec1,'*End Step');
fprintf(fileID,formatSpec1,'**');
fprintf(fileID,formatSpec1,'**********************************');

%step 3: buoyancy adjust
fprintf(fileID,formatSpec1,'**STEP3: buoyancy adjust');
fprintf(fileID,formatSpec1,'*Step, name=buoyancy adjust, nlgeom=YES, inc=1000000');
fprintf(fileID,formatSpec1,'*Static');
fprintf(fileID,formatSpec1,'1.000000e-07, 1, 1.000000e-16, 1');
```

```
fprintf(fileID,formatSpec1,'**');
fprintf(fileID,formatSpec1,'*Cload, OP=NEW');
for i=1:18;
    fprintf(fileID,formatSpec13,'cable_',i,'_side_sw, 3,',cable_cl(i,2));
end
for i=1:18;
    fprintf(fileID,formatSpec13,'cable_',i,'_side_ne, 3,',cable_cl(i,3));
end
for i=1:18;
    fprintf(fileID,formatSpec13,'cable_',i,'_main_sw, 3,',cable_cl(i,4));

end
for i=1:18;
    fprintf(fileID,formatSpec13,'cable_',i,'_main_ne, 3,',cable_cl(i,5));
end
fprintf(fileID,formatSpec1,'mooringpontoon13, 3, -5146949.81');
fprintf(fileID,formatSpec1,'mooringpontoon20, 3, -5251744.93');
fprintf(fileID,formatSpec1,'mooringpontoon27, 3, -4848341');
fprintf(fileID,formatSpec1,'buoyancy_pontoon3, 3, 37195769.34');
fprintf(fileID,formatSpec1,'buoyancy_pontoons1, 3, 37195769.34');
fprintf(fileID,formatSpec1,'buoyancy_pontoon13_mooring, 3, 55795508.65');
fprintf(fileID,formatSpec1,'buoyancy_pontoon20_mooring, 3, 55795508.65');
fprintf(fileID,formatSpec1,'buoyancy_pontoon27_mooring, 3, 55795508.65');
fprintf(fileID,formatSpec1,'** OUTPUT REQUESTS');
fprintf(fileID,formatSpec1,'*Restart, write, frequency=0');
fprintf(fileID,formatSpec1,'*Output, field, frequency=1');
fprintf(fileID,formatSpec1,'*Node Output');
fprintf(fileID,formatSpec1,'CF, COORD, RF, U');
fprintf(fileID,formatSpec1,'*Output, field, frequency=1');
fprintf(fileID,formatSpec1,'*Element Output, directions=YES');
fprintf(fileID,formatSpec1,'S');
fprintf(fileID,formatSpec1,'*End Step');
fprintf(fileID,formatSpec1,'**');
fprintf(fileID,formatSpec1,'************************************');

%step 4: temperature
fprintf(fileID,formatSpec1,'**STEP4: temperature');
fprintf(fileID,formatSpec1,'*Step, name=temperature, nlgeom=YES, inc=1000000');
fprintf(fileID,formatSpec1,'*Static');
fprintf(fileID,formatSpec1,'1.000000e-07, 1, 1.000000e-16, 1');
fprintf(fileID,formatSpec1,'**');
fprintf(fileID,formatSpec1,'*BOUNDARY, OP=NEW');
fprintf(fileID,formatSpec1,'40001,   1,     6,     0');
fprintf(fileID,formatSpec1,'40269,   1,     6,     0');
fprintf(fileID,formatSpec1,'30035,   1,     6,     0');
fprintf(fileID,formatSpec1,'30070,   1,     6,     0');
fprintf(fileID,formatSpec1,'60001,   1,     6,     0');
fprintf(fileID,formatSpec1,'60003,   1,     6,     0');
fprintf(fileID,formatSpec1,'60005,   1,     6,     0');
fprintf(fileID,formatSpec1,'60007,   1,     6,     0');
fprintf(fileID,formatSpec1,'60009,   1,     6,     0');
fprintf(fileID,formatSpec1,'80001,   1,     6,     0');
fprintf(fileID,formatSpec1,'80004,   1,     6,     0');
fprintf(fileID,formatSpec1,'80007,   1,     6,     0');
fprintf(fileID,formatSpec1,'80010,   1,     6,     0');
fprintf(fileID,formatSpec1,'80013,   1,     6,     0');
fprintf(fileID,formatSpec1,'80016,   1,     6,     0');
```

```
fprintf(fileID,formatSpec1,'80019,   1,     6,     0');
fprintf(fileID,formatSpec1,'80022,   1,     6,     0');
fprintf(fileID,formatSpec1,'80025,   1,     6,     0');
fprintf(fileID,formatSpec1,'80028,   1,     6,     0');
fprintf(fileID,formatSpec1,'80031,   1,     6,     0');
fprintf(fileID,formatSpec1,'80034,   1,     6,     0')

fprintf(fileID,formatSpec1,'*MODEL CHANGE, add, type=element');
for i=1:18;
    fprintf(fileID,formatSpec8,'cable_ne_side_A',i);
    fprintf(fileID,formatSpec8,'cable_sw_side_A',i);
    fprintf(fileID,formatSpec8,'cable_ne_main_A',i);
    fprintf(fileID,formatSpec8,'cable_sw_main_A',i);
end
for i=1:4;
    fprintf(fileID,formatSpec7,'mooring_element_13_line',i,'b');
    fprintf(fileID,formatSpec7,'mooring_element_13_line',i,'w');
    fprintf(fileID,formatSpec7,'mooring_element_13_line',i,'t');
end

for i=5:8;
    fprintf(fileID,formatSpec7,'mooring_element_20_line',i,'b');
    fprintf(fileID,formatSpec7,'mooring_element_20_line',i,'w');
    fprintf(fileID,formatSpec7,'mooring_element_20_line',i,'t');
end

for i=9:12;
    fprintf(fileID,formatSpec7,'mooring_element_27_line',i,'b');
    fprintf(fileID,formatSpec7,'mooring_element_27_line',i,'w');
    fprintf(fileID,formatSpec7,'mooring_element_27_line',i,'t');
end

fprintf(fileID,formatSpec1,'*Cload, OP=NEW');
for i=1:18;
    fprintf(fileID,formatSpec7,'cable_',i,'_side_sw, 3, 1.00E-12');
    fprintf(fileID,formatSpec7,'cable_',i,'_side_ne, 3, 1.00E-12');
    fprintf(fileID,formatSpec7,'cable_',i,'_main_sw, 3, 1.00E-12');
    fprintf(fileID,formatSpec7,'cable_',i,'_main_ne, 3, 1.00E-12');
end
fprintf(fileID,formatSpec1,'mooringpontoon13, 3, 1.00E-12');
fprintf(fileID,formatSpec1,'mooringpontoon20, 3, 1.00E-12');
fprintf(fileID,formatSpec1,'mooringpontoon27, 3, 1.00E-12');
fprintf(fileID,formatSpec1,'buoyancy_pontoon3, 3, 37195769.34');
fprintf(fileID,formatSpec1,'buoyancy_pontoons1, 3, 37195769.34');
fprintf(fileID,formatSpec1,'buoyancy_pontoon13_mooring, 3, 55795508.65');
fprintf(fileID,formatSpec1,'buoyancy_pontoon20_mooring, 3, 55795508.65');
fprintf(fileID,formatSpec1,'buoyancy_pontoon27_mooring, 3, 55795508.65');
fprintf(fileID,formatSpec1,'*Temperature');
fprintf(fileID,formatSpec1,'temperature, 0.');
fprintf(fileID,formatSpec1,'** OUTPUT REQUESTS');
fprintf(fileID,formatSpec1,'*Restart, write, frequency=0');
fprintf(fileID,formatSpec1,'*Output, field, frequency=1');
fprintf(fileID,formatSpec1,'*Node Output');
fprintf(fileID,formatSpec1,'CF, COORD, RF, U');
fprintf(fileID,formatSpec1,'*Output, field, frequency=1');
fprintf(fileID,formatSpec1,'*Element Output, directions=YES');
fprintf(fileID,formatSpec1,'S');
```

```
fprintf(fileID,formatSpec1,'*End Step');
fprintf(fileID,formatSpec1,'**');
fprintf(fileID,formatSpec1,'************************************');

%step 5: cable gravity
fprintf(fileID,formatSpec1,'**STEP5: cable gravity');
fprintf(fileID,formatSpec1,'*Step, name=cable gravity, nlgeom=YES, inc=1000000');
fprintf(fileID,formatSpec1,'*Static');
fprintf(fileID,formatSpec1,'1.000000e-07, 1, 1.000000e-16, 1');
fprintf(fileID,formatSpec1,'**');
fprintf(fileID,formatSpec1,'*DLOAD');
for i=1:18;
    fprintf(fileID,formatSpec7,'cable_ne_side_A',i,', GRAV, 9.81, 0., 0., -1.');
    fprintf(fileID,formatSpec7,'cable_sw_side_A',i,', GRAV, 9.81, 0., 0., -1.');
    fprintf(fileID,formatSpec7,'cable_ne_main_A',i,', GRAV, 9.81, 0., 0., -1.');
    fprintf(fileID,formatSpec7,'cable_sw_main_A',i,', GRAV, 9.81, 0., 0., -1.');
end
fprintf(fileID,formatSpec1,'** OUTPUT REQUESTS');
fprintf(fileID,formatSpec1,'*Restart, write, frequency=0');
fprintf(fileID,formatSpec1,'*Output, field, frequency=1');
fprintf(fileID,formatSpec1,'*Node Output');
fprintf(fileID,formatSpec1,'CF, COORD, RF, U');
fprintf(fileID,formatSpec1,'*Output, field, frequency=1');
fprintf(fileID,formatSpec1,'*Element Output, directions=YES');
fprintf(fileID,formatSpec1,'S');
fprintf(fileID,formatSpec1,'*End Step');
fprintf(fileID,formatSpec1,'**');
fprintf(fileID,formatSpec1,'************************************');

fclose(fileID);
```

Published with MATLAB® R2016b